THE 5th INDONESIA INTERNATIONAL GEOTHERMAL CONVENTION & EXHIBITION 2017

2 - 4 August 2017

Jakarta Convention Center

"Moving Forward Under Current Challenges, Obstacles and Oppurtunities toward Achieving Geothermal Development 2025 Target"

PROCEEDING BOOK

Hosted by

Indonesian Geothermal Association

Supported by

Organized by

MOVING FORWARD UNDER CURRENT CHALLENGES, OBSTACLES AND OPPORTUNITIES TOWARD ACHIEVING GEOTHERMAL DEVELOPMENT 2025 TARGET

Proceeding

The 5th Indonesia International Geothermal
Convention and Exhibition 2017
2 - 4 August 2017, Cendrawasih Hall - Jakarta Convention Center

Editor:
Abadi Poernomo
Suryantini
Doddy Astra
Aquardi Suminar

Indonesian Geothermal Association

2018

MOVING FORWARD UNDER CURRENT CHALLENGES, OBSTACLES AND OPPORTUNITIES TOWARD ACHIEVING GEOTHERMAL DEVELOPMENT 2025 TARGET

Editor:
Abadi Poernomo
Suryantini
Doddy Astra
Aquardi Suminar

Reviewer:

Ali Ashat
Aquardi Suminar
Arias Sugandhi
Boyke Bratakusuma
Doddy Astra
Doddy Darmawan
Ginanjar
Imam Raharjo
Jafar Maarif
Khasani
Rex Soeparjadi
Suryantini
Uum Komarudin
Yudi Kusumah
Yunus Daud

COMMITTEE

ADVISOR
Rida Mulyana

STEERING COMMITTEE
Yunus Saefulhak
Abadi Poernomo
Paul Mustakim
Prijandaru Effendi
Ahmad Yuniarto
Sanusi Satar
Tafif Azimudin
Ali Mundakir
Heribertus Dwiyudha
Fazil Alfitri
Riki F. Ibrahim

CHAIRMAN
Suharsono Dharmono

VICE CHAIRMAN
Dodi Herman

SECRETARIAT
Sudarwo
Andry Susanto
Rachma Nilamsuri
Ade Aznam

TREASURY
Nisriyanto
M. Ikbal Nur
Dwidy Zaraski

MARKETING & FUND RAISING
Rully Subakat
Mukawi Djumadin
Mawardi
Win Sukardi
Manthovani
Tungga Dewa
David L. Aulia

PUBLICATION/ OPENING CLOSING
Ifnaldi Sikumbang
Leila Rima
Noke Sudarman
Siska tan
Gladis Sondakh
Reva Sasistiya
Dimas P. Purnama
Esti Hayati

TECHNICAL PAPER
Uum Kamarudin
Doddy Astra
Yunus Daud
Khasani
Suryantini
Boyke Bratakusuma
Ali Ashat
Imam B. Raharjo
Jafar Maarif
Rex Soeparjadi
Aquardi Suminar
Arias Sugandhi
Nofi Ganefianto
Hilman
Yudi Kusumah

PROTOCOL & GOVERNMENT RELATION
Ismoyo Argo
Wisnu Subroto
Agdya Pratami P.
Murdiono
Reza Arsyad
Iwan S. Azof
Ida Bagus Wibatsya
Chandra Bachtiar
Murtiah Anggraini
Fachry Singka
Sentot Yulianugroho
Irfansyah Alam
Arga Surawidjaja

CONVENTION & PRE-CONFERENCE WORKSHOP
Amin Hartoni
M. Yasin P.
Nasir Bagis
Doddy Darmawan
Novianto
Supremelehaq
Dellas

PHOTO COMPETITION
Yulnofrins
Noor Faiz
Willy Ekariyono
Syaiful Hidayat
Kustiyah Yasin
Darel Nasri

FIELD TRIP
Fadruzil
Yusep Akbar
M. Kholifan
Gede Giri
Hendi Dedi
Yudi Kusumah
Hadi Kuswoyo

SPEAKERS

KEYNOTE SPEAKERS

- *Dr. Ir. Agus Hermanto, MM.*, Vice Speaker for Industry and Development, The House of Representatives of the Republic of Indonesia
- *Sri Mulyani Indrawati* represented by Mardiasmo as Vice Minister of Finance
- *Supramu Santosa*, Advisory Board of Indonesian Geothermal Association / Representative of Indonesian Geothermal Industry Community
- *HE Dr. Trevor Matheson*, New Zealand's Ambassador to Indonesia
- *Ir. Rida Mulyana* represented by Yunus Saefulhak as Director of Geothermal
- *Syamsu Alam* represented by Irfan Zainuddin as President Director of PT Pertamina Geothermal Energy

KEYNOTE SPEAKERS

- *Hendra Soetjipto Tan,* President Director of Star Energy Geothermal Salak Darajat
- *Hilmi Panigoro*, President Director of Medco Energi
- *Emma Sri Martini* represented by Darwin Trisna Djajawinata as Project Development and Advisory Director of PT Sarana Multi Infrastruktur (Persero)
- *Alexander Richter*, President of International Geothermal Association Dr. Alex Dolya, ACCA, CFA., Principal of Boston Consulting Group
- *Marcelo Augusto de Camargo*, President of GeothermEx a Schlumberger Company
- *Amnon Gabbay*, VP of ORMAT Business Development for Asia Pacific

Published by:
Asosiasi Panasbumi Indonesia (API)
2018

ISBN 978-602-52132-0-5

FOREWORD

By law, Indonesian Geothermal Association (INAGA) is obliged to conduct the Annual Scientific Gathering (PIT - Pertemuan Ilmiah Tahunan) in order to increase the knowledge and capacity of its geothermal community. This Annual Scientific Gathering (PIT) was held in conjunction with the Annual Indonesian International Geothermal Conference & Exhibition (IIGCE) which was the 1st IIGCE organized and hosted by INAGA in 2013 and thereafter continued annually with the support from Ministry of Energy & Mineral Resources.

The 5th IIGCE was held successfully on August 2nd - 4th, 2017 at the Jakarta Convention Center (JCC) and attended by more than 1000 people around the globe that consist of Central and Local Government Officials, Policy makers and regulators, investors, developers. Service companies, practitioners as well as academicians.

The committee of PIT as part of the 5th IIGCE event, have received 188 abstracts with various topics that focused on Earth Science, Engineering, Resources Management, Exploration & Drillings, Special Topics such as Social Lesson Learned, HSE etc.

From those 188 Abstract, after carefully reviewed by the Committee of Technical Papers that consist of lecturers from University and Professionals from the geothermal developers, 143 papers have been accepted for full paper to be presented in the Technical Papers Session during the 2 (two) days conference.

In this opportunity, I would like to express my gratitude and appreciation to the Technical Paper Committee, the Chair persons of Technical Paper Presentation, Authors, Presenters and all parties who have made the 2017 Technical Papers Session was successful.

Last but not least, I really appreciate all the hard work for my colleagues from ITB Geothermal Master Program to support and proceed all papers to be registered to ISBN.

I believed that the content and the quality of all the papers with various interesting topics were a great and best papers produced by our scientist and engineers, therefore once again on behalf of INAGA, I have the pleasure to share these papers for increasing the capacity and also for lesson learned of our geothermal community.

Yours truly,

Abadi Poernomo
President of INAGA

TABLE OF CONTENTS

AN INNOVATIVE METHODOLOGY BASED ON LOW FREQUENCY PASSIVE SEISMIC DATA ANALYSIS TO MAP GEOTHERMAL RESERVOIR STEAM SATURATED AREAS

A. Kazantsev[1,4], P. Egermann[1], Irvan Ramadhan[2], F. Huguet[1],
C. Formento[1], M. Peruzzetto[1,4], H. Chauris[4], J.-P. Metaxian[3]

[1]Storengy (Engie group), [2]Supreme Energy
[3]Institut de Recherche pour le Développement (IRD), [4]MINES ParisTech

e-mail: alexander.kazantsev@storengy.com, irvan-ramadhan@supreme-energy.com, frederic.huguet@storengy.com, catherine.formento@storengy.com, marc.peruzzetto@mines-paristech.fr, jean-philippe.metaxian@ird.fr, herve.chauris@mines-paristech.fr

ABSTRACT

In the context of exploration, development and monitoring, it is highly valuable to have access to the steam saturated regions of a geothermal resource. During exploration phase, it consists of a strong evidence that a sufficiently hot system is still present before the drilling decision. Then it allows to identify the best locations for the future exploration and development wells. During the production phase, it is important to monitor the steam saturated area extension due to the field depletion (production induced reservoir pressure decrease) in order to optimize the positioning of the make-up wells. This work presents an innovative methodology to detect relevant reservoir steam saturated areas which can be applied at different stages of high enthalpy geothermal projects. A field survey was recently conducted in the Muara Laboh geothermal field. The obtained results were in complete agreement with observations made on all the exploration wells. They enable to map the extension of the potential steam saturated region at the top of the structure and also to identify another potential steam area associated with a secondary top. The identified steam cap extension remains to be confirmed by the development wells which will be drilled and tested during the course of this year. These preliminary results have demonstrated the applicability and the potential of this promising new steam detection method for high enthalpy geothermal resources.

Keywords: geothermal, steam, exploration, monitoring, geophysics, low frequency passive seismic

CONTEX AND INTRODUCTION

A new reservoir characterization technique based on the interpretation of ambient, natural, low frequency passive seismic signal meets currently a growing success to detect subsurface reservoirs saturated with multiphase fluids. It has been used in various domains such as hydrocarbon detection and volcanic eruption prediction (Ferrick et al., 1982). This technique was also successfully evaluated by Storengy on a natural gas storage asset using an advanced and innovative workflow developed internally (under patent procedure since 2016). As the spectral anomaly is related to the presence of several coexisting phases in a reservoir and the basic properties of a gas/water and steam/brine system are of the same order in terms of surface tension, density and viscosity, there is no fundamental reasons why this technique could not be applicable also in the geothermal context to detect steam saturated areas.

An accurate mapping of geothermal reservoir two-phase regions is of primary importance to guide the targeting of development and even exploration wells. On a longer term, it is also very important to map the extension of the steam area related to the reservoir depletion in order to guide the drilling of future make-up wells. Unfortunately, mapping two-phase regions is usually difficult in geothermal fields since the top reservoir is picked from the MT data whose vertical resolution is low, even though the steam/water interface is identified in some exploration wells. Therefore, it is highly valuable to develop new techniques to access this information directly in an accurate and cost effective manner. This is the main objective of this paper.

The first part of the present paper explains the principle of the methodology which relies on the acquisition and the analysis of Low Frequency Passive Seismic (LFPS) data. This approach was originally used and further developed by Storengy to monitor gas saturation in the context of natural gas storage activity (Lavergne, 2015). Ocean waves permanent activity generates coherent noise (seismic surface waves) at the ocean bottom, which then propagates across continents. This so called Ocean Wave Peak (OWP), or microseism for seismologists, provides us with a natural diffuse seismic source which interacts with multi-phase inclusions in subsurface leading to a modification of the energy spectrum. In the geothermal context, volcanic tremors can be an additional natural source at the same frequencies.

The interest of extending the application of such a technology in the context of high enthalpy geothermal reservoirs is tackled in the second part of this paper and illustrated through a LFPS field survey recently conducted in the Muara Laboh geothermal field (Situmorang et al., 2016).

LOW FREQUENCY PASSIVE SEISMIC PRINCIPLE

The method is based on measuring the interaction between low frequency ambient waves and multi-phase inclusions in subsurface. Permanent activity of the ocean waves generates seismic ambient noise at the ocean bottom, which then propagates across continents mainly in the form of Rayleigh waves. The main sources of this noise have been investigated by different authors (Schimmel, 2011; Ardhuin et al., 2011). The left panel in Figure 1 (after Ardhuin et al., 2011) illustrates their distribution on the globe in 2008.

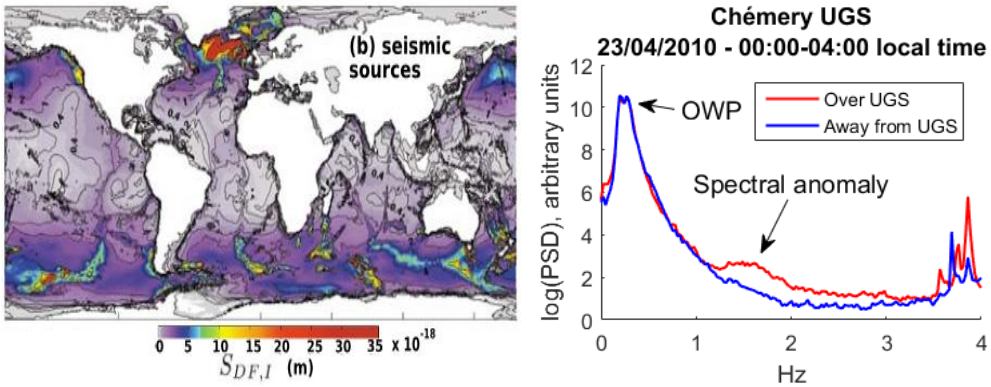

Figure 1: Source zones of seismic ambient noise (after Ardhuin et al., 2011) - Typical spectra of seismic signals outside (blue) and over (red) an Underground Gas Storage

Though these waves have most of their energy contained into the [0.1-0.2] Hz spectral band, they are still visible on the spectra up to 1-2 Hz. As we noted on various datasets, other sources can be active even at low frequencies. Human activities, such as industry and traffic, usually become visible above 1 Hz, and mainly contain surface waves. As it will be illustrated below, in the geothermal context, a volcanic system can be source of body waves dominating the ambient wavefield at frequencies as low as 1 Hz, and even lower. Whatever its origin, characterizing and exploiting a natural source avoids using costly artificial sources in seismic acquisition surveys.

Natural waves are likely to be scattered when crossing geological formations containing multi-phase inclusions because of the effective elastic and anelastic contrasts. The spectral content is modified, giving rise to an anomaly that can be mapped over the zone with multi-phase inclusions. Dangel et al. (2003) observed spectral anomalies above more than ten oil and gas fields around the world. In Figure 1 (right), the anomaly of the vertical component power spectral density (PSD) is observed above the Chémery natural gas storage in France. The aforementioned forward modeling approach based on scattering is currently being developed by Storengy and presented in more detail in Kazantsev et al. (2017). We must stress out that this approach is at reservoir scale, unlike the pore scale interface oscillation model proposed by Holzner et al. (2006) in order to explain the spectral anomaly in the hydrocarbon context.

A typical survey consists of deploying an array of three-component seismic sensors installed into 50 cm deep holes over the zone of interest (Figure 2). The recording should last at least 24 hours under good weather conditions. The array can be shifted from one day to another to improve the spatial resolution of the resulting map. Some reference sensors must stay at the same location during the whole survey. The band pass of the sensors should be at least [0.1–10] Hz. This light protocol enables to cover a large surface in a short period of time which makes it cost-effective compared to standard seismic surveys.

Figure 2: Typical sensor and its deployment

The analysis / interpretation process includes several steps:

- Pre-processing of the data to remove all the time windows where the signal was affected by external perturbations,
- Processing through the calculation of the energy spectra and the source signal propagation direction,
- Interpretation using several attributes representative of the spectral anomaly modification due to a multi-phase reservoir.

The method has been tested and validated over the Chémery natural gas storage by a consortium involving Gaz De France (now Engie). Following the preliminary results from Spectraseis in charge of the interpretation (Duclos et al., 2011), Storengy has developed its own improved processing workflow from the raw data, which has yielded very promising results (Kazantsev, 2015). Figure 3 shows the anomaly map in Chémery, compared to the gas accumulation computed by a flow simulation using a 3D reservoir model matched on 50 years of production data.

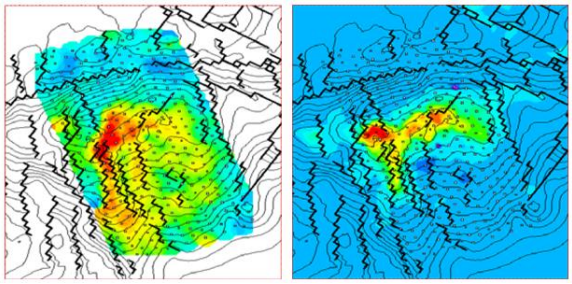

Figure 3: Spectral anomaly (left) compared to the simulated gas accumulation (right) [after Kazantsev (2015)]

A very good consistency can be observed between the two maps. As the gas distribution in the reservoir model, the spectral anomaly appears very sensitive to the presence of N-S faults located in the southwestern part of the storage (bold black lines in Figure 3 left). Moreover, the maximum spectral anomaly corresponds very well to the structural tops of the reservoir where the maximum gas column height is located.

Other successful applications of similar techniques can be found in the literature for hydrocarbon detection before drilling exploration wells (Holzner et al., 2005; Graf et al., 2007; Riahi et al., 2013) and for volcanology to monitor the low frequency tremors attributed to the magmatic chamber activity evolution before eruption (Ferrick et al., 1982; Ripepe and Gordeev, 1999).

ACQUISITION OVER A GEOTHERMAL SITE

The LFPS methodology has been tested on the Muara Laboh geothermal field (West Sumatra) which was extensively described by Situmorang et al. (2016). PT Supreme Energy Muara Laboh (SEML) drilled six full diameter exploration wells which yielded an estimation of temperature distributions, resource size, permeable structures, and hydrology of the system. The conceptual model relies on a hot geothermal fluid upwelling from the deep part of the resource in the southern part. The fluid then flows globally to the northern direction. The reservoir fluid temperature ranges between 200°C to 310°C. In the most part, the reservoir contains a single liquid phase but a small extension steam cap was detected at the shallowest part of the reservoir from wellpad A as shown in Figure 4.

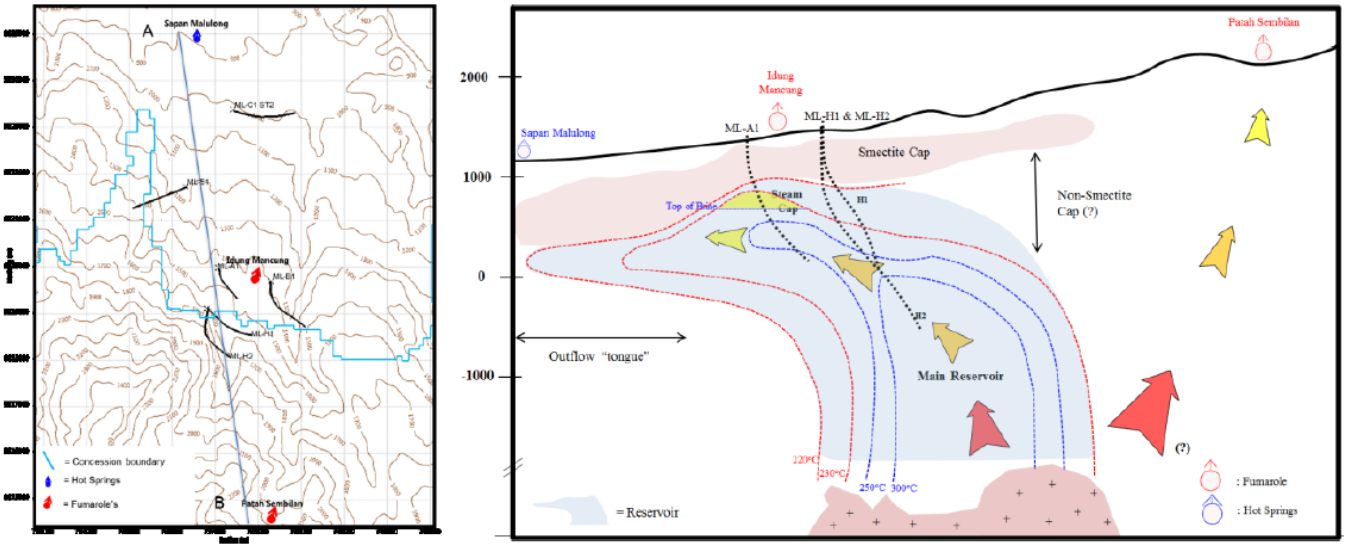

Figure 4: North-south cross section showing conceptual model of Muara Laboh field (Situmorang et al., 2016)

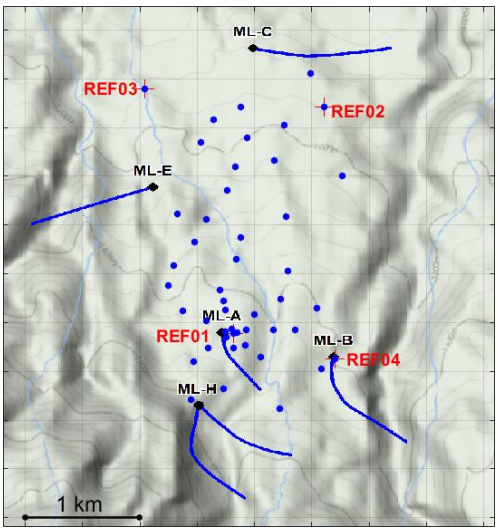

Figure 5 : Broadband seismic network deployed in Muara Laboh. Each blue location corresponds to 48 hours of available recording

11 low frequency 3-component broadband seismometers (Güralp 6TD 30s) were deployed from 31/05/2016 until 14/06/2016. Three of them (REF01, REF02, REF03) remained at permanent locations. Another 7 stations were deployed in a circular configuration whose location changed every two days. This configuration enables the array processing of the ambient noise in order to characterize the incident wavefield. The network is shown in Figure 5. Another permanent station (REF04) was added on 15/06/2016. The permanent stations remained installed until 14/08/2016 in order to check the stability of the measured attributes.

RESULTS

After pre-processing, the power spectral density (PSD) was estimated on all the 3 components. An example is shown in Figure 6.

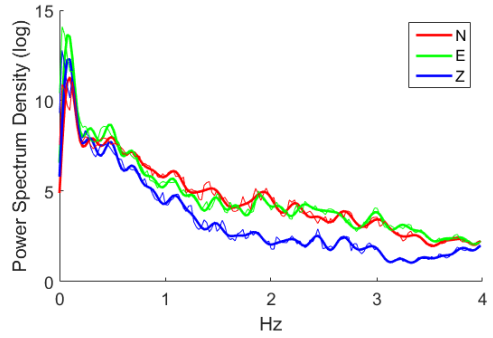

Figure 6 : Example of spectra estimated for the REF03, 03/06/2016. Bold curve : smoothed spectra.

Then the V/H spectral ratio was calculated as

$$\chi_{V/H} = \frac{PSD_z}{\sqrt{\frac{1}{2}(PSD_N^2 + PSD_E^2)}}$$

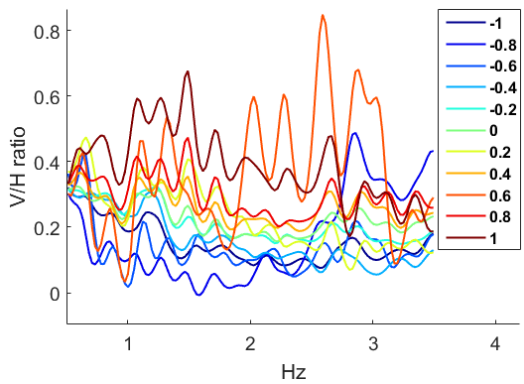

Figure 7 : Result of the V/H spectral curves classification

Following the patented procedure, an automated classification was applied to the recorded V/H spectral curves according to their shape. The classification output is quasi-continuous between -1 and 1. The spectra with values close to 1 exhibit a stronger V/H ratio between 1 and 2.5 Hz (Figure 7). The evolution of the mean V/H ratio between 1 and 2.5 Hz recorded by the reference stations during two months following the survey is shown in Figure 8. It can be seen that the high V/H ratio at REF01 is a stable feature over time.

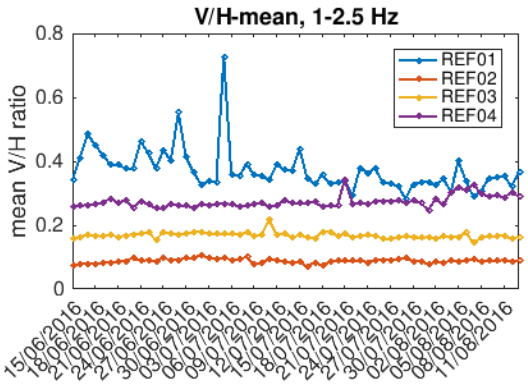

Figure 8 : Mean V/H ratio evolution in [1-2.5] Hz over a two-months recording period

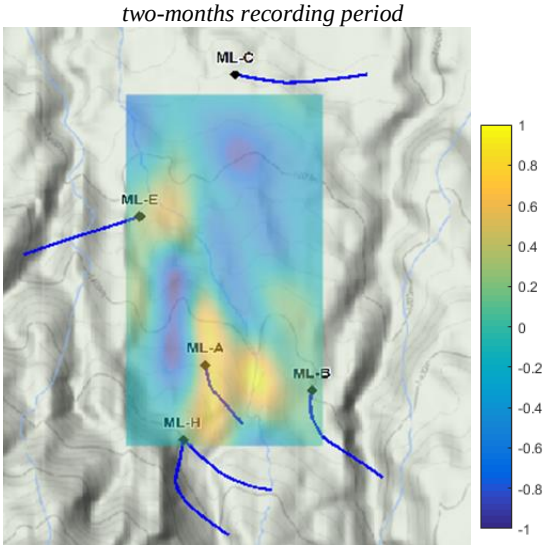

Figure 9 : Final anomaly strength map after classification and kriging

The classification results were then mapped onto the surveyed area by kriging, taking into account the uncertainties related to the time variability of the spectra (Figure 9). This map shows two "anomalous" zones characterized by a high V/H ratio (classification output close to 1) : a stronger one in the south of the field close to the well A, and a weaker one in the eastern vicinity of the well E.

Our current hypothesis is that these zones are generated by the scattering of the ambient wavefield on the steam bearing zones. The ambient wavefield was analyzed with two arrays of different apertures to address 2 frequency bands : [1-2] Hz and [5-7.5] Hz (see Figure 10 for configuration and response functions).

MUSIC algorithm (Schmidt 1986) was applied to retrieve histograms of apparent slowness and back-azimuth over overlapping 5 minutes time windows. The results shown in
Figure 11 suggest that there is no consistent velocity decrease with frequency in the [1-2] Hz band (array 2) as it would be expected for surface waves. Moreover, the values of apparent velocities range from 1500 to 3000 m/s, which is more typical for body waves at these frequencies.

The results of the array 1 exhibit velocities between 1000 and 2000 m/s into the [5-7.5] Hz band, which again seems too high for surface waves, though a decrease over frequencies is observed. Finally, the back–azimuth is stable over frequencies and is close to the Kerinci volcano's direction, as shown in the back-azimuth histograms in Figure 11. This leads us to conclude that the wavefield in the frequency band of interest is dominated by body waves originating from volcanic tremors. The next step of the work will consist of modeling the scattering of such waves by a contrast intended to mimic a steam-bearing zone.

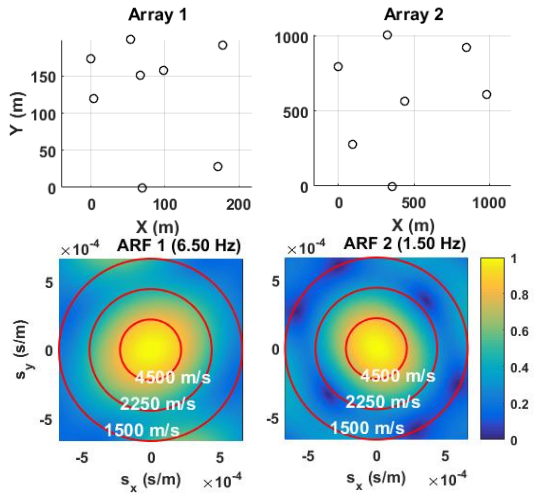

Figure 10 : Geometry of the two arrays (top) and their response functions at the relevant frequencies (bottom)

DISCUSSION

The results obtained by the empirical LFPS approach presented above are in complete agreement with the observations made on all the exploration wells (Figure 12). They enable to map the extension of two steam saturated regions :

- The main one at the top of the structure (A wellpad) were the most prolific exploration well have been drilled with a steam production under bottom hole conditions.
- In the northern part near the area of wellpad E. This latest steam anomaly is less intense and could be associated with a shallow steam zone. This is suggested by the heating-up temperature profiles recorded after drilling which are showing a significant temperature anomaly behind the casing at shallow depth (Figure 12).

Although the identified steam cap extension remains to be confirmed by development wells in the course to be drilled and tested this year, these first results are very encouraging and very consistent with the current knowledge of this geothermal reservoir

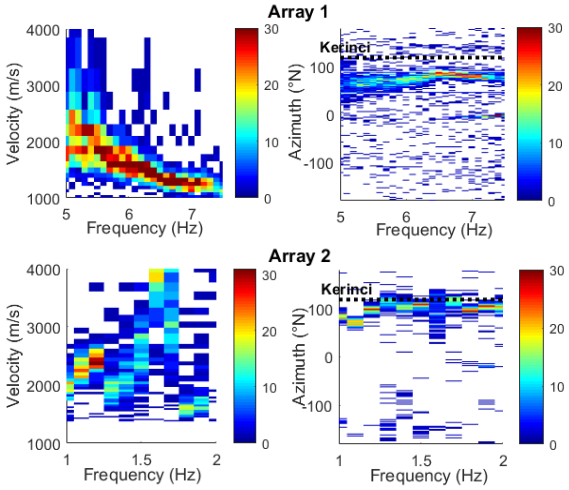

Figure 11 : MUSIC : velocity-frequency and back-azimuth histograms over analyzed windows

.

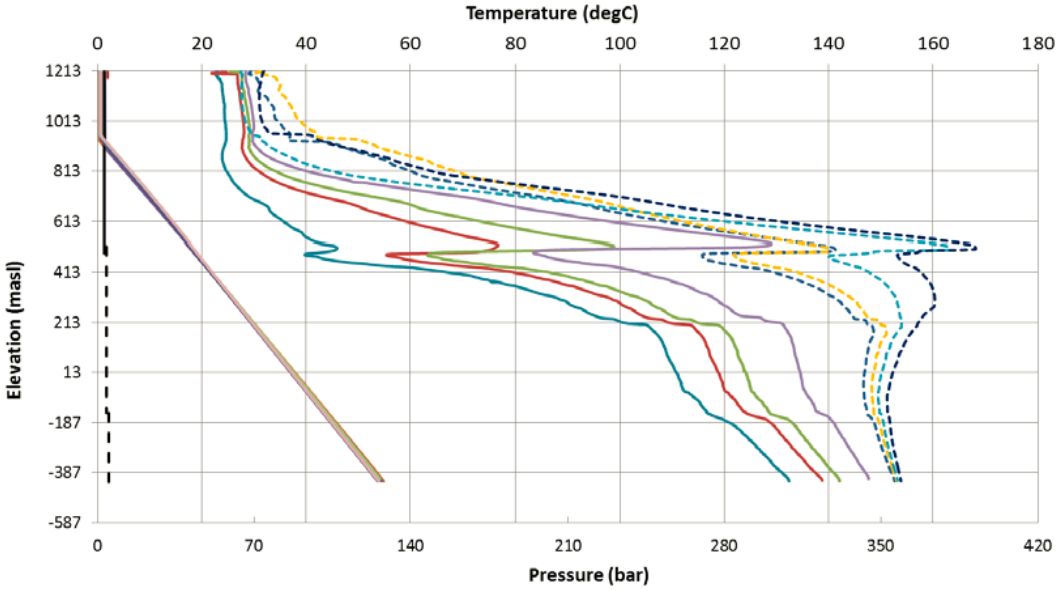

Figure 12: Anomaly in temperature recovery behind casing observed on E1 well that could be attributed to shallow steam

CONCLUSIONS

A new methodology based on the acquisition and the analysis of Low Frequency Passive Seismic (LFPS) data has been successfully tested on the Muara Laboh geothermal reservoir to map the steam saturated areas.

The protocol for data acquisition is simple and the survey can be conducted over a short period of time which makes it a cost effective solution. The data analysis and interpretation consist of the key part to obtain accurate energy spectra and relevant attributes representative of the

spectral anomaly modification due to steam saturated reservoir areas.

The first results are very promising since already consistent with the current knowledge of the reservoir. The ongoing field development drilling campaign should enable to strengthen the accuracy of these preliminary results. The application of this new steam saturated areas detection method for high enthalpy geothermal resources is very promising for both the exploration and field development phases. It may improve the success ratio of the wells through a better targeting of the most prolific areas.

REFERENCES

Anne Mangeney. 2011. 'Ocean Wave Sources of Seismic Noise'. *Journal of Geophysical Research* 116 (C9), doi: 10.1029/2011JC006952

Dangel, S, M.E Schaepman, E.P Stoll, R Carniel, O Barzandji, E.-D Rode, and J.M Singer. 2003. 'Phenomenology of Tremor-like Signals Observed over Hydrocarbon Reservoirs'. *Journal of Volcanology and Geothermal Research* 128 (1–3), doi: 10.1016/S0377-0273(03)00251-8

Duclos, M., B. Artman, B. Birkelo, F. Huguet, J. F. Dutzer, and R. Habiger. 2011. 'Low Frequency Seismic Survey at a Gas Storage Reservoir'. *73rd EAGE Conference and Exhibition incorporating SPE EUROPEC 2011*, doi: 10.3997/2214-4609.20149602

Ferrick, M. G., Anthony Qamar, and W. F. St Lawrence. 1982. 'Fluid Dynamic Analysis of Volcanic Tremor'. *Cold Regions Research and Engineering Laboratory (U.S.)*

Graf, R., S. Schmalholz, Y. Podlachikov, and E. H. Saenger. 2007. 'Passive Low Frequency Spectral Analysis: Exploring a New Field in Geophysics'. *World Oil 01/2007*, 47-52

Holzner, R., P. Eschle, M. Frehner, S. Schmalholz, and Y. Podlachikov. 2006. 'Hydrocarbon Microtremors Interpreted as Oscillations Driven by Oceanic Background Waves'. *68th EAGE Conference and Exhibition Incorporating SPE EUROPEC 2006*.

Holzner, R., P. Eschle, H. Zürcher, M. Lambert, R. Graf, S. Dangel, and P. F. Meier. 2005. 'Applying Microtremor Analysis to Identify Hydrocarbon Reservoirs'. *First Break* 23 (5).

Kazantsev, A., H. Chauris, P. Dublanchet, and F. Huguet. 2017. 'Near-Field Elastic Scattering of Rayleigh Waves - A Model for Interpreting Hydrocarbon Micro-Tremors'. *79th EAGE Conference and Exhibition 2017*, doi: 10.3997/2214-4609.201700868

Kazantsev, Alexandre. 2015. 'Extraction et Analyse l'anomalie Sismique Basse Fréquence Sur Le Site de Stockage de Chémery'. *Storengy report OI-CE/DESS-AKA-2015-00237*.

Lavergne, Damien. 2015. 'Innovative Technology for Monitoring an Underground Gas Storage : Low Frequency Passive Seismic Analysis'. *World Gas Conference 2015*, Paris, France.

Riahi, N., A. Goertz, B. Birkelo, and E. H. Saenger. 2013. 'A Statistical Strategy for Ambient Seismic Wavefield Analysis: Investigating Correlations to a Hydrocarbon Reservoir'. *Geophysical Journal International* 192 (1), doi: 10.1093/gji/ggs031

Ripepe, Maurizio, and Evgenii Gordeev. 1999. 'Gas Bubble Dynamics Model for Shallow Volcanic Tremor at Stromboli'. *Journal of Geophysical Research: Solid Earth 104 (B5)*, doi: 10.1029/98JB02734

Schimmel, M., E. Stutzmann, F. Ardhuin, and J. Gallart. 2011. 'Polarized Earth's Ambient Microseismic Noise: POLARIZED MICROSEISMIC NOISE'. *Geochemistry, Geophysics, Geosystems* 12 (7), doi: 10.1029/2011GC003661

Schmidt, Ralph O. 1986. 'Multiple Emitter Location and Signal Parameter Estimation'. *IEEE Transactions on Antennas and Propagation* AP-34 (3).

Situmorang, J., R. Martikno, A. Perdana Putra, and Ganefianto, N. 2016. 'A Reservoir Simulation of the Muara Laboh Field, Indonesia'. *41st Workshop on Geothermal Reservoir Engineering*. Stanford University, Stanford, California.

GEOTHERMAL 3D SUBSURFACE MODELING A CASE STUDY FROM SORIK MARAPI FIELD, INDONESIA

A.C. Licup, Jr.[1], Z.F. Sarmiento[3], X.L. Omac[2], F.C. Maneja[2], V.R. Chandra[1], M.B. Esberto[2], M.J.Z. Villareal[2], A.S.J. Baltasar[2], S. Mulyani[4], P.P. Sari[4], Jhonny [4], D. Juandi[4]

[1]PT Sorik Marapi Geothermal Power, [2]FEDCO
[3]KS Orka Renewables PT Ltd, [4]Schlumberger

e-mail: armando.licup@ksorka.com; zammy.sarmiento@ksorka.com; omac.xl@gmail.com; felix_maneja06@yahoo.com; vicky.chandra@ksorka.com; mig.esberto@gmail.com; mjzvillareal@gmail.com; smulyani@slb.com; ppsari@slb.com; jjhonny@slb.com; djuandi@slb.com

ABSTRACT

Indonesia is considered to have the largest geothermal potential in the world, estimated at 29,000 MW and distributed from high, medium and low enthalpy geothermal systems. To date, only less than 5% have been utilized, but many other geothermal concessions are being developed and offered for further exploration and development. The Sorik Marapi geothermal field has been recently drilled with results indicating the existence of a high temperature-neutral resource. Maximum temperature measured so far has been recorded as 290°C, with three wells currently tested and producing an average of 11.5 MW.

Initial modeling works in the field has been completed and discussed in FEDCO (2017) NORC report paving the way forward for a strategy that prioritizes the development of the Sibanggor area. This paper deals with the 3D modeling studies conducted in the geothermal field, based on available data from surface exploration (3G-geological, geochemical and geophysical) surveys, and shallow and deep drilling in the 4 identified prospect areas. The 3D modeling utilizes Petrel® software from Schlumberger which allows interfacing of limited and non-standard data formats for easy and fast processing. The 3D model is structured to integrate the structural model, lithology and alteration zone, the 3D MT resistivity model and the temperature distribution collected from the 6 wells in the area.

The workflow in the models starts with data loading and quality control, creation of structural framework for fault modeling and generating 3D grid for reservoir property modeling to capture the lithology, resistivity and temperature distribution. Special workaround algorithms are required to ensure correct data loading. The final result of this study is the 3D subsurface static model defining the vertical and lateral resource boundaries as well as the prime resource areas which would be the basis of designing future well targets to achieve the targeted 240 MW installed capacity in the field. The same model would then be expanded in constructing the numerical model to match the natural state condition of the resource, and subsequently for making forecasts on the future reservoir behavior at different operating conditions.

Keywords: 3D subsurface model, structural, lithology, resistivity and temperature model, Petrel, Sorik Marapi, Indonesia

INTRODUCTION

The Sorik Marapi geothermal field is one of the liquid dominated systems located along the Great Sumatran Fault System (SFS). Several surface exploration works have been undertaken to characterize the field's geothermal potential. These include geophysical surveys, geochemical sampling and structural mapping based on LiDAR image interpretations. Now on its exploration drilling and early development stage, SMGP recently completed its first few production wells. To better visualize the field, both surface and subsurface geoscientific data obtained were utilized to develop various 3D models using Petrel® software. The output of this project consist of a 3D structural and lithological model of SMGP, as well as resistivity and temperature distribution in the field.

The model boundary used in this project is shown in Figure 1, encompassing the entire SMGP geothermal concession.

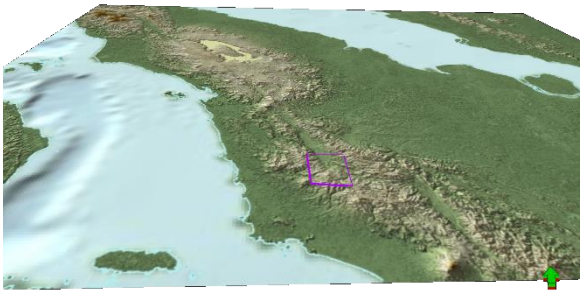

Figure 1: Model boundary location (purple square) at area study Sorik Marapi

REGIONAL GEOLOGY AND TECTONIC SETTING

Structural Geology

The Sumatran Fault System (SFS) is a long right-lateral strike-slip fault which traverses the entire length of the Sumatra Island. This zone of active deformation is attributed to the subduction within the Sunda Trench. The geomorphology of the SFS was found to be highly segmented, consisting of second order geometrical irregularities which splits the fault extent to at least nineteen (19) segments (Sieh and Natawidjaja, 2000). Such irregularity and an important tectonic feature of the SFS lie on the equator (between 0.1°S and 1.5°N), coined as the "*equatorial bifurcation*", where the fault splays to

two sub-parallel structures – Angkola and Baruman segments, with a widest separation of 35km at 0.7°N (Figure 2). This is known as the Panyabungan pull-apart basin, one of the thirteen (13) pull-apart basins mapped along the extent of the SFS (Muroaka et al., 2010). The SFS runs the length of the Barisan Mountains in Sumatra, the volcanic arc related to the Sunda trench. The Barisan Mountain is comprised of at least thirty-five (35) volcanoes, one of which is the active strato-volcano – Sorik Marapi (2,145 masl).

Stratigraphy

The stratigraphic units in the SMGP may be summarized into four (4) formations. From oldest to youngest, these are: (1) The ***Basement*** consisting of Mesozoic to Paleozoic metasediments (including shale and limestone), which are possibly intruded by plutonic rocks (including granodiorite and quartz diorite) (SKM, 2011), this unit has not been intercepted in the subsurface, thus far; (2) The ***Sibanggor Volcanic,*** formerly referred to as Old Volcanics, possibly of Tertiary Age, consisting of undifferentiated generally altered volcanics / volcaniclastics units with hardly distinguishable original composition and fabrics; (3) ***Roburan Volcanics***, predominantly dacitic to andesitic exhibiting pumiceous and porous texture with common primary micas; and (4) ***Sorik Marapi Volcanics***, consisted of young andesitic to basaltic lava flows and pyroclastic deposits that radiate outwards from the active Sorik Marapi volcano. Shown in Figure 3 is the stratigraphic cross-section of these formations as encountered in SMGP wells.

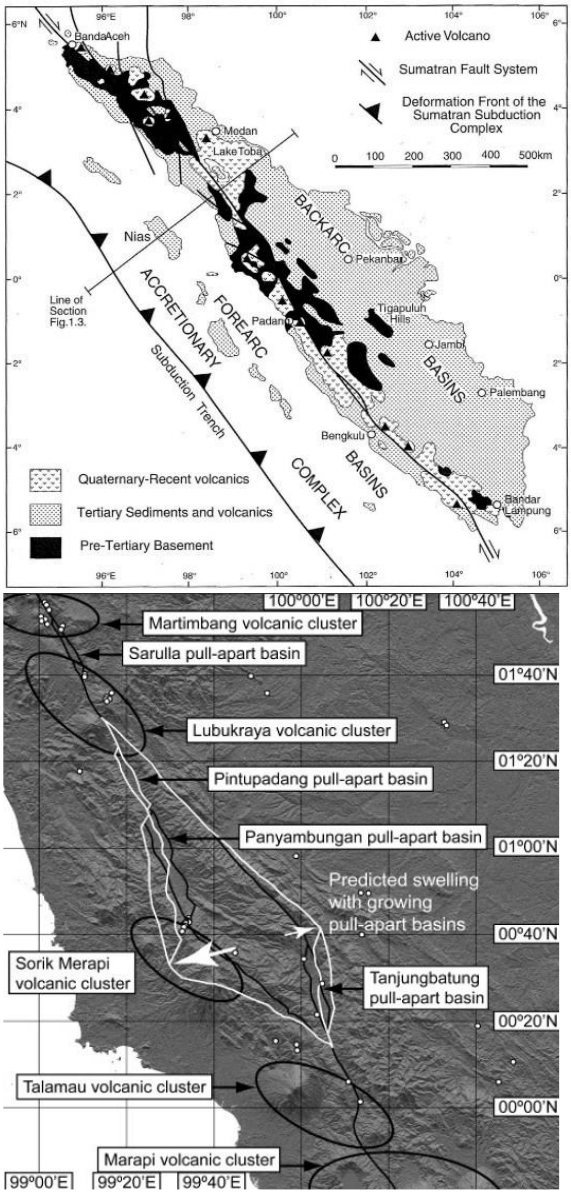

Figure 2: Volcano-tectonic setting of Sorik Marapi showing localized fault stresses in response to the dextral movement along the Sumatran Fault System (adapted from Muraoka, et al., 2010)

.

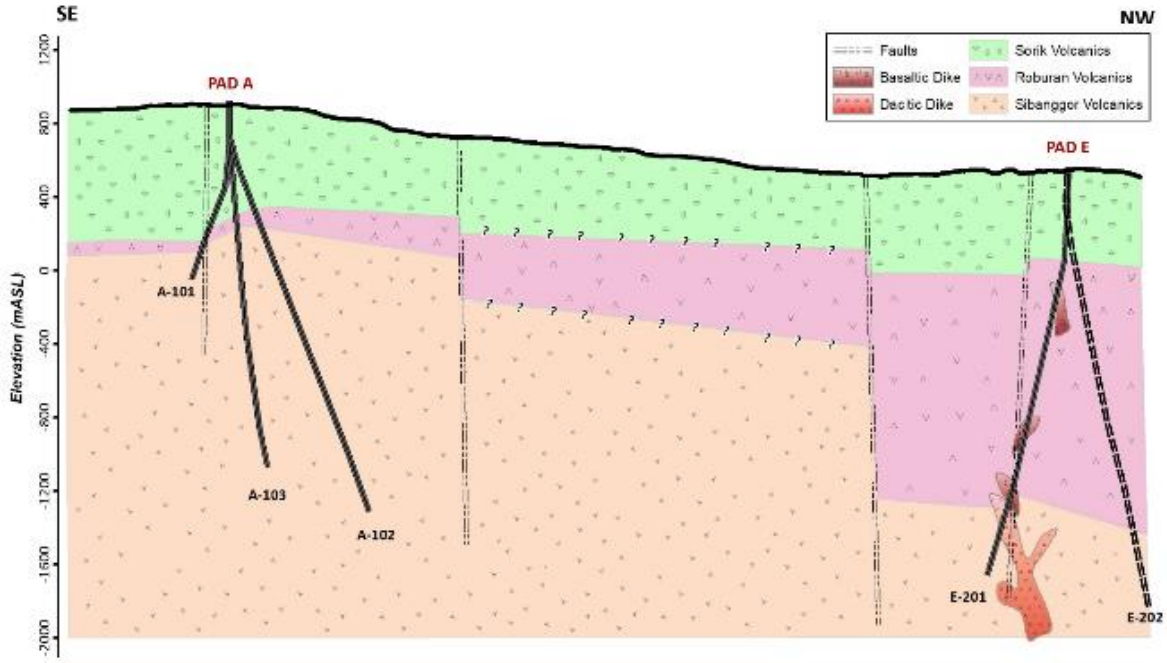

Figure 3: Stratigraphic Cross section based on encountered lithology among SMGP wells

Hydrothermal Alteration

The dominant alteration mineral assemblage of wells drilled in PAD A exemplified an alteration suite largely resulting from neutral pH geothermal fluids. At shallow levels (surface to 50masl), the alteration assemblage is composed of silica + chlorite + smectite + calcite ± iron oxides ± pyrite, which comprise the argillic zone or clay cap of the reservoir. The presence of common bladed calcite in Pad A wells at around +100 to +500masl insinuates boiling condition along these depths. At deeper levels, neutral to alkaline environment remain evident with the noted presence of rare secondary amphiboles, epidote and wairakite suggesting a formation temperature in excess of 250ºC. The ubiquitous presence of calcite suggests neutral pH fluids with high CO_2 fugacity which hinders the growth of epidote even at high temperatures.

On the other hand, Pad E wells showed a hydrothermal alteration assemblage that is lower in rank as compared to Pad A wells. Moreover, the clay zone is thicker in two Roburan wells where smectite persisted down to -930m msl. The abundance of Fe oxides throughout these wells suggest that the volcanic formation may have been deposited in a water-lain environment. Based on alteration mineralogy, predicted temperatures from E series wells may reach 220°C, which is relatively lower than A series wells.

GEOTHERMAL SYSTEM

The Upflow Zone

Previous studies conducted in Sorik Marapi have suggested varying conceptual models of the geothermal resource. SKM (2011) proposed that there are four (4) separate upflow zones in the project based on several MT resistivity anomalies. FEDCO (2016, 2017) favored a typical single geothermal system with an upflow zone that is associated and located near or directly beneath Mt. Sorik Marapi volcano. This interpretation is shared by ISOR (2016) in their due diligence study report for the area. This model is depicted with the main resource centered between Sorik Marapi and Sibanggor Tonga and overlain by a low resistivity layer. In view of the lack of MT data at Mt Sorik Marapi, a more definite shape and size of the upflow zone cannot be ascertained. However, such resistivity structure provides a good indication on the location of the nearest upflow zone. Recent drilling in Pad A confirmed the existence of hot geothermal fluids in Resource Area 1 in Sibanggor sector.

Two-phase Liquid Dominated System

Figure 4 shows the updated integrated conceptual model of Sorik Marapi geothermal resource (Fedco, 2017). It shows that mixtures of fluids and magmatic gases ascend vertically to the summit of Mt. Sorik and from there discharges magmatic gases, highly saline fluids with very low pH. Part of the mixtures of fluids finds its way laterally and channeled through fractures or faults leading to the Sibanggor area and appear at the surface as thermal springs and fumaroles. As the fluids migrate, the acidic fluids interact with the rocks and the overlying aquifer forming a mature geothermal system with a neutral pH as manifested in the thermal springs. This is supported by stable isotope ($\delta^{18}O$ and δD) data showing that samples from fumarole condensates, except from the Mt. Sorik crater, lie to the left of the meteoric water line. Geochemical samples from Sibanggor Tonga insinuate that the fluids come from a source with a temperature of 280°C while Roburan samples indicate that they are secondary fluids from steam-heated groundwater.

The temperature distribution from the wells drilled in Pad A shows a broad isothermal section and slight reversal-like in SMA-102 at deeper levels, suggesting the northern part of Sibanggor area is probably at the periphery of the main thermal plume. As inferred from the trend of hydrothermal alteration and isotherms and interpretation of the MT data, it is likely that the deep, near-neutral pH geothermal resource in Sibanggor might be centered beneath the eastern slope of Sorik Marapi volcano.

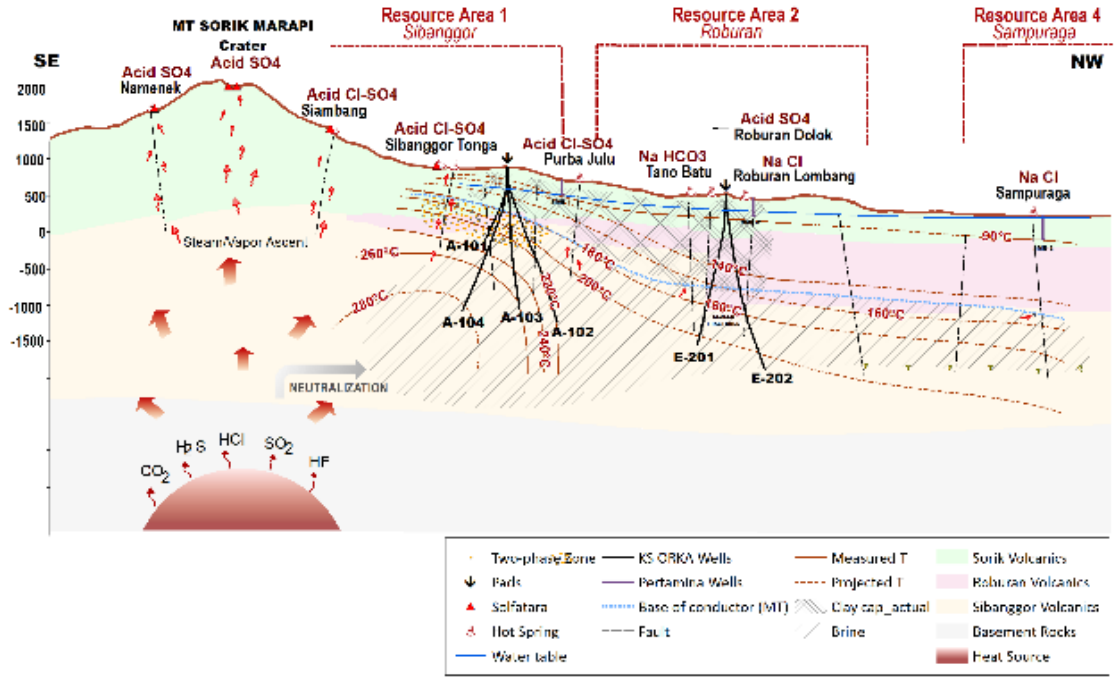

Figure 4: Updated Conceptual Model of the Sorik Marapi Geothermal Project

The benign nature of fluids tapped by Pad A wells has confirmed that the up flowing fluids have already undergone substantial neutralization. The main characteristic of this system is that a two-phase zone exists at the top of the main brine reservoir which was undoubtedly predicted even during the drilling stage due to the presence of common bladed calcite in all the wells from +100 to +500 mASL. All wells have temperature profiles falling within the boiling point for depth (BPD) curve from 100-200m MSL suggesting boiling condition at depth. Well SMA-103 exhibited highest temperature of 290°C at 1400m during shut condition.

The Cap Rock

The capping mechanism conspicuously differs between Pad A and Pad E wells. In Sibanggor sector, a comparatively thin conductive layer was recognized from MT survey. This can be correlated to the interpreted reservoir cap above +100m MSL among Pad A wells. The cap rock is characterized by widespread development of silica and interstitial calcite with generally minor smectite and interlayered clays. Fractures are hemmed in by amorphous quartz which are probably deposited due to pressure fluctuations as a consequence of episodic rupturing and silica sealing at the roof of the reservoir.

In Roburan sector, a thick conductive body was inferred through analysis of MT data. This roughly corresponds to predominant argillic alteration assemblage until -800m MSL. The conductive layer is made up of prevalent smectite, interlayered clays, iron hydroxides, amorphous silica and interstitial calcite. The extensive silica sealing at the base of cap rock was not observed in Pad E wells which suggests the lack or absence of hot fluid flow in the area in the recent past.

The Reservoir Host Rock

At the production section of Pad A wells (+100m to -1300m MSL), intensely altered rocks with hardly discernible original fabric and composition and exhibiting high-temperature alteration minerals are encountered. These rocks belong to the Sibanggor Formation where a general increase in well-formed secondary mineral crystals and abundant vein materials are observed specially within zones of fault intersections. The type of lithology, degree of alteration and existence of open fractures all indicate that this volcanic formation acts as the host for the geothermal reservoir. Reservoir temperatures exceeds 250°C as temperature gradient tends to increase towards the upflow zone.

On the other hand, Sibanggor Formation in Pad E wells was intersected deeper and are mostly altered to low and medium rank mineral assemblage and normally devoid of crystallinity. This further signify that Roburan sector is an impervious barrier that prevents vertical or lateral migration of geothermal fluids.

Outflow Zone

The signature of the outflowing fluids to the lowlands and possibly associated with the Mt. Sorik Marapi is exhibited by hot springs (96°C) in Sampuraga area, some 17 kilometers to the north of Sorik Marapi Crater (Figure 5). Whether Sampuraga is hydrologically connected with Sibanggor resource as suggested by geochemical data, it is not corroborated by the drilling results of wells SME-201 and SME-202. The steep thermal gradient from pad A to pad E, poor permeability and low hydrothermal alteration rank among pad E wells insinuate that Roburan sector is not part of the main lateral flow path from upflow region in Sibanggor en route to Sampuraga.

If there is some hydrological connection between Sampuraga and Sibanggor, the path should pass in area outside the low-lying corridor that stretches from Sibanggor to Roburan. A possible circuitous route would be through an area east of South Sumatran Marapi Central Fault. However, if this is true, well SMA-102 should be

very permeable and SME-202 should at least show some resemblance of alteration halo at depth.

Pursuing further the possibility of having hydrological connection between Sampuraga and Sibanggor, by some reckoning, is beneath the western mountain range. The limited MT resistivity data to the west provides a hint on this conjecture. Resistivity profiles has shown that there is possible domal MT resistivity structure west of Roburan which can be construed as possible flow of hot fluids. The solfataric activity at Roburan Dolok could just be a surface leak from that hydrological corridor. This mountain range is seemingly composed of volcanic chains that includes Sorik Marapi, an unnamed preserved crater and a cinder cone. An alternative explanation is that there is really no connection between Sampuraga and Sibanggor and they are actually separated by a cold block. This concept requires a heat source other than the Sibanggor upflow that supplies the hot geothermal fluids in Sampuraga. Figure 5 below shows location of volcanic centers within the mountain range that could be possible heat sources.

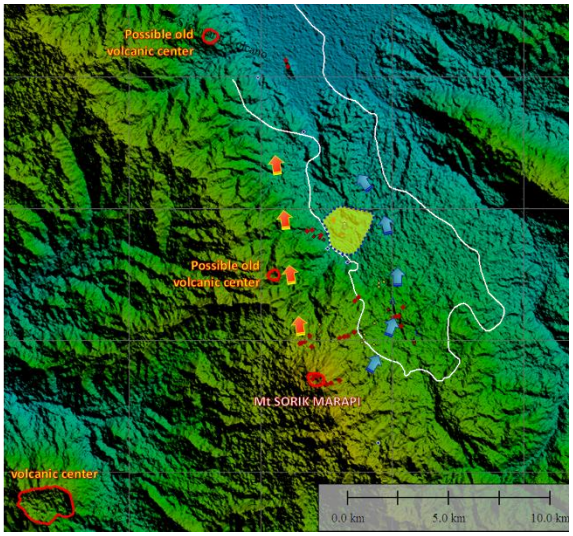

Figure 5: Interpreted outflow path from Mt. Sorik Marapi Upflow Zone to Sampuraga

DATA AND METHODOLOGY

Modeling process for the study area is done by updating the previous study which was created without well data. Several data from that study are still used for current modeling, they are fault polygons from surface mapping and LIDAR interpretation, 3D resistivity from magnetotelluric method and topography point data. There are 6 wells from 2 pad locations that are used as input data. The additional subsurface data consists of lithological information (cuttings), secondary mineral distribution, and temperatures at several depths (Figure 6).

The final model came from integration of those data. Structural model comprises of topography surface and fault planes which were generated from topography point data and fault polygons previously interpreted. On the other hand, lithology models were created based on cross sections of lithology facies from well data as shown at Figure 3. Supplementary lithological and alteration mineral data from wells have been used as additional information for this lithological model. Distribution model of resistivity value in the study area was extracted from 3D magnetotelluric points data (Figure 7).

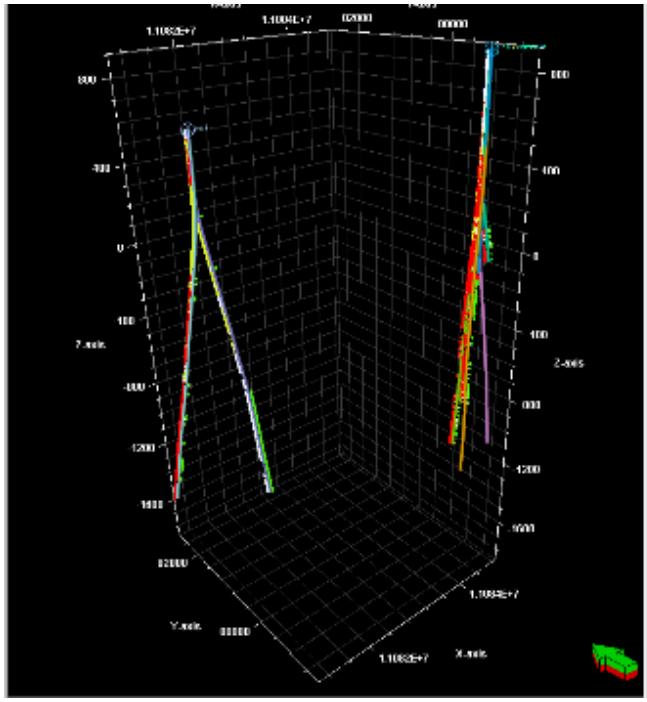

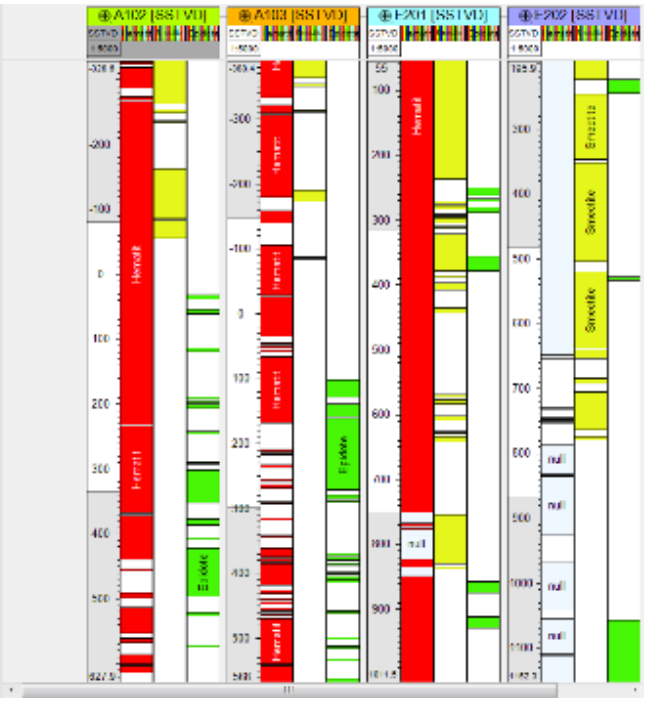

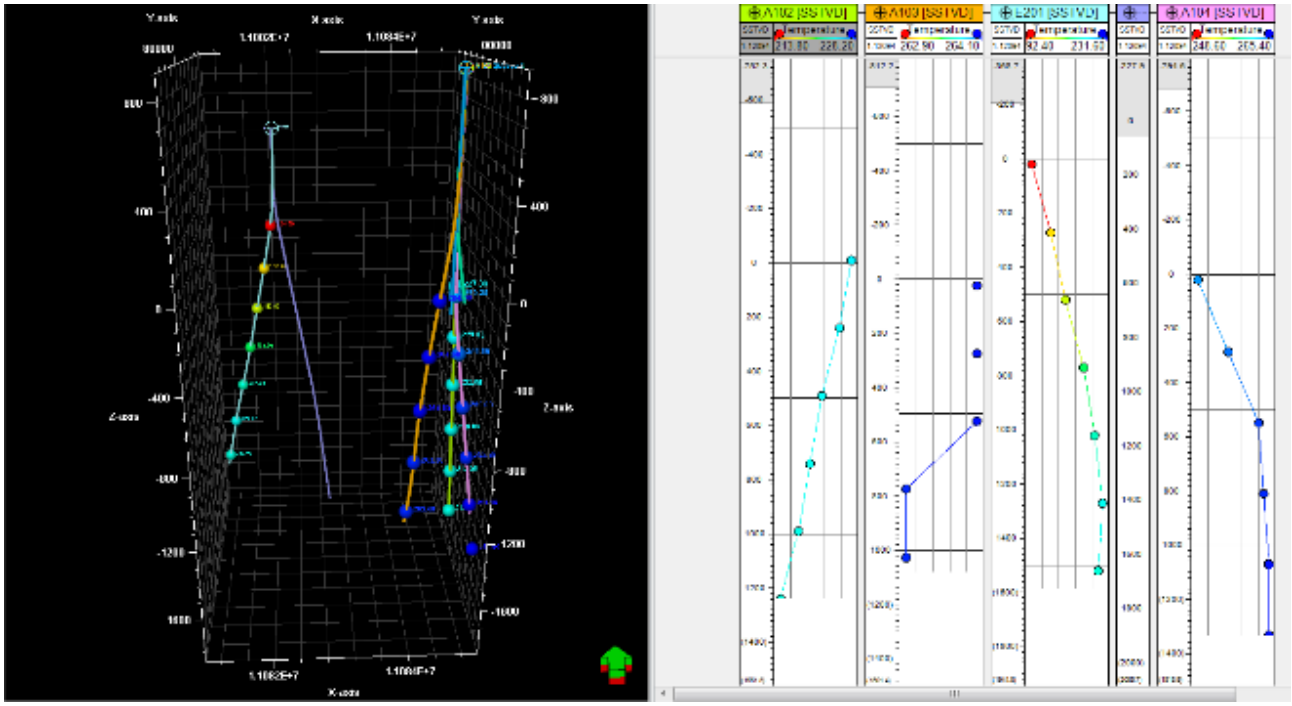

Figure 6: Additional information from well data including distribution of secondary minerals (above) and temperature at some depth (below)

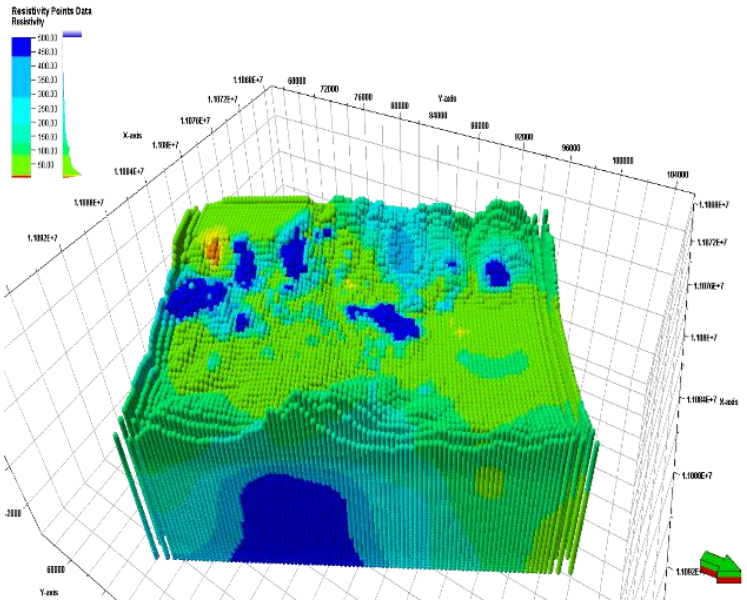

Figure 7: 3D resistivity MT point data for resistivity modeling (colors based on depth of points location)

The results of resistivity 3D models were also used as driver to populate the temperature values from well data to create 3D temperature model. Table 1 enumerates the data required for each modeling process.

Table 1: Data list for 3D subsurface modeling.

3D Models	Data
Structural	a. Topography point data b. Fault polygon from surface mapping
Lithology	a. Lithological data from wells b. Alteration minerals from wells c. Cross section of facies lithology
Resistivity	a. 3D Magneto telluric point data
Temperature	a. Measured well temperatures

The workflow for the 3D modeling of Sorik Marapi geothermal resource was adapted from similar study conducted in Aydin, Turkey, which used Petrel® as the modeling software (Akar, S. et al., 2011). Generally, there are four main steps in this workflow, they are: data input, structural modeling, property modeling, and Quality Check for the results (Figure 8).

Loading data into software are defined based on the files type. Topography, 3D resistivity and fault polygons were simply loaded as points and polygon. Lithology and temperature were imported as well data, while cross sections or map data were inputted as image. The Coordinate Reference System (CRS) was needed to make

sure all data are inputted correctly. This will influence the positions of data and the 3D visualizations. Structural modeling started by defining project boundaries that can cover all data and diversity. For this modeling process, a square polygon with and area of 7.4 x 10^8 m^2 was chosen as the lateral boundary. Then, surface map is gridded based on that boundary with topography point data as the main input. Topography condition of project area was represented by surface elevation map. The fault polygons were edited to enable them as input in fault framework. In this process, fault polygons that were expressed in the surface as 2D data has been transformed into fault planes which are 3D objects. There are 490 fault polygon data available for this project. In this case, fault data were classified into 4 classes based on LIDAR and surface evidences, they are either major or minor faults with high to medium confidences (Figure 9).

All fault planes can be modeled and used for a framework in the succeeding steps. However, modeling too many faults is a very tedious process and may result into unreasonably complicated 3D visuals. To simplify the approach, 73 fault planes were selected for the succeeding steps. Fault modeling defines the skeleton of 3D grid model and fault pillar based on selected fault planes. The skeleton will serve as guide for horizon modeling process to generate horizon data which represents the facies boundary. To get proper model, lithology cross section from well data has been used in the process. After that, zoning and layering were conducted to set the cell thickness. It is important to get more layers such that all point data will be captured into the 3D grid. When the 3D grid is ready, property modeling can now be performed. This process consists of geometrical modeling for lithology model, and petrophysical modeling for resistivity and temperature distributions. The final results of these models were verified by applying several methods such as creating cell volume to ensure that all cells at 3D grid model are correct, check the histogram for every result of petrophysical modeling, and view well section to validate the relationship between actual well data and results model

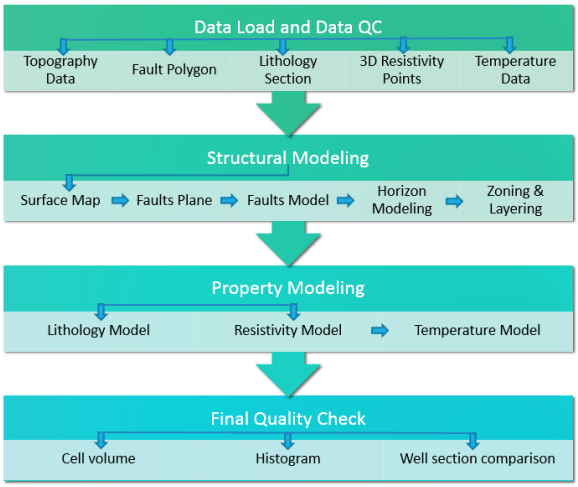

Figure 8: Workflow for 3D Subsurface Modeling using Petrel® software with four main stages: load data, structural, property modeling and final QC.

.

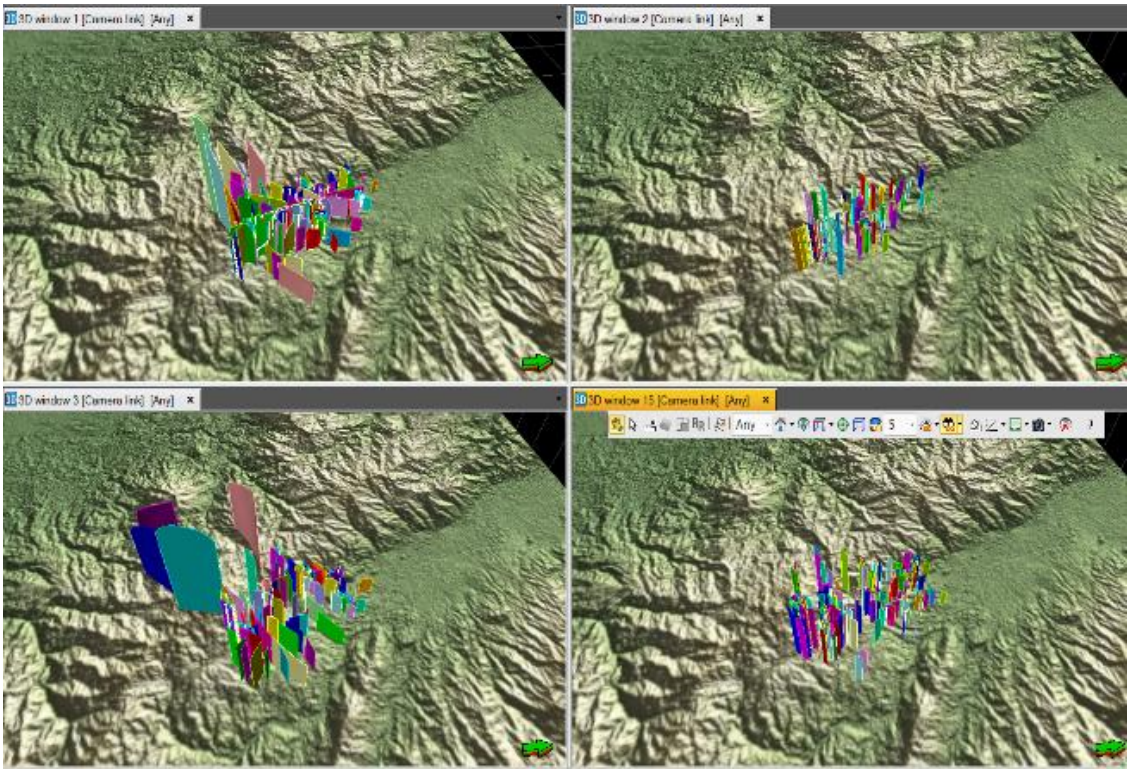

Figure 9: Faults plane data from faults polygon which classified into four classes: Major Minor faults with high confidence (1st row) and Major Minor faults with medium confidence (2nd row).

RESULTS MODEL

The final various 3D subsurface models of geothermal resource will be integrated to develop a single model. This comprises the fault model, the horizon model, and properties information such as lithology, resistivity and temperature. All of the results were created sequentially from structural fault model to property distribution in the 3D grid.

Structural and Lithological Models

The result of structural modeling is shown in Figure 10. Fault planes were modeled using process structural framework to 3D grid in Petrel®. Based on surface mapping and actual well-fault intersectio[illegible] were assigned with a dip range of 85º to [illegible] model demonstrated the complexity of structural framework in the project due to the movement along Sumatra Fault system and the formation of Panyabungan Graben. As more subsurface data become available, this model can be used in establishing the plumbing mechanism in SMGP.

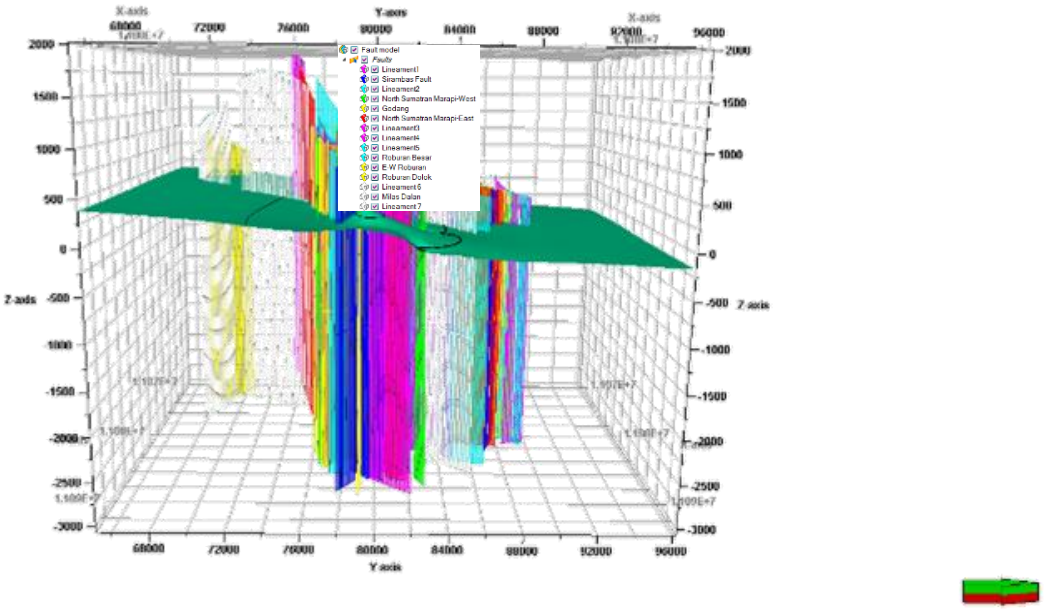

Figure 10: 3D Fault Modeling Subsurface results

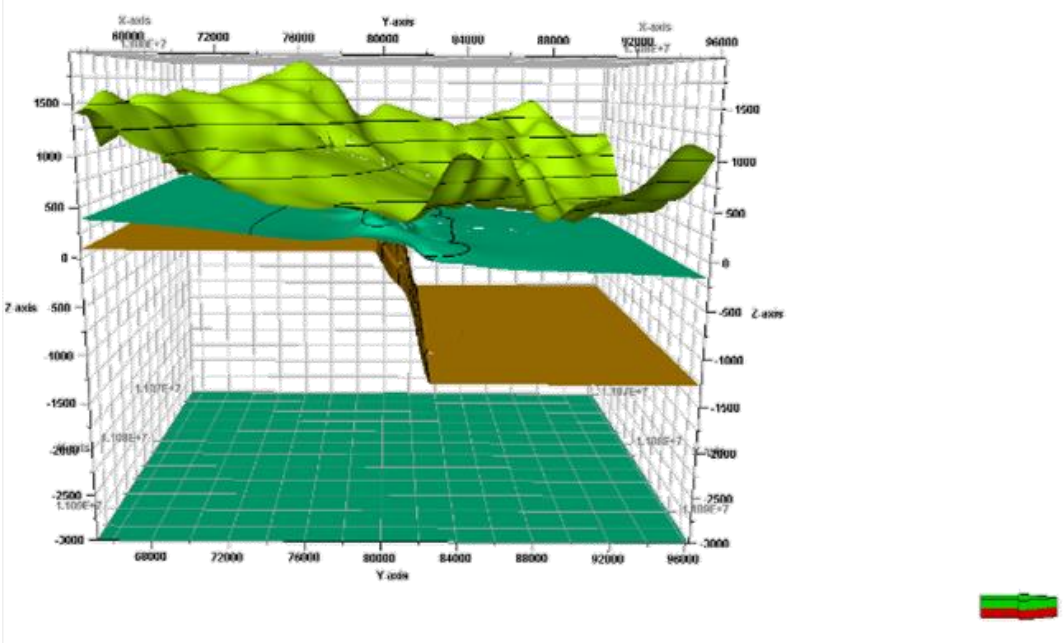

Figure 11: Horizon modeling results

From the structural model, horizon model is created on a skeleton grid with lateral resolution of 50m x 50m. The horizon model was generated using well lithology as main input. The several horizons inside the model represent facies boundary. These boundaries correspond to the tops of Sorik Volcanics, Roburan Volcanics, Sibangor Formation and a bottom layer at -3000m MSL which was assumed as vertical limitation for the model (Figure 11).

Prior to deep exploratory drilling, a 3D stratigraphic model was constructed using gravity data and other third party 3D visualization software. That model was

reconstructed using Petrel® and the result is shown in Figure 12. However, after drilling several deep wells, it was established that the basement was not intersected contrary to initial geological prognosis. It is possible that the basement is too deep and beyond the reach of the exploration wells.

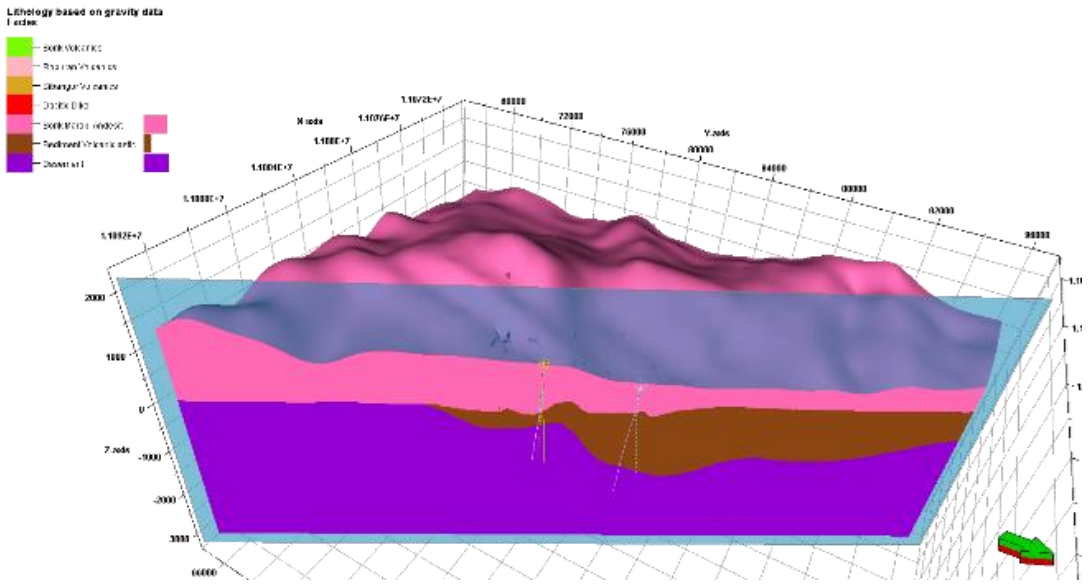

Figure 12: 3D Lithology model based on gravity data from previous study without any well data.

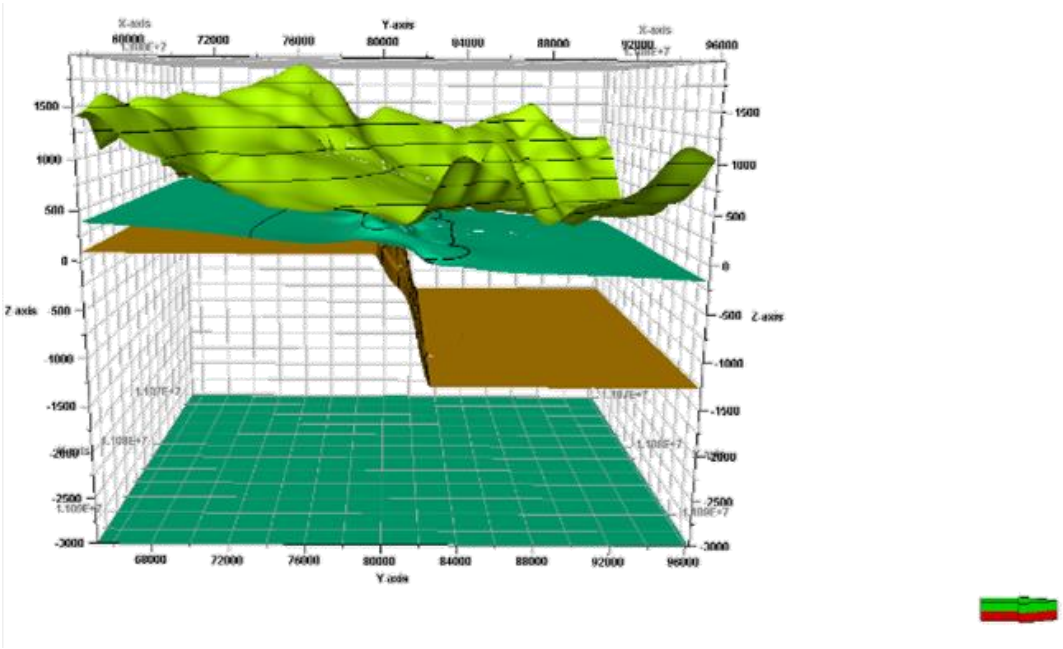

Figure 11: Horizon modeling results

VBased on drill cuttings analyses, the subsurface stratigraphy was remodeled into the 3D grid (Figure 13) and the outcome is quite consistent with the cross-section shown in Figure 3. This model has supported the previous FEDCO (2017) observation that Roburan sector was once a depression where Sibanggor Formation was down thrown and where the bulk of Roburan Volcanics subsequently accumulated. Preponderance of iron hydroxides in cuttings samples implies that volcanics in Roburan was deposited in aqueous environment.

Resistivity Model

For this study, the resistivity distribution data from magnetotelluric (MT) surveys were used in geophysical modeling. The MT measurements were considered as resistivity attributes for point data. The final product of MT data processing is the resistivity distribution in 3D subsurface (Figure 7).

To extract the point data into 3D grid model, the values should be extracted by well log upscaling process. The 3D grid which was previously built consisted of numerous cells where single value can be assigned. In the upscaling process, all values from point data within a cell in 3D grid were assigned as attributes. The cells without any values (due to lack of field measurements) were assigned with values interpolated from neighboring cells. To populate the upscale data for entire 3D grid, petrophysical modeling with kriging method was applied to generate the resistivity model (Figure 14).

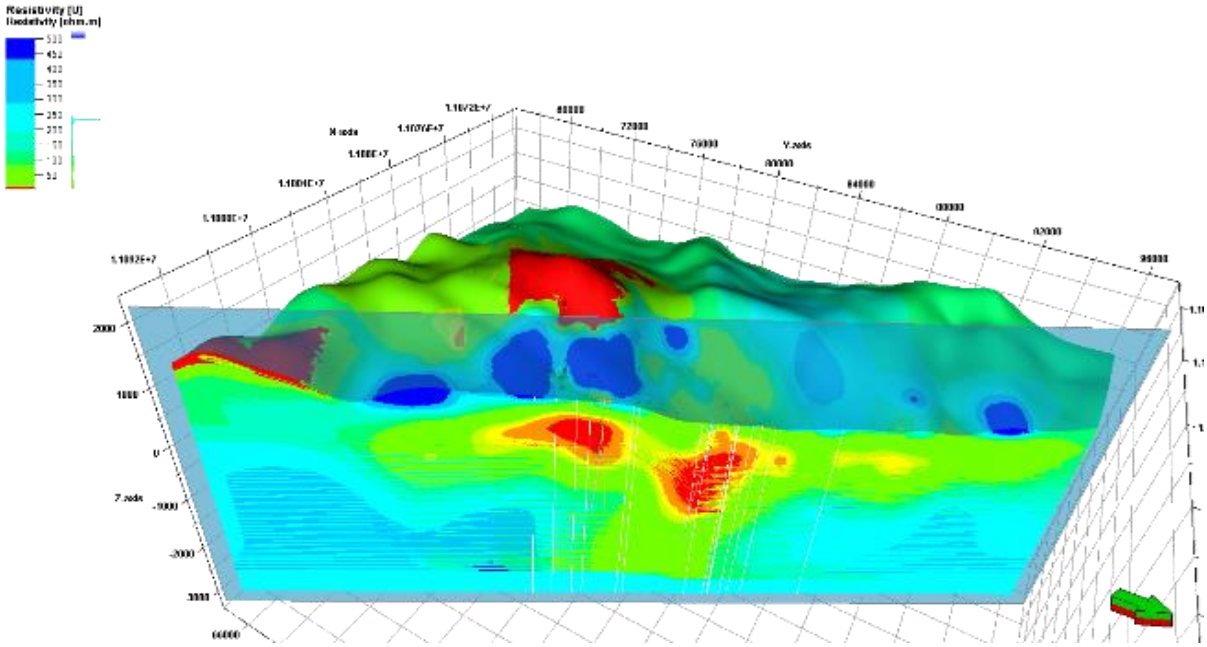

Figure 14: 3D Resistivity model based on points data with resistivity attribute from MT

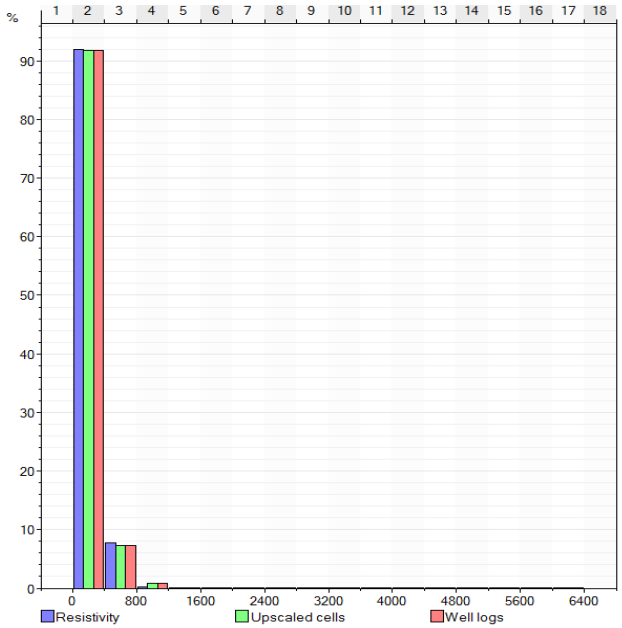

Figure 15: Histogram view which shows the comparison of original data from points, upscaled data and resistivity in the 3D grid model.

This model shows the distribution of resistivity values especially near the wells drilled in pads A and E with characteristic low resistivity. The resistivity value for entire model ranged from1 to 6,300 Ωm.

Quality control for this model was done by checking histogram data of the resistivity model. This histogram showed the comparison between original data, upscaled data and properties model data (Figure 15). Based on the histogram, there was substantial similarity between them which means almost entire value from data has been captured into 3D grid model.

Temperature Model

Being one of the most essential features of a geothermal system, subsurface temperature distribution model is considered as one of the main goals in this study. For this model, temperature data are available from four wells (A102, A103, A104 and E201) that were drilled from pads A and E. The deepest elevation attained by the 4 wells was -1400m MSL. Due to scarcity of data, the best way to model temperature is by using stochastic approach. But the results entail a lot of uncertainties. Thus, temperature modeling was done by deterministic approach similar to resistivity modeling.

The challenge for this method is how to optimize the utilization of available data from the wells to attain a more realistic representation of the resource model. To address this issue, a new attribute for original resistivity point data was created. This new attribute represents the value of temperature at each point. To get that temperature attribute for every point data, the calculator function of Petrel® was applied. This function formula determines the relationship between the measured temperatures of well and resistivity model value at the same location. By plotting Temperature against resistivity, a formula that expresses the relationship between two parameters was generated (Figure 16). Based on the graph, the following equation was derived:

$$y = 202.628 + 0.85288\,x - 0.00265004\,x^2$$

where x =Resistivity(Ωm) and y=Temperature (°C)

Using the above equation, the temperature attributes were established based on resistivity data and used as input for property modeling. The workaround was similar with resistivity modeling previously discussed. Point data attributes were upscaled into 3D grid model, then the values populated into entire grid by doing petrophysical modeling with kriging method. The results show temperatures values ranging from 25°C to 270°C inside the 3D grid model (Figure 17).

Quality control for this model can be done by checking its histogram data similar to what has been done to resistivity model. In addition, well section window was used to compare original temperature data from wells and the resulting model (Figure 18).

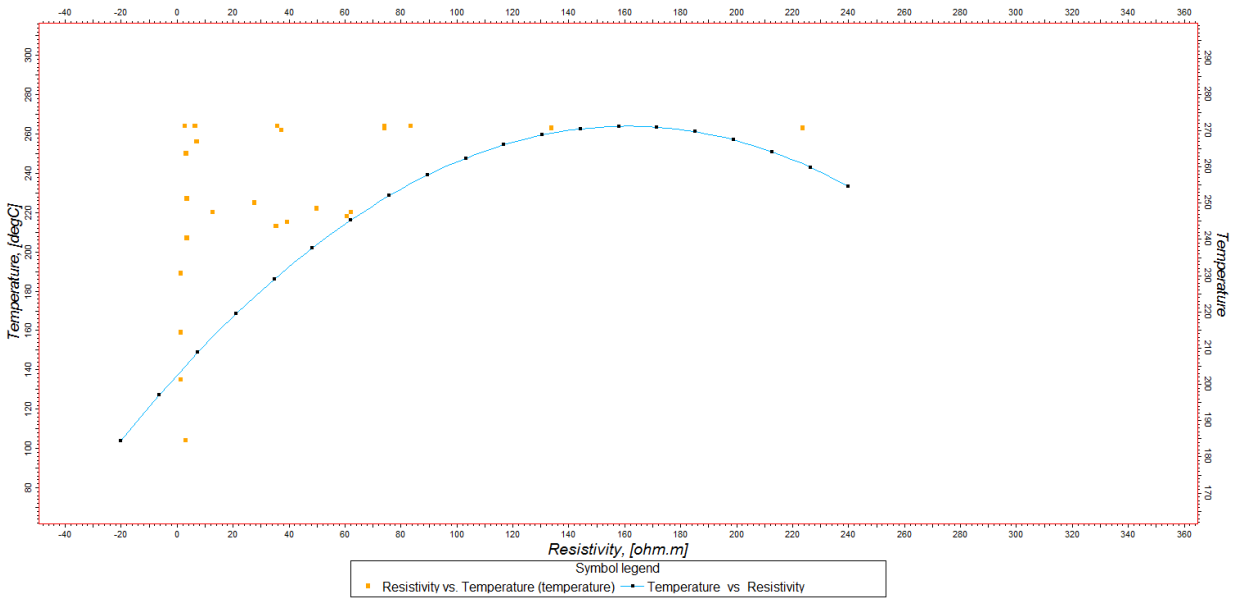

Figure 16: Non-linear function graph generated from resistivity and temperature data relationship.

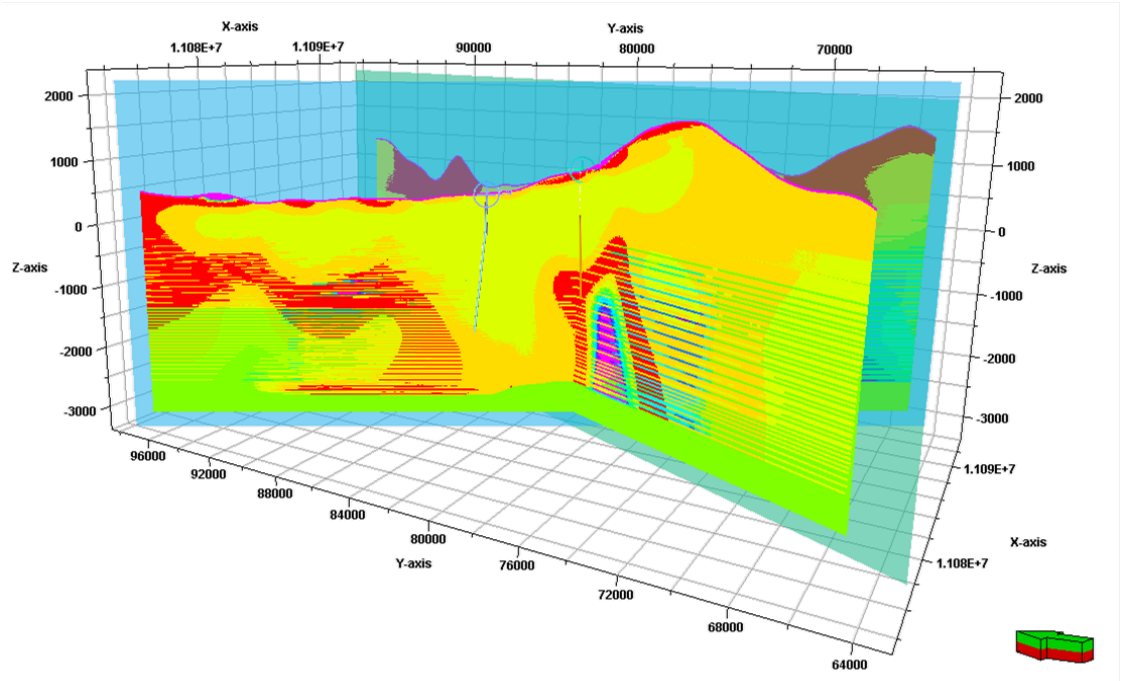

Figure 17: 3D Temperature model based on points data with temperature attributes extracted from resistivity data

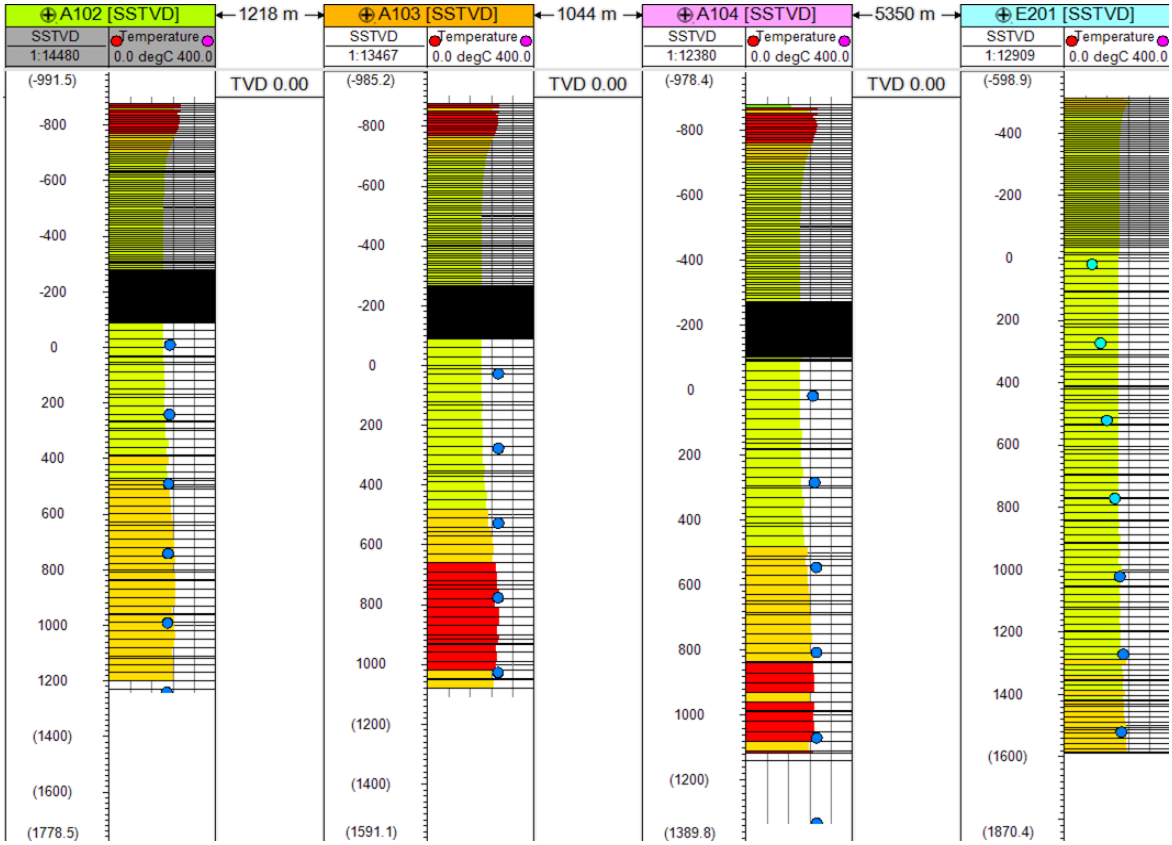

Figure 18: Well section window to compare original well data temperature (blue circle symbol) and result model of temperature

Basing on the 3D visualization and testing at well section window, we can consider that temperature value distribution is reasonably accurate except for locations that were too far from existing wells. It is expected that this temperature model will be improved in the future as more wells are drilled.

DISCUSSION

The model created using the resistivity-derived temperatures demonstrated that the hottest section or the main resource is located in the vicinity of the eastern flank of Mt. Sorik Marapi volcano. The geothermal reservoir is indicated by near vertical feature that may represent the thermal plume emanating from an area beneath Mt. Sorik Marapi. The chimney-like form of the reservoir may have been influenced by scarcity of data at and west of Sorik Marapi volcanic center. It is possible that the size of the resource could even be broader should more MT measurements are conducted within Sorik Marapi volcano and to the west where a large, seemingly ancestral caldera is located.

On the other hand, the model does not clearly define the outflow path of the reservoir nor the possible hydrological connection between the main resource area and the northern chloride springs in Sampuraga area, where the main outflow was previously postulated. The vague hot lateral feature in this sector may denote possible flow path of hot fluids but apparently originating from a different source.

The Model has also shown that the Roburan sector - where wells SME-201 and SME-202 were drilled – is characterized by relatively cold block at the middle of the concession. This area is shown in the model as a possible cold barrier between Sorik Marapi-Sibanggor upflow and Sampuraga chloride hot springs.

CONCLUSIONS

1. The challenges encountered during the modeling processes is the scarcity or even absence of data in some areas. However, the possibility of improving the result model is encouraging, especially when new subsurface data becomes available.
2. 3D subsurface model for the geothermal system was built sequentially from structural model, lithology model, resistivity model and temperature model. Since they are built in the same 3D grid, all of the results should be compatible with each other.
3. This study has shown that, with ample data availability, it is possible to visualize a 3D representation of the geothermal reservoir with reasonable accuracy. This model can be useful for resource assessment, development drilling strategy and future reservoir management.

ACKNOWLEDGEMENTS

The authors would like to thank the managements of KS Orka, PT SMGP and Schlumberger for allowing us to use the data and software in the preparation of this manuscript.

REFERENCES

Akar, S., Atalay, O., Kuyumcul, C., Solarog'lul, U.Z.D., Colpan, B., Arzuman, S., 2011. 3D Subsurface

Modeling of Gümüs¸köy Geothermal Area, Aydın, Turkey. *GRC Transactions*, Vol. 35.

Blanco, D.F., Philippon, M., Hagke, C.V., 2015. Structure and Kinematics of the Sumatran Fault System in North Sumatra (Indonesia). *Tectonophysics*. pp 1-12.

Cattin, R., Chamot-Rooke, N., Pubellier, M., Rabaute, A., Delescluse, M., Vigny, C., Fleitout, L., Dubernet, P., 2009. Stress change and effective friction coefficient along the Sumatra-Andaman-Sagaing fault system after 26 December 2004 (Mw = 9.2) and the 28 March 2005 (Mw = 8.7) earthquakes. *Geochemistry, Geophysics, Geosystems* Vol. 10, Q03011.

Filtech Energy Drilling Company, 2017, Sorik Marapi Geothermal Power Plant ("PLTP Sorik Marapi") 240 MW, Notice of Resources Confirmation, Unpublished Technical Report.

Hamilton, W., 1979. Tectonics of Indonesia Region. *US Geological Survey Professional Paper* 1078. pp. 18-38

Hochstein, M.P., Sudarman, S., 1993. Geothermal resources of Sumatra. *Geothermics Vol. 22*, pp 181–200.

Muraoka, H., Takashi, M., Sundhoro, H., Dwipa, S., Soeda, Y., Momita, M., Shimada, K., 2010. Geothermal systems constrained by the Sumatra Fault and its pull-apart basins in Sumatra, Western Indonesia. In: *Proceedings World Geothermal Congress* – Bali, Indonesia, pp. 1–9.

Petrel*, 2010, Schlumberger Information Solution, Petrel Software Online.

HelpSieh, K., Natawidjaja D., 2000. Neotectonics of Sumatra fault, Indonesia. *Journal of Geophysical Research* Vol. 105, pp. 1-30.

Weller, O., Lange D., Tilmann F., Natawidjaja D., Rietbrock A., Collings R., and Gregory L., 2011. The Structure of the Sumatran Fault revealed by local seismicity. *Geophysical Research Letters*, Vol. 39, pp. 1-7

HYDROTHERMAL ALTERATION CHARACTERIZATION OF GEOTHERMAL FIELDS IN INDONESIA BY ROCK PETROLOGY AND MODELLING

Fiorenza Deon[1], Caroline Lievens[2], Auke Barnhoorn[1], Chiel Welink[2], Tulus Imaro[1], Riskiray Ryannugroho[3], Ehsan Reyhanitash[5], David Bruhn[1,4], Freek van der Meer[2], Rizki Hutami[3], Besteba Sibarani[3], Christoph Hecker[2], Oona Appelt[4], Franziska Wilke[4], Yunus Daud[6] and Tia den Hartog[2]

[1]Delft University of Technology, Faculty of Geosciences and Engineering, Delft, the Netherlands
[2]University of Twente Faculty of Geo-Information Science and Earth Observation, Enschede, the Netherlands
[3]Bandung Institute of Technology ITB, Bandung Indonesia
[4]Helmholtz Centre Potsdam, German Centre for Geosciences, Potsdam, Germany
[5]University of Twente Faculty of Science and Technology, Enschede, the Netherlands
[6]University of Indonesia (UI), Jakarta, Indonesia

e-mail: F.Deon@tudelft.nl

ABSTRACT

Indonesia with its large, but partially unexplored geothermal potential is one of the most interesting and suitable places in the world to conduct geothermal exploration research.

This study focuses on geothermal exploration based on fluid-rock geochemistry/geomechanics and aims to compile an overview on geochemical data-rock properties from important geothermal fields in Indonesia. The research carried out in the field and in the laboratory is performed in the framework of the GEOCAP cooperation (Geothermal Capacity Building program Indonesia- the Netherlands).

The application of petrology and geochemistry accounts to a better understanding of areas where operating power plants exist but also helps in the initial exploration stage of green areas. Because of their relevance and geological setting geothermal fields in Java (Wayang Windu, Tanguban Perahu) have been visited so far. Mount Salak, Gunung Slamet (Java) and Flores surveys are planned in the near future. Operators, universities and governmental agencies will benefit from this approach as it will be applied also to new green-field terrains.

By comparing the characteristics of the fluids, the alteration petrology and the rock geochemistry we also aim to compile an overview of the geochemistry of several geothermal fields in Indonesia. The gathering of this information is the base for the geomechanical experiments on-going at TUD.

At the same time the rock petrology and fluid geochemistry will be used as input data to model the reservoir fluid composition along with T-P parameters with the geochemical workbench PHREEQC. The field and laboratory data are mandatory for both the implementation and validation of the model results. If successful, this approach can be applied in many geothermal fields characterized by steep terrain and tropical vegetation, which hampers the classical seismic-geophysical exploration methods.

Keywords: geothermal exploration, capacity building, fluid chemistry and rock petrology

INTRODUCTION

In a conventional approach, several methods need to be adopted and integrated to understand the geochemical and geophysical signatures of active geothermal systems (e.g., Rybach and Muffler 1981). These methods also apply for green-field studies and include: (a) geochemical investigations (e.g., using chemical geo-thermometers to infer the temperature of the geothermal reservoir and measurements of gas isotopes, such as $^{3}He/^{4}He$, to constrain the origin (mantle or crust) of fluids; (b) drilling of exploration wells; (c) gravity measurements to map any negative anomaly associated with the steam fraction in high-porosity reservoir rocks or to locate zones of lowered density provoked by thermal expansion in magmatic bodies; (d) application of electrical methods such as resistivity to search for zones of higher-salinity fluids; (e) use of seismic methods for the determination of shallow intrusions and their vertical extension.

Young volcanic zones along convergent plate margins are prime targets for the exploration of geothermal-energy sources as active magma chambers have an intrinsically geothermal potential (Bogie et al. 2005). Heath transfer in those areas is dominated by circulating fluids and, in the case of two-phase systems, also by steam. Therefore, surface manifestations like hot springs and steam vents are indicators for geothermal activity. Prior to any geophysical surveying of geothermal systems, a field-based geological and geochemical reconnaissance is required to develop a conceptual model of a geothermal field. The exploration phase predating drilling of the first well is commonly termed Greenfield exploration, referring to the juvenile non-exploited condition of a geothermal reservoir (Hochstein, 1988). However, superficial geothermal manifestations are not manifested in all volcanic fields. Geological formations serving as barriers or seals for fluids may prevent discharge of up-flowing waters.

Java, i.e., is geologically associated with the magmatic arc of the Sunda subduction zone (Simkin and Siebert 1994). Here, geothermal waters were subject of exploration and utilization over several decades (Hochstein et al., 2000; Hochstein and Sundarman 2008). However, the efforts to explore and exploit geothermal prospects changed over the years and also with respect to their location along the island chain. For example, activities for exploitation of

geothermal energy centered on vapor-dominated system in western and central Java (in Salak or Cisolok) at the end of the 1970ies, where the infrastructure was sufficiently developed. Efforts increased in the mid 1990ies, when the Indonesian government encouraged foreign investors to take part in the exploration. Recently, the main activities are focused on existing power plants at Kamojang**,** Wyang Windu and Djeng.

Recent published works such as Deon et al. (2015) and Brehme et al. (2014, 2015, 2016) evidences the important of water and rock geochemistry when exploring tropical fields. Analyses on water and rocks deliver valuable information. An approach applied to a wider range of fields is still missing. By comparing the characteristic of the fluids, the alteration petrology and the rock we aim to contribute to compile an overview of the geochemistry in the important geothermal fields in Indonesia and to characterize the rocks for the geomechanical experiments on-going and planed at TUD. The goal is not only to obtain scientific results but also to deliver a reliable method to the governmental agencies, companies and academics.

Deon et al. (2016) describes the fluid-rock characteristics of Tanguban Perahu and Wayang Windu. (see Figure 1). In this paper we present a wider application method to detect hydrothermal alteration specifically looking at clays. A combination of X-ray Diffraction (XRD) technique accompanied by Electronmicroprobe analyzer (EMPA) has been chosed to determine if and in which extend the rocks are suitable for geomechaical experiments and further acizing tests. A first set of experiments involving temperature test are presented in Imaro et al (2017).

METHODS

Rock samples

The XRD analyses have been performed on the crushed and sieved samples using a Bruker D2 Phaser XRD installed in the laboratories of ITC, University of Twente. The rock powder has been placed on a XRD sample holder (amount approximately 1 gram) and analyzed. The patterns have been acquired from 6˚ to 80˚ (degrees 2θ). The interpretation has been carried out semi-quantitatively by using the program DIFFRAC.EVA (Brucker).

EMPA images have been collected with a JEOL JXA 8230 electron microprobe (15 kV accelerating voltage) at the Electron Microprobe Laboratory, Department of Inorganic and Isotope Geochemistry at the Helmholtz Centre Potsdam – German Research Centre for Geosciences (GFZ) in Potsdam, Germany. The measuring conditions are described in have described in Deon et al. (2016).

Water probes have been sampled in three locations as shown in Figure 2: Kawah Putih (acidic volcanic crater lake), Cimanggu (hot spring) and Cibolang (hot river). The water samples have been collected according to the procedure of Giggenbach & Gougel (1989) recommended for the quantitative analysis of the major ions. Water samples were filtrated using a 0.45 µm membrane filter to prevent the interaction of the fluid with suspended particles and algal growth. For the analysis of anions, water samples were untreated, while for cation analysis planed soon, the water samples will acidified with HNO_3. The on-site measurements covered pH, temperature (T) and carbonate content. The elements in the water samples have been measured at the University of Twente, Netherlands.

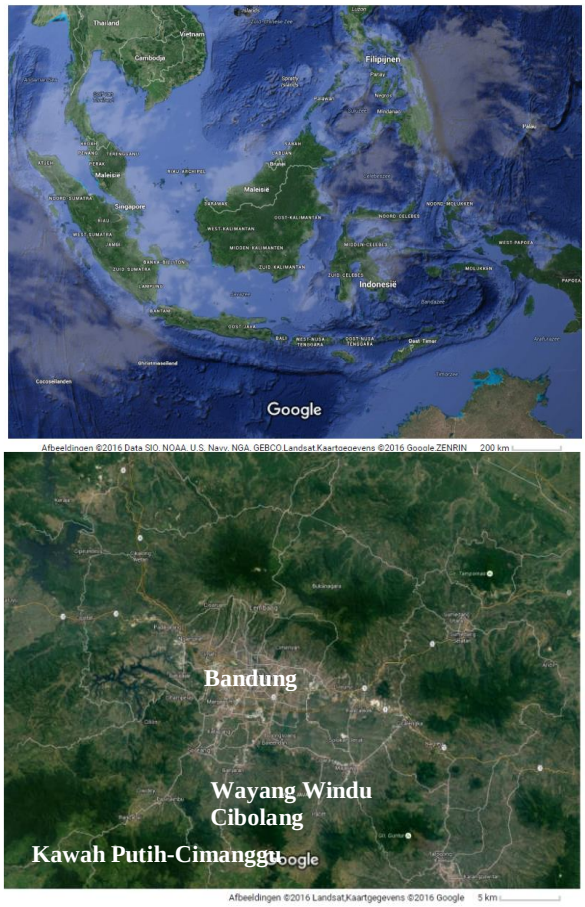

Figure 1: Map of Indonesia with the highlighted research areas. Detailed map of the fieldwork area in West Java in the proximity of Bandung. (Source Google Earth)

Figure 2: a) acidic volcanic lake crater Kawah Putih

Figure 2: b) hot spring Cimanggu

Figure 2: c) river in Cibolang.

RESULTS

Rocks

The XRD semi-quantitative (Figure 3a and 3b) interpretation results of the analyzed rocks are listed in table 1. The samples from Tanguban Perahu (basalts) mostly contain plagioclase and feldspar (B2). BB, BC show small amounts of goethite whereas BD ilmenite. The pumice XRD pattern indicates a high amount of tridymite. Nearly 90 wt. % of quartz and 9 wt. % of sulfur form CB1. KB1 (Kawah Burung) shows almost only sulfur and KW1 has a smaller amount of sulfur (60 wt.%) along with 30 wt. % of trydimyte and pyroxene (7.2 wt.%). In Table 1 the crystallinity (%) has been calculated for each compound. The mineral structures adopted with the EVA program represent an ideal match with the measured patterns and are chosen on the base of the rock type analyzed.

The analyses performed at the EMPA show plagioclase crystals (Figure 4a and b) and quartz. The element distribution mapping refers to the Al concentration on a plagioclase crystal (see Figure 5a and b). The brighter the color appears the higher the element concentration occurs to be in the spot. The samples B2, BB, BC and BD are classified as basalts; CB1 and KW1 as a silica sinter (based on the quartz amount), KB1 sulfur and PM as a pumice. Because of the concentration below 1 wt.% the clay fraction could not be identified with XRD but has been observed at the EMPA scattered in the basalts. Kaolinite $AlSi_2O_5(OH)_4$ constitutes approximately 1 wt. % of the phases amount of the analyzed samples.

Table 1: Mineral composition of the rock samples and the calculated (semi-quantitatively) mineral fractions.

Sample	Cristallinity percentage	Compound name	Compound formula	Weight percent
B2	51,1	Oligoclase	$(Ca,Na)(Al,Si)_4O_8$	73,7
		Sanidine	$K(AlSi_3O_8)$	26,3
BB	64,1	Bytownite	$(Ca,Na)(Al,Si)_4O_8$	69,4
		Microcline	$K(AlSi_3O_8)$	29,2
		Goethite	$FeHO_2$	1,4
BC	62,0	Bytownite	$(Ca,Na)(Al,Si)_4O_8$	89,8
		Sulfur	S_8	8,8
		Goethite	$FeHO_2$	1,4
BD	80,3	Bytownite	$(Ca,Na)(Al,Si)_4O_8$	59,7
		Anorthoclase	$Na,K(AlSi_3O_8)$	36,4
		Ilmenite	$FeTiO_3$	3,9
CB1	85,7	Quartz	SiO_2	88,7
		Sulfur	S_8	9,9
		Anatase	TiO_2	0,8
		Cristobalite	SiO_2	0,6
KB1	85,4	Sulfur	S_8	94,3
		Cristobalite	SiO_2	5,7
KW1	52,2	Sulfur	S_8	60,4
		Tridimyte	SiO_2	32,4
		Diopside	$MgCaSi_2O_6$	7,2
PM	68,6	Tridimyte	SiO_2	65,6
		Biachellaite	$(Na,Ca,K)_8(Si_6Al_6O_{24})(SO_4)_2(OH)_2 \bullet H_2O$	26,2
		Anatase	TiO_2	8,2

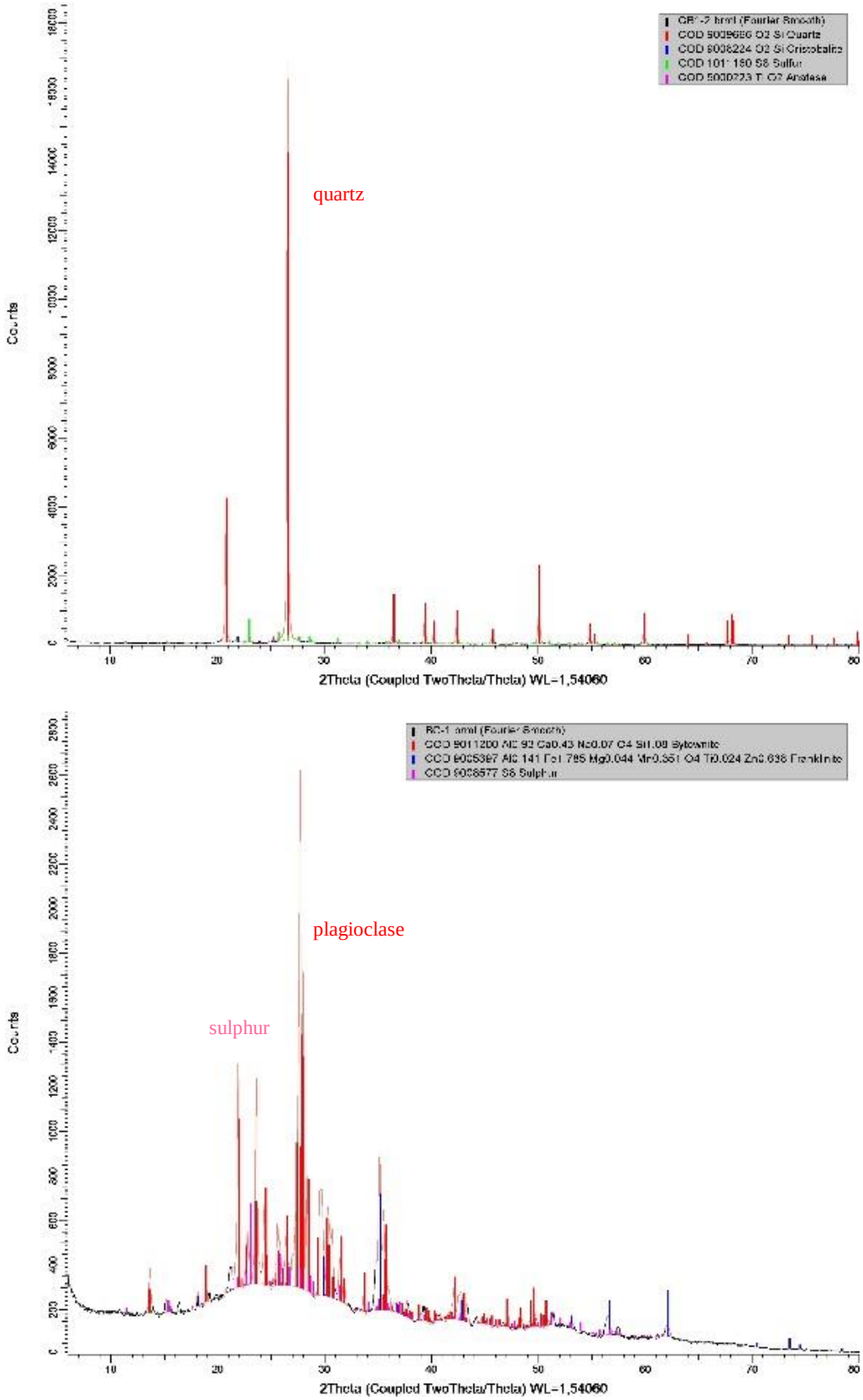

Figure 3: XRD patterns with the peak match and identification. a) sample CB1 where the intense high red peaks have been assigned to quartz (top figure). b) BC 1 where the most intense peaks belong to plagioclase (bottom figure). The bumps indicate the amorphous fraction.

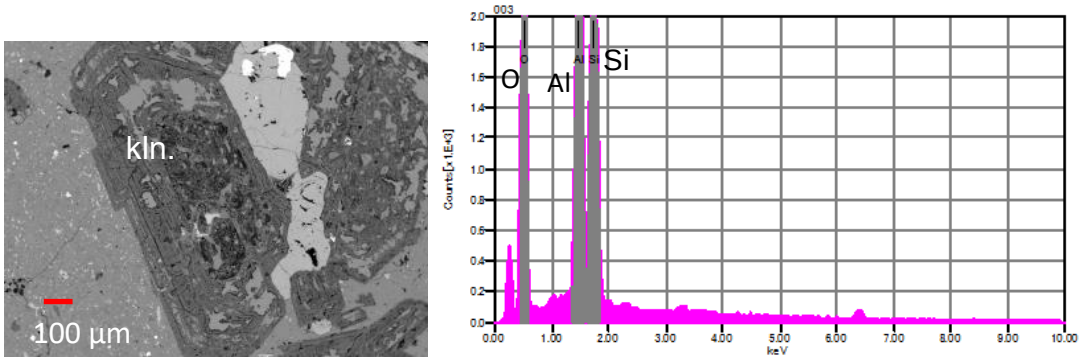

*Figure 4: a) EMP image aquired on a plagioclase crystal where **the alteration patterns** are clearly visible in the plagioclase grain (left). b) EBS sprectum aquired on the alteration rims showing **kaolinite** occurrence (right).*

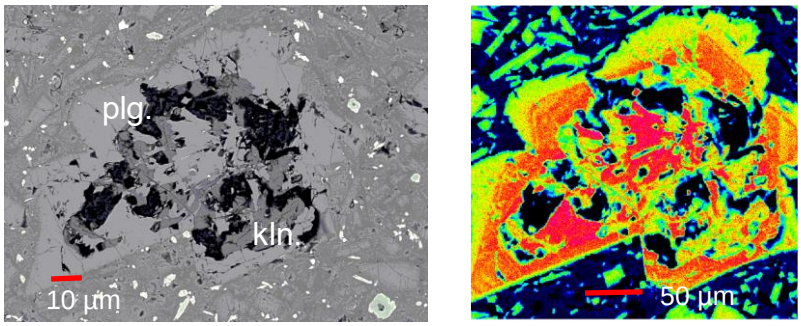

Figure 5: a) BSE image of a plagioclase crystal (left).
b) related Al distribution mapping on the altered plagioclase crystal (right).

Fluids

All the water samples have failed the bicarbonate test in the field due to the weather conditions (heavy rain) and / or absence of bicarbonate. The major anions are listed in Table 2. The temperature measured on-site ranges from 29.3 ˚C (KP1 Fig. 2a) to 90.3 ˚ C (CB1 Fig 2c). The pH of KP1 0.8 is more acidic than the other two springs CB1 (2.5) and CM1 (5.1). High sulfate concentration characterize both KP1 and CB1. A considerable amount of chlorine (˜ 600 ppm) has been detected on KP1 whereas the other two samples show no chlorine (CB1) and a smaller amount (˜40 ppm). Major cations have not been measured yet because the springs will be monitored and re- sampled in summer/fall 2017 during the dry season.

Table 2: Field parameter and water chemistry.

Sample	T(˚C)	pH	HCO_3^- (ppm)	SO_4^{2-} (ppm)	Cl^- (ppm)
KP1	29.3	0.8	n.d.	310	595
CB1	90.3	2.5	n.d.	474	-
CM1	64.6	5.1	n.d.	40	44

DISCUSSION

Rocks

The XRD patterns in Figure 3a and b show the peak interpretation of the samples CB1 (3a) and BC (3b). The two diffractograms have been selected based on the mineralogy of the rocks and the relevance applied to the Indonesian geothermal fields. CB1 is a typical silica sinter which can be often found in several geothermal fields such as Wayang Windu (this study) but also in other locations with hydrothermally altered outcrops. Intense and sharp quartz peaks can be observed in Figure 3a. Their intensity corresponds to the highest concentration (quartz) as shown in Table 1. Generally when the peak appears so sharp and high one can rely on the semi-quantitative interpretation. An absolute quantification of the mineral phases in the probes investigated in this paper could not be performed because of the amorphous fraction characterizing them. Manifestations such as silica sinters are often found near volcanic craters or high temperature hot springs (Deon et al. 2016). BC, basalt from the Tangkuban Perhau area, is characterized by a high amount of plagioclase in our XRD interpretation identified as bytownite. The bumps, visible in the pattern, are caused by the amorphous fraction detected in the samples as the crystallinity % (see Table 1) have been estimated to be 62 %. Basalts with this composition not only characterize many geothermal areas in Java but are often classified as the reservoir rock. It is therefore very important to gather as many details as possible on the samples (or cores whenever available) in order to determine the rock properties. The response to the temperature of these rocks and the variation of properties such as permeability-porosity is described in Imaro et al. (2017). Geomechanical experiments with acidizing are planned at TUD with the goal to test these rock types in order to improve the production in several active fields in Indonesia with already operating plants.

The clay fraction plays a very important role in the rock's response to temperature and stress but also on properties such as permeability, porosity and swelling. The amount could not be identified with the XRD due to the extremely limited amount lying below the detection limit (˜1 wt.%). This is why we have conducted detailed image acquiring and chemical analyses at the EMPA.

Selected well-formed plagioclase crystals have been chosen for the images acquirement at the EMPA as shown in Figure 4. Clear alteration rims spreading towards the inner part of the grain can be observed on the grain (Figure 4a). The chemical analyses (Figure 4b) indicates kaolinite as alteration phase. This rock have been collected in the Wayang Windu crater and therefore we relate the kaolinite occurrence to the hydrothermal alteration on going in the crater caused by high temperature steam and bubbling hot springs (see Deon et al. 2016).

A more detailed and precise technique to map the alteration has been applied to a second crystal (Figure 5). The grain has been selected and chemically analysed to confirm the alteration. Al has been chosen as element for the mapping because its different occurrence (concentration) in plagioclase and kaolinite. Thus, the identification of clay is supported by the Al different concentration in the grain. By looking at the different intensity of the colours related to Al in the image one can distinguish between the areas with high Al concentration (yellow) and lower (green). The regions with smaller Al content are those where kaolinite can be detected as alteration of the plagioclase shown in the Figure 5a.

Commonly the clay fraction is determined with XRD on a separated portion of the sample. This technique is reliable but very time–consuming and bounded to the available amount of clay. Very small fractions (below 1 wt. %) can hardly be identified and quantified. The EMPA, if available, allows a "relatively" quick and reliable determination of the clay type (based on the chemistry) directly on the thin section.

Fluids

The sampled springs have been analyzed only in terms of two major anions (sulfate and chlorine). The results have been plotted in the Giggenbach ternary diagram in Figure 6. The concentration of the major anion allows to classify the water samples in terms of vicinity to reservoir. However, without cation concentration it is not possible to estimate the reservoir temperature and apply the geothermometers. More sampling and monitoring are planed on those springs. Sample KP1 plots in the mature water field whereas CB1 in the steam heated water. The high concentration of Cl (˜600 ppm) in KP1 is likely to be expected because of the very acidic pH of the volcanic crater lake Kawah Putih. The samples CM1 is most likely chracterized by a high concentration of bicarbonate because of the very low measured concentration of sulfate and chlorine. More sampling and analyses are needed in order to better investigate this springs and their geochemistry.

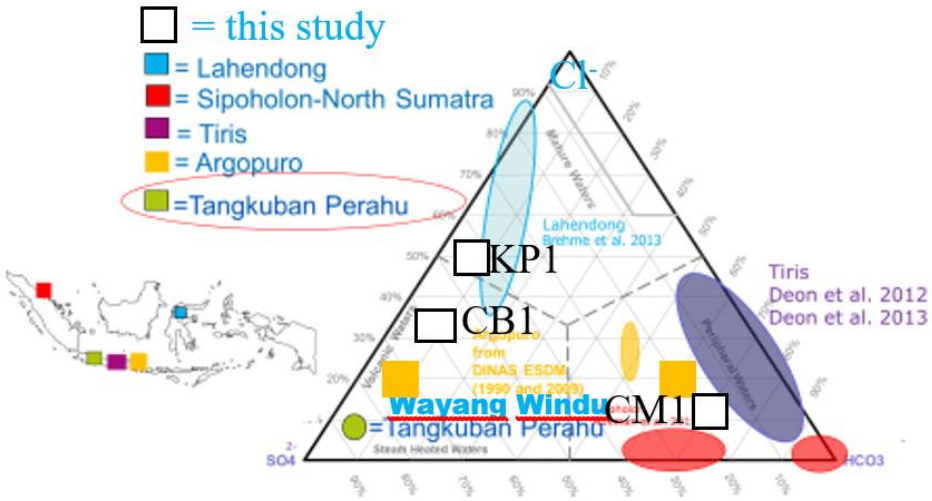

Figure 6: Ternary diagram of the major anions Cl^-, SO_4^{2-}, HCO_3^-. Data from the literature show significant differences in the geochemistry from different fields and are included for comparison.

CONCLUSION AND OUTLOOK

The additional data presented in the work complete those included in Deon et al. (2016). We aim to apply this approach to other fields in Java: Mount Salak and Mount Slamet. By sampling water and rocks additional information will be gathered on theses areas. The data will be implemented in the PHREEQC geochemical workbench in order to simulate the reservoir fluid composition. The novely in this study is the binary appproach which is followed: not only we are going to test PHREEQC with data from green fields but also with data from areas where plants are already operating. This will allow to verify whether the reservoir temperatures-composition estimation for the areas under exploration is correct by validating the results on already explored and known areas.

This paper is the follow up of the paper presented at the IGCE 2016. More steps and field campaigns are planed with our Indonesian partners along with capacity building activities within the Dutch-Indonesian cooperation GEOCAP (Geothermal Capacity Building Program the Netherlands-Indonesia).

ACKNOWLEDGEMENTS

The Dutch Ministry for foreign affairs is thanked for funding this research project.

Our gratitude goes to the Indonesian GEOCAP project coordinator Sanusi Satar.

The authors wish to thank Star Energy Wayang Windu Geothermal for their involvement in the study and permission to publish this paper.

REFERENCES

Bogie, I., Lawless, J.V., Rychagov, S., Belousov, V., 2005. Magmatic – related hydrothermal systems: classification of the types of geothermal systems and their ore mineralization. In: Proceedings of Geoconference in Russia, Kuril 2005.

Brehme, M., Moeck, I., Kamah, Y., Zimmermann, G., Sauter, M., 2014. A hydrotectonic model of a geothermal reservoir – A study in Lahendong, Indonesia. Geothermics 51, 228–239. doi:10.1016/j.geothermics.2014.01.010

Brehme, M., Wiegand, B., Deon, F., Blöcher, G., Cacace, M., Kissling, W., Haase, C., Erbas, K., Kamah, Y., Regenspurg, S., Moeck, I., Zimmermann, G., Sauter, M. 2015. Structurally Controlled Fluid Flow in a High-Enthalpy Geothermal System – Case Study Lahendong, Sulawesi (Indonesia) - Proceedings, World Geothermal Congress 2015 (Melbourne, Australia 2015).

Brehme, M., Deon, F., Haase, C., Wiegand, B., Kamah, Y., Sauter, M., Regenspurg, S. 2016. Fault controlled geochemical properties in Lahendong geothermal reservoir Indonesia. - Grundwasser, 21, 1, p. 29-41.

Deon, F., Förster H.-J., Brehme, M., Wiegand, B., Scheytt, T., Moeck, I., Jaya, M.S., Putriatni, D.J, 2015 Geochemical/hydrochemical evaluation of the geothermal potential of the Lamongan volcanic field (Eastern Java, Indonesia). Geothermal Energy, 3-20, DOI 10.1186/s40517-015-0040-6.

Deon, F., Barnhoorn, A., Lievens, C., Saptadij, N., Sutopo, van der Meer, F.D., den Hartog, T., Brehme, M., Bruhn, D., de Jong, M., Ryannugroho, R., Hutami, R., Sule, R., Hecker, C.A. and Bonté, D. 2016 Exploration and comparison of geothermal areas in Indonesia by fluid-rock geochemistry. In: Proceedings of the 4th Indonesia international geothermal convention & exhibition 2016, 10-12 August 2016, Jakarta, Indonesia

Giggenbach, W.F., Gougel, R.L., 1989. Collection and analysis of geothermal and volcanic waters and gas discharges. DSIR Report CD 2401, 4th edition, Pertone, New Zealand.

Hochstein, M.P., 1988. Assessment and Modeling of Geothermal Reservoirs (Small Utilizations Schemes). Geothermics, 17, 15-49.

Hochstein, M.P., Browne, P.R.L. 2000. Surface manifestations of geothermal systems with volcanic heat sources, In: H. Sigurdsson (Ed.), Encyclopedia of Volcanoes, Academic Press, 835–855.

Hochstein, M.P, Sudarman, S., 2008. History of geothermal exploration in Indonesia from 1970 to 2000. Geothermics 37, 220-266.

Imaro, T., Deon, F., Bakker, R., and Barnhoorn, A. 2017 Thermal Fracturing of Volcanic Rocks for Geothermal Field Applications. 19th EGU General Assembly Vienna. Austria.

Nukman, M., Moeck I., 2013. Structural controls on a geothermal system in the Tarutung Basin, north central Sumatra. Journal of Asian Earth Sciences 74:86-96.

Rybach, L., and Muffler, L.J.P., 1981. Geothermal systems: Principles and Case Histories. Joun Wiley & Sons New York.

Simkin, T., and Siebert, L., 1994. Volcanoes of the World (2nd ed), Tucson: Geoscience Press, 349 pp.

 ISBN 978-602-52132-0-5

MARGINAL RECHARGE IDENTIFICATION BASED ON TRITIUM IN DARAJAT AND SALAK GEOTHERMAL FIELDS

Hanna M. Paramitasari, Yunia Syaffitri, Christovik H. Simatupang

Star Energy Geothermal Salak and Darajat II, Ltd.
Sentral Senayan II, 26th Floor, Jl. Asia Afrika No.8, Jakarta 10270, Indonesia

e-mail: HParamitasari@starenergy.co.id, YSCL@starenergy.co.id, christovik@starenergy.co.id

ABSTRACT

Marginal recharge (MR) presents in the peripheral of a geothermal field to support the sustainability of the natural state of the system. There are several types of MR that determined by their sources, namely groundwater, steam-heated water, old condensate, and etc. The influx rate of these liquids into reservoir can be accelerated as the mass extraction is begun. The presence of these liquids near the wellbore has been identified to be responsible on several bad impacts at the production wells, such as decrease in temperature, deposition of scale minerals, and decline in production.

Since these liquids are very distinct in chemistry and temperature as compared with reservoir liquid, thus geochemistry surveillance program is designed to monitor the penetration of these liquids into reservoir. In Darajat and Salak geothermal fields, tritium (^3H) has been collected to investigate the type and distribution of MR. The result of the study in both fields shows that each field demonstrate its own characteristic of MR.

Keywords: Recharge, Tritium, Darajat, Salak

INTRODUCTION

Darajat and Salak geothermal fields are located within a mountain range of inactive andesitic volcanoes. They lie along the main trend of Sunda Volcanic Arc which extends from Sumatra to Flores (Hamilton, 1979; Hutchinson, 1989) (Figure 1). Both fields have been operated commercially since 1994. Darajat geothermal field with vapor-dominated system has been generating 271 MW from 3 power plants. Meanwhile, Salak geothermal field with liquid-dominated system has been producing 377 MW from 6 power plants. Continuous mass extraction from both fields consequently invites "foreign" liquids to the reservoir due to pressure drawdown.

There are four types of liquid that have been commonly identified in geothermal systems, namely reservoir liquid, brine injectate (only in two-phase geothermal system), condensate injectate, and marginal recharge (MR). There are several distinguishable signatures that imprinted by the aforementioned liquid types, such as temperature and fluid chemistry. In term of temperature, brine injectate, condensate injectate, and MR have relatively lower temperature than reservoir liquid. Meanwhile, in the case of fluid chemistry, they have distinct concentration in chloride (Cl), bicarbonate (HCO_3), sulfate (SO_4), silica (SiO_2), boron (B), magnesium (Mg), stable isotopes ($\delta\ ^{18}O$ and $\delta\ ^{2}H$), tritium (^3H), and pH.

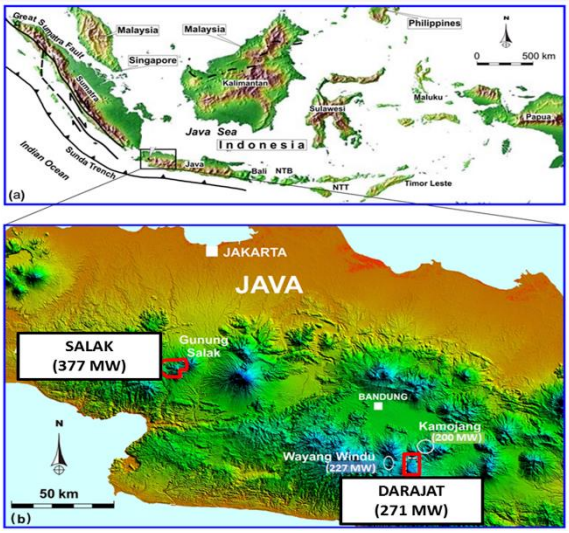

Figure 1: Location map shows Darajat and Salak contract area (red polygons).

Simatupang and Molling (2010) have determined four types of MR based on its distinctive chemistry, such as groundwater, old condensate, acid sulfate-magmatic driven, and mixed outflow. Groundwater which is usually found at the shallowest part of the geothermal system and originated from rain water and/or stream water is identified by its elevated Mg content. The precipitation of this liquid into depth increases its exposure to the heat and/or ascended steam from the geothermal fluids. As the result, increase in HCO_3, SO_4, B concentration and decrease in pH are expected. The SiO_2 concentration is the parameter that used to recognize the water-rock interaction. The product of this process is known as steam heated water. If this water is preserved from this natural process, then it is classified as old condensate. The acid sulfate-magmatic driven is another type of MR that originated from magmatic source. Unlike the steam heated water which is also called acid sulfate, this liquid has relatively heavier isotopes and consists of magmatic chemical species. The last MR type is mixed outflow liquid. It is the mixture of the outflow brine and groundwater. This liquid is characterized by relatively lower Cl concentration.

The presence of this cooler fluid near the wellbore at Darajat and Salak geothermal fields has been observed to be responsible on several detrimental impacts, such as decrease in temperature, deposition of scale minerals, and decline in production at production wells. In fluid chemistry observation, Down Hole Sampling (DHS) and surface sampling are the techniques that used to collect the fluid sample. Conversely, Pressure-Temperature (PT) and Pressure-Temperature-Spinner (PTS) are utilized to identify the appearance of this "foreign" liquid from

temperature data. Since MR has been historically observed to give more severe impact at both fields, thus MR becomes the main attention in geochemistry surveillance. The identification of MR type helps determining the "fit-for-purpose" surveillance plan to locate the liquid source and monitor the penetration of this liquid into reservoir. The ultimate objective is to prevent the negative impact and prepare better well planning and targeting for future production well.

MR at Salak geothermal field typically has low to medium Cl, high Mg, and high SO_4. Meanwhile, the MR at Darajat geothermal field has elevated N_2 and A_r even during the absence of drilling activities (Simatupang and Molling, 2010). The ^3H is observed as another chemical signature that helps to distinguish the young groundwater with the other MR liquid types. This MR becomes a concern due to its very low temperature and dissolved oxygen content. The ~20 years geochemistry surveillance of Darajat and Salak fields has been showing the use of ^3H in MR monitoring.

The ^3H, a radioactive isotope, exists in the atmosphere in two forms, natural and anthropogenic (Bishop et al., 1961). This isotope is naturally produced in the stratosphere (the upper layers of the atmosphere) by cosmic radiation on nitrogen (^{14}N):

$$^{14}N + n \rightarrow {}^3H + {}^{12}C$$
$$^{14}N + n \rightarrow 3{}^4He + {}^3H$$

The production rate of ^3H in the whole atmosphere has been estimated at 0.25 atoms/cm^2/s (Fontes, 1983). The ^3H that enters hydrologic cycle as "tritiated" water is rapidly oxidized. The precipitated concentration arising from this source varies between 5 to 20 TU (TU=Tritium Units; 1 TU corresponds to 1 ^3H atom per 10^{18} ^1H atoms) depending on the geographic locations in the northern hemisphere. It generally increases with increasing latitude (IAEA, 1983).

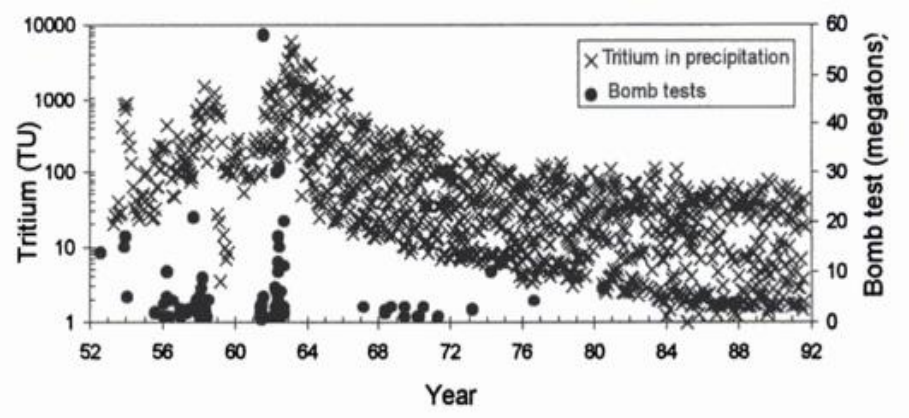

Figure 2: Tritium precipitation from thermonuclear bomb tests since 1952. Tritium data for selected stations in North America and Europe, from the IAEA GNIP database. Bomb test data are summarized from various sources by Rath (1988) and Gonfiantini (1996) in Clark and Fritz (1997).

Atmospheric testing nuclear devices between 1952 and 1980 generated a tremendous quantity of ^3H. It contaminated global precipitation system for over three decades (Figure 2). The bomb test in 1962 created a huge peak which was appeared in ^3H concentration in 1963. This 1963 peak became a marker that was used in many hydrological studies. Concentration of ^3H in precipitation (Figure 2) shows significant decrease to 1-100 TU in 1990's at the northern hemisphere as the responds to its decay. Therefore, the current ^3H concentration in groundwater at Darajat and Salak fields can be simply determined by its decay with the assumption that the initial ^3H input into a groundwater is known (Tritium's half life, $t_{1/2}$ = 12.43 years). The equation can be written as follow (Clark and Fritz, 1997):

$$t = -17.93\, ln \frac{a_t{}^3H}{a_0{}^3H}$$

$a_t{}^3H$ = The remaining measured tritium concentration (expressed TU) in sample after decay over time (t)
$a_0{}^3H$ = The initial tritium (expressed in TU)
t = decay time

The formula above can be used by assuming the 1990's ^3H in the groundwater (after the thermonuclear) at the southern hemisphere (e.g., Indonesia) is similar to the ^3H levels at the northern hemisphere (Figure 2). The current estimated residual ^3H in groundwater at the southern hemisphere after decay is at 0.19-18.77 TU (Table 1). This decay series calculation (Table 1) shows that the natural ^3H can be utilized to trace the young groundwater influx in geothermal system up to the next 20 years if the low ^3H level measurement technique is applied. Clark and Fritz (1997) reported that propane synthesis or ^3He ingrowth techniques allows low-level ^3H content measurement (±0.1 TU).

Table 1: Estimated measured ^3H in groundwater as the result of decay series after 1990's. The estimation of current residual ^3H in groundwater is higlighted in green cells.

$a_o{}^3H$ = The initial tritium concentration in 1990's is 1 TU

Years	0	10	20	30	40	50	60
TU	1	0.57	0.33	0.19	0.11	0.06	0.04

$a_o{}^3H$ = The initial tritium concentration in 1990's is 10 TU

Years	0	10	20	30	40	50	60
TU	10	5.73	3.28	1.88	1.07	0.62	0.35

$a_o{}^3H$ = The initial tritium concentration in 1990's is 100 TU

Years	0	10	20	30	40	50	60
TU	100	57.25	32.78	18.77	10.74	6.15	3.52

METHODOLOGY

The existence of cooler water influx in nearby production wells is usually evidenced by temperature changes, scale deposition, and production decline (Figure 3). In order to identify the characteristics of the cooler water influx, hence further analysis in fluid chemistry is performed (Figure 3). However, this paper only discusses the application of ^{3}H in identifying the young groundwater.

The ^{3}H sampling was firstly conducted at Salak in 1996 and firstly implemented at Darajat in 1999. This activity has been performed by in-house sampling team in non-regular schedule. The sample is collected at selected production wells (steam condensate samples only), main header of injection wells, and surface water. Since the required amount of sample for ^{3}H laboratory analysis is ~1000 ml, thus the ^{3}H sampling at thermal features (i.e., springs) has only been performed at Salak and never been conducted during downhole sampling. Unlike the sampling activity, the laboratory analysis was performed by the 3rd party company. The approximate laboratory error analysis is ±0.09 TU.

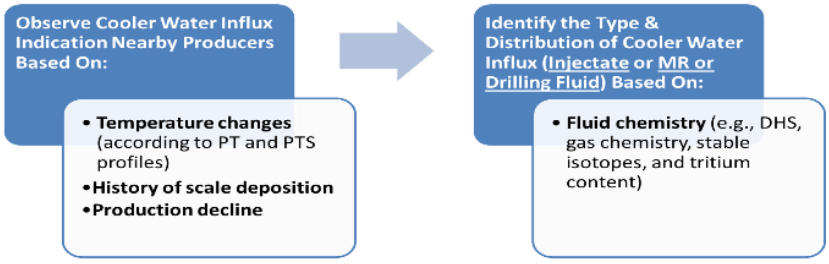

Figure 3: Flowchart to investigate the cooler water influx type and its distribution at Darajat and Salak geothermal fields.

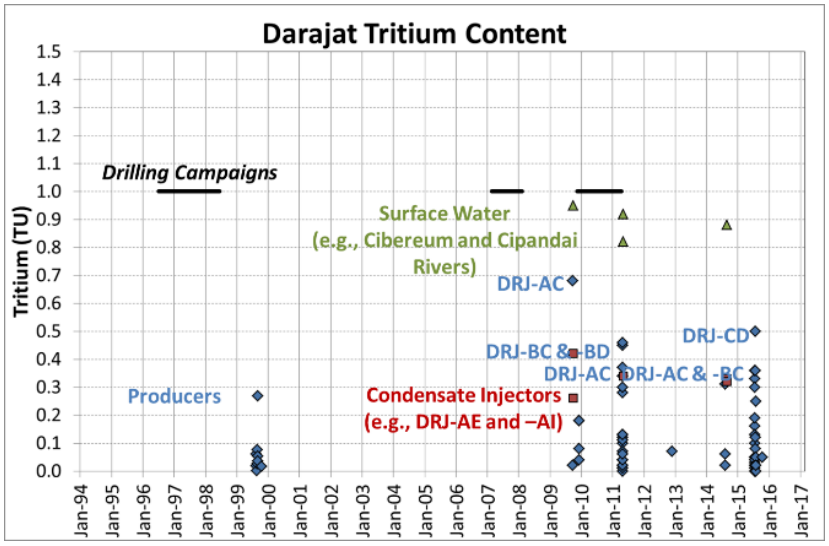

Figure 4: Historical tritium content at producers, condensate injectors, and surface water of Darajat geothermal field.

DISCUSSION

MR seems to enter the system through periphery at both Darajat and Salak geothermal fields as the result of pressure sink due to continuous exploitation (Figure 5 and 9). Tritium monitoring program is designed to measure the detectable tritium-rich liquid and its lateral distribution. Some potential sources of tritiated liquid are condensate injectate (which has been exposed to the atmosphere in the cooling towers) and young groundwater (which can comprise the MR).

Tritium Distribution at Darajat

Historically, ^{3}H content of condensate injectate at Darajat injectors (e.g., DRJ-AE and -AI) is ~0.3 TU; while the tritium content of surface water from the nearby stream is ~0.9 TU. Several producers at Darajat (i.e., DRJ-AC, -CD, -BC, and -BD) have been consistently showing higher ^{3}H content than condensate water (Figure 4). The producers with high ^{3}H content (>0.3 TU) are observed in the southern area of Darajat (Figure 5). However, DRJ-CA that uniquely produces water has low tritium content at 0.02-0.04 TU. This fact led the hypothesis of this phenomenon to the invasion of steam heated water instead of groundwater (Simatupang et al., 2015).

The high tritium distribution (>0.3 TU) at southern Darajat area indicates the presence of groundwater MR. It implies to the degree of temperature impact due to the penetration of this tritiated liquid. It is strongly related with the hypothesis that young groundwater has lower temperature than the older MR (Syaffitri and Molling, 2013). As the consequence, it potentially gives more

severe impact in temperature and steam production of the well.

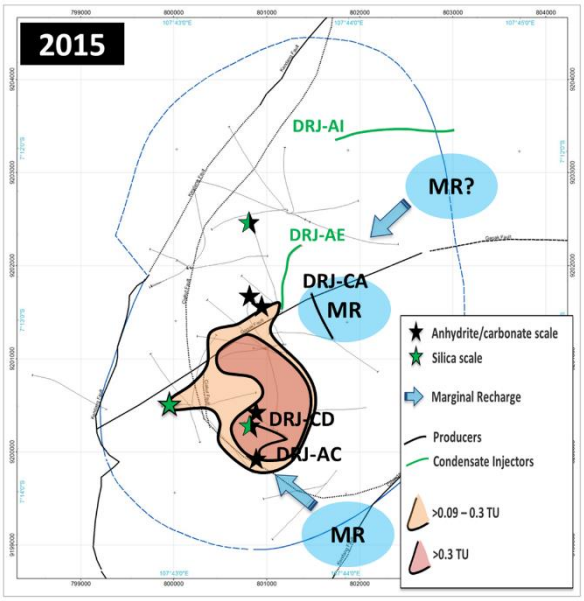

Figure 5: Tritium distribution at Darajat geothermal field based on 2015 tritium sampling colletion (Modified from Syaffitri et al., 2016).

Among all the producers at Darajat field, DRJ-AC showed an anomalous ^{3}H concentration at 0.68 TU in 2009 (Figure 4). Meanwhile, the ^{3}H concentration was only 0.36 TU at DRJ-AC and 0.50 TU at DRJ-CD during the absence of drilling/workover activity in 2015. This 2015 ^{3}H concentration was considerably higher than the ^{3}H concentration from condensate injectate (Figure 4). Therefore, the high ^{3}H content at DRJ-AC in 2009 was suspected to be related with acid stimulation program because this anomalous content cannot be explained by the decay time formula. Quenching with surface water is commonly conducted at Darajat prior to the acid stimulation.

The presence of young groundwater within southern area (Figure 5) appears to be responsible for scale deposition that leads to production decline in the wellbore (e.g., DRJ-AC and -CD). DRJ-AC has been known to have series of scale deposition events. The temperature reversal at 584-932 m ASL as shown by PT profile of this well indicates the location of the entry point of the MR influx (Figure 6).

Flowing Well Head Pressure (FWHP) is also suspected as another factor that contribute to the invasion of this cooler liquid. The intermittent FWHP helps re-deposition of the scale mineral in the wellbore. The increase in FWHP appears to saturate the area around the wellbore and allow nearby MR liquid to move closer to the well. On the other hand, the decrease in FWHP triggers the boiling of MR liquid. These processes eventually result to scale deposition in the wellbore due to increasing superheat (Figure 7).

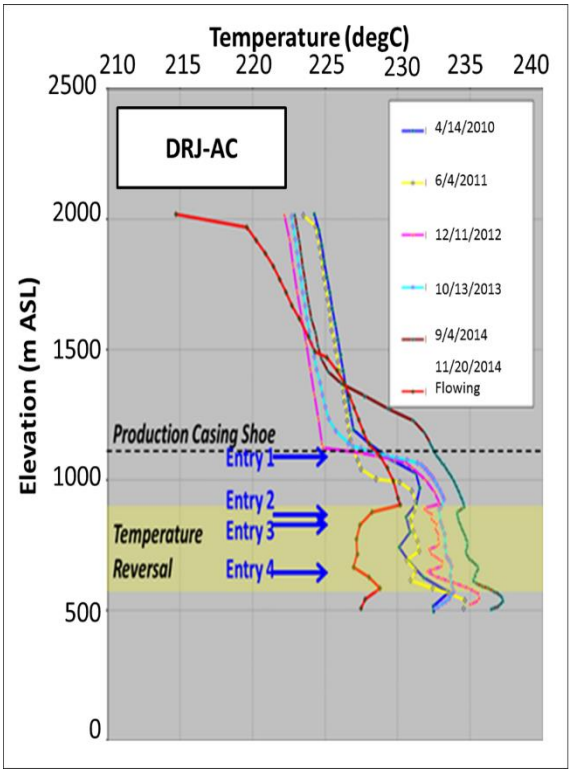

Figure 6: Historical PT profiles of DRJ-AC shows temperature reversal at 584 - 932 m ASL.

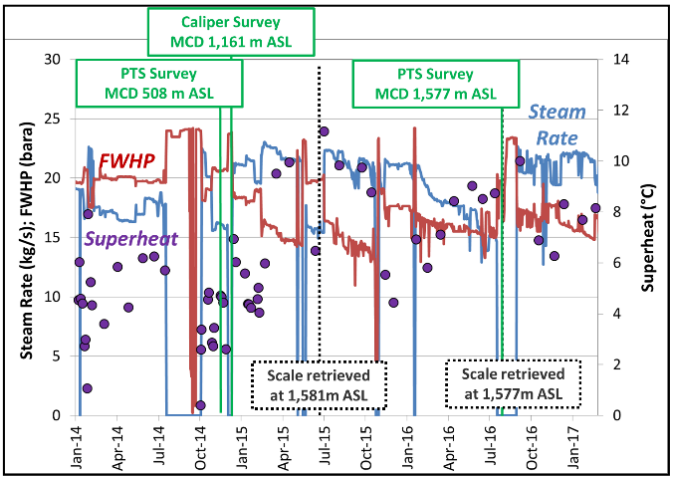

Figure 7: Historical steam rate, FWHP, superheat, and Maximum Clear Depth (MCD) at DRJ-AC during 2014-2017.

Tritium Distribution at Salak

The ^{3}H content of Salak producers is <0.1 TU meanwhile the ^{3}H content of condensate injectors is ~0.2 TU. The lower ^{3}H content in the production wells is either due to the absence of the condensate injectate in produced liquid or insignificant contribution of condensate injectate in produced liquid (Figure 8). The anomalous ~0.6 TU in injected condensate at AWI-AB-3 in 1996 was possibly related with drilling activity. The wellbore is flushed thoroughly with water after drilling completion test. The 1996 drilling campaign is suspected to be responsible for this high tritium content at AWI-AB-3.

During the absence of drilling campaigns, the producers at northeastern wells (e.g., AWI-G and -H) have tritium

content >0.05 TU while the northwestern wells (e.g., AWI-A and -AF) have tritium content <0.02 TU. The tritium distribution at northwestern wells >0.05 TU in 2012 possibly related to drilling activity at AWI G-8 (Figure 9). The highest tritium content (0.09 TU) observed in 2012 at AWI-A-5. AWI-A wells (e.g., AWI-A-5 and -7) have historical of scale deposition due to MR existence that leads to production decline.

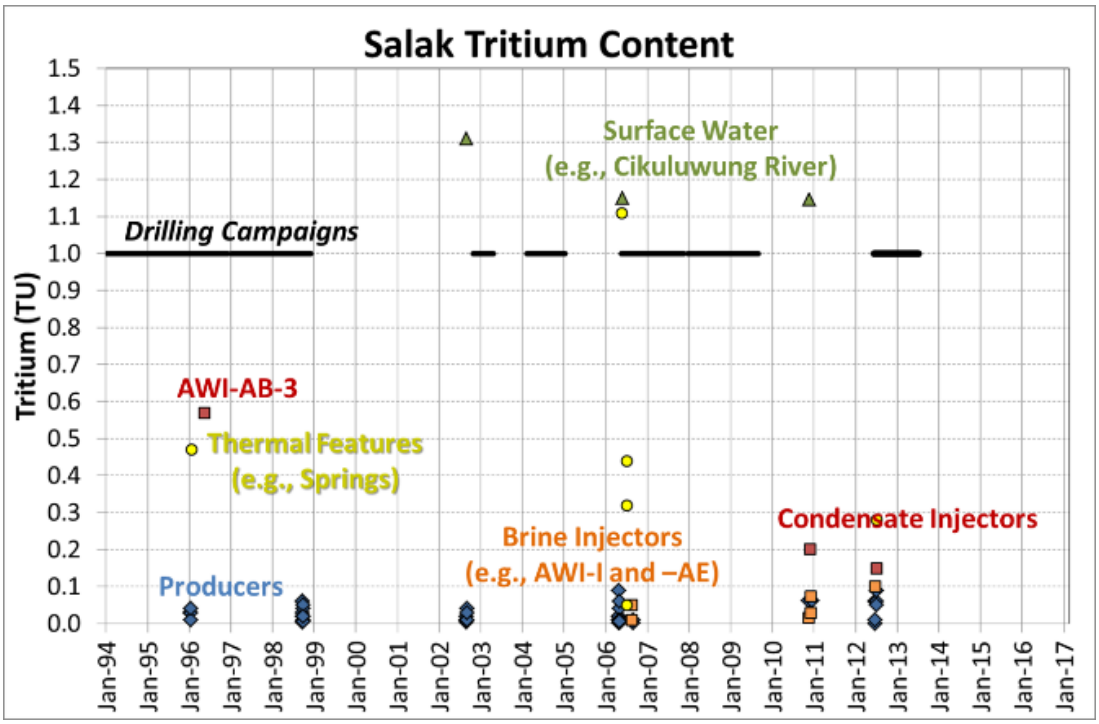

Figure 8: Historical tritium content at producers, brine injectores, condensate injectors, and surface water of Salak geothermal field.

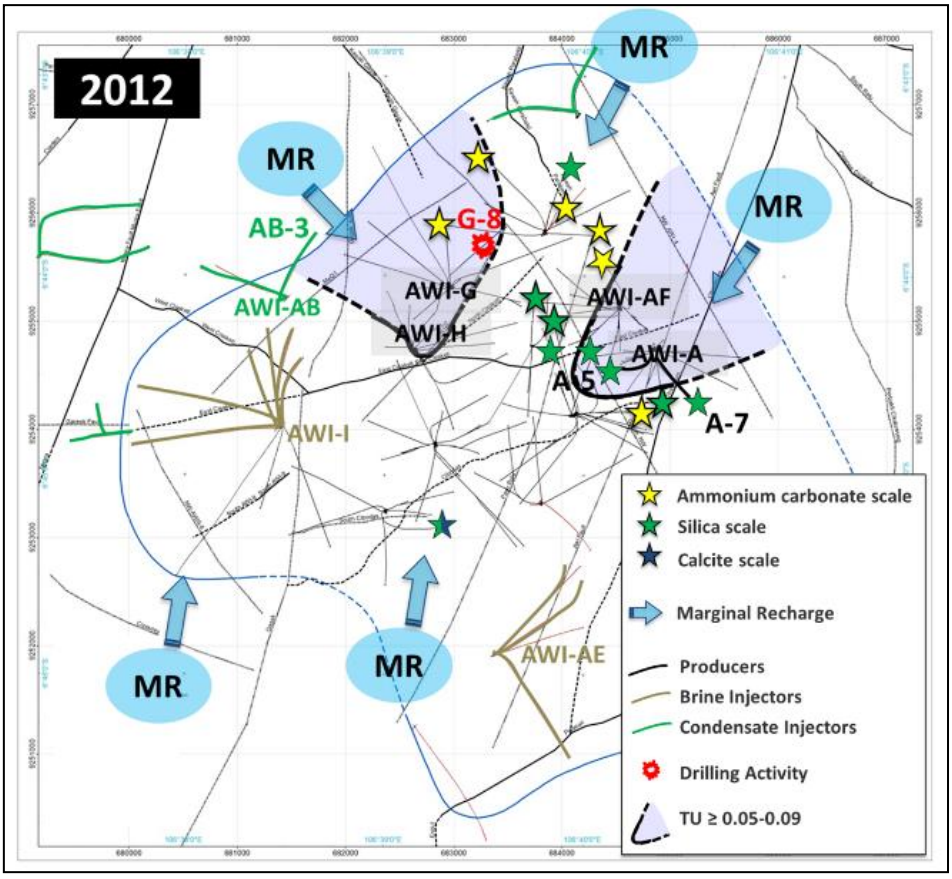

Figure 9: Tritium distribution at Salak geothermal field based on 2012 tritium sampling colletion (Modified from Syaffitri and Molling, 2013).

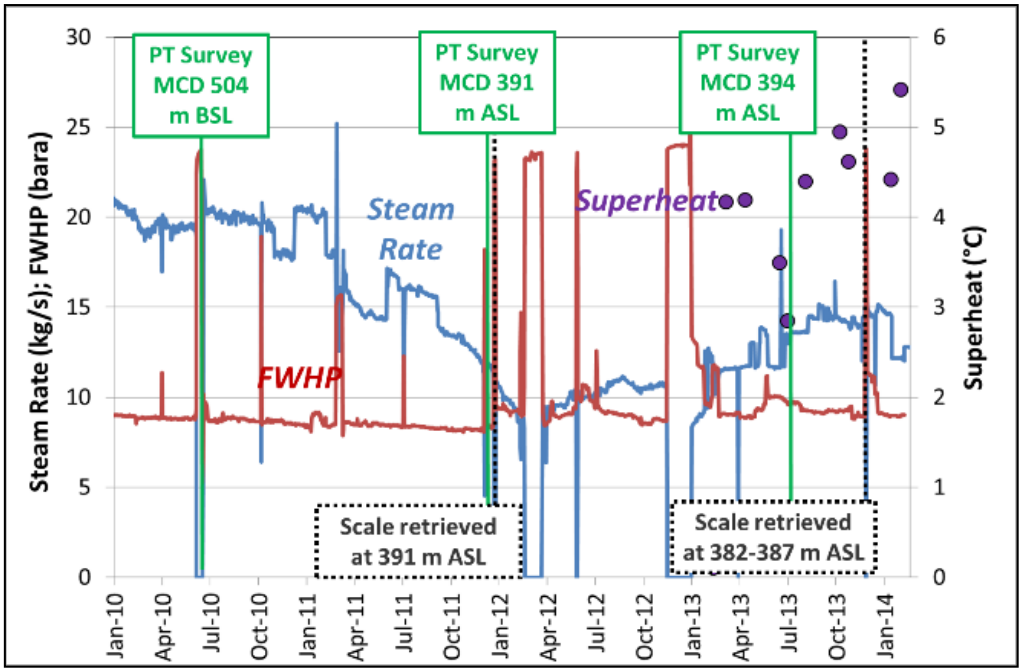

Figure 10: Historical steam rate, FWHP, superheat, and MCD at AWI-A-7 during 2010-2014.

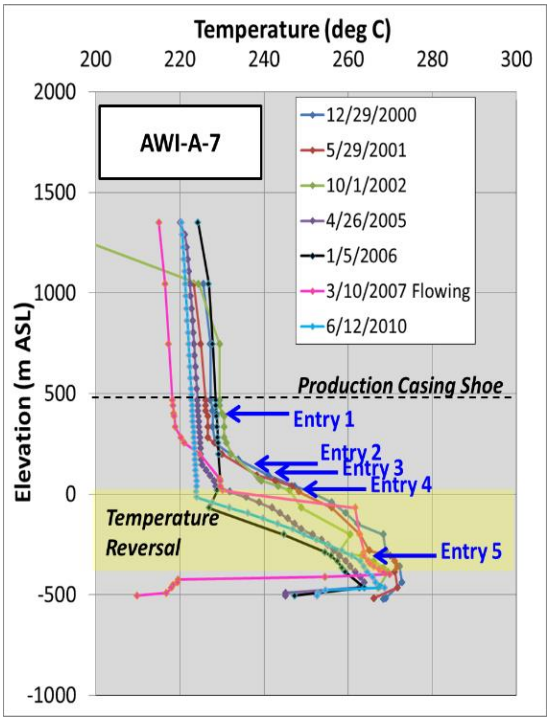

Figure 11: Historical PT profiles of AWI-A-7 shows temperature reversal at 19 - 465 m BSL.

Table 2: DHS sample of AWI-A-7 in April 22, 2007.

Well	Depth (m ASL)	pH	Na (ppm)	Cl (ppm)	B (ppm)	SO_4 (ppm)	HCO_3 (ppm)	Mg (ppm)	SiO_2 (ppm)
AWI-A-7	536	5.01	3216	5634	207.9	6.83	42.94	0.1	300
AWI-A-7	134	4.91	680.54	1366	57.87	3.33	123.04	0.09	90.8
AWI-A-7	-240	5.45	4980	9450	357	12.2	43.7	0.016	581

Temperature reversal has been historically observed at the deeper part of AWI-A-7 (Figure 11). Initial reservoir chloride content at Salak field is ~6,000 ppm. Stimac, et al. (2007) reported that the eastern part of Salak where AWI-A wells are located characterized by dilution compared to other parts of the field. The 2007 DHS sample data of AWI-A-7 demonstrated diluted chloride content (1,366 ppm) at 134 m ASL (Table 2). This DHS sample indicates MR presence at AWI-A-7 with relatively lower in Cl composition and relatively high HCO_3, Mg, and NH_4 concentrations (Molling at al., 2007). This MR type appears to precipitate scale mineral in superheated well like AWI-A-7 because the liquid is dried out (Figure 10).

However, the amount of ^3H content at most Salak producers is lower than laboratory detection limit of tritium analysis (±0.09 TU). Thus, it suggests that the MR liquid at Salak is not young groundwater.

CONCLUSIONS

Since the estimated ^3H content in the next 20 years is still within 0.06-6.15 TU, thus the ^3H monitoring is still applicable to trace young groundwater influx in geothermal system if the low-level ^3H content measurement technique is used.

The result of ^3H study at both fields concludes the young groundwater invades in greater contribution at southern area of Darajat meanwhile the young groundwater appears to absence or invade in insignificant contribution at Salak.

ACKNOWLEDGEMENT

We thank Star Energy Geothermal Darajat II, Limited (SEGD) and Star Energy Geothermal Salak, Ltd. (SEGS) for supporting this project and Pertamina Geothermal Energy (PGE) granting permission to publish this paper.

REFERENCES

Arnórsson, S. (2000), "Isotopic and Chemical Techniques in Geothermal Exploration, Development, and Use," *International Atomic Energy Agency (IAEA)*, Vienna, 351 pages.

Bishop, K. F., Delafield, H. J., Eggleton, A. E. J., Peabody, C. O., and Taylor, B. T. (1961), "Tritium in the Physical and Biological Science Vol. I: The Tritium Content Of Atmospheric Methane," *IAEA*, Vienna, 14 pages.

Clark, I. and Fritz, P. (1997), "Environmental Isotopes in Hydrogeology," *Lewish Publishers*, Boston, 312 pages.

Fontes, J-Ch. (1983), "Guidebook on Nuclear Techniques in Hydrology: Dating of Groundwater," *Technical Series No. 91*, IAEA, Vienna.

Hamilton, W. (1979), "Tectonics of the Indonesian Region," *United States Geological Survey Professional Paper 1078*, 45 pages.

Hutchinson, C. S. (1989), "Geological Evolution of South-East Asia," *Claredon Press*, Oxford Science Publications, Oxford, 368 pages.

IAEA (1983), "Guidebook on Nuclear Techniques in Hydrology," *Technical Report Series No.91*, IAES, Vienna.

Molling, P. A., Sunio, E. G., and Wijaya, B. A. (2007), "Interpretation of Downhole Sampling (DHS) Results at Awibengkok Geothermal Field, Indonesia," *In-house Chevron Geothermal Report*, November 9.

Simatupang, C. H., and Molling, P. A. (2010), "The Case For An External Origin For MR-Based On Liquid Chemistry," *In-house Chevron Geothermal Presentation*, August, 45 slides.

Simatupang, C. H., Intani, R. G., Suryanta, M. R., Irfan, R., Golla, G. U., Cease, C., and Molling, P. A. (2015), "Evaluation of Water Produced from a Steam Dominated System, a Case Study from the Darajat Field," *Proceedings World Geothermal Congress 2015*, Melbourne, Australia, April 19-25, 8 pages.

Stimac, J., Nordquist, G., Suminar, A., and Sirad-Azwar, L. (2007), "An Overview of the Awibendkok Geothermal System, Indonesia," *Geothermics 37*, 32 pages.

Syaffitri, Y. and Molling, P. A. (2013), "2012 Salak Tritium Survey," *In-house Chevron Geothermal Presentation*, September, 27 slides.

Syaffitri, Y., Molling, P. A., and Paramitasari, H. M., 2016, "The Characteristics and Distribution of Marginal Recharge (MR) at Darajat Field," *In-house Chevron Geothermal Presentation*, March 18, 2017 slides.

RESULTS OF I-I DEEP WELL: IMPACT ON THE CONCEPTUAL MODEL OF THE SALAK GEOTHERMAL SYSTEM

Nur Vita Aprilina, Fanji Junanda Putra, Satrio Wicaksono, Tri Julinawati, Reka Tanuwidjaja, Aditya Hernawan

Star Energy Geothermal Salak Ltd.
Sentra Senayan 2, Jl. Asia Afrika No.8, Jakarta Pusat, Indonesia

e-mail: nvaprilina@starenergy.co.id; Fanji.J.Putra@starenergy.co.id; satriowicaksono@starenergy.co.id; Tri.Julinawati@starenergy.co.id; reka.tanuwidjaja@starenergy.co.id; AdityaH@starenergy.co.id

ABSTRACT

I-I deep well, the last well of 2012-2013 Salak Drilling Campaign, was drilled at Pad I with two objectives, namely, (1) augment steam supply and (2) reduce the uncertainty of the base of reservoir (BoR) in the inferred upflow region southwest of Salak (also known as Awibengkok) Geothermal System. Although the well was completed about 20% shallower than planned to 10,402' MD (3,170 m) only, it is now the deepest well drilled in the Salak reservoir.

Interpretation of borehole image logs indicates that I-I deep well intersected predominantly pyroclastics (volcanics) with interbedded lavas and sedimentary rocks below 10,000' MD. These units appear to be a member of the Marine Sediments and Volcaniclastics (MSV) Formation which is now deeper than what were previously interpreted as continuous sedimentary rocks. Before, it was believed that sedimentary rocks (called Continuous Sediments Formation) underlie the MSV Formation to form the basement of the Salak reservoir.

I-I deep well successfully encountered the deepest permeable entry to date at ~6,350' BSL at Salak. It confirmed the presence of deep permeability (likely related to the geothermal system's upflow) in this part of the field and prompted a revision of the P10 BoR. Geology, geochemistry, and Pressure-Temperature (PT) data also support the interpretation of a high-temperature upflow in the Pad I area. However, both Qtz and NKC geothermometries don't work very well because brine injection at Pad I since 1994 has impacted the reservoir and has camouflaged the original chemistry of Pad I wells. These favorable results at I-I deep well confirm previous interpretations that the upflow of the geothermal system is beneath the southwest area. The presence of the deep feed zone in the MSV Formation indicates that this formation is not the basement of the geothermal reservoir and supports further drilling of deep wells in this area.

Keywords: Salak, Deep Well

INTRODUCTION

The Salak geothermal field is located in West Java, Indonesia along the Sunda Volcanic Arc (Figure 1). It is situated in a mountainous area with elevation ranging from about 950 to 1,500 m above sea level (ASL). The field is about 60 kilometers from Jakarta, capital city of Indonesia. Salak is one of the world's largest liquid-dominated geothermal fields with a current total installed capacity of 377 MWe. Six power plants are found in Salak with 180 MWe from the PLN Units-I/II/III and 197 MWe from the Star Energy Geothermal Salak Units IV/V/VI.

The Salak geothermal system lies in a highland on the southwestern flank of the Gunung Salak volcano (2211 mASL). The commercial resource is spatially associated with andesitic-to-rhyolitic volcanism that has occurred over the past 330 ka, especially silicic volcanics erupted in the last 280 ka along a major NNE-trending structure. It is fracture-controlled reservoir with benign chemistry, low-to-moderate non-condensable gas (NCG) content, moderate-to-high temperature (240–312°C) geothermal resource with high fracture permeability, moderate porosity (mean = 10.6%) and moderate-to-low matrix permeability (geometric mean = 0.026 md) (Stimac et al., 2007).

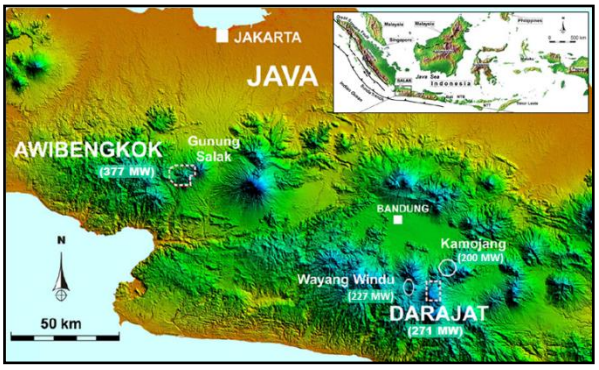

Figure 1: Map of West Java showing major cities and volcanic centers. Also shown are the Awibengkok/Salak and Darajat geothermal contract areas (dashed polygons) and other producing geothermal fields in the general area (Aprilina et al., 2015).

BACKGROUND OF I-I DEEP WELL DRILLING

Salak geothermal field is one of three geothermal fields operated by Star Energy Geothermal which has been produced for more than 20 years of commercial operations. In order to maintain steam supply to support full generation, one of the strategies is steam production program through drilling campaign. The latest drilling campaign in Salak field was conducted in 2012-2013 which has been completed 13 new drilling wells.

I-I deep well was targeted to the south from the I pad and was drilled primarily for steam supply and Value of Information (VOI) to test temperature and permeability at depth in the area of the inferred upflow region of the Salak reservoir, to reduce uncertainty about the Base of Reservoir in the southwestern area of the field, below elevation -5,500 ft.sl (Figure 2).

Pad I is located at area where the highest reservoir temperature was measured, with distinct fluid chemistry

showing stronger magmatic influence, and petrographic evidence of intrusive rocks and contact metamorphism (Stimac et al., 2008). The MEQs directly beneath the I pad are believed to be related to injectate and/or pressure transients down a deeply extending vertical fracture system. These evidences support the interpretation of deep fluid convection and that the fracture system related to upflow of the geothermal system is in West Salak.

The base of a geothermal reservoir is defined when the permeability of the rock is not enough to sustain commercial production. This corresponds (more or less) to a permeability of 1 - 10 mD, which is the permeability assigned to the deepest active block layer at -6,000 ft.sl. in the Salak reservoir model (Kusumah et al., 2013). Data from recently drilled deep wells (O-CRD; I-G; I-H; and J-D) show potential for an extension of permeability at depth. Also, the depth of recorded MeQ / micro-seismicity events indicates the possibility that permeability could extend as deep as -13,000 ft. ASL in the southwestern area of the field in the vicinity of the I pad (Figure 3). In other geothermal field (e.g. Larderello, Italy; Bulalo, Philippines), substantial reserves have been found below what previously was thought to be a reservoir bottom. A very deep well at the I pad will help to reduce uncertainty about a possible deep reservoir at Salak.

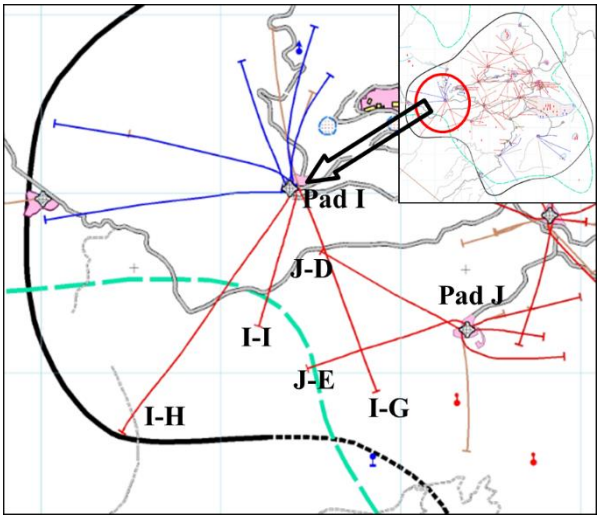

Figure 2. Map showing the location of Pad I, Pad J, I-I deep well, and surrounding wells. Upper right map showing well locations and commercial reservoir boundary of Salak Geothermal Field.

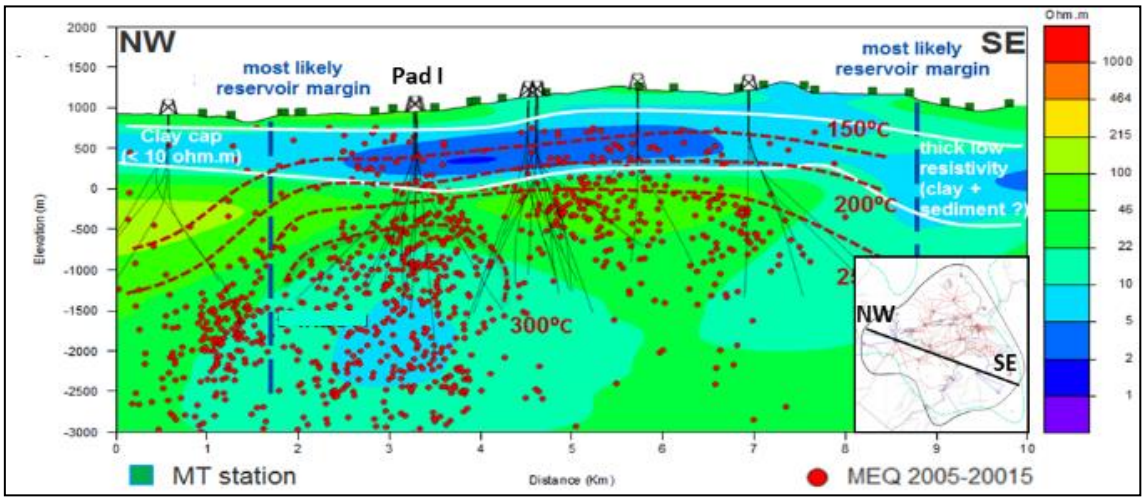

Figure 3. Cross-section across the seismicity zones in south Salak. Profile also showing the low-resistivity clay cap as defined by the 1D MT layered model (invariant mode; white dashed lines) and the 3D MT inversion model (colored background) with the isotherm contour. The low-resistivity body below the 200°C isotherm is an artifact of the 3D modeling.

I-I DEEP WELL DRILLING SUMMARY

I-I deep well was designed as a low inclination (17°) standard 2D directional well targeting production from the deep brine reservoir south of the I pad. I-I deep well was planned to be drilled to 13,000 ft.MD /12,481 ft.TVD (9,175 ft.BSL) and to be completed with 4 different diameter holes (26", 17-1/2", 12-1/4" and 9-7/8") and 1 contingency hole (7-7/8"). The drilling was started with 26" hole section to depth of 1798 ft.MD and then followed with 17-1/2" hole section to the top of reservoir depth at 4314 ft. The 13-3/8" production casing was set and cemented at 4304 ft.MD in altered (silicified) dacite tuff. Epidote was first observed in drill cuttings at 4309 ft.MD and became persistent below about 4960 ft.MD. Reservoir section was drilled with 12-1/4" hole section to the depth of 9702 ft.MD and followed by landing the 10-3/4" perforated casing to the bottom. This section was completed with 2 bit ran safely with no stuck pipe event and also during drilling those section were successfully managed the return to the surface. After drilled out 10-3/4" casing shoe, while continuing drilling about 300 ft.MD of 9-7/8" hole section, the well experienced big total losses that lead to hydrostatic column dropped significantly in the wellbore and followed by increasing wellbore temperature and pressure that lead to well control issue. Due to the high risk of wellbore phenomena uncertainty then the team decided to suspend drilling in order to be able to do study for better understanding the wellbore phenomena (Souvanir et al., 2015). I-I deep well actual schematic depict in Figure 4.

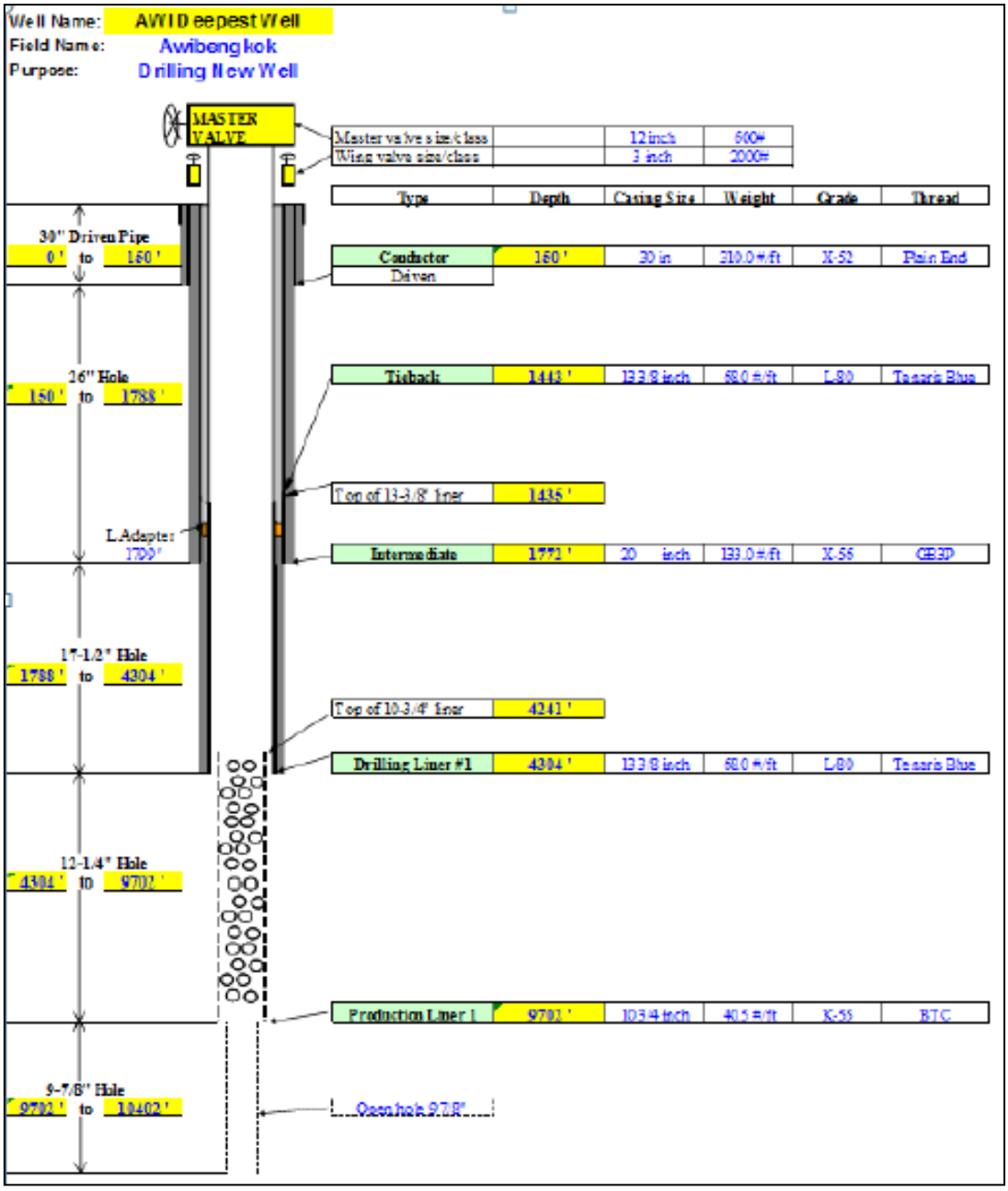

Figure 4. I-I deep well actual schematic.

I-I DEEP WELL RESULTS

The lithological sequence intersected by I-I deep well is similar to that encountered in offset wells I-G, I-H, and J-D especially above the reservoir hole section. In general, the lithological sequence of I-I deep well based on cutting description can be divided into six major formations, namely Upper Dacite, Upper Andesite, Middle Dacite, Middle Andesite, Rhyodacite Marker (RDM), and Lower Andesite. However this well was blindly drilled starting at 6,505' MD until TD. In this hole section which was drilled without mud returns, the only means of obtaining lithologic data were come from Total Count Gamma Ray (GR), Spectral Gamma Ray (HNGS), and borehole resistivity image logs which was conducted at 9734-10359 ft.MD (Figure 5). A previous study about identifying reservoir rocks using drilling data mentioned that the Rhyo-Dacite Marker (RDM) at Salak has a high GR response that is discernible in the GR log. In addition, the Marine Sediments and Volcaniclastics (MSV) Formation exhibits another increase in GR response (Pamurty et al., 2015).

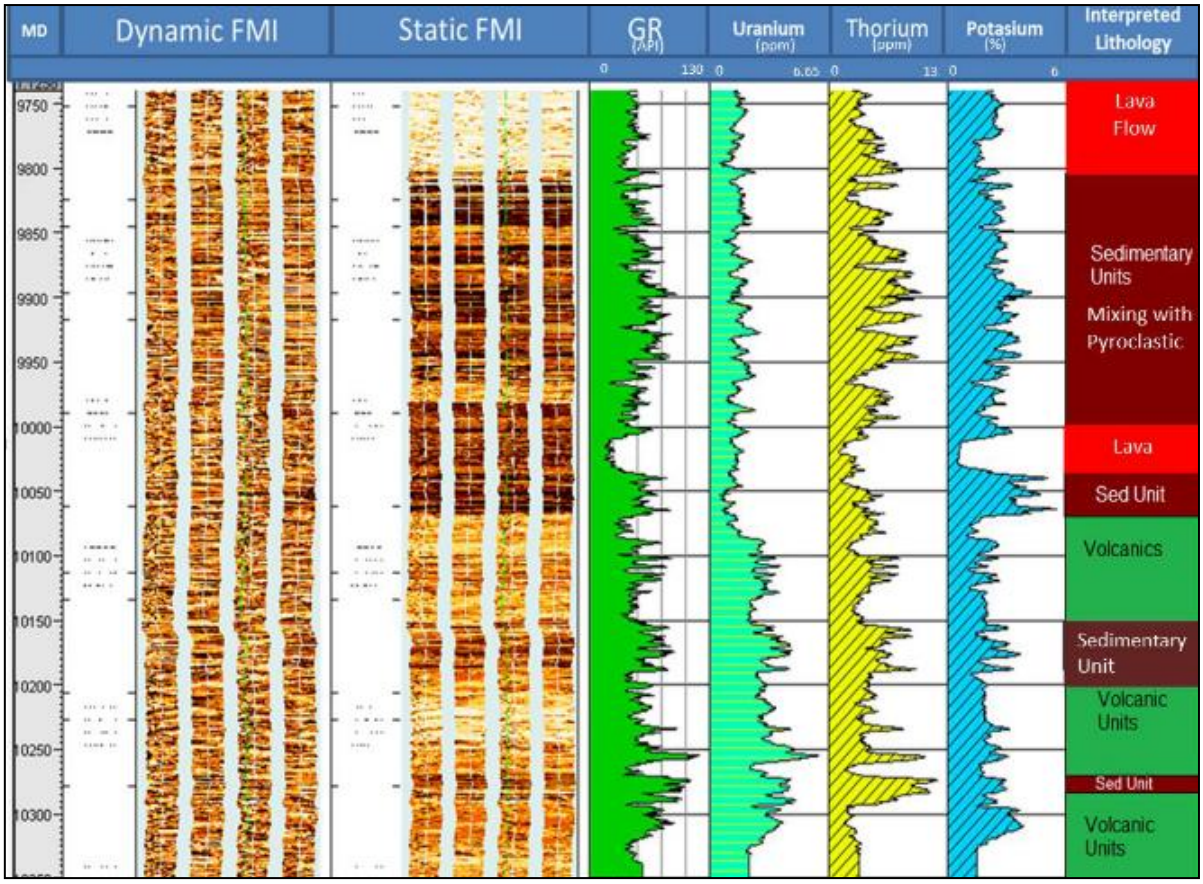

Figure 5. I-I deep well lithology interpreted from borehole resistivity image log, total count Gamma Ray (GR), and Spectral Gamma Ray (HNGS) showing occurrence of volcanic rocks (Marine Sediment Volcanic Formation) at depth.

Lithology interpreted in this blind drilling section predominantly consists of breccias interlayered with clastic sediments and carbonate rocks. The carbonate rocks are interpreted to be correlated with the Bojonglopang (or Bantargadung) Formation that has a similar Middle Miocene age. Volcanic rocks mixing with these sedimentary rocks are common in the deep wells. The deep section petrography suggests that the marine sediments and other sedimentary units are mixed with the volcanics instead of being deposited as a continuous sequence. The volcanic materials found in the sedimentary units are believed to be reworked materials due to natural sedimentation process and/or orogenic movement rather than volcanic activity. It is supported by image log interpretation which indicates that the sedimentary rocks at Salak are strongly folded (Figure 6). These bedded units have various strikes and dips, from gentle to steep, and are interpreted as folded and maybe faulted. Both Martodjojo (1984) and Clements and Hall (2007) theorized that sedimentation decreased due to uplifting or orogenesis in the southern part of West Java in Late Miocene. Volcanogenic materials were deposited by turbidity currents and debris flows (Bantargadung and Saguling Formations) in the middle part of the Bogor Basin (Clements and Hall, 2007). The Bantargadung and Saguling Formations are dominated by breccia with boulder-sized fragments of andesite and limestone.

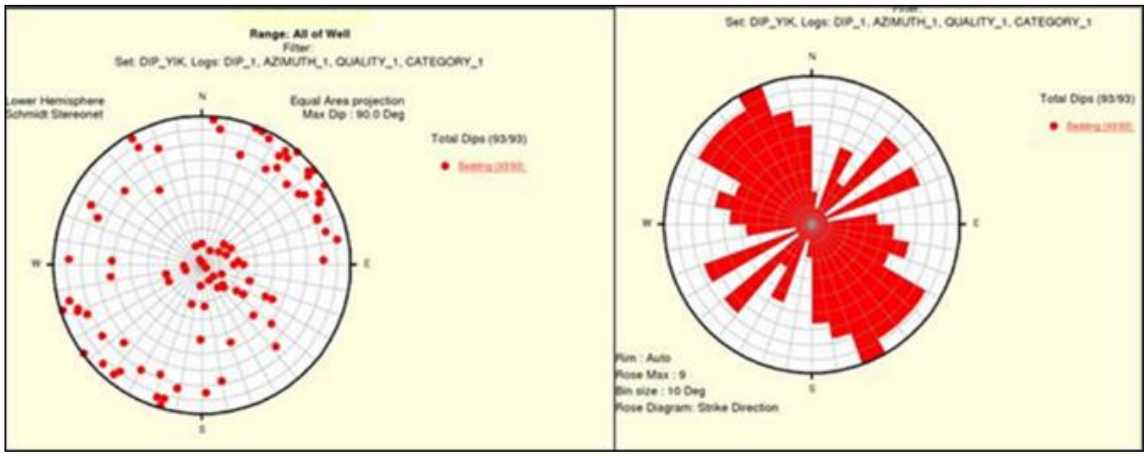

Figure 6. Dipmeter plot show that the dips of the bedded sedimentary rocks can be grouped into both shallow (<45°) and steep (>60°). The steeply dipping beds support the theory that these sediments may be folded.

Based on Pressure-Temperature-Spinner (PTS) and heat-up survey data, I-I deep well encountered three permeable zones at 6,150 ft.MD, 6,530-7,030 ft.MD, and 10,030 ft.MD (Figure 7). The deepest feed zone at 10,030' MD has high temperature (610° F), high pressure (1,300 psi), and high enthalpy inflow. Eventhough borehole resistivity image log indicates no direct correlation between the feed zone location to the structure data, the interval range of this feed zone to permeability indication (fractures/fault cluster , and significantly drop in pressure while drilling/PWD) is 67 ft.MD. This suggest that feed zone may still correspond to the large fractures occured at 9960-9965 ft.MD (Figure 8).

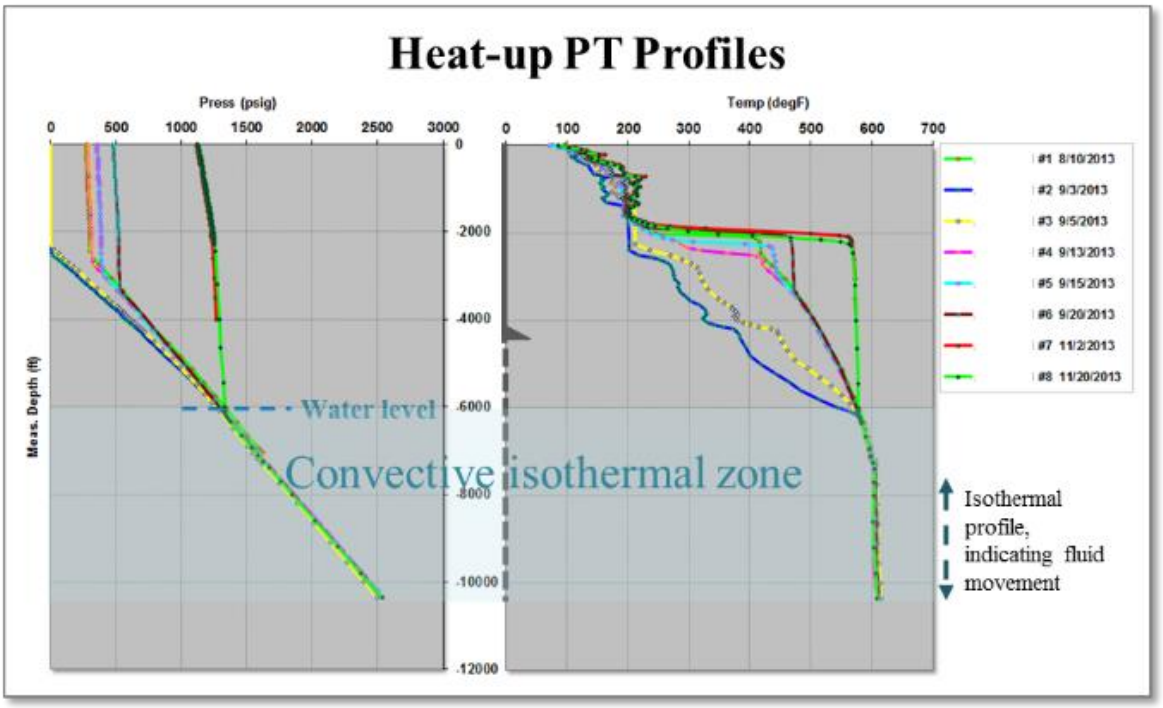

Figure 7. Heat-up PT Profiles of I-I deep well. Deep upflow creates convective isothermal zone that was undisturbed during completion test.

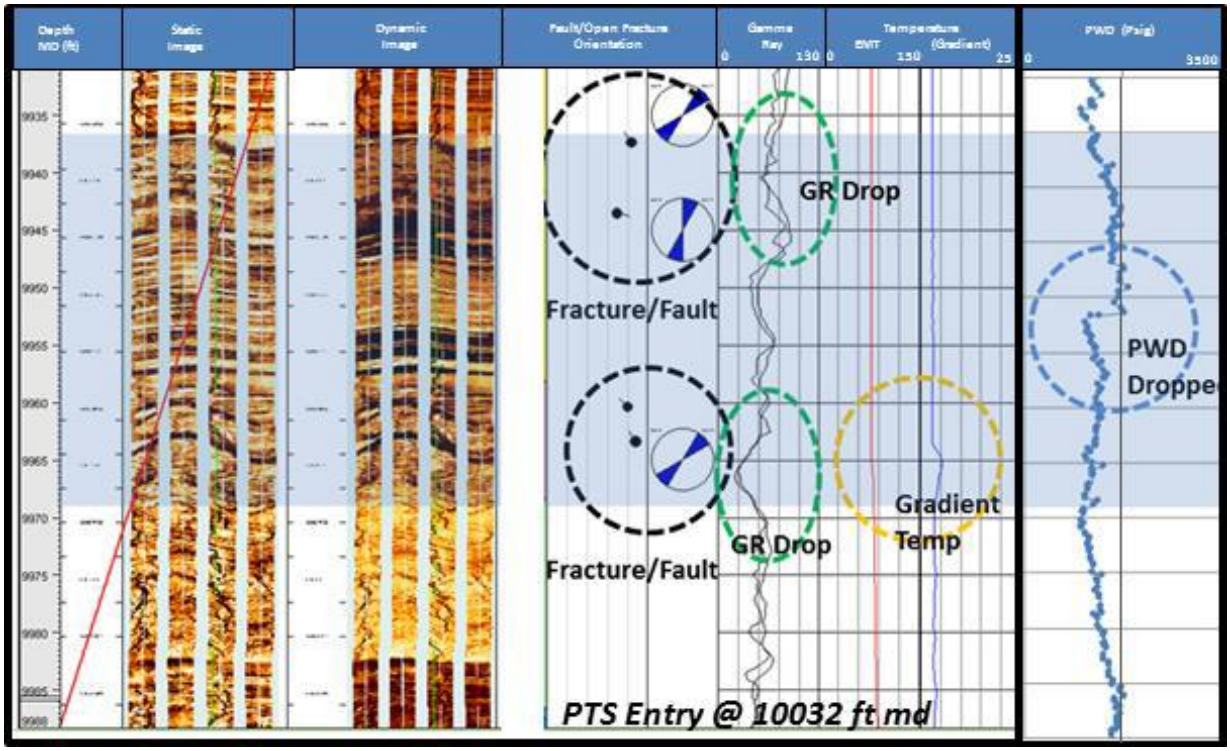

Figure 8. Borehole resistivity image log shows fractures/fault cluster at 9960-9965 ft.MD that coincident with significantly drop in pressure while drilling (PWD). These features may correlate with thee deepest entry in I-I deep well at 10,030 ft.MD.

IMPACT TO THE SALAK CONCEPTUAL MODEL

Interpretation of borehole image logs indicates that I-I deep well intersected predominantly pyroclastics (volcanics) with interbedded lavas and sedimentary rocks below 10,000 ft.MD. These lithology units are deeper than what were previously interpreted as continuous sedimentary rocks. Wells that penetrated the deeper, more continuous sedimentary sequence often show conductive temperature gradients suggesting that the sediments represent the basement of the Salak reservoir in some portions of the field. Before, it was believed that sedimentary rocks (called Continuous Sediments) underlie the Mixed Volcanics-Sediments (MVS) to form the basement of the Awibengkok reservoir. However, this deep sequence of pyroclastics and sedimentary rocks at I-I deep well suggests that the MVS is present deep in Salak. Furthermore, this new interpretation suggests that separating the sedimentary rocks into the Mixed Volcanics-Sediment (MVS) and Continuous Sediments (CS) based on the occurrences of volcanic materials and predominant carbonate rocks, respectively, is impractical now. It is probably best to combine the MVS and the carbonate-rich CS (now herein called the Marine Sediments and Volcanics or MSV).

The deep entry at 10,030 ft.MD (6,350 ft.BSL), now the deepest fluid entry identified to date at Salak, confirmed the presence of deep permeability (likely related to the geothermal system's upflow) in this part of the field and prompted a revision of the P10 BoR (low case). These favorable results at I-I deep well confirm previous interpretations that the upflow of the geothermal system is beneath the I Pad. The presence of the deep feed zone in the Marine Sediments Volcanics (MSV) indicates that this formation is sufficiently permeable to sustain commercial production and suggests that this formation is not the basement of the geothermal reservoir.

ACKNOWLEDGEMENT

We thank Star Energy Geothermal Salak Ltd. (SEGS) for supporting this study and granting permission to publish this paper.

REFERENCES

Clements, B. and Hall, R. (2007), "Cretaceous To Late Miocene Stratigraphic and Tectonic Evolution of West Java", *Proceedings 31st Annual Convention of the Indonesia Petroleum Association*, pp 87-104.

Kusumah, Yudi Indra, Ryder, Andrew, Aprilina, Nur Vita, Souvanir, Tommy, Pasikki, Riza Glorious, Peter, Libert, Frederick Titoes, Hidayaturrobi, Abu Dawud, and Hidayati, Nurul (2013), "Drilling Proposal of Salak Deep Well", *In-house Chevron Geothermal Report*, pp 1-28.

Martodjojo, S. (1984), "Evolution of Bogor Basin", *Unpublished Doctoral Thesis*, Bandung Institute of Technology.

Pamurty, Perdana Noverda, Satya, Drestanta Yudha, and Golla, Glenn U. (2015), "Identifying Reservoir Rocks Using Drilling Data", *In-house Chevron Report*, pp 1-34.

Souvanir, Tommy, Putra, Redha Bawika, Putra, William Maha, and Dumrongthai, Panurach (2015), "Deepest Geothermal Well in Indonesia: A Success Story", *Proceedings World Geothermal Congress*.

Stimac, James, Nordquist, Gregg, Suminar, Aquardi Rahmat, and Azwar, Luthfie Sirad (2007), "An Overview of the Awibengkok Geothermal System, Indonesia", *Geothermics paper*.

Wicaksono, Satrio, Aprilina, Nur Vita, Tanuwidjaja, Reka, Putra, Fanji Junanda, Julinawati, Tri, Aditya, Hernawan, and Mubarok, Zaky (2016), "Southwest Salak Evaluation", *In-house Chevron Geothermal Report*, 46 pages.

IDENTIFICATION OF PERMEABILITY GEOTHERMAL RESERVOIR IN AN ACTIVE FAULT ZONE

Jamaluddin[1], Emi Prasetyawati Umar[2], Li Yong[1], Cheng Fuqi[1]

[1]Geological Engineering Department, School of Geosciences, China University of Petroleum, Qingdao, China
[2]Mining Engineering Department, Faculty of Industrial Technology, Universitas Muslim Indonesia, Makassar, Indonesia

e-mail: jamaljamaluddin1994@gmail.com; emiprasetyawati.umar@umi.ac.id;
1158782814@qq.com; chengfuqi@upc.edu.cn

ABSTRACT

The Indonesian state on the ring of fire is an area that has geothermal potential. The existence of geothermal systems is generally closely related to the activities of volcanism and magmatism. Although producing geothermal systems occur in both compressional and extensional regions of strain in volcanic arcs. Volcanic areas have dominant lithology in the form of igneous rocks, and have complex geological structures. Rocks in the geothermal field are usually volcanic rocks. Which have small primary permeability of the fracture, the rock have a secondary permeability, so that the total permeability becomes larger. Fault is a fracture system that will help rocks have a large total permeability. Another relationship between fault and geothermal heat is that a fault create vertical permeability of a rock. So in the field of geothermal, there is usually a pattern of alignment between the location of a manifestation with the location of other manifestations in a similar fault system.

Keywords: Fault, Geothermal, Permeability, Reservoir

INTRODUCTION

The decrease in fossil energy resources has led to an increase in demand for efficient utilization of unconventional and sustainable energy resources, such as geothermal reservoirs. Additionally, the increasing impact of carbon dioxide has led to the development of geological storage of carbon dioxide. In this context of geothermal development and carbon dioxide storage within a sedimentary formation, one important aspect for the siting of future wells is to locate zones where fluid circulation occurs. Productive heated land reservoirs should have high porosity and permeability, considerable size, high temperatures and sufficient fluid content. Permeability is generated by stratigraphic characteristics and structural.

The high correlation between the presence of geological structures in a region can form the permeability of rocks to circulate due to warming by heat sources. When the fluid circulates in a reservoir, it can form a shielding layer that causes the rocks on the surface to be transformed (clay alteration rocks), in response to the heat pressures from within the earth. On the other hand, the continuous hydrothermal activity can result in a high fracture in the geothermal environment, causing rock formation on deformed surfaces and eventually forming certain morphologies. This environment becomes a single geothermal system. Thus, the geothermal system in the active fault line can be created by environmental permeability factors of rock and hydrothermal activity.

The permeable igneous rocks usually contains fracture zones. Based on the direction, the fracture permeability is divided into two: vertical permeability and horizontal permeability. Fault strongly supports the formation of vertical permeability, because the geothermal fulid can pass to the surface along the fault plane. This is characterized by the presence of surface geothermal. Basically, the development and management pattern of geothermal energy is only based on three main factors, namely temperature, permeability and geothermal fluid (Hanano, 1999).

BARASANGA GEOTHERMAL FIELD

Regionally, structures of Lasusua-Kendari Sheet are faults, fold, and joint. Fault and straightness are generally northwest-northwest directions in the direction of Lasolo fault. Lasolo fault is sinistral slip-sliding fault which allegedly still active until now, as evidenced by the hot springs in Batugamping reefs that aged Holocene on the Fault Line in Southeast Tinobu, precisely in Barasanga District Lasolo. A rising fault is found at Tanjung Labuandala in the south of Lasolo, ie the rock from iolite rocks over the Meluhu Formation rocks. Fault Lasolo is North-West-trending, dividing the Kendari Sheet into two parts. The north-east side of the fault section is called the Hialu Lane and the southwest is called the Tinondo Lane (Rusmana, et al, 1993). Hialu Lane is generally a set of rocks characterized by the origin of Ocean Crust and Tinondo Lane is a set of rocks that are characterized by the origin of continental exposure.

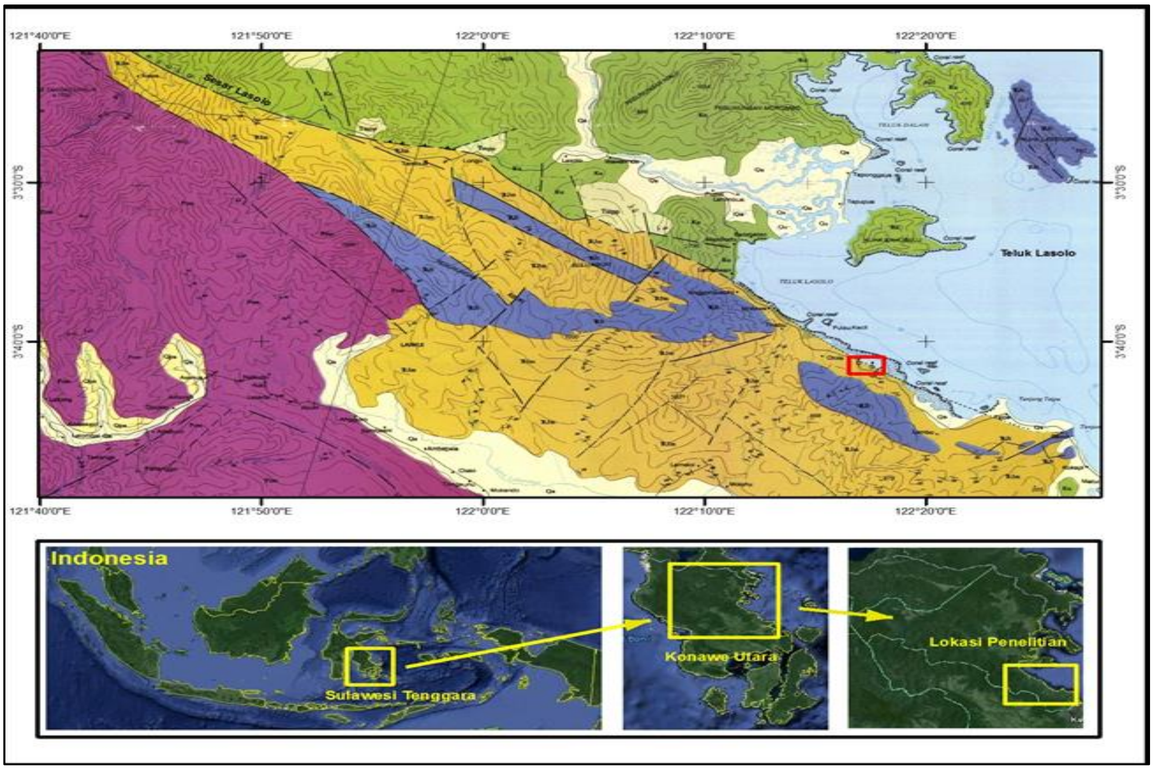

Figure 1: Geological map of the Lasusua-Kendari, Indonesia.

PERMEABILITY

Permeability is important because it is a rock property that relates to the rate at which hydrocarbons can be recovered. Values range considerably from less than 0.01 millidarcy (MD) to well over 1 darcy. A permeability of 0.1 MD is generally considered the minimum for production. Highly productive reservoirs commonly have permeability values in the Darcy range.

Permeability is expressed by Darcy's Law:

$$Q=A\left(\frac{k}{\mu}\right)\left(\frac{\Delta P}{L}\right)\ldots\ldots\ldots\ldots\ldots\ldots\ldots\ldots\ldots\ldots\ldots\ldots(1)$$

Where Q is rate of flow, k is permeability, μ is fluid viscosity, $\frac{\Delta P}{L}$ is the potential drop across a horizontal sample, and A is the cross-section area of the sample. Permeability is a rock property, viscosity is a fluid property, and $\frac{\Delta P}{L}$ is a measure of flow potential.

The basic concept of permeability is closely related to the basic law of fluid flow through porous media, known as Darcy's Law, which is the first empirical law first introduced by Henry Darcy in 1856 (Rivera. J., 1995) Conceptually Rivera (1995) subsequently divides permeability based on its medium to matrix permeability, and fracture permeability. Matrix permeability is generally defined as a single porosity system especially in materials such as rocks whereas fracture permeability is related to a fracture or a series of fractures. The concept of permeability in geothermal is more proportionally oriented to the container, namely primary permeability and secondary permeability (Browne, 1996). Primary permeability includes rocks, contacts of rock layers, unconformity and ancient solution features that are also overall known as stratigraphic approaches. Secondary permeability includes fractures, hydraulic fracturing, joints and hydrothermal leaching.

The search for the permeable zone of the geothermal area reservoir can be performed using structural analysis, stratigraphy, structural and stratigraphic combinations, microearthquakes and drilling. The search for structural signs includes the analysis of the appearance of geothermal symptoms through aerial photography and Landsat imagery, a review of rock distribution patterns and rock contacts and the appearance of regional lineament deployment. Identify potential fault zones through the appearance of symptoms during the drilling process, among others, loss of fluid circulation, powder analysis and rock core, and others. Permeable zone search can also be done by looking at the distribution of microseismicity. The greater the degree of seismicity, the greater the flow of fluid below the surface into the reservoir.

RESULT AND DISCUSSION

The fault zone is usually the most important fracture zone of a geothermal geology. This zone is usually a way out of geothermal fluid to the surface or as a recharge media to catch water from the soil. Fault zone usually consists of 2 parts of the fault core and damage zone (Caine et al, 1996). In the active fault zone (usually frequent earthquakes at that location), the hydraulic conductivity of the fault core usually increases with the increase of the earthquake magnitude (Gudmundsson, 2000). When the fault is inactive, the fault cores are very narrow, but still sufficient to pass the fluid (Gudmundsson, 2000) Damage zone on the fault lies on both sides of the fault core Damage Zone consists of many fractures of varying sizes and usually also the same direction as the main fault.

The geothermal field usually associated with the volcanic landscape, one of the areas that usually has a constituent rock in the form of igneous rock and has a complex geological structure. In relation to geological structures related to geothermal, important geological structures to

be considered are fracture structures, especially faults and minor faults (fracture). In the reservoir, the fluid flow in the fracture zone or the minor faults is usually larger and may be almost all in this zone. Fracture is related to the permeability of the reservoir. The magma interactions in igneous rocks usually have very little permeability. Fracture structure is very important because the structure is closely related to the escape of hydrothermal fluid and hydrological cycle. Fracture will make igneous rocks that have this small primary permeability to have a large secondary permeability. So the influence of fracture will cause the total permeability becomes bigger.

Fracture structures are essential for the hydrothermal migration process because they play very important role in the escape of hydrothermal fluid. In the process of passing fluid to the surface, it requires a high permeability.

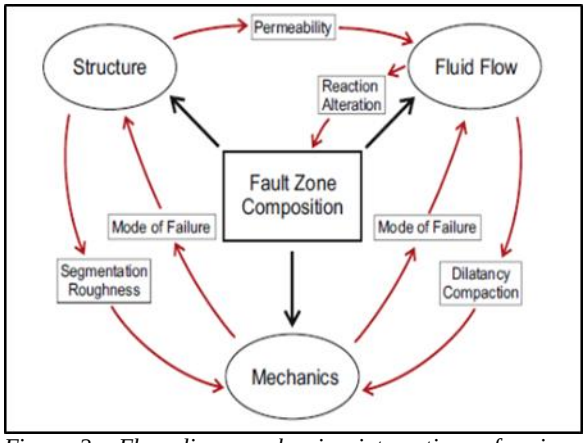

Figure 2 : Flow diagram showing interactions of main topics of structures, mechanics, and fluid flow. Mode of failure refers to whether or not seismic slip occurs (Faulkner, 2010).

The potential for geothermal heat can be identified by the presence of surface geothermal manifestations. One of the controllers on the emergence of such manifestations is the presence of the exit medium or the permeable zone (Hochstein and Browne, 2000). The geological structure of a fracture or fracture zone is one of the permeable zone indications which is an important aspect of geothermal exploration. Its existence is the path to the process of migrating the geothermal fluid (Soengkono, 1999).

Manifestations of surface geothermal occur because of fractures that allow hot fluids to the surface. Fractures can be formed due to the geological structure of the Lasolo fault found in the Baruata Region. Lasolo fault is estimated to be active until now which is marked by the availability of hot springs in Barasanga area (Rusmana, et al., 1993). Structural and stratigraphic combination analysis involves collectively the two elements forming a localized permeable zone such as a combination of fractures with rock contacts or joints with rock contacts or with dissonance. Rocks contact sometimes act as a means of forming a normal fault structure (gravity fault).

Figure 3 : Seepage of hot springs Barasanga.

Refering to the geothermal system that is the availability of heat source, reservoir, Caprock, and water source that is heated the ground water (ground water). This study focuses on the presence of hot water in rock layers in order to obtain geophysical models of subsurface rock layers suspected as layers of hot-water rocks. The first layer at the sounding points G1 and G2 based on field geological conditions and petrographic analysis and guided by the classification table by (Telford, 1990 and Loke, 2004), is an emerging area of hot springs. Presumably in this layer is a limestone (travertine) which has a layer thickness of 1.4 meters and a depth of 1.4 meters with resistivity 266 Ω.m. At the sounding point G1 to the point of sounding G2 with a depth of 2.52 meters and a layer thickness of 1.13 meters is a manifestation formed due to the dissolution process of limestone around due to the hot chemistry of hot springs. Travertine is manifold incoherent travertine is travertine where the material of the preparation is not mutually binding strongly. This layer is medium or hot spring and has a distribution from the West-Northwest until the East to Organize at the point of sounding G1 continuously to the sounding point G2. The presence of a layer of hot-water rocks is thought to be a sandstone with a resistivity value between 20-95m because sandstones have good porosity and permeability so that the ability to absorb and pass water is very good. This layer is a container or place of heating of water sources.

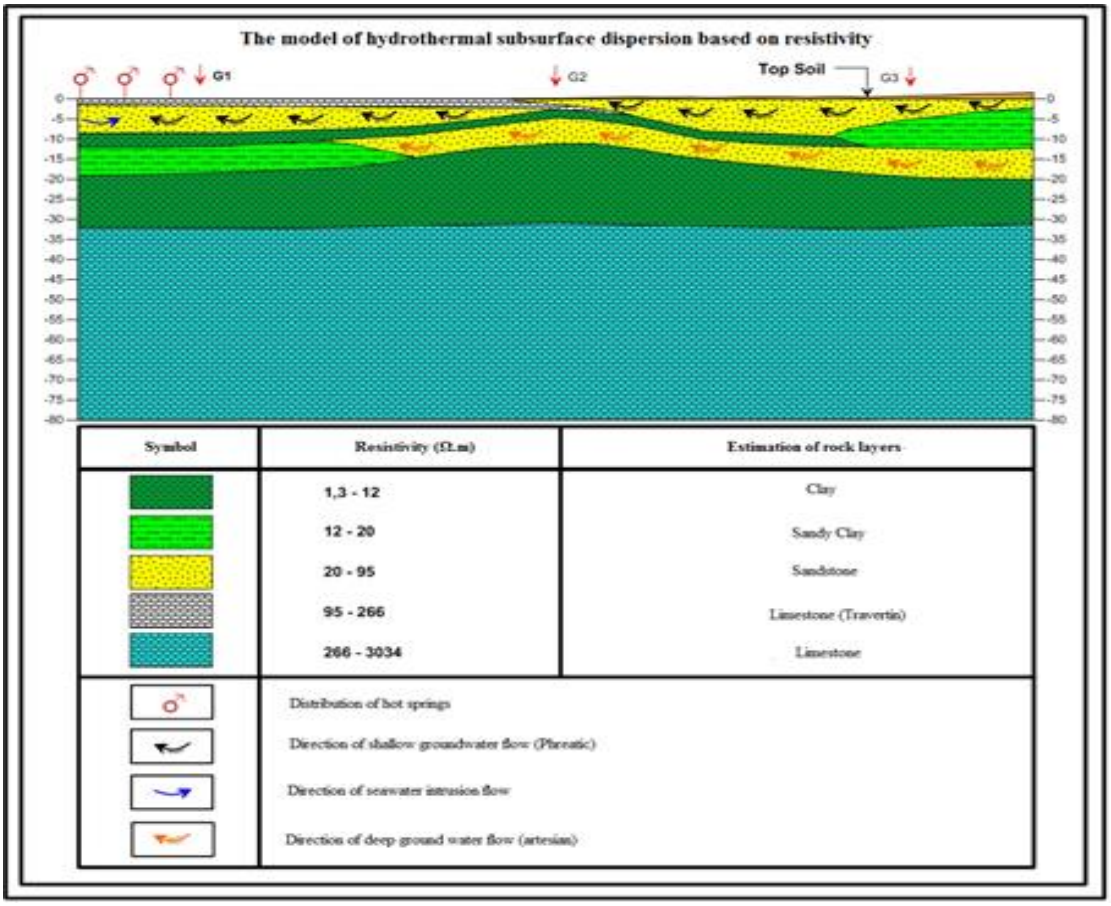

Figure 4 : Model of surface rock distribution of hydrothermal based on resistivity.

Groundwater flowing into the structural zone will be heated and pass through rock zones. The source of heat comes from the activity of geologic structure which is estimated to be active in the form of Lasolo shear fault. The ground water will continue to accumulate and heated, resulting in increased water temperature, increased volume, and increased pressure. Due to the constant pressure, temperature and volume of groundwater from below the Earth's surface due to geological structure activity, the hot fluid suppresses the rocks above it and seeks a breakthrough path to release the pressure. The hot fluid then breaks through the weak zones of the rocks above, resulting in a geothermal heat manifestation in the North-Northeast region.

The existence of manifestations in the Barasanga region in accordance with the results of the analysis of the manifestation of geochemical analysis of the six samples of hot springs that show the type of hot water chloride (chloride). Contains a higher chloride (Cl) element than other elements. And based on the result of physical analysis of hot springs with a surface temperature below 1000ºC that is with average about 480ºC and manifestation of geothermal in the form of travertine sedimentation is characteristic of the heat source of the non-volcanic area caused by the activity of geological structure in the form of Lasolo shear fault.

CONCLUSIONS

- Manifestations of surface geothermal, estimated to occur due to heat propagation from below the surface or due to fractures that allow the geothermal fluid to flow to the surface.

- Distribution surface rock layers are suspected as sandstone with resistivity values between 20-95 Ω.m from the southwest direction to the north-east of the Sea, with geothermal sources derived from geologic structural activity such as the Lasolo shear fault leading from the East to Northwest.

REFERENCES

Browne, P.R.L.. (1996), "Geothermal Exploration Technology Pre-advanced Class", 1-30.

Caine, J.S., Evans, J.P. and Forster, C.B. (1996), "Fault zone architecture and permeability structure", *Geology*, **24**, 1025–1028.

Faulkner, D.R., Jackson, C.A.L., Lunn, R.J., Schlische, R.W., Shipton, Z.K., Wibberley, C.A.J., Withjack, M.O. (2010), "A review of recent developments concerning the structure, mechanics and fluid flow properties of fault zones", *J. Struct. Geol*. **32**, 1557 – 1575.

Gudmundsson, A. (2000), "Active fault zones and groundwater flow" , *Geophys. Res. Lett*., **27**(18), 2993– 2996,

Hanano, M. (2000), "Two Different Roles Of Fractures in Geothermal Development", *Proceed.in WGC Kyushu- Tohoku Japan*, 2597-2602.

Hanano, M. and Kajiwara, T. (1999), "Permeability associated with natural convection in the Kakkonda geothermal reservoir", *Trans. Geotherm. Resour. Council* , **23**, 351-360.

Hochstein, M.P., and Browne, P.R.L. (2000), "Surface Manifestations of Geothermal Systems with Volcanic Heat Sources". *Encyclopedia of Volcanoes. Academic Press A Harcourt Science and Technology Company.*

Rivera, L.. (1995), "Reservoir Engineering Aspects Related To Injection". *Course on Injection Tech., IGA.*, 1-64.

Rusmana, E., Sukido, Sukarna, D., Haryono, E., Simandjuntak, T.O. (1993), "Keterangan Peta Geologi Lembar Lasusua – Kendari, Sulawesi, skala 1:250.000", Puslitbang Geologi, Bandung.

Soengkono, S. (1999), "The Kopia geothermal system (New Zealand) - the relationship between its structure and Extent". *Geothermics* **28**, 767-784.

STRUCTURAL GEOLOGY ANALYSIS USING REMOTE SENSING METHOD AND ITS CORRELATION TO GEOTHERMAL OCCURENCE AT LEBAK REGENCY, BANTEN

Rifqi Alfadhillah Sentosa, Hasbi Fikru Syabi, Iyan Haryanto

Departement of Geological Engineering, Faculty of Geological Engineering, Padjadjaran University.
Jl. Raya Bandung Sumedang Km. 21, Sumedang 45363 – Indonesia

e-mail: rifqi14008@mail.unpad.ac.id ; hasbi14002@mail.unpad.ac.id; iyan.haryanto@unpad.ac.id

ABSTRACT

Research area is located in Cibeber and Malingping District of Lebak Regency, Banten Province. The research location is located approximately 80 kilometers southwest of Jakarta. This area has a complex geological structure, as well as found many intrusive and metamorphic rocks. In this research area, geothermal manifestations were found in the form of four hot springs i.e. three Pamancalan hotsprings in Cibeber District, and Citando hotspring in Malingping District.

The method used is geological structure analysis of research area using remote sensing on ASTER-GDEM satellite imagery. Structural analysis methods performed in the form of lineament delineation, determination of lineament density and major trends, and application of wrench system model. The results of structural analysis will be correlated with the existense of geothermal manifestations with the aim of identifying the most influential structural patterns as the pathway for geothermal fluid to reach surface in the study area.

Structural analysis of study area shows major trends developed in study area are NS and EW trends. The result of delineation of lineaments is in the form of lineament density map which shows the distribution of high value density that is almost evenly distributed in all area of research. The study area also indicates compatibility with the concept of wrench fault and its structure model.

Pamancalan hot springs are associated with high value of lineaments density, which are 3600-4400 m/km2, associated with an NS oriented lineament and also associated with primary right lateral wrench in the model of the Wrench Fault model. Citando hot springs are associated with a very high density area of lineament density value, which is over 4800 m/km2. These springs are also associated with directional tendencies of NS and structures of the secondary left lateral wrench.

Keywords: Geothermal, Structural Geology Analysis, Surface Manifestation, Lineament Density, Bayah

INTRODUCTION

Lebak is a administrative area in the southern of Banten Province, adjacent to West Java Province at the east. This regency is located approximately 40 kilometers at the southwest of Jakarta. Geographically, Lebak Regency is located at coordinates 105 25 '- 106 30' BT and 6 18' - 7 00' LS. The northern part of this regency is lowlands, while in the southern part it is mountains with Mount Halimun at the southeast end. Ciujung River flows to the north, and is the longest river in Banten.

In the southern area of Lebak Regency, two districts is known to have geothermal manifestations, which are hot springs located in Cibeber and Malingping districts in the southeast and southwest of the regency respectively. Geothermal manifestation is an indicator of the underlying geothermal potential that formed when geothermal fluids find a path to reach the surface. Hot water in Cibeber district is found on the banks of river, flowing from rock slits. While hot water in Malingping district has been utilized by citizens to be used for bathing.

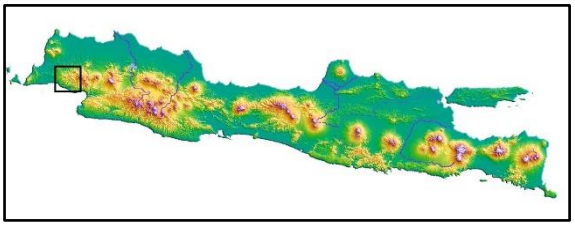

Figure 1. Lebak Regency as the study area

This study aims to determine the relationship between the structural geology that developed in Lebak Regency with its geothermal potential characterized by the existences of manifestations in the form of hot springs in Cibeber and Malingping districts. This research is expected to provide some of the preliminary data and descriptions for advanced geothermal research in the area, particularly regarding the understanding of the geological relationships of structures and geothermal manifestations.

GEOLOGICAL SETTING

Tectonic and Geological Structures

The geological structures in the western part of Java show different structural features in each region. This may occur due to different geological backgrounds in each region, such as the difference of inclination of Benioff Zones in each segment, to the reactivation of old fault by younger tectonics (Haryanto, 2013).

According to Haryanto (2013) Bayah area at the southern part of Lebak Regency is a series of sedimentary hills that have EW orientation extends to Walat in Sukabumi, West Java. This structure pattern is classified as the structure of Java Trends (Martodjojo, 1984 as cited in Haryanto, 2013).

This Bayah area is cut by two fault systems. The first system is a NNE-SSW oriented fault with almost vertical traverse direction. This first system is interrupted by the second system that trails EW. Along with this second system, the block from Bayah Complex has subsidenced in the south (Bemmelen, 1949).

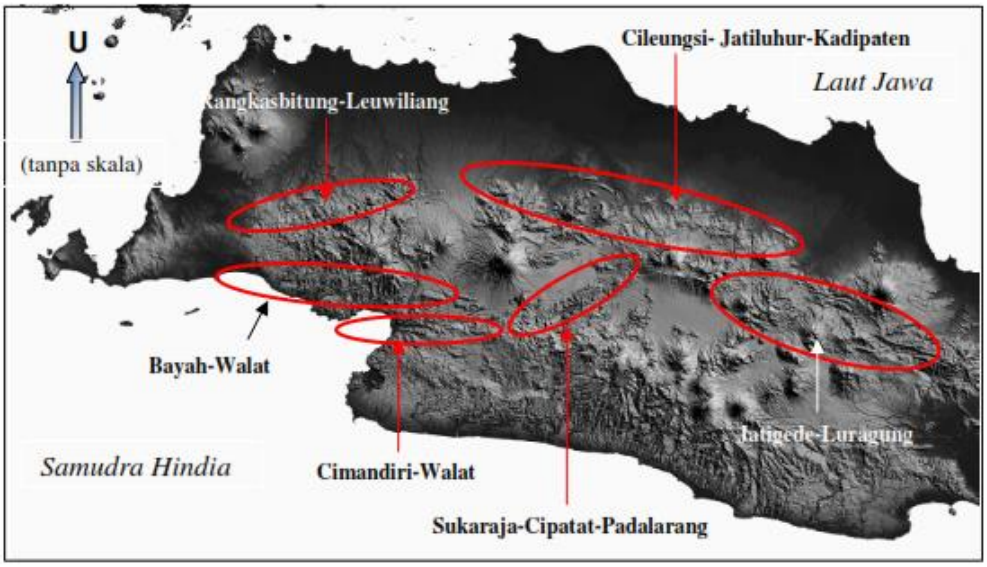

Figure 2. Bayah-Walat at the western side of Java Island has sediment hills with EW orientation (Figure after Haryanto, 2013)

Stratigraphy

The stratigraphy of study area according to Sujatmiko and Santosa (1992) in Geological Map of Leuwidamar Quadrangle, Jawa (1109-3) are composed from the youngest to oldest formations as follows:

- Alluvium (Qa): Pebble to mud
- Coastal deposits (Qc): Gravel to clay, detritus of corraline limestone and mollusk, reef limestone
- Quaternary volcanics (Qv), Basalt (Qb), Tapos breccia (Qvb), Halimun lavas (Qvl), Endut volcanics (Qpv)
- Bojong Formation (Qpb): Tuffaceouss sandstones, marl
- Cipacar Formation (Tpc): Tuffaceous sandtsones, breccia tuff, conglomerate, marl
- Citorek Tuff (Tpv), Malingping Tuff (Tpmt)
- Genteng Formation (Tpg): Pumice tuff, tuffaceous sandstones, breccia, conglomerate, marl
- Cimanceuri Formation (Tpm): Conglomerate, calcareous sandstones, dacitic tuff, breccia, limestone
- Cikasungka tuff (Tmkt): Tuff, silicified wood, tuffaceous breccia
- Andesite (Tma): basalt, diabase, hornblende andesite
- Bojongmanik Formation (Tmb): mudstone, limestone, sandstone
- Quartz diorite (Tmqd), Dacite (Tmda)
- Badui Formation (Tmd): Limestone, tuff
- Saraweh Formation (Tms): Limestone, claystone
- Cimapag Cimapag (Tmc): Limestone, tuff, claystone.
- Citarete Formation (Tmt): Limestone, tuff
- Cihara granodiorite (Tomg), Metamorphic rocks (Tomm)
- Cikotok Formation (Temv): Volcanic breccia, tuff, lava
- Cijengkol Formation (Toj): sandstone, conglomerate, breccia, tuff, and coal seams
- Ciracurup Formation (Tet): sandstone
- Bayah Formation (Teb): Sandstones, limestone, claystone, dan conglomerate

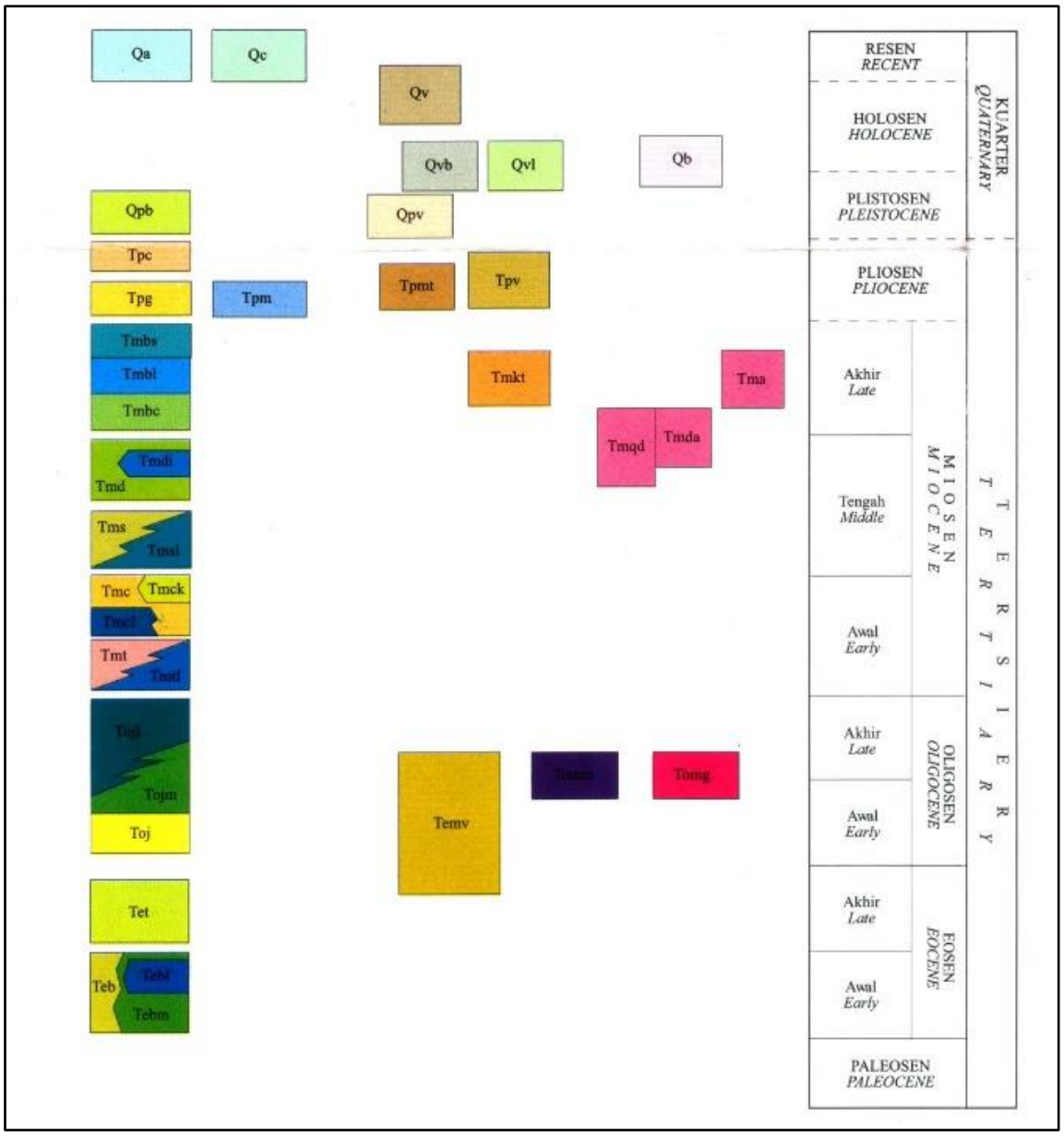

Figure 3. Stratigraphy of formations in study area (after Sujatmiko & Santosa, 1992)

METHODOLOGY

The structural analysis methods used in this research use remote sensing method on ASTER-GDEM satellite imagery. Stages in structural analysis are done in the form of lineaments delineation, determination of lineament density, determination of main trend and application of Wrench Fault Concept by Moody and Hill (1956) to regional area of research. The results of this analysis will be attributed to the presence of geothermal manifestations in the research area. The result will be a conclusion about the structure associated with the manifestation.

Lineaments Delineation

Lineaments delineation performed on satellite imagery is done using hillshading technique. Hillshading is a technique used to recognize lineament with visualize terrain as shaded relief. Digital elevation model represented from four illumination directions to optimize the delineation step. The four angles of illumination that is 0º, 45º, 90º, and 315º will support each other in showing the delineations in the image. Methods with this technique can be accessed on GIS software such as MapInfo and ArcGIS.

Lineament Density

This analysis show the concentration of the lineaments that has been delineated from the previous stage. This method calculates the frequency of the lineaments per unit area (length/km^2) that will produce an lineament density map. The grid sections will be counted in length in each grid box of 2 km x 2 km and then the result of the calculation is represented by a middle point at the center of each grid. The results of the representation will be made contours that show the large concentration of contour obtained.

Major Trend Determination and Wrench Fault Concept Application

The concept of Wrench Fault is a concept devised by Moody and Hill (1956) about the primary compression stress and its relationship to the structural elements formed in an area. This concept states that if a homogeneous isotropic material is subjected to a compression force, the material will experience wrench at an angle of 30º to the direction of the maximum principal compressive stress to which it is involved.

This assumption considers several things, such as lineament orientation, slip direction of the lineament, and literature study from regional geological map of research area by Sujatmiko and Santosa (1992). The purpose of this analysis is to know the direction of the main stress that causes the development of structural pattern, the properties of the geological structure associated with the geothermal manifestation in the research area, as well as to know to know the dominant orientation of the lineament with the help from data analysis from previous steps

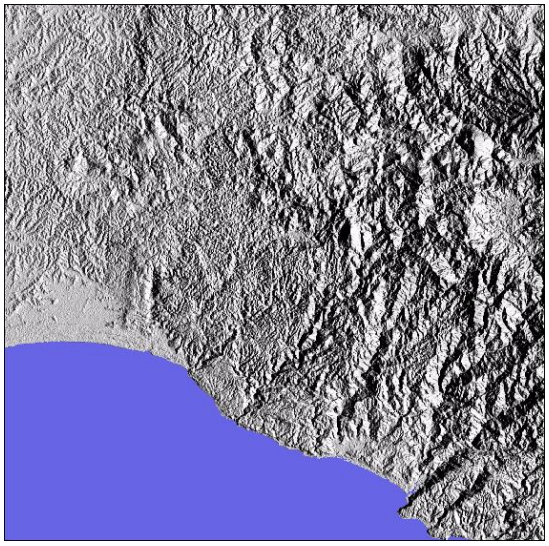

Figure 4. ASTER-GDEM satellite image from research area with a width of 50 km x 50 km. Approximately 30% of the research area is the Indian Ocean (blue color) that goes into the study area, but will not be the target of the structural analysis

.

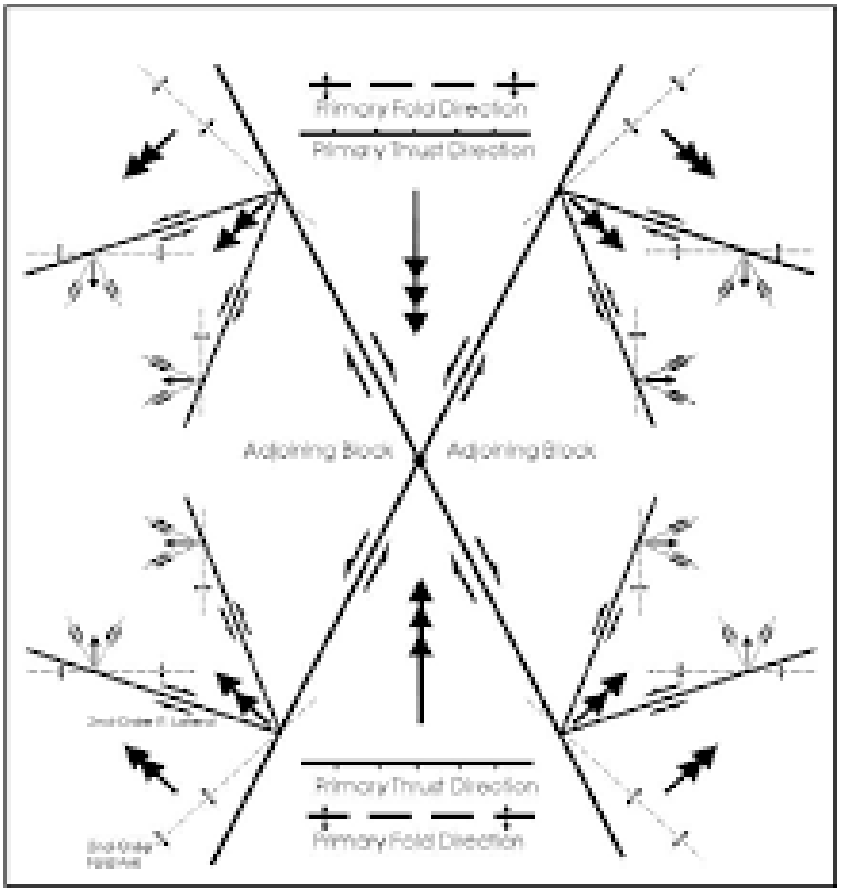

Figure 5. Model of Wrench Fault Concept (Moody & Hill, 1956)

RESULT AND DISCUSSION

Lineament Delineation

Lineaments delineation is done on all the possible lineaments that can be recognized on satellite imagery in a designated study area, utilizing four angles of illumination that cause all lineaments to be visible. The results of this method can be seen in Figure 6.

A total of 1398 lineaments were drawn at this stage and assumed to represent all areas of the study area. Delineation with a light angle of 0º has more lineaments delineated than the other three illumination angles, with 606 lineaments. Delineation with 45º illumination angle resulted in 221 lineaments, 90º angle resulted in 329 lineaments, and 315º angles resulted in 243 lineaments.

The results of all lineaments delineation are compiled into one for use in the analysis and construction of lineament density maps.

Lineament Density

The result of a lineaments compilation that has been drawn in the previous stage is a map showing the lineaments length per unit area (length / km2) using a 2x2 kilometer grid in each of each box. The map can be seen in figure 7.

The lineament density map shows a nearly equal distribution of lineaments across the study area. Areas with high densities are shown as orange to red zones on the map, which is more than 3600 m / km2.

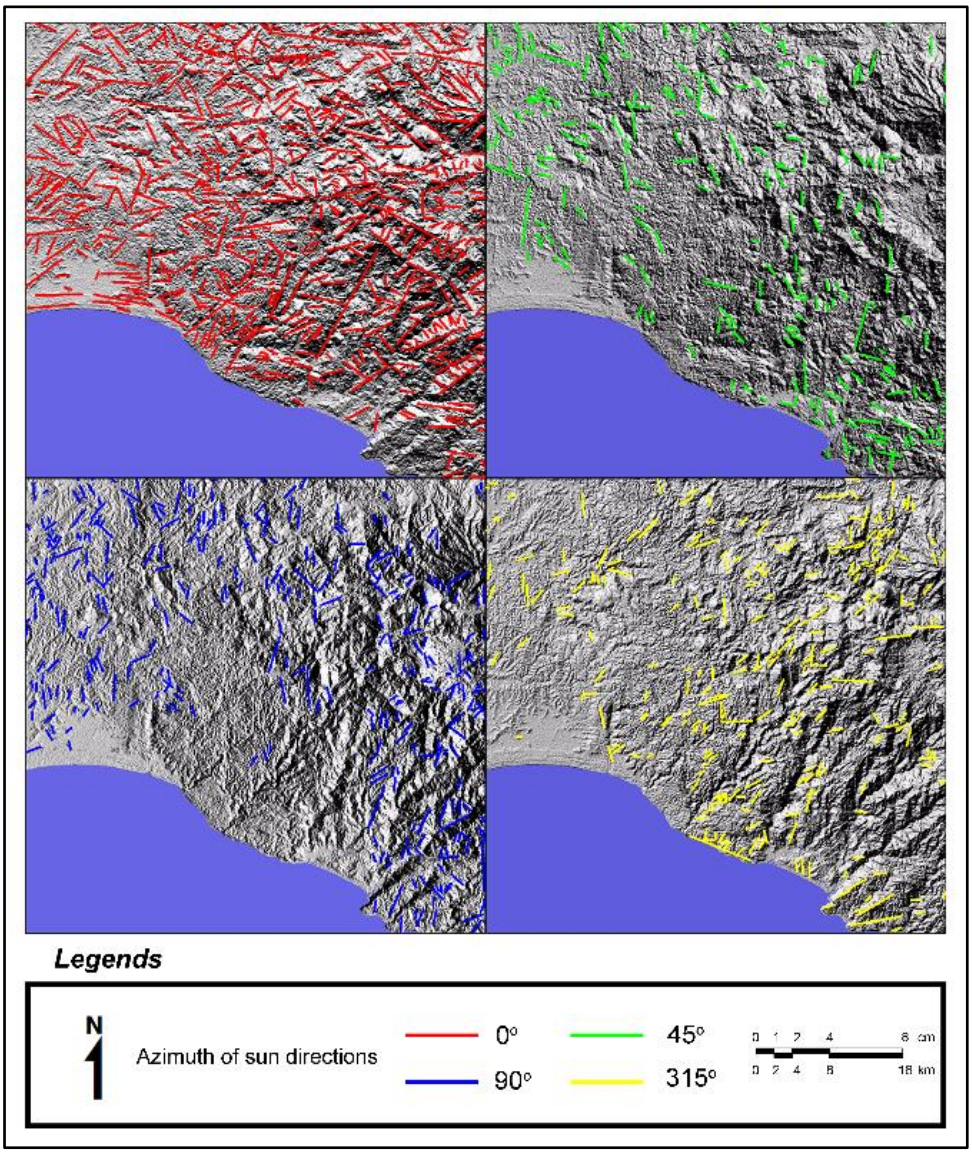

Figure 6. Results of lineaments delineation method from four different illumination directions, i.e. 0º, 45º, 90º, 315º.

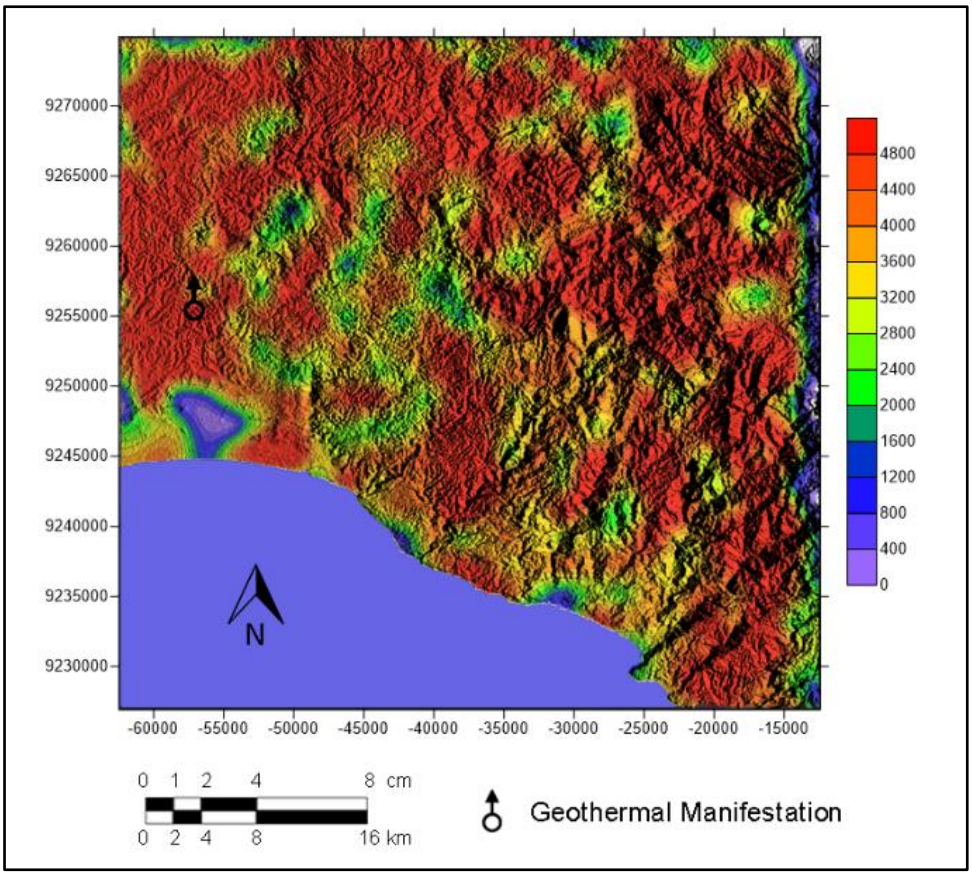

Figure 7. Lineament density map

Major Trend Determination

Results from the analysis of the two previous stages were used in determining major trends in the study area. All of delineation step results are compiled and Rose diagrams are made to find out the dominant orientation of the lineament drawn.

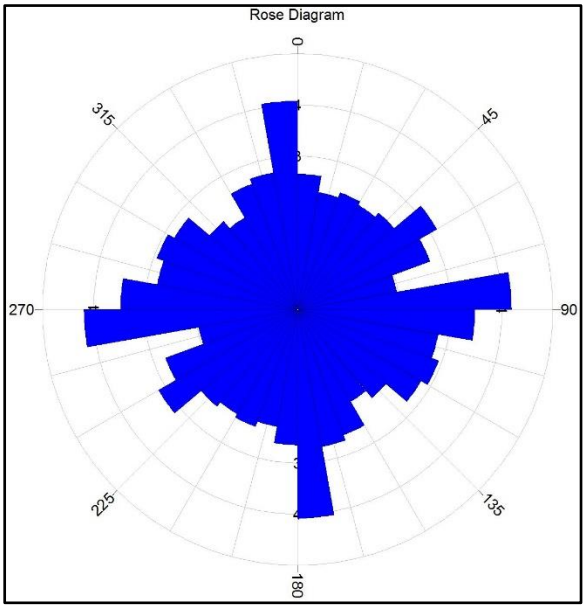

Figure 8. Rose Diagram of study area

Rose diagram above shows two trends of lineament that dominate the abundance in the research area are the NS and EW directions. These two main trends shown in the diagram to have the same dominance.

The EW trends are assumed to be associated with the Java Trends with the same orientation. According to Haryanto (2014) the pattern of EW structures began to form at Early Tertiary due to a new fault that is formed, not from the reactivation of old faults. This pattern controls highs and low lands in Java, including foreland basin, accretional prism, volcanic arc, and back arc (Haryanto, 2014).

The NS trends are assumed to be associated with the Sunda Pattern. This pattern is dominant in the western part of Java Island, while in the east it is hardly visible. According to Haryanto (2014) this structure pattern began to form at the beginning of Paleogen and control the distribution of Eocene sediments and early Miocene in Java.

Wrench Fault Concept Application

In the model of the Wrench Fault concept of Moody & Hill (1956) the three-way stresses effect of compression will produce wrench of varying scales. Order 1 represents the primary wrench that has an angle of approximately 30 º to the direction of the main firm. Order 2 represents secondary wrench. Order 3 is a continuation of Order 2 but not applied in the current study because it is difficult to distinguish the difference from order 1 in the study area. In addition, primary thrust and primary fold was applied in this study. The position of every said elements can be seen at Figure 9.

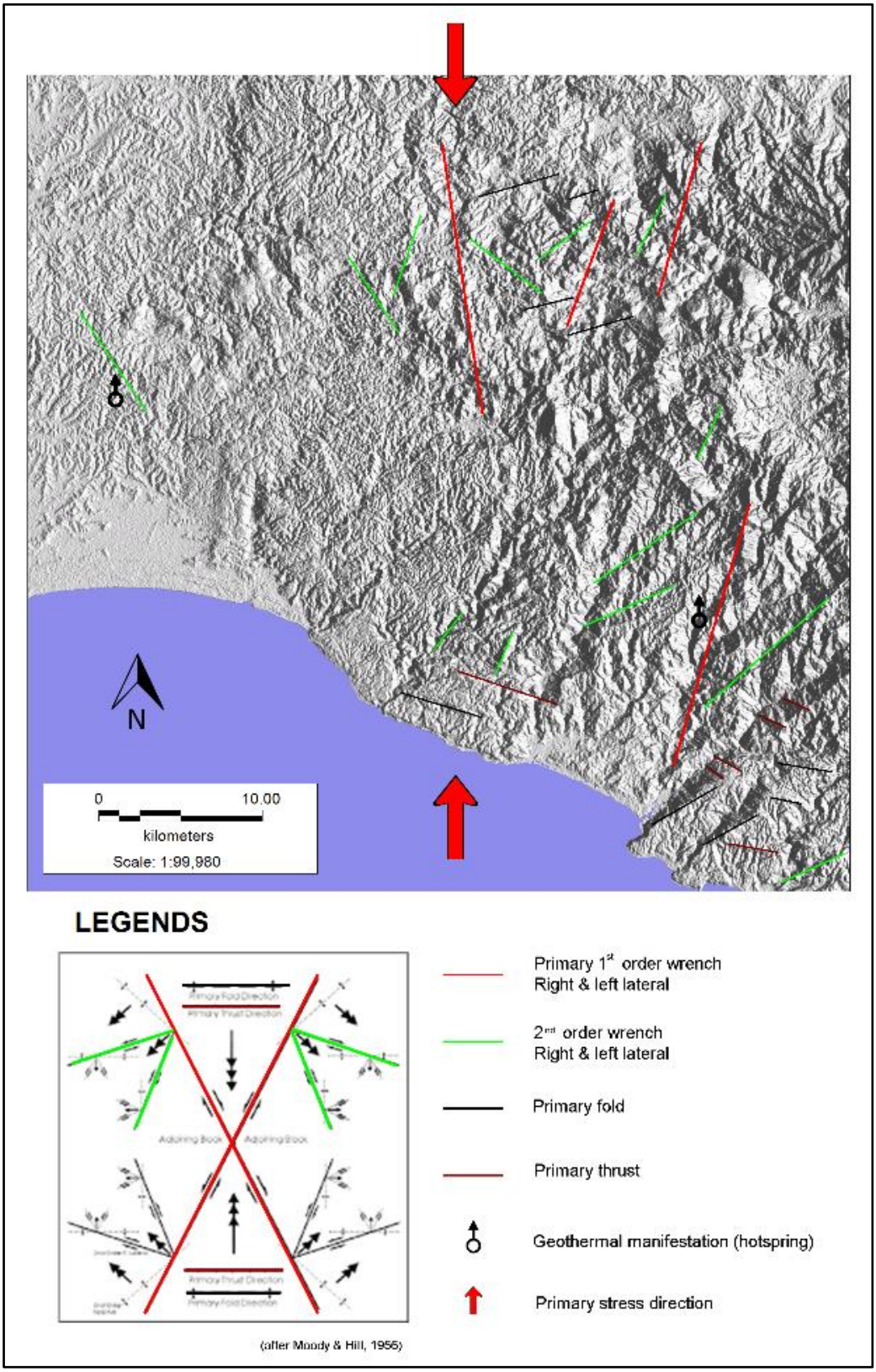

Figure 9. Application of Wrench Fault Concept (Moody and Hill, 1956) in study area

The figure contains the application result of Wrench Fault concept in study area. Four large red lineaments i.e. three NE-SW directional majors are assumed to be primary right lateral wrench and one direction of NW-SE is assumed to be primary left lateral wrench. These four lineaments form an angle of approximately 10º - 30º with NS direction.

The green lines on the map represent the secondary wrench. NNE-SSW and WNW-ESE directional alignment is assumed to be a secondary right lateral wrench. While the orientation of the oriented ENE-WSW and NNW-SSE is assumed to be a secondary left lateral wrench.

The black line is assumed to be the primary fold due to the main stress. While the brown line is assumed to be the primary thrust. In the study area, primary fold and primary thrust are tend perpendicular to the NS direction.

Looking at the results of the concept application, it can be deduced that the main direction of compression stress of the research area is from NS direction, according to the fault and fold in the model orientation. The red line that is assumed to be the primary fault forms an angle of ± 30 º with NS direction. The green colored lines that are assumed to be secondary fault have an orientation that corresponds to the Wrench Fault concept model. Similarly, the primary fault and primary fold that are perpendicular to the direction of main stress direction make the interpretation more convincing.

Geothermal Manifestation

Manifestations in the research area are located in two districts, namely Cibeber District in the southeast and Malingping District in southwest of Lebak Regency. Through the structural analysis that has been done, these two manifestations show a relationship with the existing majors.

Pamancalan hot springs are located in Sukamulya, Cibeber District, located in the southwest region of Lebak Regency. Pamancalan hot springs are divided into three springs. The first hot spring come out of the rock gap and spread over 20 meters. The second hot spring located across the location of the first hot spring. While the third hot spring is on the river bank.

Citando hot spring is located in the village of Senang Hati, Malingping District, located in the southeastern region of Lebak Regency. At this spring there is precipitated iron oxide and sinter carbonate. These hot springs have been utilized for baths.

On the lineament density map, the Pamancalan hot springs are in the orange contour area, indicating areas of high density value of lineament, ranged about 3600-4400 m/km^2. While Citando hot springs appear on red contours that indicate the highest value of lineament density, which value is over 4800 m/km^2.

Based on the determination of the major trends, hot springs Pamancalan and Citando seems to associated with lineaments that tends to orient toward the NS. This trend is one of the main trends that the development is dominant in the research area.

Based on the results of the Wrench Fault model application, the Pamancalan hot springs have an association with the lineament that is assumed to be the primary right lateral wrench. While the Citando hot spring has an association with the lineament that is assumed to be secondary left lateral wrench.

CONCLUSION

Distribution of lineaments and structural patterns are important parameters for permeable zones indicated by geothermal manifestasion occurrence. The research area shows a good distribution of lineaments with almost all of research areas fall into the category of high lineaments density of above 2000 m / km^2. The study area shows the main trends of directional directional NS and EW, which are assumed to be associated with Sunda Trends and Java Trends, respectively. The study area also showed compatibility with the Wrench Fault system model from Moody and Hill (1956) with the main stress of NS direction.

Pamancalan hot springs are associated with high value of lineaments density, which are 3600-4400 m/km^2, associated with an NS oriented lineament and also associated with primary right lateral wrench in the model of Wrench Fault model.

Citando hot spring is associated with a very high density area of lineament density value, which is over 4800 m/km^2. This spring is associated with a lineament with NNW-SSE directional tendencies and also with secondary left lateral wrench.

ACKNOWLEDGEMENT

The authors would like to express sincerest gratitude to Yuda Maulana, Santy Liesdayanty, and Agil Gemilang Ramadhan for very helpful advices during the writing of this paper. The authors also would like to thank every KKNM participant at Mulyasari, Losari District, Cirebon who have been supporting author during the writing of this paper.

REFERENCES

van Bemmelen, R. W. The Geology of Indonesia vol. IA : General Geology of Indonesia and Adjacent Archipelagoes, (second edition 1970 – reprint), Martinus Njhoff, The Hague.

Harding, T. P., Lowell, J. D. Structural Styles, Their Plate-Tectonic Habitats, and Hydrocarbon Traps In Petroleum Provinces. The American Association of Petoleum Geologists Bulletin V.63 No. 7 (July 1979) P. 1016-1058.

Haryanto, I., Sunardi, E., Sudrajat, A., Abdurrokhim & Jamal. Plate Tectonic and Regional Structural Geology in West Java. 1st International Conference – Geoscience for Energy, Mineral Resources, and Environment Applieds 2014.

Haryanto, Iyan. Struktur Sesar di Pulau Jawa Bagian Barat Berdasarkan Hasil Interpretasi Geologi. Bulletin of Scientific Contributoion, Volume 11, Nomor 1, April 2013: 1-10.

Patonah, A., Syafrie, I., Ayasa, H. & Permana, H. New Perspective on High Grade Metamorphic Regional in Bayah Complex, Banten Province. 1st International Conference – Geoscience for Energy, Mineral Resources, and Environment Applieds 2014.

Patonah, A., Helmi, F., Prakoso, J. & Widiaputra, T. Basement Komplek Bayah, Kabupaten Lebak, Propinsi Banten. Bulletin of Scientific Contribution, Volume 13, Nomor 3, Desember 2015: 182-191.

Sujatmiko, Santosa, S. Geological Map of The Leuwidamar Quadrangle, Jawa. 1992. Geological Survey. Bandung.

Geological Resource Center Survey Team. Survei Terpadu Geologi Dan Geokimia Daerah Panas Bumi Pamancalan Kabupaten Lebak, Provinsi Banten. 2011. Geological Resource Center Library.

A CONCEPT OF RELIABILITY CENTRED MAINTENANCE APPLIED TO GEOTHERMAL POWER PLANT

Hari Agung Yuniarto[1], Ruly Husnie Ridwan[2], Khasani[1], Imam Bhaskara[3]

[1]Dept. of Mechanical and Industrial Eng. UGM, Yogyakarta, Indonesia
[2]PT Geo Dipa Energi (Persero), Jakarta, Indonesia
[3]PT Pertamina (Persero), Jakarta, Indonesia

e-mail: h.a.yuniarto@ugm.ac.id

ABSTRACT

In pursuance of increasing power plants' competitiveness in energy market, these power plants need to embrace a proper operating and maintenance methodology in order to lessen the level of O & M (operation and maintenance) costs. Similar to this, Geothermal Power Plants ought to embrace as well the corresponding strategy, so that they can vie for their productivity and competitiveness. The prominence methodology needed should be able to achieve the equipment's availability at maximum level whilst attaining cost of maintenance at optimum level. Reliability is a parameter which is successfully used to serve as a warning signal for maintenance managers to respond to the lower level of availability. This paper demonstrates the application of Reliability Centred Maintenance (RCM) in Geothermal Power Plants. A case study of a geothermal power plant in Dieng - Central Java, Indonesia- operated by PT. Geo Dipa Energi was conducted. In this research, a framework for the implementation of RCM into Geothermal Power Plants was developed. The results include recommendations for 52 maintenance tasks to eliminate 36 malfunction of equipment that never happened, in the form of four lubricating task, four visual check task, 15 inspection tasks,18 scheduled restoration task, one scheduled discard task, and 10 no scheduled maintenance task.

Keywords: RCM, geothermal power plant, maintenance, assets management

INTRODUCTION

Indonesia is one country in the world that have high levels of production and generating capacity of geothermal power is great. According to the US. Energy Information Administration (US. Energy Information Administration, 2015), Indonesia is ranked third, after the United States and the Philippines, as the country with the level of production of electricity and geothermal power generation capacity by 2014. Currently, Indonesia is able to generate electrical energy for 1.3 gigawatts of all geothermal power plants in Java, Bali, North Sumatra and North Sulawesi. According to the Ministry of Energy and Mineral Resources (Ministry of Energy and Mineral Resources, 2014), the amount of electrical energy generated currently uses only five percent of a total of 29 gigawatts of electric potential that can be generated from geothermal power. Seeing the potential of electrical energy produced from geothermal power in Indonesia is still very large, the potential development of geothermal power plants in Indonesia is expected to grow rapidly.

In pursuance of increasing power plants' competitiveness in energy market according to Misra (Misra, 2008), these power plants need to embrace a proper operating and maintenance methodology in order to lessen the level of O & M (operation and maintenance) costs. Similar to this, Geothermal Power Plants ought to embrace as well the corresponding strategy, so that they can vie for their productivity and competitiveness. The prominence methodology needed should be able to achieve the equipment's availability at maximum level whilst attaining cost of maintenance at optimum level. Reliability is a parameter which is successfully used to serve as a warning signal for maintenance managers to respond to the lower level of availability (Moubray, 1997). These problems can arise due to many factors, ranging from the life of the equipment, maintenance procedural error, until contact between the equipment and the working environment and equipment continuously. Based on research conducted by Akar and his colleagues (Akar, et al., 2013), there are five maintenance problems are most common in geothermal power plants, namely corrosion, defects in the installation, maintenance errors, defects in electronic components, and the issues that have an impact on the environment.

Some researchers are trying to find solutions to the problems in geothermal power plants. Bore in 2018 (Bore, 2008) investigated the comparison between the methods of management *(six-sigma,* RCM, and *lean* maintenance) used in the maintenance system with AHP and *cost* modeling. Kariuki in 2013 (Kariuki, 2013) researched the relationship between the *operation and maintenance costs* and *outages forces* on the *availability* of equipment in geothermal power plants. Adele in 2009 (Adele, 2009) examines the evaluation methods for systems of geothermal power plants with a method of *benchmarking* with other geothermal power plants. Unfortunately, to date no single study has offered a systematic procedure of applying RCM (Reliability Centred Maintenance) to geothermal power plants.

This paper demonstrates the development of a framework for implementing RCM to a geothermal power plant. A case study of a geothermal power plant in Dieng - Central Java, Indonesia- operated by PT. Geo Dipa Energi was conducted.

RESEARCH METHOD

The first step in this research is to conduct literature study which includes gathering information and knowledge related to this research, that is RCM method as compilation of maintenance system built in this research, geothermal power plant system as a research object and historical data of maintenance at PT. Geo Dipa Energi - Dieng Unit. Literature studies on geothermal power plant system generate knowledge about the types of plants, equipment that work on each type of the plant, how each type of plant works, and common problems occur in a

geothermal power plant system. The literature study of RCM produces knowledge and steps that must be taken in designing an integrated systematic maintenance system. Literature study of historical data of maintenance at PT. Geo Dipa Energi - Dieng Unit - produces operation procedure on geothermal power plant systems, equipment working on geothermal power plant and documents of historical data of equipment failure.

Next step is to develop framework for implementing RCM to the geothermal power plant. And parallel to this is to collect data of existing maintenance system at PT Geo Dipa Energi - Dieng Unit. Whilst the framework is established and the existing maintenance data is available, RCM is then applied to the geothermal power plant at the case study company. The following step is a stage where a web-based database software is built. This devised software will be used to store the input documents required by the maintenance system. The developed database software aims to support the maintenance system for recording documents that were initially done manually changed to online so that the resulting maintenance system could be more effective and efficient. Figure 1 shows all steps of the research method explained above.

RESULTS AND DISCUSSIONS

The devised framework for implementing RCM to a geothermal power plant consists of three parts namely Input, Process and Output. As can be seen in Figure 2, the inputs used (Input) at the beginning of implementation of a maintenance system (Process) come from all documents generated during the implementation of the systematic RCM programme which is comprised of eight activities (see Figure 3). In the Process, the maintenance tasks that have been selected in the final outcome of the systematic RCM programme are applied accordingly, so that it is expected the maintenance activities could effectively improve reliability of the system to be maintained and optimally solve the existing maintenance problems with cost efficient (Output).

The implementation of the devised framework alongside the systematic RCM programme on the case study company results in the selection of 52 particular maintenance tasks comprised of 4 *lubricating task*, 4 *visual/operational check tasks*, 15 *inspection/functional check tasks*, 18 *scheduled restoration tasks*, 1 *scheduled discard task*, and 10 *no scheduled maintenance tasks*. The results of implementation are represented by certain parameters which are tabulated in Table 1. Four parameters are measured to assess performance of the RCM based maintenance system applied to the geothermal power plant of PT. Geo Dipa Energi - Dieng Unit - in which they are *the number of equipment failure, mean time between failure, availability* and *average kWh loss per day*. Compared to the performance before the RCM based maintenance system was implemented, the results after implementation shows that *the number of equipment failure* decreases, MTBF increases, *availability* increases as well as *average kWh loss per day* decreases as illustrated in Figure 4. In conclusions, Figure 4 provides evidence that performance of the case study's geothermal power plant shows an upward trend.

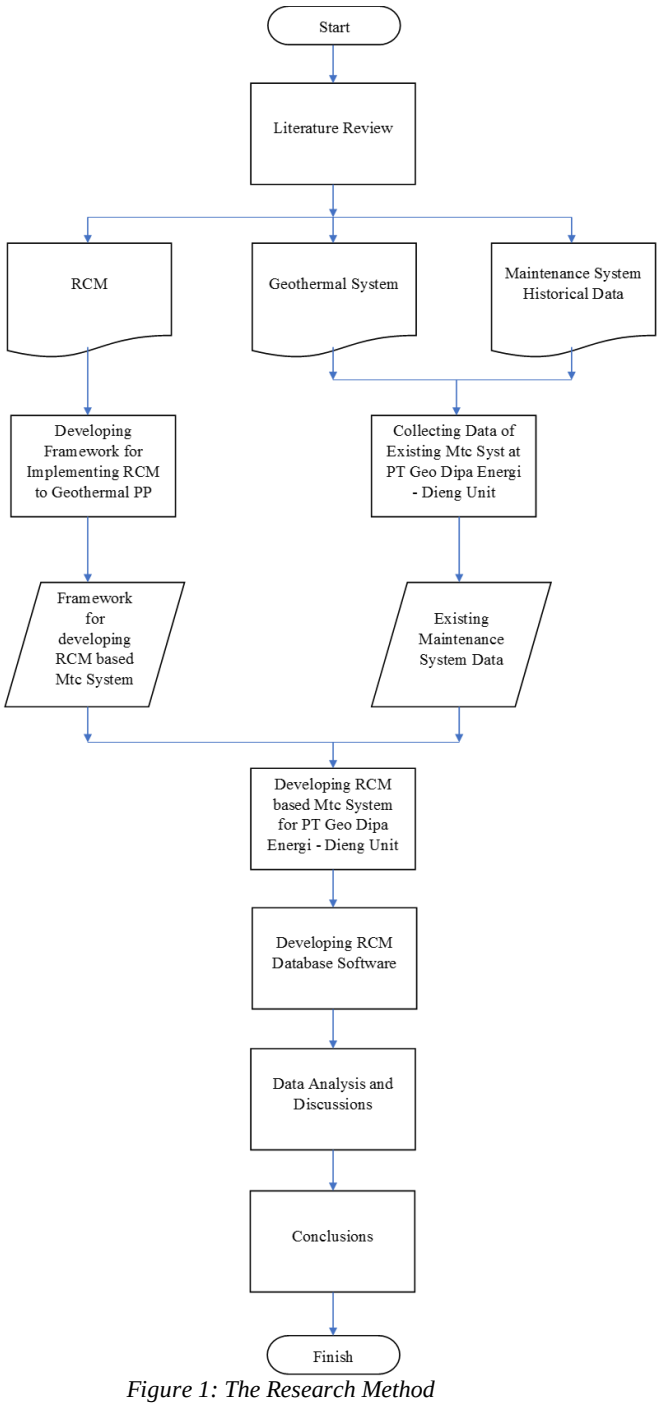

Figure 1: The Research Method

Table 1: The Implementation Results of RCM based Maintenance System

No	Parameters	Results (Nov 2016 – Mar 2017)
1	The number of equipment failure	4
2	Mean Time Between Failure (day)	33
3	Availability (%)	98,79
4	Average kWh loss/day (kWh)	8.911

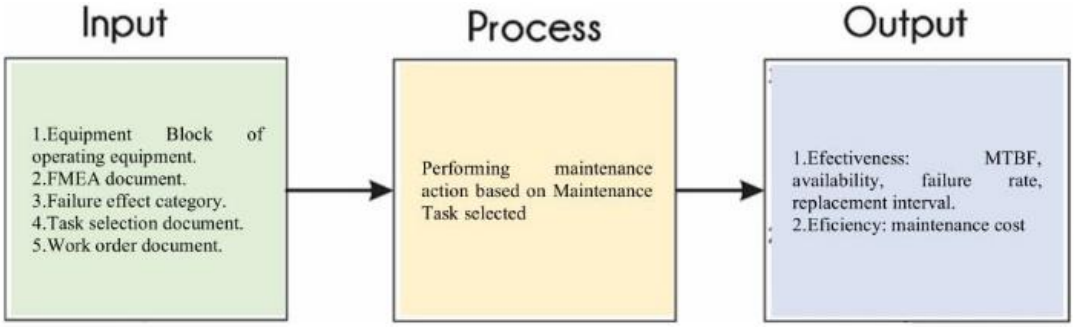

Figure 2: The Framework of RCM Implementation

CONCLUSIONS

A devised framework for implementing RCM to geothermal power plants alongside its systematic RCM programme has been well established. Once validated in the case study company, it can help select 52 appropriate maintenance tasks comprised of 4 *lubricating task*, 4 *visual/operational check tasks*, 15 *inspection/functional check tasks*, 18 *scheduled restoration tasks*, 1 *scheduled discard task*, and 10 *no scheduled maintenance tasks*. The results of implementation show an upward trend in the performance of the case study's geothermal power plant compared to the condition before the devised framework was implemented. Those parameters of performance are represented by *the number of equipment failure, mean time between failure, availability* and *average kWh loss per day.*

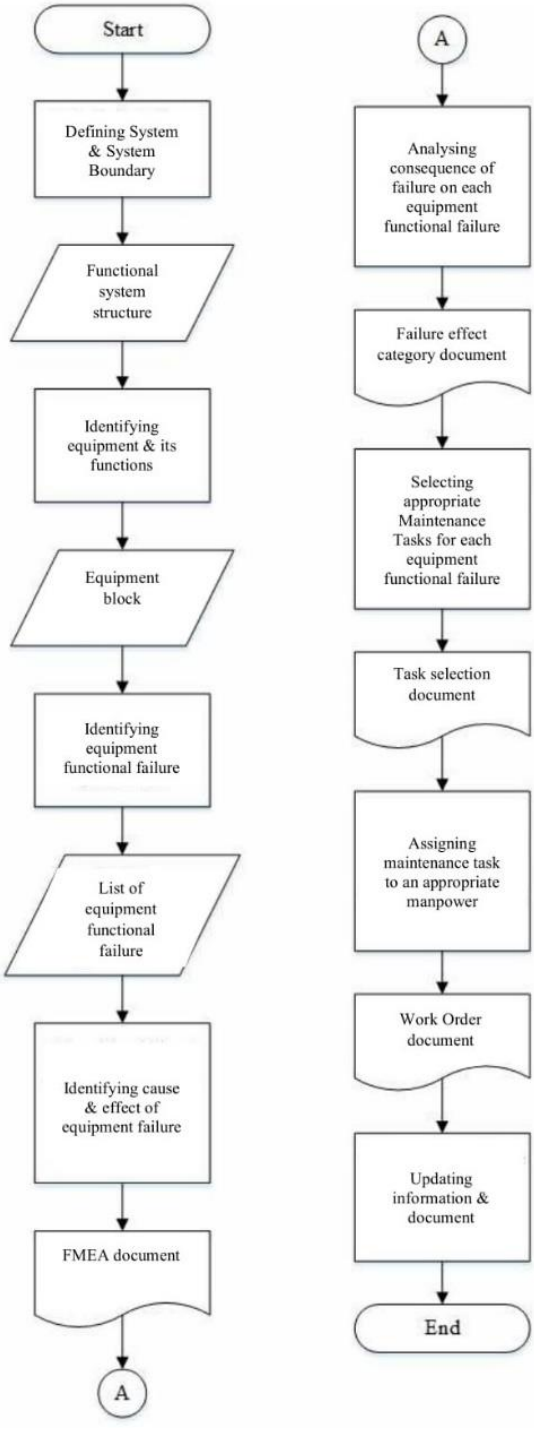

Figure 3: The Systematic RCM Programme

ACKNOWLEDGMENT

The authors wish to acknowledge full support of The Geothermal Capacity Building Programme - Indonesia-Netherlands (GEOCAP) for the accomplishment of this research. The authors also appreciate the comments and suggestion on this work from Bart in't Groen, Koen Broess and Kees van den Ende of DNVGL Netherlands.

REFERENCES

Adele, M. A., 2009. *Evaluation of Maintenance Management Through Benchmarking in Geothermal Power Plant*, Iceland: United Nations University.

Akar, N. et al., 2013. Risk Analysis of Geothermal Power Plants Using Failure Modes and Effects Analysis (FMEA) Technique. *Energy Conversion and Management*, Volume 72, pp. 69 - 76.

Atlason, R. S., Oddsson, G. V. & Unnthorsson, R., 2014. Geothermal Power Plant Maintenance: Evaluating Maintenance System Needs Using Quantitative Kano Analysis. *Energies*, Volume 7, pp. 4169 - 4184.

Bore, C. K., 2008. *Analysis of Management Methods and Application to Maintenance of Geothermal Power Plants*, Iceland: United Nation University.

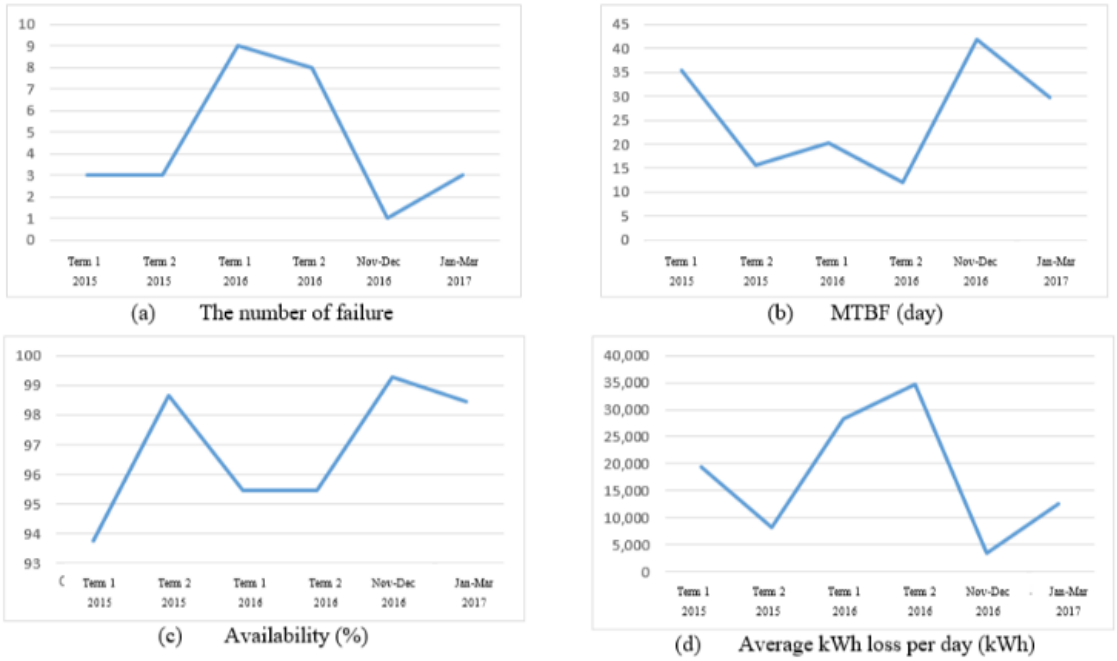

Figure 4: Before and After Implementation

Kariuki, S. K., 2013. *Maintenance Practice and Performance of Power Sector in Kenya*, s.l.: University of Nairobi.

Ministry of Energy and Mineral Resources, 2014. *Handbook of Energy & Economic Statistics of Indonesia.* Jakarta: Pusdatin ESDM.

Misra, K. B., 2008. Maintenance Engineering and Maintainability: An Introduction. In: *Handbook of Performability Engineering.* London: Springer-Verlag, pp. 755 - 772.

Moubray, J., 1997. *Reliability-Centered Maintenance.* 2nd ed. New York: Industrial Press.

US. Energy Information Administration, 2015. *Indonesia has significant potential to increase geothermal electricity production.* [Online] Available at: https://www.eia.gov/todayinenergy/detail.cfm?id=23392

ISBN 978-602-52132-0-5

FRONTIER FLUID INJECTION MANAGEMENT IN DIENG GEOTHERMAL FIELD TO PREVENT SILICA SCALING: EFFICIENCY FOR GREATER OPTIMAL PRODUCTION

Muhammad Ali Akbar Velayati Salim, Navendra Chista Yogatama, Arief Budiman Ustiawan

Geological Engineering Department, Universitas Diponegoro
Universitas Diponegoro, Jalan Prof. Soedarto, Tembalang, Semarang, 50275, Jawa Tengah

e-mail: research.aliakbar@gmail.com; navendra100@gmail.com; arief.lord@gmail.com

ABSTRACT

As a severe production issue in Dieng geothermal field, silica scaling has been a major threat in various hydrothermal field dominated with water, thus affecting severely on production and electricity generation of the field. To overcome the damaging effect of silica scaling, an innovative and suitable fluid injection management is a must. This research is conducted by gathering geothermal field data from previously observed fields and comprehensive data analysis in order to achieve the best possible solution. The amount of silica deposition is estimated by calculating the difference between dissolved SiO2 with the solubility of amorphous silica curve. At 180°C and 160°C, the induction time for polymerization was not reached. Scaling rates were 0.2 to 0.3 mm/yr at 180°C (assuming density 2.2), increasing to 0.3 to 0.4 mm/yr at 160°C. At 140°C and 120°C, there was measurable polymer formation, even at the pipe inlet, and the polymer concentration increased through the pipeline; the increase at 120°C was twice that at 140°C. Therefore, scaling in the pipeline decreased dramatically along the length of the pipe, as monomeric SiO2 was removed from solution into the suspended polymer. In all cases, the scale which formed was hard and glassy, with density about 2 gm/ cc. Accordingly, researchers found that the deposition process of silica scaling in Dieng Geothermal Field highly depends on temperature and fluid pH. With those dependence in mind, it is possible to assume low-level scaling confidently enough for purposes regarding production, injection system and mechanism. This can be achieved by suppression technology with the main purpose is to reduce the pH of the fluid by mixing with non-condensable gases and steam condensate. Improved developments in the future on predictive technique will result in uniformity in data collection and experiment design.

Keywords: Fluid injection management, Dieng, silica scaling, temperature, solubility.

INTRODUCTION

Dieng Plateau is located on the border between Wonosobo regency and Banjarnegara regency with an area of 620 hectares surrounded by cluster of mountains such as Mount Sumbing, Mount Sindoro, Mount Perahu, Mount Rogojembangan and Mount Bismo. Dieng Plateau is a caldera with volcanic activity beneath its surface. Dieng geothermal field which is managed by PT. Geo Dipa Energi has two locations of Geothermal Power Plant Complex. The field is located in the Dieng volcanic plateau at an altitude of more than 2000 meters (Layman et al., 2002).

In general, geothermal system is divided into two categories: vapor domination system and water domination system. Dieng Geothermal Field is in the water dominated category with its fluid production composition is 60% water and 40% steam. As a severe production problem at Dieng geothermal field, silica scaling has become a major threat in various hydrothermal fields dominated by water, which greatly affects production and power generation in the field. Scaling is a precipitate or crust derived from mineral salts dissolved in water on a particular contact medium which results in scaling of the contact medium, for example the reduction of pipe diameter or even total blockage of the pipe. Dieng field geothermal fluid production which has a high silica content of ± 900 mg/L. The silica content of high production fluids causes silica scaling problems in geothermal steam production wells and in the brine injection path at Dieng geothermal field.

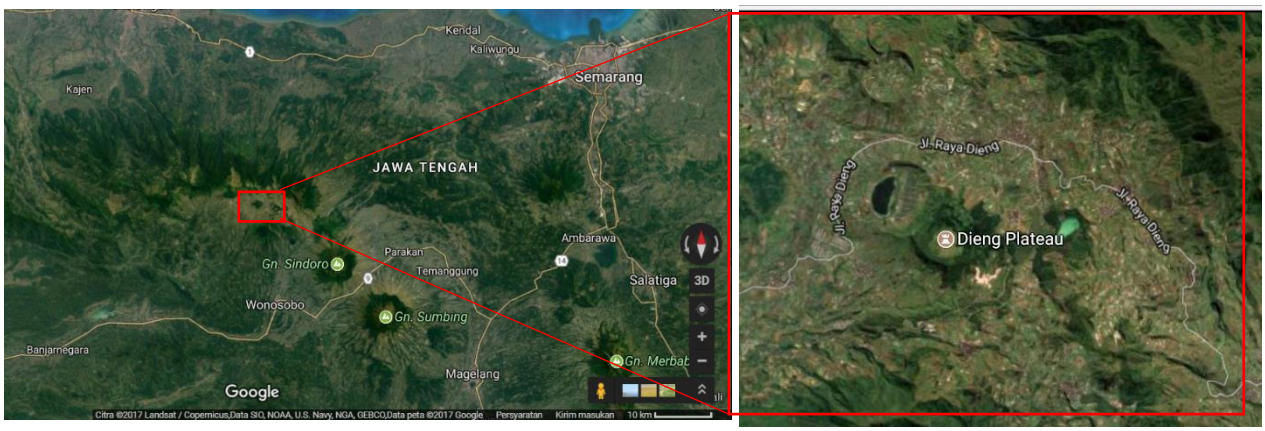

Figure 1: Dieng Plateau Location

Figure 2. Silica Scaling at Dieng field (Felix Arie Setiawan, 2015)

Despite the success of the geothermal industry in learning to manage the severe deposition of hot geothermal hypersaline water in the Salton Sea region of California, United States can show that silica scaling problem can be solved, because to overcome the damaging effects of silica scaling, an innovative and appropriate fluid injection management is a must.

This study aims to implement a concept of fluid injection management based on temperature and fluid pH associated with the rate of pipe diameter reduction process on the brine injection path or production well by silica scaling at Dieng geothermal field. The benefit of this research is to find out suitable method or mechanism to reduce silica scaling so that it can increase production based on the parameters which influence the rate of silica scaling thickening. Where the development of the results of this future-enhanced research on predictive techniques will result in uniformity in data collection and experimental design.

METHODOLOGY

This research is conducted by collecting data obtained from previous studies in the past. Data were obtained from previous literature and researches on silica scaling such as data obtained from the representative wells.

The data has been collected is then processed so that it can be developed to the next phase. In order to create research works that can be utilized widely it is required to do the following stages of data processing which includes:

a) *Examination of data*. The data that has been collected is then checked whether it is complete in order to support the hypothesis to be presented in this paper.

b) *Data analysis*. The data obtained is then analyzed quantitatively or mathematically so as to obtain an objective result which is then continued with a qualitative analysis or conveying interpretation based on data that has been obtained.

c) *Conclusion and further project development*. Data that has been analyzed is then drawn conclusions that can generate a new innovation that may be applied or researched further.

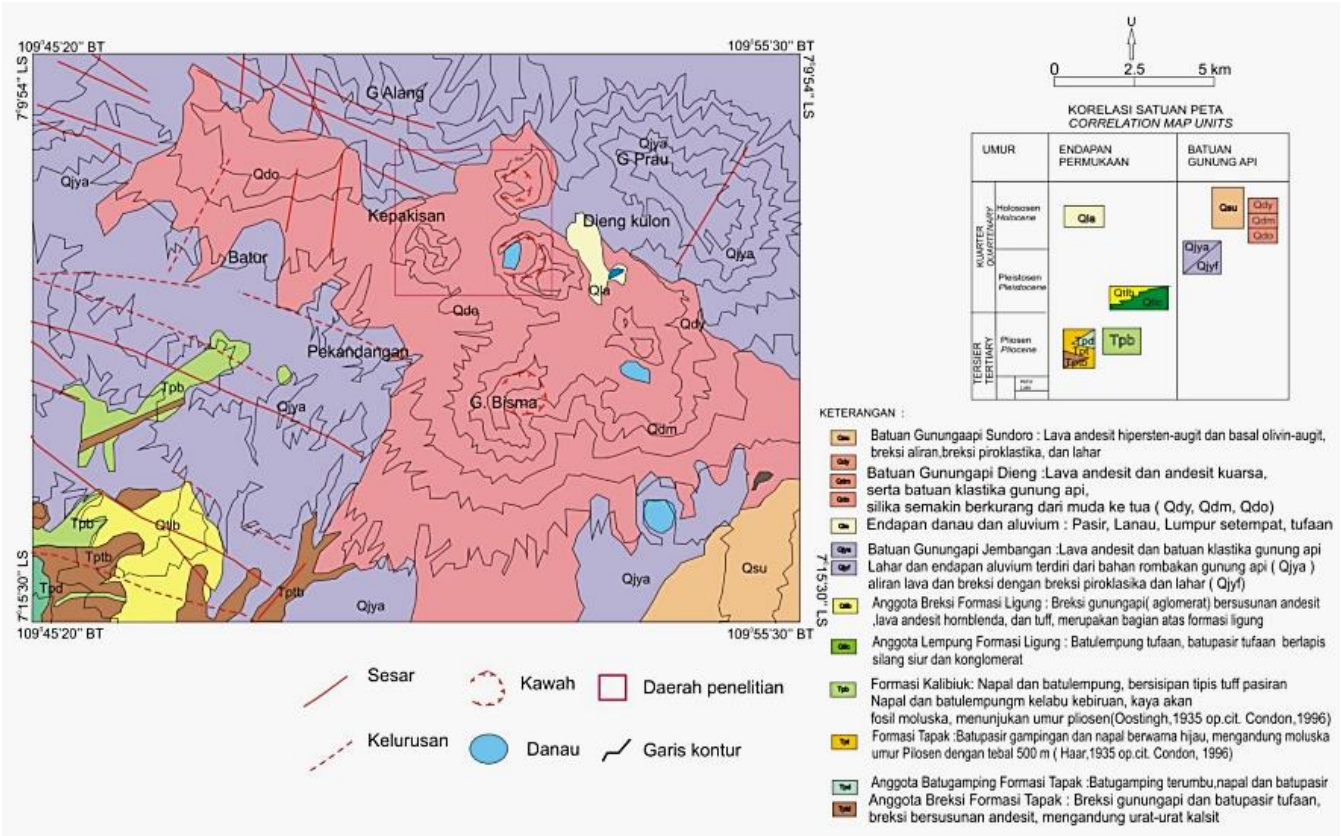

Figure 3. Regional Geology Map of Banjarnegara-Pekalongan (Condon et al, 1996)

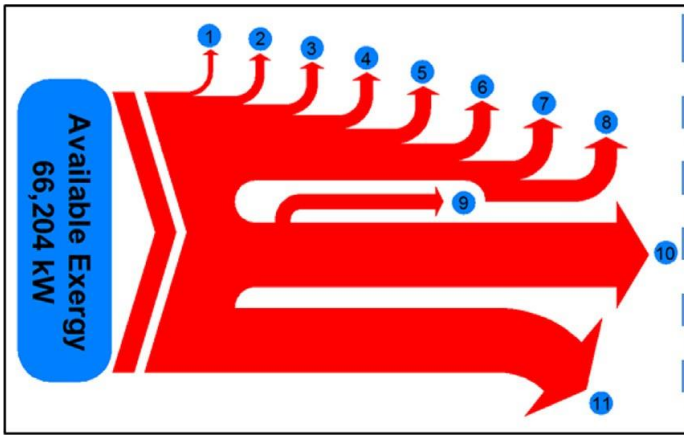

	Components	Losses	%
1.	Purifier	146.9	0.22
2.	Inter-condenser	1019	1.54
3.	After-condenser	1584	2.39
4.	Cooling tower	2832	4.28
5.	Main-condenser	3639	5.50
6.	Turbine	5,492	8.30
7.	Flasher	3652	5.52
8.	Separator	8334	12.59
9.	Parasitic load	2600	3.93
10.	Net Power output	24300	36.70
11.	Waste brine	12,605	19.04

Figure 4. Exergy diagram for exergy flow from the single-flash of Dieng geothermal power plant (Pambudi, 2015)

GEOLOGICAL SETTING

Physiographically, the area of Central Java is divided into 4 East-West trending zones (Van Bemmelen, 1949). These 4 zones are the Central Coast of Central Java, the North Serayu, Serayu Selatan Mountains, and the South Coast Plains of Central Java. Meanwhile, the Dieng Plateau itself is included in the North Serayu zone is limited by its western side Karangkobar and its western area bounded by Ungaran (Van Bemmelen, 1949).

According to Pardiyanto (1970), geomorphology and the area surrounding the Dieng Plateau can be divided into two kinds consisting of mountainous areas and the highlands (Plateau). The mountainous area covers almost all parts of the edge consisting of one straightness of volcanoes (Mount Srodja, Mount Kunir, Mount Pakuwadja, Mount Kendil, Mount Butak, Mount Patarangan, Mount Prahu, Mount Patakbanteng, Mount Djurangsawah, Mount Blumbang, and some domes solitary such as Mt. Bisma and Mount Nagasari). Meanwhile, the plateau area itself is located between rows of volcanoes and dome solitary, generally have filled volcanic material consisting of Dieng, Batur Highlands and Highlands Sidongkal).

Regional stratigraphy in the study area according to Condon et al. (1996), consists of eleven lithologies in the order of old to young is Unit Members Breccia Formation Tapak, Unit Members Limestone Formation Tapak, Unit Formation Tapak, Unit Formation Kalibiuk, Unit Members Clay Formation Ligung, Unit Members Breccia Formation Ligung, Unit Stone Mountain fire Jembangan, Lake and Alluvium Sediment Unit, Unit Dieng Volcano rocks, rocks Unit Volcano Sundoro, Alluvium Deposition Unit.

According to Gunawan (1968) op.cit. Zaenudin (2006) The geological structure of Dieng and its surroundings is influenced by tectonic movements of Quaternary which is still active to date. A great fold does not occur, but clearly there are two Quaternary fractures that can be observed. The first fracture was found in the west part in the formation of Ratamba Block accompanied by fracturing. The second fracture is influenced in the eastern region of Sigedang graben from Tlerep-Butak Volcano and Graben Watumbu from Prahu. Meanwhile, the study summarized by Condon et al. (1996) states that the existing geological structures consist of fault, straightness, and fractures involving rocks aged from Cretaceous to Holocene (Figure 3).

DIENG GEOTHERMAL FIELD

Exergy diagram of the field's single-flash system

The available exergy the power plant received from the fluid and where it is used in the power plant process correlates to the main objective of the power plant which is to convert available exergy into electricity (Figure 4). Although, several losses and waste is expected during this process. The total available exergy in Dieng has been calculated to be around 76,204 kW, which arrives from the reservoir in the form of hot fluid. The net electricity produced is 24,300 kW after reduction by a parasitic load of 2600 kW. This parasitic load is used by several pumps, including the hot well pump (HWP),the auxiliary pump, and the fan. Losses from all the components such as the purifier, the inter-condenser, the after-condenser, the cooling tower, the main condenser, the turbine, the flasher, and the separator are 146.9, 1019, 1584, 2832, 3639, 5492, 3652, and 8334 kW, respectively. The amount of brine sent to the formation uses 12,605 kW in state number 11. This represents 19.04% of the total available exergy that goes to the plant (Pambudi, 2015).

Deposition rate

Previous studies found the estimation of Dieng geothermal field silica scaling deposition rate from representative wells by determining the mass per time units. The higher the potential deposit of silica, the greater the deposition rate. This calculation was done with the assumption that there was no inhibitor liquid has been injected to the brine pipelines. The amount of silica scaling produced are mainly affected by the concentration of potential silica deposits within the fluid and the mass flow rate values.

pH and temperature effect

Utami et al (2014) conducted research on the effects of pH and temperature change in correlation with silica scaling based on two representative wells at Dieng geothermal field. It is found that the process of silica scaling formation at surface facilities in Well A and B are strongly influenced by the very high SiO2 concentration of resevoir and also the significant change of temperature and pressure which induced flashing to occur and the solution pH. There are only a very slight difference of silica deposition between the temperature-controlled silica

solubility curve and pH-controlled silica solubility curve. Beside the abundance of silica concentration within the water, mass flow rate of the fluids also affect the amount of silica deposition. The higher the mass flow rate, the higher the deposition rate over time.

PROJECT DEVELOPMENT

In order to prevent and/or minimize the formation of silica scaling, an understanding, thorough planning and research is essential to establish the suitable fluid injection management.

Scaling mechanism

a well-controlled and documented experimental work to elaborate scaling mechanism by Mroczek and McDowell (1990) was conducted by passing separated brine from a well through a pipeline for 29 to 35 days. Then the pipeline was cut into even sections and the amount of scale in each section determined. Eight experiments were run, two each with separator pressure set for 180°C, 160°C, 140°C and 120°C. At each pressure there was one experiment with a brine f1owrate of 3 I/sec, and another with a rate of 30 I/sec; this produced total residence times of 7 minutes and 0.7 minutes. Total Si02 and monomeric Si02 were measured in water samples collected at the inlet and outlet. Salinity and pH were not reported, but saturation ratios and T-Si02 values suggest that there was essentially no ionized silica (Klein, 1995).

At 180°C and 160°C, the induction time for polymerization was not reached, even at 7 minutes. Scaling rates were 0.2 to 0.3 mm/yr at 180°C (assuming density 2.2), increasing to 0.3 to 0.4 mm/yr at 160°C. At 140°C and 120°C, there was measurable polymer formation, even at the pipe inlet, and the polymer concentration increased through the pipeline; the increase at 120°C was twice that at 140°C.

Therefore, scaling in the pipeline decreased dramatically along the length of the pipe, as monomeric Si02 was removed from solution into the suspended polymer. In all cases, the scale which formed was hard and glassy, with density about 2 gm/ cc (Klein, 1995).

Gas suppression

Hirowatari and Yamaguchi (1990) discussed about gas mixing to lower the solution pH and suppress scale development. A model of dissolving various amounts of CO2 into the injection line brine, after separating the brine from steam at 175°C, is illustrated in figure 5. The particular case modeled starts at 50 ppm oversaturation. Between 25 ppm and 500 ppm total C in solution as CO2, there is a dramatic drop of pH from 7.2 to 5.8, while unionized Si02 climbs from 822 ppm to 850 ppm and oversaturation increases from 50 ppm to 75 ppm. The increase of oversaturation is completely counterbalanced by the lowered pH, and molecular deposition rate drops from 0.15 to 0.01 mm/yr. This should also effectively eliminate any tendency for particle formation and deposition. pH and scaling potential can be lowered further with additional CO2, but this hardly seems necessary. It should be noted that P C02 for 500 ppm is only 1.5 bar. The 500 ppm level is achieved by mixing about 0.025 t/hr non-condensable gases (13 m3 at 1 atm.) per 50 t/hr of water flow.

For comparison with the gas mixing, it is noted that: 1) mixing 50 t/hr water flow with 17.5 t/hr condensate at 60'C also lowers the molecular deposition rate to 0.01 mm/yr; 2) all oversaturation in 175'C water would be removed by mixing with an equal amount of 60'C condensate; and 3) mixing with a combination of gas and condensate may have a beneficial effect by reducing wintertime freezing of vapor in the gas line (Klein, 1995).

CO2 source

The need of CO2 to decrease silica scaling formation by lowering the molecular deposition rate of injection fluid means the need of CO2 resources around Dieng geothermal field. This can be solved either by purchasing from CO2 suppliers or establishing integrated system by transferring CO2 from coal-fired power plants. Pipeline facilities interconnecting the coal-fired power plant with the geothermal field would transfer simultaneously the extracted CO2 into the fluid injection management. In this case, the available nearby coal-fired power plants are PLTU Adipala, PLTU Karangkandri in Cilacap and PLTU Batang, Central Java.

Table 1. The calculation of deposition rate in Well A and Well B at Dieng Geothermal Field. The potential deposit unit mg/L is assumed to be equal with mg/kg to simplify the calculation (Utami, 2014)

Well	Location	Potential Deposits	Mass Flow Rate*	Deposition Rate			
		mg/kg	kg/s	ton/hour	ton/day	ton/month	ton/year
A	Separator	100	2.75	0.00099	0.02	0.71	8.55
	Weirbox	630		0.01	0.15	4.49	53.89
B	Separator	660	9.6	0.02	0.55	16.42	197.07
	Weirbox	600		0.02	0.50	14.93	179.16

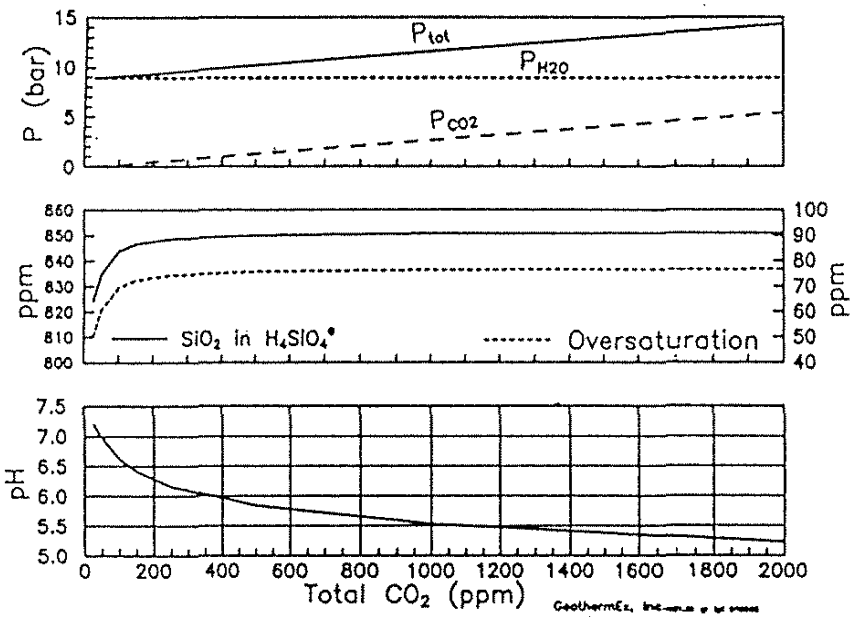

Figure 5. The effect of CO2 mixing into water at 175°C (Klein, 1995)

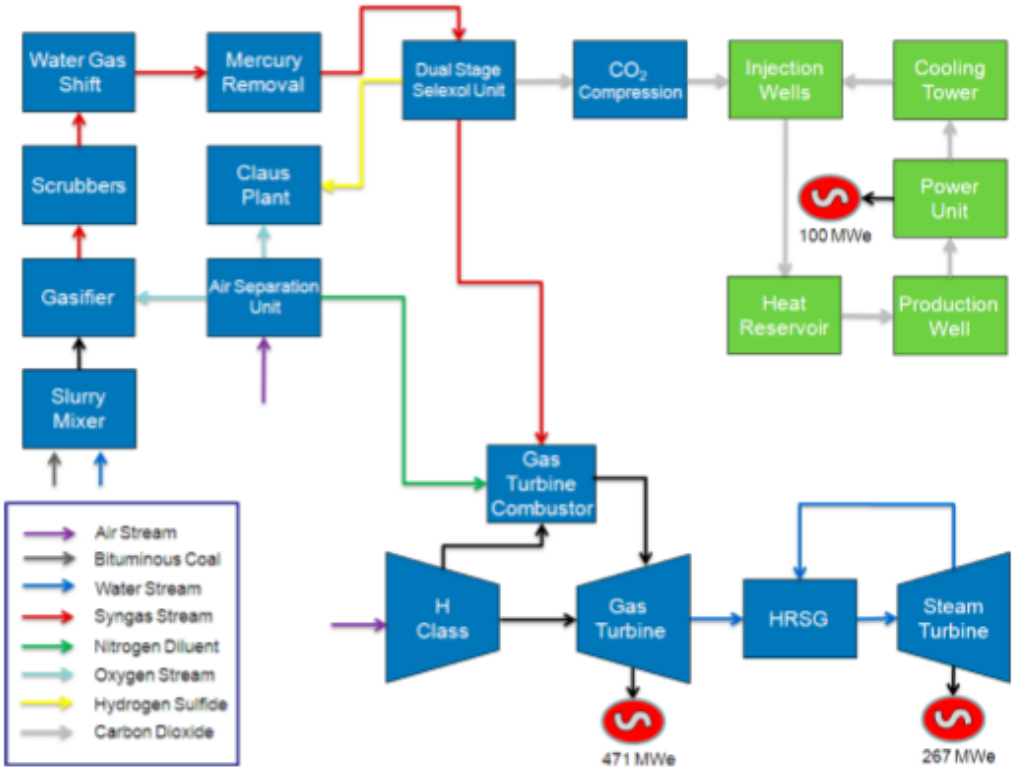

Figure 6. CO2-circulated EGS combined with IGCC system as integrated schematic system of geothermal field and coal-fired power plant (Chandra, 2012)

CONCLUSION

There are several results of this research. First, the amount of silica deposition is estimated by calculating the difference between dissolved SiO2 with the solubility of amorphous silica curve. Silica scaling in the Dieng geothermal field is caused by the influence of fluid pH. From the results of research that has been done previously known that the silica deposit will decrease along with the increase of fluid pH in well A and B at Dieng geothermal field. Where, the solubility of amorphous silica increased significantly at pH > 7 in the separator, and pH > 8 in the weirbox. One way to increase and decrease the pH of geothermal fluid conditions is through fluid management. Fluid management that can be done is by utilizing injection fluid inhibitor (usually sulfuric acid (H2SO4) to reduce the pH unit, or caustic soda (NaOH) to rise the pH unit) into the brine pipeline is able to halt the formation of silica scaling for several hours (Brown, 2011). Alternatively, the separator pressure adjustment can also be applied. But sometimes, this can be unacceptable for the economic power generation.

Second, From the findings above it is known that the higher the temperature of geothermal fluid, the higher the pressure would eventually be resulting in less silica scaling in the pipe. Therefore, the required actions to prevent or minimize silica scaling alternatively are engineering the fluid temperature rise, preserving the pressure of the reservoir and establishing integrated system of geothermal field and coal-fired power plants interconnected by pipeline facilities in order to conduct CO2 suppression into the injection fluid.

Then, using another exploration method in Dieng geothermal field such as by changing the single-flash separation become a double-flash separation is one of possible solution.

The higher the temperature of geothermal fluid, the higher the pressure would eventually be resulting in less silica scaling in the pipe. So, to prevent silica scaling alternatively is to engineering the fluid temperature rise.

The implementation of scCO2 EGS-IGCC will reduce annual emissions by 8,200 tons of NOx, 20,000 tons of SO2, and 4.35 million tons of CO2 over conventional thermal plants in an optimal pairing.

RECOMMENDATION

Establishing integrated system of geothermal system fluid injection management along with coal-fired power plant would be better in the long run as it will continuously supply CO2 by pipeline from the coal-fired power plant while also capturing carbon underneath and reducing CO2 emission to the atmosphere in general.

In addition to scale suppression strategies in Dieng geothermal field, the following is recommended for scale management at low levels of oversaturation (Klein, 1995):

a) Design the injection system to minimize residence time and avoid turbulence.
b) Install pressure ports on injection lines to allow monitoring for scale-related impedance.
c) Install inspection ports and scaling coupon ports
d) on the injection lines.
e) Install ports at both ends of injection lines to allow inserting a clean-out.

REFERENCES

Guerra, C. E.; Jacobo, P. E. 2012. *pH Modifications for Silica Control in Geothermal Fluids.* Short Course on Geothermal Development and Geothermal Wells, UNU-GTP and LaGeo, Santa Tecla, El Salvador.

Gunnarsson, I.; Arnórsson, S. 2003. Silica scaling: The main obstacle in efficient use of high-temperature geothermal fluids. International Geothermal Conference, Reykjavík.

Klein, Christopher W. 1995. Management Of Fluid Injection In Geothermal Wells To Avoid Silica Scaling At Low Levels Of Silica Oversaturation. Geothermal Resources Council Transactions, Vol. 19, October 1995 Edition.

Layman E.B., Agus I., WarsaA S.: The Dieng Geothermal Resource, Central Java, Indonesia. Geothermal Resource Council Transactions, Vol.26, p. 573-579, (2002).

Mroczek, E. K., and G. McDowell. 1990. *Silica Scaling Field Experiments*. Geothermal Resources Council Transactions, Vol. 14, Part II, August 1990, pp. 1619-1625.

Pambudi, N. A.; Itoi, Ryuichi .2015. *Performance improvement of a single-flash geothermal power plant in Dieng, Indonesia, upon conversion to a double-flash system using thermodynamic analysis*. Renewable Energy: an International Journal.

Pardiyanto, L. 1970. *The Geology of The Dieng Area, Central Java*. Minister of Mines, Geological Survey of Indonesia, Bandung.

Setiawan, F. A.; Panthron, Hedrik; Alfredo, et al. 2015. *Mitigation of Silica Scaling from Dieng s Geothermal Brines using Ca(OH)2*. Proceedings Indonesia International Geothermal Convention and Exhibition : Jakarta.

Utami, W. S.; et al. 2014. *The Effect of Temperature and pH on the Formation of Silica Scaling of Dieng Geothermal Field, Central Java, Indonesia*. PROCEEDINGS, Thirty-Ninth Workshop on Geothermal Reservoir Engineering 2014. Stanford University, Stanford, California.

Wahyudityo , R; Harto, A. W.; Suryopratomo, K. 2013. *Analisis Scaling Silika pada Pipa Injeksi Brine di Lapangan Panas Bumi Dieng dengan Studi Kasus di PT. Geo Dipa Energi*. TEKNOFISIKA Vol.2 No.1, January 2013 Edition.

Chandra, Divya; Conrad, Caleb; et al. 2012. *Pairing Integrated Gasification and Enhanced Geothermal Systems (EGS) in Semiarid Environments.* Energy & Fuels. Texas, United States.

USE OF DEEP SLIMHOLE DRILLING FOR GEOTHERMAL EXPLORATION

K.M. Mackenzie, G.N.H. Ussher, R.B. Libbey, P.F. Quinlivan, J.U. Dacanay and I. Bogie

Jacobs (formerly SKM)

e-mail: ken.mackenzie@jacobs.com; gregory.ussher@jacobs.com; ryan.libbey@jacobs.com; paul.quinlivan@jacobs.com; julius.dacanay@jacobs.com; ian.bogie@jacobs.com

ABSTRACT

Deep slimholes were used very effectively in Indonesia in the 1990's for geothermal resource delineation and potentially again have a major role in assisting early exploration of geothermal prospects that are increasingly challenging because of ambiguous surface indications and more remote and difficult terrain.

The capital expenditure required to drill deep geothermal exploration wells to prove any geothermal system can be substantial particularly if a project is remotely located and requires large infrastructure work to facilitate the exploration and resource proving process. In the absence of tariffs commensurate with the risks in exploration drilling, developers are cautious to embark on high cost drilling, particularly where the probability of successfully finding a resource with the first few wells may be low because of resource uncertainties.

Deep slimhole drilling using equipment that is smaller and requires less road and water supply infrastructure can achieve exploration outcomes at lower cost. However, successful application of this technology requires a solid foundation comprising five elements: an appropriate well design; a simple and clear strategy covering major drilling decision points; a robust procurement and implementation plan; a suitably experienced and equipped drilling contractor; and experienced technical supervision of the operation. Following this approach it is possible to obtain exploration and resource characterisation equal to that provided by full sized exploration wells.

The use of deep slimholes can improve the success rate of subsequent appraisal drilling using conventional or large diameter wells and so it can provide cost savings on the total project cost. The use of deep slimholes for exploration reduces the early capital spend on a project, and therefore improves the success-weighted Net Present Value (NPV) of a project, particularly where there is a reduced probability of successfully finding a resource. In combination, the reduced capital and improved scheduling of expenditure plus reduced cost of failure for a project (or for a portfolio of projects), has the ability to reduce the tariff required for geothermal projects in Indonesia.

Small diameter wells can potentially produce geothermal fluids sufficient for several hundreds of kW of electricity, raising the possibility of a group of such wells supplying electricity economically in areas where demand is low such as small, remote or isolated grids. The feasibility of doing this in Eastern Indonesia is currently being considered.

Keywords: geothermal exploration, resource uncertainty, financial risk, conceptual model, deep slimhole drilling

INTRODUCTION

There is a range of drilling alternatives that can be considered for purposes of geothermal exploration and assessment of resource potential. The applicability of one or more of these alternatives is ultimately dependent on key project considerations such as schedule, cost and risk management, and is usually evaluated on a case by case basis depending on the objectives for a particular project and the extent of existing resource knowledge.

This has become increasingly important as the "low hanging fruit" exploration projects in which pre-drilling exploration results were sufficiently good that initially successful drilling could be conducted with full size wells have already been exploited.

With the high cost of drilling, it is becoming increasingly important to optimise well targeting, particularly for the first wells in a geothermal system. Where there is uncertainty as to the resource potential, location and extent; or in the location, nature and orientation of permeability, there can be good reasons to use slimholes initially. The primary reason for drilling slimholes is twofold:

- to reduce the overall risk (cost) of failure in exploration drilling
- to improve the probability of success of appraisal, delineation and production wells.

The significant lower upfront capital expenditure and reduced financial risk makes this approach particularly attractive for the early part of the drilling phase where the level of risk is normally the highest (Figure 1).

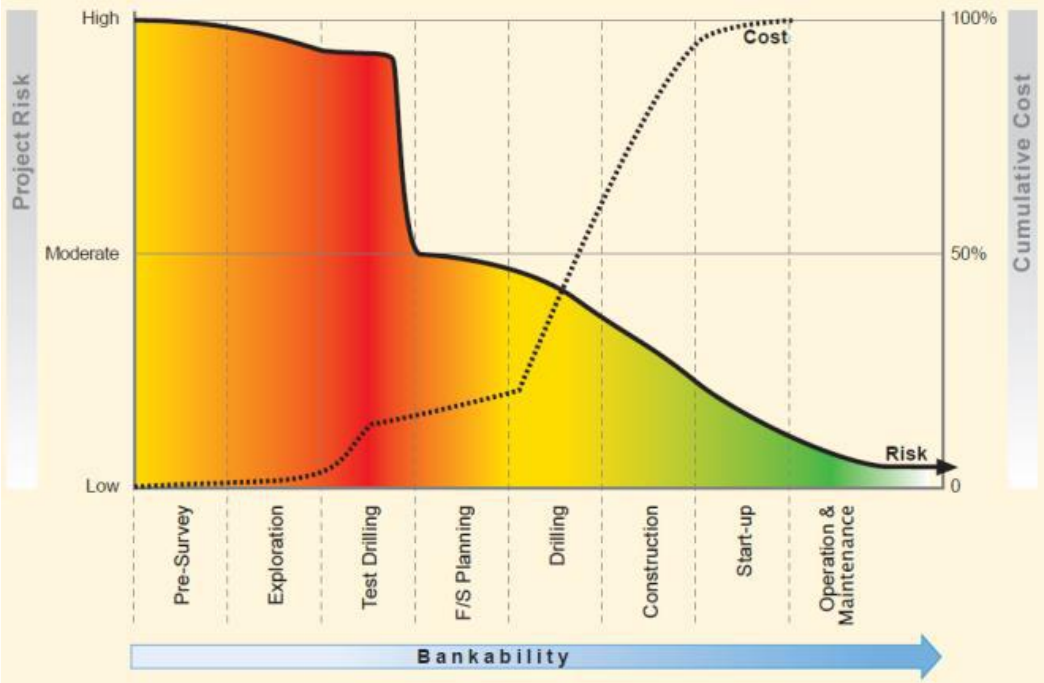

Figure 1: Bankability versus risk for a geothermal project, note the strong drop in risk engendered by successful test drilling. From: Gehringer and Loksha (2012).

Deep slimhole drilling was used effectively for geothermal exploration in Indonesia in the 1990's notably at Wayang Windu, Darajat (Riza and Berry, 1998), and Sarulla (Gunderson et al, 2000). Over the past 25 years, slimhole drilling has become increasingly utilized for geothermal resource exploration and delineation in other regions notably in the USA, Japan, New Zealand, the Caribbean, Central America and Chile, and even recently in Malaysia (see for example White et al., 2012; Garg and Combs, 1993; Nielson and Garg, 2016; Nielson and Garg, 2017; Libby et al., 2017).

This paper summarises the relative advantages and disadvantages of slimhole drilling, and describes the typical equipment and infrastructure requirements for this approach. It also provides some examples of where deep slimhole drilling has been successfully implemented on geothermal projects to address different project objectives with focus on application in Indonesia.

TERMINOLOGY AND ASSUMPTIONS

Within the geothermal industry there are two generic well types normally considered for exploration drilling; these are slimhole wells and what are typically referred to as 'conventional' sized wells. Each generic well type has two variants that are normally selected according to the objectives of a particular drilling program and other factors such as cost. These generic well types are summarised in Table 1 and depicted schematically in Figure 2.

Table 1: Generic Well Definitions and Applications

Type	Variant	Description
Slimhole Well	Temperature Gradient	Well completed above the level of the productive reservoir to establish presence of clay conductor, confirm temperature, and validate conceptual model. ~200 – 800 mVD.
	Deep Slimhole (2 3/4" – 7" PC)	Drilled into the reservoir to confirm commercial temperature (primary objective) and can test productivity (secondary objective). ~500 – 2,000 mVD.
Conventional Well	Standard (9 5/8" PC)	Wells that penetrate substantial thickness of the reservoir, enable comprehensive testing of resource productivity, and may be used for production or injection in a development. ~2,000 – 3,000 mVD.
	Large (13 3/8" PC)	

Notes: PC = production casing, VD = vertical depth

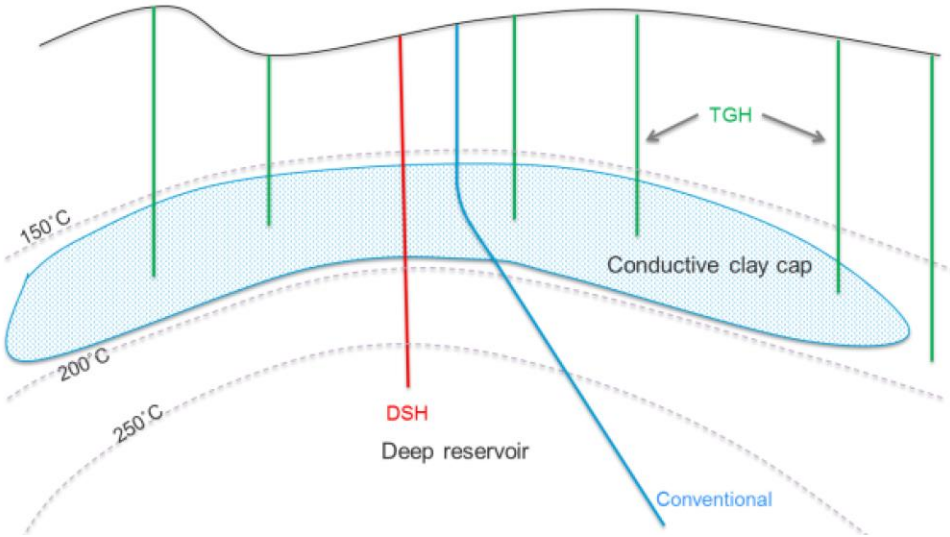

Figure 2: Generic drilling options (TGH = temperature gradient hole, DSH = deep slimhole)

A deep geothermal slimhole is defined as a well that is drilled with a continuous wireline core rig or a small rotary drilling rig with the specific aim of drilling into the geothermal reservoir. Note that a "reservoir" is simply defined as a permeable hot aquifer, which is commonly, but not always situated beneath a hydrothermal clay cap. The target reservoir is most often linked to a zone of deep upflow, however, some smaller projects target shallow permeable zones that reside within the clay cap and/or along shallow outflow paths.

Slimholes have been designed and constructed to safely core or drill into hot formations up to 275˚C. Generally the finished hole size ranges from NQ size (75.7 mm diameter) to 6-1/4" (normally using rotary drilling techniques and tricone bits).

Slimhole depths are mostly limited by the rig capacity and well designs prepared by Jacobs have mostly targeted maximum depths of 2,000 m. Most wells are continuously cored for their full depth or rotary drilled in the shallow sections using a tricone bit, then cored in the main interval of interest through the hydrothermal clay cap and underlying reservoir rock. Slimholes are usually drilled straight, either vertically or at an angle to the horizontal (slant) depending on exploration targeting requirements. There is also the technology to drill directional holes, most particularly using coiled tubing with a mud motor, but so far the use of this technology appears to be restricted to the oil and gas exploration industry.

Temperature gradient holes are a shallow type of slimhole aimed at helping to define the upper part of the geothermal system and which are terminated above the level of the productive reservoir, primarily due to rig and well control (blow out prevention) restrictions, and most particularly depth limitations on setting the final cemented casing. Such holes are normally used to help define the shallow geological environment, in particular the extent of the geothermal clay cap and to confirm whether it has associated shallow heat flow or is a relict feature. Collectively this information can be used to validate and refine the conceptual model. It can be used to estimate what the deep reservoir temperatures might be, although care needs to be exercised when extrapolating shallow temperature information. This is most particularly the case in andesitic volcanic piles where perched groundwater aquifers are common and can severely reduce temperature gradients.

Temperature gradient hole drilling uses the same type of equipment and associated infrastructure required for deep slimhole drilling, including all of the necessary precautions required for well control and overall site safety.

INFORMATION SECURED FROM SLIMHOLES

In general, slimholes obtain very similar information regarding the geothermal reservoir to that obtained with conventional larger diameter holes, but with some important differences.

Geology:

Continuous coring means that an almost complete geological section is obtained compared with only cuttings in most geothermal wells, possibly supplemented by a short length of "spot" core. Within conventional rotary drilled holes there is also the likelihood of obtaining no cuttings below any major loss zones, unless drilling with aerated fluids is successful in maintaining circulation. Coring enables much greater confidence in identifying the lithologies, alteration and veining, and the relationships between different units or events. In addition, potential problem units (e.g., smectite-rich lithologies within the reservoir) may be identified at an early stage before they cause potentially costly drilling problems in larger diameter production wells. For example, it was only through data from cored slimholes at Wayang Windu in the 1990's that our geologists were able to understand the rather thin formations that were causing major problems in drilling conventional production wells and eventually saved a large amount of drilling time.

The availability of continuous core samples also provides an opportunity for detailed profiling of rock properties, including porosity, permeability, resistivity and density. This can be useful for helping to validate the conceptual geothermal model and geophysics profiling, and for constraining numerical models of the reservoir that will be used throughout the project life. Oriented cores can also be obtained (at some extra cost) to help characterise geological structure within the reservoir. Where there are concerns over subsidence, obtaining a good core record

will be an advantage for determining geotechnical properties of formations.

Temperature:

Slimholes are ideally suited for collecting temperature measurements. Temperature measurements that approximate undisturbed reservoir temperatures can be made during drilling, using small temperature logging tools easily run during short operational pauses. Simple maximum registering thermometers (MRT) can provide temperature data in excess of 250°C, and where a wireline coring rig is used, can provide a temperature for each interval drilled. Small electronic temperature data loggers (e.g., the HOBO® U12-015) are available to log temperatures at all depths and at temperatures up to 150°C.

The reason that these measurements when drilling are so viable is that very little drilling fluid is circulated during slimhole drilling in comparison to a full size operation, thus a 2-3 hour heat-up can be sufficient to give a temperature that is nearly representative of natural state conditions (especially near the bottomhole). Evidence for this is provided by a comparison between MRT/HOBO® data collected during drilling and temperature logs made after months of heating in Libbey et al (2017). Conventional pressure-temperature-spinner logs using standard geothermal industry wireline tools (e.g., 1.75" Kuster K10 PTS tool) can also be run in slimholes following well completion to characterise the conditions over the full length of the well.

The early collection of temperature data is useful for two reasons. Firstly, if there are major drilling difficulties that lead to premature abandonment of the well there will still be some temperature data available. Secondly, if low temperatures are found down to reservoir depths the well can be terminated early thereby saving on additional drilling cost while other well targets can be reviewed.

Permeability:

Permeability will be noticed when found with slimholes, just as with larger diameter wells (e.g., drilling breaks, fluid losses, kicks, etc.). Completion tests can measure injectivity indices, and provide general guidelines for whether good permeability has been found. A normal type of completion test is run in slimholes, measuring water loss, injectivity and pressure fall off.

Productivity:

Provided that slimholes are properly designed (see the section on well design in this paper), slimholes can be flowed if they encounter suitable temperature, pressure and permeability. Our research indicated over 16 projects where slimholes have been flowed. Garg and Coombs (1993) report several wells at Oguni in Japan that flowed with about 6-8 tph of steam or close to 1 MWe. Jacobs has tested wells at the Mita project in Guatemala with a reservoir temperature of only 205 °C, but with good permeability. In this example the 4" diameter wells provided flows equivalent to over 1 MWe (Figure 3).

Figure 3: A flow test of 1,300 m deep angled slimhole in Mita, Guatemala. Final hole size was HQ (100 mm). Production was about 1 MWe.

Chemistry:

Provided a slimhole encounters suitable permeability and temperature (or artesian pressure), it will be possible to discharge the well and obtain samples of hot water and separated steam for analysis. In this way, the chemistry and enthalpy of the deep reservoir fluid may be characterised prior to the first production well being drilled. This can be a useful risk reduction approach, particularly in areas where there may be indications of acid magmatic chemistry or secondary bicarbonate fluids prone to scaling. Information related to fluid chemistry (past and/or present) is also provided by the hydrothermal mineralogy observed in the core and cuttings.

SLIMHOLE DESIGN AND DRILLING

Slimhole well design follows the same process as for conventional wells. It is a step by step process that requires consideration of the anticipated conditions of the particular geothermal resource to be drilled, followed by the design of appropriate pressure containment and casing loading limitations. The recommended well design process is defined by the New Zealand Standard Code of Practice for the Drilling of Deep Geothermal Wells (NZS2403:2015).

However, there are special or unique design issues related specifically to slimholes that need to be considered and managed in the design process. In particular the small annular spaces for cementing, type of slurry design required, methods for centralising casing, and choice of the smaller tubing connections (or core rod connections) are important considerations. It has to be noted that slimholes can reach the same very high temperatures that conventional drilling encounters, and although well control is generally easier than with larger diameter wells, the casings are put under similar stresses and cementing integrity is just as essential for safe well completion. An example well design outline for a 1,000 m deep slimhole is provided in Figure 4.

Casing Details	Hole Size	Casing Shoe Vertical Depth (meters)	Casing Shoe Temperature	Remarks
9-5/8" OD Grade K55 43.5 or 36 ppf	12-1/4"	6	Ambient near surface	Conductor - drilled and set with rig
6-5/8" OD, Grade K-55 20 ppf R3 Seamless	PQ core, open out to 8-1/2"	100	< 100 °C	Cement casing back to surface. Set-up 7-1/16" BOP equipment on 6-5/8" casing
4-1/2" OD Schedule 40 pipe welded connections	PQ core, hole size open out to 5-3/4"	400	210 °C	Cement casing back to surface. Set up 7-1/16" (or 4-1/16") BOP equipment on 4-1/2" casing
3-1/2" OD Schedule 40 flush joint connection perforated	HQ	1000	250 °C	Squat on bottom (can core NQ and leave NQ rod perforated if encounter HQ coring difficulties. Uncemented liner

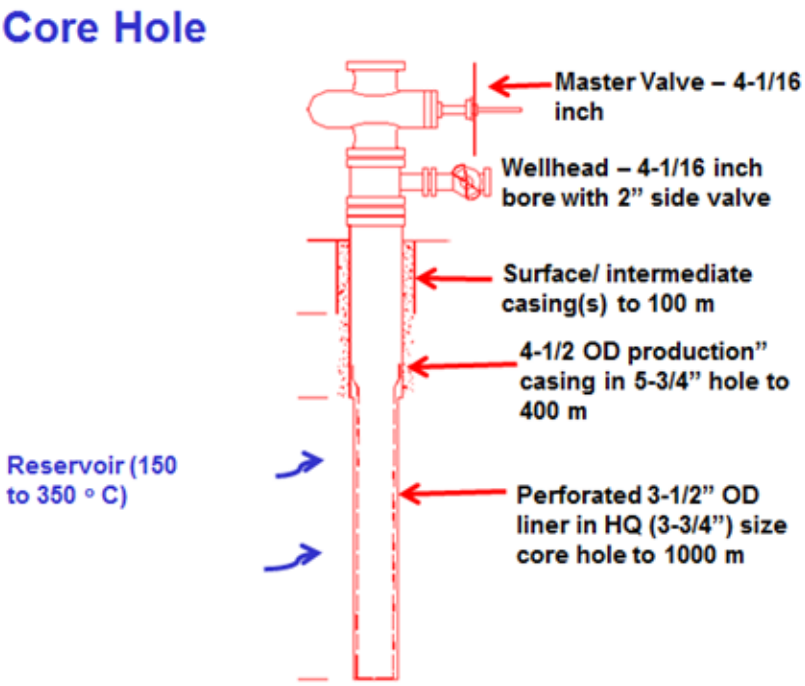

Figure 4: Typical well construction details for a 1,000 m cored slimhole

Compared to large rigs used for production drilling the rigs used for slimhole drilling are relatively small, often self- propelled and have to be jacked up above the ground to accommodate the Blowout Prevention Equipment (BOPE) needed to maintain a safe drilling operation for any geothermal well. For coring rigs without any pony sub or any headroom below the rotary table, the vertical clearance required to accommodate the BOPE is provided by constructing a shallow cellar.

Depending on site accessibility and well targeting objectives a slimhole can be drilled vertically or slant. For a slant hole, the mast can be tilted to allow for the drilling of a straight slant hole at any angle ranging from vertical to 45 degrees from vertical. A typical core rig uses high rotational speeds to cut the rock with relatively light core rods. Generally these rigs provide their own cementing equipment, mud services and directional instrumentation.

For the production casing string, the flush jointed connections of core rods are not designed to withstand compressive loadings during thermal cycling in a well. On the first heat up of the well there is a high risk of failure if threaded connections are used in the production casing string. It is for this reason the production casing used for slimhole wells is recommended to be installed using welded casing connections.

Figure 5 shows a typical slimhole coring rig while Figure 6 shows a typical wellhead set up with the BOPE installed on a slant hole – this was drilled at the Mita project in Guatemala (White et al., 2010).

In addition to the pure technical requirements of a slimhole rig there is also a need that operators and crew have a sufficient level of previous geothermal slimhole experience as indicated by a track record of recent successfully drilled wells. Careful contracting is also required with clear evidence for the drilling contractor's financial robustness such that unexpected requirements for additional consumables and spare parts can be immediately met.

Figure 5: Typical slimhole coring rig

Figure 6: Blowout Preventer for slanted slimhole drilling

The water supply requirements for slimholes can vary greatly depending on the type of slimhole drilling. When drilling with smaller diameter rotary drilling, the water requirements tend to scale down from conventional well drilling in proportion to hole area – so may be of the order of 50% of that for conventional wells. Continuous coring systems however require very small maximum flowrates (~40 lpm, compared to 2,000-3,000 lpm for conventional wells) and can readily be supplied by water carried by small tanker. The challenges with available water supplies may dictate the type of drilling that can be achieved initially. In very challenging locations, slimholes may give the confidence necessary to invest in water supply infrastructure to provide the necessary requirements for larger and deeper wells.

One of the differences with conventional drilling is that slimhole drilling operations are more commonly undertaken by a single contractor who is typically the rig owner. This contractor will provide all of the services and materials on site under one umbrella contract.

Such contracts are still best delivered using an independent engineer that provides well design, drilling plans and supervision so as to look after the Owner's interests in the operation. While a fixed price per metre (as sometimes used in the minerals industry) may provide some protection for the Owner, the drilling company will want to complete the well but may not do everything necessary to have a sound and stable geothermal well that provides the necessary data and long-term mechanical integrity for the Owner. If the contractor comes from a minerals background and proves to be "out of their depth" in geothermal drilling, then it is possible that without good supervision the wells will take unduly long or not reach their targets, which is not in the Owner's interest. Table 2 provides a summary of the technical aspects of slimhole and conventional wells.

Table 2: Comparison between common slimhole and conventional drilling approaches

Item	Slimhole Drilling	Conventional Drilling
Rig size for at least 1,000 m deep well	Small truck mounted	Large (more horsepower)
Number of truckloads for moving rig/ consumables	6 to 10	40 to 80
Production hole diameter	2.98" (NQ) to 3.78" (HQ)	8-1/2" (standard), or 9 5/8" (large)
Approximate time to complete 1,000 m	40 days (24 hours per day, 7 days per week)	20 days (25 days for 1,500 m), (24 hours/ day, 7 days/week)
Approximate rig pad size	40 m x 40 m	100 m x 70 m
Storage area	40 m x 40 m	200 m x 200 m
Access road	Single lane track or helicopter	2 lane with no steep grades
Highest structure	Mast up to 15 m above ground	Mast up to 45 m above ground
Waste sump volume	250 cu m approximately.	1, 000 cu m approximately, maybe larger.
Noise	Not a significant issue.	Significant in close proximity to site.
Peak water supply requirements	2,000 cu m per day for small rotary holes, 60 cu m per day for coring HQ holes.	3,500 cu m per day.

PROJECT DEVELOPMENT IMPLICATIONS

The following are some of the characteristics of slimholes that will have an impact of project risk, cost and schedule.

Early Infrastructure:

With many projects now being explored in remote and challenging terrain, the scale of access roads and water supplies required can have costs greater than the actual well drilling process. Conventional drilling with many personnel and services and large volumes of consumables and materials requires good all weather access for the high volume of traffic and large truck loads. The very high day cost of conventional drilling drives a high quality of infrastructure to avoid any costly down time on drilling operations. Typically this infrastructure is built to a semi-permanent standard on the assumption that when the resource is discovered drilling operations will continue past the exploration stage.

The smaller scale of equipment, materials, water supply and services needed for slimhole drilling may enable the use of smaller and lower standard access infrastructure. Roads may be of a quality typical to those used for mineral exploration drilling and only upgraded later if the resource is discovered. In some settings a helicopter supported operation might be a preferred option for accessing a remote exploration location in difficult terrain. This approach has been successfully applied for several slimhole drilling campaigns in Chile (e.g., Laguna del Maule, Tolhuaca). The water supply needed for cored type slimholes is less than 10% of that for conventional drilling and is thus easier to source locally near the drilling operation (e.g., with a temporary stream catchment).

Drilling and Infrastructure Cost:

Depending on the location and rig availability, a 1,500 m deep slimhole (with HQ bottomhole dimensions) may cost approximately US$1.3-1.8 million. A standard 8-1/2 inch diameter geothermal production well to this depth would typically cost 3-4 times as much. This means that an operator can theoretically drill several slimholes for the same cost of one standard diameter well, and achieve exploration coverage of a wider area.

In addition to the actual cost of drilling, the construction of roads, well pads, and water supply (see above) should all have lower cost (typically ~50 % or less) for a slimhole rig where the supporting infrastructure requirements are substantially less than those needed for a normal rotary drilling approach.

Permits and Land Access:

Conventional exploration wells are expected to be retained as a productive asset for any subsequent project development and so the land for exploration needs to be secured (through ownership or suitable lease) for the expected life of the project. This process can take considerable time and may mean early relocation of existing occupants, which may not be necessary if the project does not proceed. If slimholes are not intended to be permanent assets (possibly being abandoned after testing) then land acquisition may be avoided by more temporary lease arrangements that suit all parties.

Environmental permitting will typically also be quicker and cheaper in some jurisdictions due to the smaller environmental footprint, lower site impacts and temporary nature of the exploration drilling and testing activities.

Schedule:

The time for construction of roads, well pads, water supply and rig mobilisation can be very much less for a slimhole rig campaign compared to one using large rotary drilling rigs. The smaller footprint for well pads can mean they are constructed faster and may be located in more ideal locations possibly even closer to populations.

Typically slimhole drilling with a coring rig will involve a single contractor for materials and services and so procurement may be simpler and faster than a multi-package drilling program. However, an initial shortage of experienced slimhole drilling contractors in Indonesia may require mobilisation of an international contractor.

Where time is critical to achieve exploration outcomes (e.g. to meet regulatory or financial deadlines or limited budget), slimholes may be the only realistic option.

A deep slimhole approach, when used to deliver exploration outcomes (primarily being the proving of the presence of a useful reservoir, and possibly extending to define the areal extent of such a reservoir) should not extend a development schedule because it is not inserting an additional drilling stage. Instead it is achieving the exploration/discovery stage with a different method, with subsequent delineation and appraisal drilling still being achieved with conventional wells. A good exploration drilling program with several deep slimholes should be able to drive increased rates of success in the subsequent drilling phases.

In some projects, slimhole drilling has been done in parallel with conventional exploration drilling to help accelerate the schedule for resource delineation (proving that sufficient reservoir exists to support long term production). An example of this was at Wayang Windu where 4 x 1,500 m deep vertical slimholes were drilled to help confirm reservoir extent while production drilling focused on the central resource area. This not only saved on drilling costs, but helped accelerate the time needed to meet the lender's requirements for proving resource bankability.

Perhaps the biggest impact that using slimholes can make on schedule is when the cost or difficulty of conventional drilling means that this exploration phase of drilling does not start until a range of other factors (such as risk equity funding and a high tariff) are in place. In these cases, the projects can be stalled for decades following the surface exploration activities.

PROJECT FINANCIAL IMPACTS

Return on Investment - Internal Rate of Return (IRR):
Where projects are developed on an Independent Power Producer (IPP) basis they are oftentimes owned by a Special Purpose Company (SPC) and developed on a Non-Recourse Finance basis. In this situation Developer equity is usually required to fund the SPC activities up to the Financial Investment Decision (FID) gate. Greenfield geothermal projects usually take at least 4 years from concession capture to FID, and frequently longer. During this period exploration, delineation and finally appraisal wells are progressively drilled to respectively prove the resource, then delineate the resource and finally get to the proven MWe under wellhead that the lenders require at FID. Where the exploration and delineation drilling involves full size wells rather than slimhole wells, the Developer equity is larger and has to wait longer for its return. This means the tariff required must be higher.

An argument often made in favour of full size exploration wells is that since slimholes produce very little if any MWe (megawatt electrical equivalent), then more appraisal wells will be required and all the slimholes are doing is adding more total cost to the project. But actual analysis shows that the increased success rates of conventional drilling due to earlier slimholes more than offsets the cost of the slimhole drilling.

This is demonstrated in Figure 7 showing reduced capital over a similar timeframe is required to reach Commercial Operation Date (COD) using deep slimholes. The reduced

capital cost has the opportunity to allow a reduced tariff for a given Internal Rate of Return (IRR), or increased IRR for a given tariff.

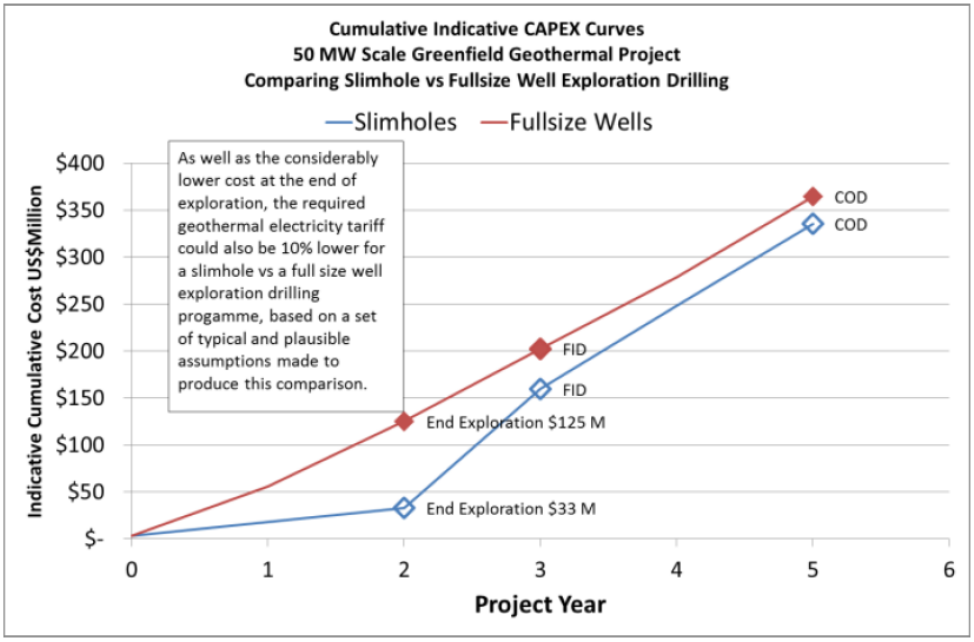

Figure 7: Indicative CAPEX for a 50 MWe project with and without use of deep slimholes. Red curve is using only conventional drilling, blue curve is using deep slimholes for the exploration phase. FID = Financial Investment Decision, COD = Commercial Operation Date.

Cost of Failure:

Throughout the exploration and delineation drilling phases of a greenfield geothermal project there is a risk that there is no resource, or that the resource will be too costly to develop, or that the project may not proceed to FID. Developers will commonly apply a decision tree process to assess the probability that they will exit the project at each of the main decision gates. At exit, some or all of the cost expended to that point will be lost for no return.

Geoscientific data collected may indicate a significant chance that exploration drilling may not find a useful resource. For example, this may be because there are few, if any, strong thermal features, and much of the evidence for a system rests on geochemistry from weakly flowing springs and positive geological and geophysical indications. We see some projects at this stage where the probability of discovering a useful resource may be much less than 50%. Under these circumstances there is a considerable chance that equity invested in exploration and delineation drilling may be lost. If the decision is made to abandon the project based on the results of the first wells, then the best result for the Developer would be to have spent the smallest amount of equity on the drilling campaign. This concept emphasises the utility of a slimhole exploration and delineation program for high risk projects, and is demonstrated in Figure 8.

[Note that Probability of Discovery is now officially defined for geothermal in the UNFC 2009 resource classification system which is endorsed by the International Geothermal Association (IGA): "Specifications for the application of the United Nations Framework Classification for Fossil Energy and Mineral Reserves and Resources 2009 (UNFC-2009) to Geothermal Energy Resources"].

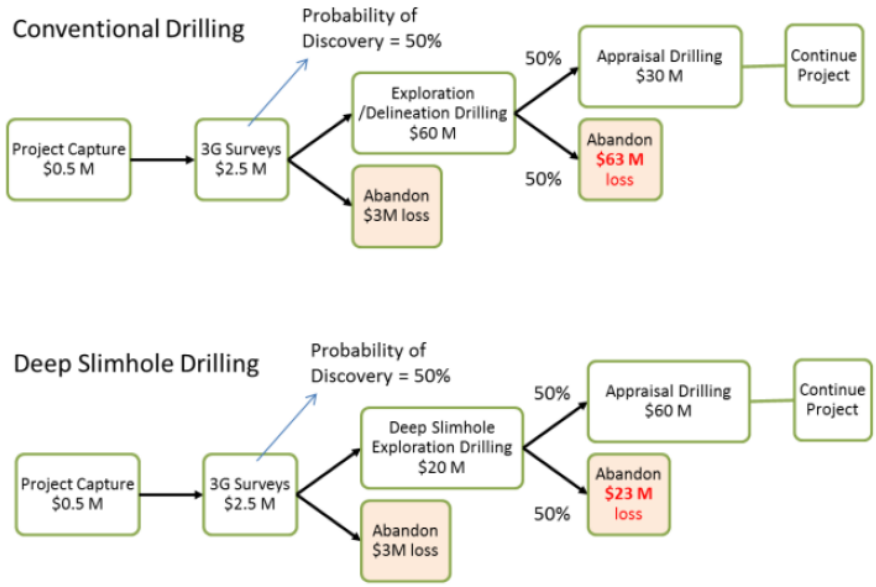

Figure 8: There is potential to exit a project at each major phase if the project does not prove viable. If Probability of Discovery from exploration drilling is low, then the use of deep slimholes puts less capital at risk than when using conventional wells for the exploration phase.

Risk Adjusted Net Present Worth (rNPV):

This burden of the cost of failure has to be evaluated and can be estimated using probability weighting of the NPV stream for the project.

The highest risk adjusted net present value (rNPV) for the project may be achieved by a slimhole exploration and delineation program, particularly where the Probability Of Discovery (POD) of actually finding a resource is low.

As one of our very experienced geothermal development clients recently noted "We try and prove that the resource DOES NOT EXIST as cheaply as possible".

A big reason for following this approach is that for a geothermal developer with a portfolio of projects, they have to carry the cost of failures across the business. It is not enough to just do the economics for the success case: a competent and responsible developer has to account for the "failures" as well.

Any tariff structure for geothermal should consider this, but equally in a fixed tariff environment, reducing failure cost will improve the viability of projects.

CASE STUDY EXAMPLES

We have compiled a dataset of 45 geothermal fields from 14 countries where slimholes have been utilized (Figure 10 and Table A1). Slimholes have been flowed at 28 of these projects (62%), and slimholes at 33 of these projects (73%) have successfully intersected the target reservoir. Below are some specific examples of projects included in this database.

Wayang Windu, Indonesia

The first exploratory slimhole was drilled at the Wayang Windu field in 1993-1994 by Pertamina. Another four slimholes were drilled in 1996 by Mandala Nusantara Limited, the initial developers of the field. This later slimhole drilling was undertaken in parallel with the drilling of initial deep production wells in the central part of the field, as part of an accelerated exploration and development drilling program. The objective of slimholes was to delineate the geothermal reservoir to help accelerate financial closure (Figure 9). The slimholes were rotary drilled in the upper section and then continuously cored to a total depth of 1,500 m and constructed as permanent monitoring wells.

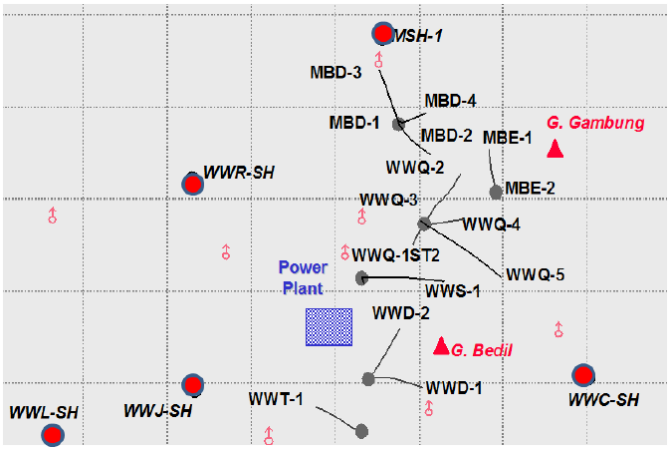

Figure 9: Wayang Windu early well field layout. Delineation slimhole locations shown as red circles and denoted by –SH suffix

In addition to helping prove the extent of the resource and validating the field concept model, the slimholes were a key component in the development of a four facies volcanic model of the field (Bogie and MacKenzie, 1998). The continuous core samples were valuable in supplementing the geological and formation imaging information obtained from the larger production wells. The lithostratigraphic information was particularly important in helping to understand the distribution and physical characteristics of clay-rich tuffaceous siltstone beds which are widespread across the Wayang Windu area (Bogie et al., 2008). These beds were responsible for significant formation related drilling difficulties during the early stages of the deep production well drilling campaign. They were difficult to delineate from cuttings

generated by conventional rotary drilling due to their geomechanical instability when hydrated by drilling fluids and propensity to contaminate cuttings derived from the underlying strata. The continuous core samples obtained from the slimholes proved highly valuable in this regard.

The slimholes were all constructed with continuously grouted casing and a perforated liner within the deeper sections of the wells. This enabled temperature and pressure measurements to be made to total depth. One of the slimholes, WWR, also sustained discharge of low pressure steam for several days.

The four deep slimholes drilled in 1996 were all completed close to their design depth without any major technical difficulties. The drilling process was completed efficiently and, in addition to achieving the desired technical outcomes, the drilling budget and program objectives were successfully met. A key reason for this successful outcome was the use of suitably specified and well maintained drilling equipment that was procured from the USA. This equipment was provided by Tonto Drilling Inc. and comprised a truck-mounted Universal Drill Rig Model 1500 (Figure 11). The use of a drilling contractor with substantial experience in geothermal drilling conditions was also important for completing a successful drilling campaign and for the wells achieving their intended objective.

Figure 11: Combined slimhole (orange rig in foreground) and conventional well drilling (white rigs in background) approach used at Wayang Windu, Indonesia in 1996.

APAS KIRI, MALAYSIA

A recent slimhole has been drilled at the Apas Kiri project in Sabah, Malaysia in the NE of the island of Borneo (Libbey et al., 2017). The field is associated with the Pleistocene-aged Mt. Maria volcano, the westernmost of a chain of volcanic features that are situated along the Semporna Peninsula. The result of initial surface geoscientific exploration provided indications of a medium to high temperature resource (Siong et al., 1991; Barnett et al., 2015), however, there was considerable uncertainty owing to the nature of the surface manifestations (the hottest features are 75°C effervescent springs) and ambiguity in the resistivity model of the system.

To further assess the economic potential of the Apas Kiri prospect, slimhole AK-1D was drilled vertically to a depth of 1,449 m from a pad on the SE flank of Mt. Maria. The upper 310 m of the well was drilled using percussion-air and tricone methods and the remainder was drilled using a diamond core bit. The bottomhole diameter is NQ, with an HQ production casing cemented at 1,359 mMD.

Core samples from AK-1D revealed a subsurface stratigraphy dominated by massive and brecciated dacite and andesite flows, with intercalated volcaniclastic units. The rocks are highly fractured, faulted, and veined and display a prograde hydrothermal alteration sequence typical to geothermal systems situated in volcanic terranes.

Initial temperature runs were conducted during drilling pauses using a HOBO® U12-015 data logger and maximum registering thermometers (the latter which were useful for providing measurements beyond the data logger's limit of ~150°C). Data provided by these preliminary measurements correspond quite closely with more detailed temperature logs that were collected after the completion of the well (Libbey et al., 2017). Measured temperature profiles display a transition from conductive to more convective gradients at a depth of ~1,100 m, where a temperature of 180°C is reached. Maximum temperatures in the well are exhibited at the bottom of the hole and reach ~200°C. A small temperature inversion near the top of the profile reflects a shallow warm water (likely mixed steam-heated) aquifer. Multiple cement plugs were required to seal off this zone.

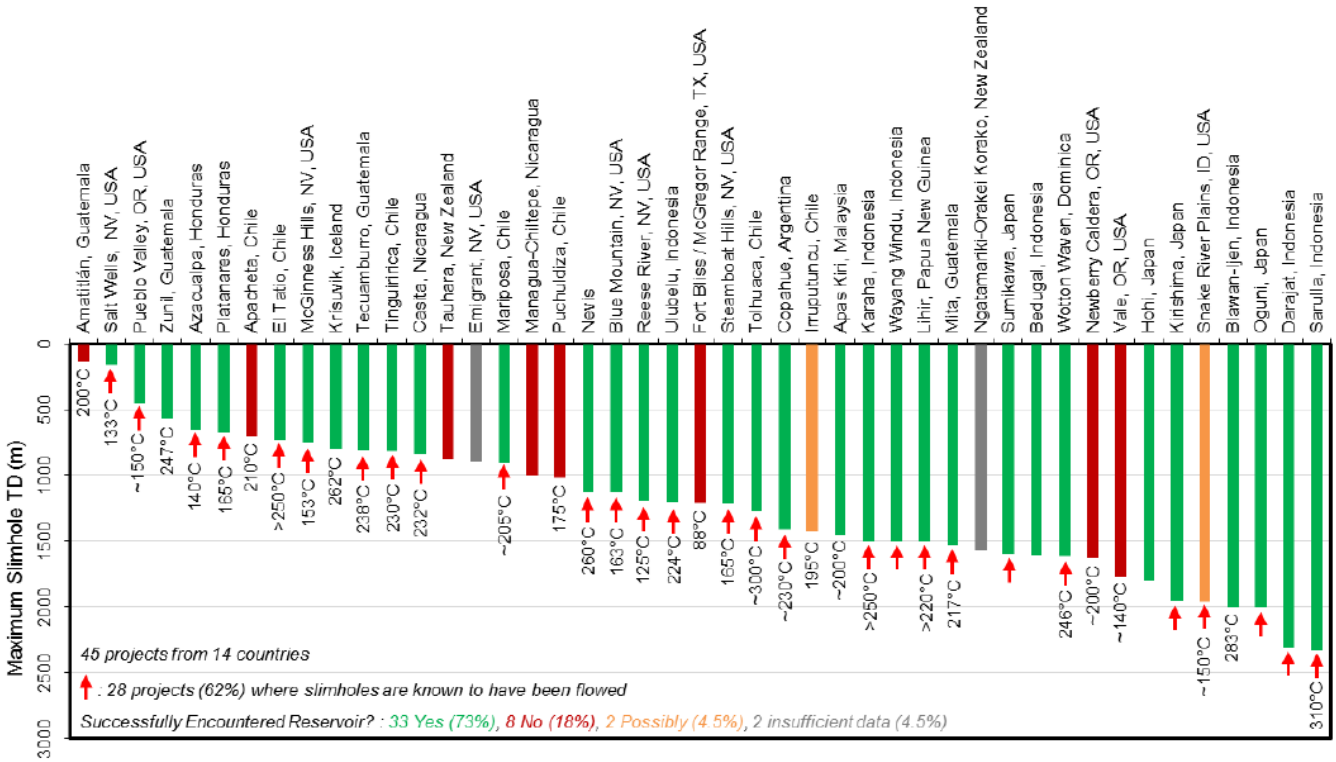

Figure 10: Maximum depth of slimholes utilised at geothermal projects. Maximum temperatures intersected also shown. Red arrows delineate projects where slimholes are known to have been flowed. See Table A1 for more detailed information.

The measured temperatures, rapid heat-up times, and largely convective temperature gradient at the base of the well were all considered successful outcomes of AK-1D. A related success for the project was the observed correlation between the downhole alteration zonation and measured temperature profiles with the conductor in the 3D MT inversion model.

The correlation between the surface and downhole geological, geophysical, and P-T datasets has proven highly valuable for confirming the presence of a medium to high temperature, neutral pH geothermal resource at Apas Kiri. Data made available from the slimhole has greatly assisted with refining the conceptual model of the geothermal resource and defining future well targets. Additionally, the identification of clay-rich volcaniclastic units and shallow warm-water aquifers has provided vital information about "problem formations" that will assist with the planning, design and successful completion of future wells.

Casita

The Casita geothermal project is located in the NW of the Cordillera de los Marrabios of Nicaragua that constitutes part of the volcanic arc that runs through the country (White et al., 2012).

A MT survey and gas chemistry from a single fumarole provided positive results indicative of a steam cap that may be sitting upon a wider liquid resource. Risks from terrain constraints, poor slope stability and the limited occurrence of thermal features that could provide valid geothermometry was addressed by drilling the CSS-1 slimhole in 2011.

Figure 12: Slimhole drilling with a very small well pad enabled well CSS-01 at Casita to be drilled on very steep slopes. Water was carried by water tanker to the site.

It was planned to drill the hole vertically to 1,000 m and to set a production casing at 600 m. Drilling difficulties lead to a reduction of these depths to 842 m and 495 m, respectively. The hole penetrated intercalated andesitic lavas and pyroclastics as had been expected. Several large losses in drilling circulation were associated with many of the fractured lava flows that were encountered and this required the placement of numerous cement plugs. Weak argillic alteration was found above the reservoir and much stronger alteration deeper in the well. This deeper alteration did not match with current conditions and appears to have formed during an earlier liquid alteration event where temperatures were lower.

The well produced dry steam (Figure 13) confirming the presence of a steam cap, but it failed to reach its full programmed depth and the occurrence of an underlying liquid reservoir was not fully tested. Nevertheless, the gas geochemistry indicated that this was most likely the case.

Figure 13: Slimhole well CSS-01 on discharge; note that the water vapour is coming out the silencer with none coming from the weir box indicative of a dry discharge.

The CSS-1 slim hole reduced the risk of constructing full size roads, pads and wells in in areas indicated by the MT survey to establish that the MT survey is indicative of the resource. It is anticipated that a full sized drilling program will take place in the near future.

Darajat, Indonesia

Three deep production wells were drilled at Darajat by Pertamina in the late 1970s, and a further 14 by Amoseas Indonesia between 1986 and 1994, when the 55 MWe Darajat Unit I was commissioned. Further exploration between 1996 and 1998 included geophysical and geochemical surveys, and 12 new production wells. Also at this time, 6 deep slimholes were drilled toward the field margins with the purpose of helping to confirm the extent of the steam zone and to develop updated resource capacity estimates. The detailed geological information from these slimholes, together with data from production and reinjection wells, meant that a detailed three dimensional volcanic facies based geological model of the Darajat geothermal reservoir could be constructed (Rejeki et al, 2010). This three dimensional geological model was then used as the basis of a numerical simulation model that Chevron used for making reservoir predictions and informing further field development and operational strategies.

One of the key reasons for using slimhole drilling at Darajat was because it provided a lower cost approach for resource delineation. Providing a reduced environmental impact in challenging terrain due to the smaller equipment and drilling infrastructure requirements was also an important driver for the slimhole drilling approach.

A detailed review of the Darajat slimhole drilling experience is provided by Riza and Berry (1998). The equipment used was the same Tonto Universal Drilling rig set-up used at Wayang Windu. The slimholes were successfully completed and met their objectives at a daily rate of about 40% of the daily cost that was applicable at the time for a large rig drilling approach. Riza and Berry (1998) describe some important learnings from the slimhole drilling campaign including:

- the use of a rotary drilling approach for hole sections which prove difficult for coring or with persistently low drilling penetration rates.
- options for retrieving any stuck pipe or 'fish' left in hole due to drilling difficulties are limited compared to a conventional large rig approach. This required needing to drill a sidetrack leg in some wells.
- some issues with increased torque when coring deeper sections successfully alleviated through the use of lubricant additives to the drilling fluid system.
- formation related drilling difficulties in friable red clay-rich units could be stabilised by cementing though did prove time consuming to deal with and drill out.

Riza and Berry (1998) tabulated the depth of the wells drilled, and we have calculated the days per 1,000 m drilled for these (Table 3). Two wells (S-3 and S4) were deepened using a larger coring rig, and eventually the reservoir was encountered with all but one well. The deepening of S-4A encountered many problems, but the average drilling rate for all other drilling was about 39 days per 1,000 m of depth.

Table 3: Depth vs drilling duration for Darajat slimhole drilling. Based on data provided by Riza and Berry (1998).

Well	TD (m)	Days / 1,000m	Entered Reservoir
S-1	1,356	38	Yes
S-2	1,449	59	Yes
S-3	1,567	41	No
S-4	1,602	32	No
S-5	2,300	24	Yes
S-6	1,932	30	No
S-3A	2,337	45	Yes
S-4A	2,213	152	Yes

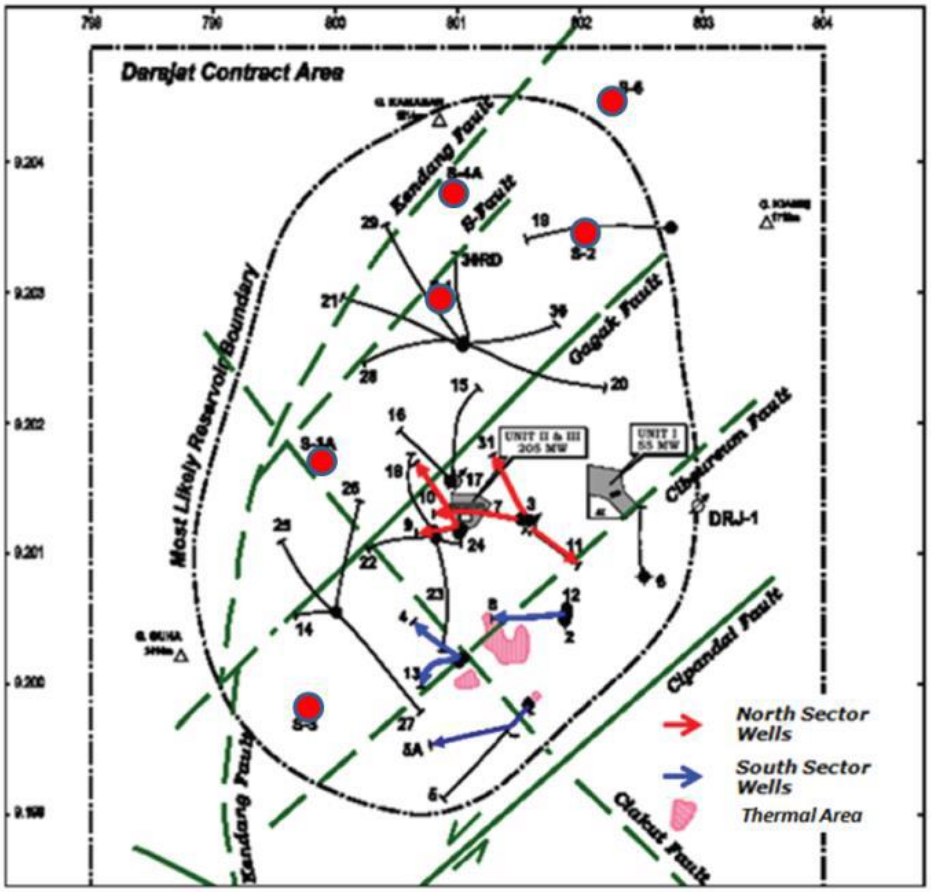

Figure 14: Darajat steamfield, with the slimholes drilled in 1996-98 circled in red. The coverage of these wells gave confidence in the extent of reservoir, particularly in the north, and deep deviated wells have not been drilled in that area.

Mita, Guatemala

The Mita geothermal system is located at Cerro Blanco in southern Guatemala and hosts a high grade epithermal gold deposit. While initially identified as a highly prospective mining project, early exploration drilling indicated a large volume of hot water in close proximity to the ore deposit. Environmental permitting requirements meant that any mining would need to be undertaken by underground methods, so a significant early challenge was to dewater and cool the rocks before mining could safely proceed. At the same time that the mine dewatering requirements were being defined it was identified that exploitation of the associated geothermal resource was an option for providing power generation to the project.

Field geology, geochemistry and geophysical surveys to investigate the geothermal resource were completed in 2007 and 2008, but there was still considerable uncertainty as to the location and conceptual understanding of the geothermal system. Because of this uncertainty, the next stage of investigation comprised four inclined (at up to 30° from vertical) slimholes drilled to depths of 1,200-1,530 m. The first of these holes targeted the interpreted upflow zone, but was not particularly hot, and had very low permeability. The core from this hole indicated that interpretation of the MT data was complicated by fossil hydrothermal alteration, including alteration associated with the epithermal mineralisation, and a thick sequence of clay-rich sedimentary rocks, overlain by young lava flows. The second and third slimholes were also not very permeable, but they were hotter and did discharge, and it was not until the fourth hole that good permeability was encountered. Long term production testing of the last well enabled detailed characterisation of the reservoir production testing and enabled the discharge chemistry to be evaluated (Figure 3).

For the Mita project, slimhole drilling was used to test the initial conceptual model, which was poorly constrained after surface exploration so was considered to have a low probability of drilling success. It enabled the resource to be outlined (to a degree) for a much lower cost than would have been the case with production wells, and helped inform a strategy for drilling production and injection wells for a potential power generation development.

Lihir, Papua New Guinea

The Lihir geothermal field is unusual in many ways, not least of which is that the first deep geothermal wells were drilled after hundreds of shallow holes, which delineate the superimposed gold deposit. To assess a proposed 40 MWe expansion to the geothermal power plant developed to supply electricity to the mining operation, four step-out deep exploration slimholes were drilled between 2007 and 2008. These wells were deviated at 30° from vertical and drilled to a total depth of 1,500 m to evaluate the extent of geothermal resource to the northeast and northwest of the existing production sector. Core samples from these slimholes provided significant new information, particularly in characterising the monzonitic intrusive complex in the reservoir, since although there are many standard geothermal wells in this area, no cores were taken during geothermal drilling, and no drill cuttings were

collected after total losses were encountered, typically at about 600 m.

Drilling and testing of two slimhole wells (GW47 and GW52) confirmed zones of fracture permeability and significant temperatures (> 220°C). The slimholes thus provided new geological data that could not be obtained from conventional geothermal wells. They provided cost-effective temperature, pressure and permeability data from the reservoir to the north and east, some 3 km beyond the previous area of proven resource. This new information was used to guide the geothermal exploration/development strategy for the mining operation.

Laguna del Maule (Mariposa), Chile

Magma Energy Corp had largely completed field geology, geochemistry and geophysical surveys at Laguna del Maule by the end of March 2009, but the exploration concession was due to expire in July and the positive results indicated by the field studies prompted the company want to apply for an exploitation concession. To do that, they had to prove that the concession contained a resource of a suitable size and temperature to support a geothermal development.

The resource size was indicated by the MT geophysics survey data, but at least one well had to be drilled into the reservoir to prove the resource temperature. With the resource located 10 km from the nearest road, and 1,200 m higher in elevation, full sized production wells were not an option within the available timeframe. However, with a helicopter supported drilling operation (Figure 15), by early June, a vertical slimhole was completed to a sufficient depth (659 m) and a sufficiently high downhole temperature (over 200°C) was recorded. An inferred resource of 140 MWe was declared, and an application for an exploration concession was submitted before the deadline in July.

Figure 15: Helicopter supported slimhole drilling campaign at Laguna del Maule, Chile

In this example, helicopter supported slimhole drilling was the only feasible option to prove reservoir temperatures in the time available. Because of equipment weight limitations, a relatively small rig was used. Despite the small rig size and challenging conditions, including the modification of Kuster PT logging procedures for running in a BQ (46 mm) sized hole and the onset of winter in the Andes, the initial well at Laguna del Maule achieved its objective by drilling down to 659 m so that downhole temperatures could be measured.

CHALLENGES OF DEEP SLIMHOLE DRILLING

The biggest challenge with using deep slimholes for reservoir exploration is achieving the required depth. The relatively small hole sizes means that there are small tolerances between drilling string and the hole such that equipment can easily be stuck. Additionally, there are fewer options for adding additional casings in the event of problems. The small diameter tubulars also can face torque issues at deep levels.

The solutions to these problems lie in planning and drawing on the available geothermal experience with slimhole drilling. Riza and Berry (1998) give a good description of the measures they took with materials and procedures at Darajat in the 1990's. Some recent slimhole drilling programs have used contractors that are familiar with coring for mineral exploration, but have not budgeted for contracting geothermal drilling engineering expertise nor the use of suitable materials. The use of high temperature drilling fluid lubricants and rod/barrel grease is essential.

The small rigs used for coring operations may limit the depth that the upper casings can be placed. However, provided that shallow upper cool aquifers are cased off, a production casing does not necessarily need to reach the top of reservoir, and setting a "production" casing in the clay cap region may be fine for exploration purposes.

In situations where a slimhole fails to meet its exploration objectives or is unable to reach the target total depth it is usually challenging to successfully work the well over in the same way that can be done for conventional sized wells. This is mainly due to the smaller equipment and casing configuration that is used for slimhole drilling, although there are some examples of slimholes that have been successfully modified during drilling due to formation related difficulties encountered. An example of this is at Darajat where several holes were either deepened and/or sidetracked to depths in excess of 2,000 m due to caving formation and stuck pipe incidents (Riza and Berry, 1998).

Slimholes can be flowed, but not at the same mass flow rates at larger diameter wells, so while they can determine the existence of good permeability, they cannot readily test for reservoir drawdown effects.

Various attempts have been made to extrapolate slimhole productivity to full sized production well productivity (e.g. Garg and Coombs 1997). While it is not possible to accurately determine the expected behaviour of production wells, modelling can provide useful indications that are good enough to evaluate expected project economics for the purpose of justifying the higher cost of larger wells in an appraisal drilling program.

ADDITIONAL USES OF SLIMHOLES

While slimholes are typically too small for production on large scale projects, they do have valuable use if retained open on a project:

Pressure Monitoring:

Slimholes are ideal for monitoring pressure in a reservoir, providing valuable early tracking of reservoir pressure possibly within the main production areas but possibly also on the margins of the field if used as delineation

wells. This is highly valuable, as typically all successful wells are used on most projects, leaving none for designated long-term monitoring purposes. With no central monitoring wells, it can be challenging to measure pressure change in some systems if relying only on well shut surveys during plant shutdown and maintenance periods.

Sentinel Monitoring:

Slimhole wells located on margins of field can monitor both pressure and temperature changes that may occur from the incursion of marginal groundwaters or previous outflows for the system. This acts as an early warning system of undesirable effects in the productive reservoir. Sentinel wells can also be used for monitoring the effects of production on neighbouring undeveloped systems to assist with proactive protection of areas which may be culturally or environmentally sensitive.

Condensate Injection:

In smaller projects (10-25 MWe) condensate flows can be modest and may be accommodated by a slimhole with good injectivity characteristics. The need for condensate disposal is often a last minute consideration after the prioritisation for obtaining the main production and injection capacity, and a good slimhole in the central part of a field may suit the purpose.

Production and Injection for Small Projects:

Slimholes drilled to explore resources in remote locations can be used for small scale geothermal generation projects that may serve long-term as remote power generation (Vimmerstedt, 1998). Such small developments may also provide the confidence for considering the cost of drilling larger wells and a transmission connection for a remote system that would not otherwise be explored.

Table 4. Comparison between slimhole drilling and conventional wells

Feature	Slimhole Drilling	Conventional Drilling
Data collected		
Geology	Full core and accurate depth and thickness information (cored slimholes) Fracture characteristics visible and measurable	Yes - Cuttings with occasional core. Sophisticated logs (FMI, acoustic) needed to get fracture imaging
Temperature	Can measure temperatures more reliably while drilling. PT logs at completion	Yes – Requires heating after well completion to get reliable temperatures
Permeability	Completion tests and injectivity	Yes - Completion tests and injectivity
Productivity (well flow)	Can flow. Must estimate larger well capacity.	Yes – can flow and test at operational conditions
Chemistry	Samples can be taken from flowing well. Less flowrate during drilling may give quicker stabilisation of flow chemistry	Samples can be taken from flowing well.
Infrastructure and Costs		
Roads and well pads	Small well pads (40 x 40 m) Single lane track (temporary) or helicopter	Large well pads (70 x 100 m) 2 lane road with no steep grades
Water Supply	Coring rig operations may need as little as 40 lpm	Circulation rates up to 3000 lpm. Major water supply infrastructure.
Land permits	Possibly temporary lease (plug and abandon) to reduce time for access	Permanent ownership / rights needed to retain wells for later production / injection.
Cost		
Infrastructure costs	Modest	Can be high for difficult terrain
Wells costs	Typically 25-40% of conventional wells	
Development Implications		
Cost of failure	Modest	High
Schedule	Reduced time to start drilling and complete Exploration stage Assist delineation and appraisal stages at lower cost	
Overall project cost	Can be less than conventional wells	

CONCLUSIONS

Some concerns commonly expressed about using slimholes for geothermal exploration are that they do not reach deep enough into the reservoir, cannot demonstrate well productivity and simply introduce another drilling stage that adds to overall project schedule and cost.

While some recent projects in Asia have had drilling problems and struggled to complete slimholes to the target depth in reasonable timeframe, slimhole wells drilled over 20 years ago were successfully drilled to depths of over 2,000 m in Indonesian geothermal systems. This approach has also been applied elsewhere in the world with good results in terms of completing wells safely and successfully, while also achieving desired exploration outcomes.

When conducting slimhole drilling programs for geothermal exploration, it is not sufficient to only draw from local mineral drilling industry experience. The special characteristics of subsurface geothermal conditions, and the complex terrain associated with many geothermal environments needs to be factored into slimhole well design and drilling plans. Supervision by personnel with geothermal-specific expertise is essential during slimhole drilling, just as it is for conventional well drilling.

With a downward pressure on tariffs because of the availability of lower cost alternative energy options, and the exploration of more challenging, higher risk prospects, the geothermal industry cannot afford the high cost of exploration drilling in many cases. This barrier of high equity capital at high risk early stages of geothermal

project is stopping projects from moving forward in many regions globally. Reducing the magnitude of capital at risk in exploration through the use of slimhole drilling programs has the opportunity to get more projects proven and eventually "bankable".

A full set of comparisons between slimhole drilling and conventional wells is provided in Table 4

ACKNOWLEDGEMENTS

The support of Jacobs in supporting the writing of this paper is gratefully acknowledged.

REFERENCES

Aravena, D. and Lahsen, A. A geothermal favourability map of Chile, preliminary results. GRC Transactions, v. 37, 2013.

Asturias, F. Reservoir assessment of Zunil I & II geothermal fields, Guatemala. UNU-GTP Reports, no. 3, 2003.

Barnett, P.R., Mandagi, S., Iskander, T., Abidin, Z., Amadaloss, A., and Raad, R. Exploration and Development of the Tawau Geothermal Project, Malaysia. Proceedings World Geothermal Congress, 2015.

Bogie, I., Kusumah, Y.I., and Wisnandary, M.C. Overview of the Wayang Windu geothermal field, West Java, Indonesia. Geothermics, Vol. 37, No. 3, pp. 347-365, 2008.

Bogie, I. and MacKenzie, K.M. The Application of a Volcanic Facies Model to an Andesitic Stratovolcano Hosted Geothermal System at Wayang Windu, Java, Indonesia. Proceedings 20th New Zealand Geothermal Workshop, 1998.

Boseley, C., Bignall, G., Rae, A., Chambefort, I., and Lewis, B. Stratigraphy and hydrothermal alteration encountered by monitor wells completed at Ngatamariki and Orakei Korako in 2011. Proc. New Zealand Geothermal Workshop, 2012.

Code of Practice for Deep Geothermal Wells. New Zealand Standard: NZS 2403:2015.

Combs, J., Garg, S. K. and Pritchett, J.W. Geothermal slim holes for small off-grid power projects. Renewable Energy, Vol. 10, No. 2/3, pp. 389-402, 1997.

Combs, J., Garg, S. K. Discharge Capability And Geothermal Reservoir Assessment Using Data From Slim Holes. Proceedings World Geothermal Congress, 2000.

Cumming, W.B., Vieytes, H., Ramirez, C.F., and Sussman, D. Exploration of the La Torta geothermal prospect, Northern Chile. GRC Transactions, v. 26, 2002.

Dal – In.te.sa. SpA. and Geotermica Italiana S.r.l. Estudio de prefactibilidad geotermica en la region central de Honduras, 6) Perforacion exploratoria y geo-petrographia, Informe Final. ENEE, Impresa National de Energia Electra, Tegucigalpa, Honduras, 1988.

Daud, Y., Nuqramadha, A., Fahmi, F., Pratama, S.A., Rahman, K.R., and Subroto, W. Discovering "hidden" geothermal reservoir in Blawan-Ijen geothermal area (Indonesia) using 3-D inversion of MT data. Draft paper, 2017.

Delahunty, C., Nielson1, D.L. and Shervais, J.W. Deep Core Drilling of Three Slim Geothermal Holes, Snake River Plains, Idaho. GRC Transactions, Vol. 36, 2012.

Finger, J.T. and Jacobson, R. Slimhole drilling logging and completion technology – an update. Proceedings World Geothermal Congress 2000.

Finger, J., Jacobson, R., Hickox, C., Combs, J., Polk G. and Goranson, C. Slimhole handbook: procedures and recommendations for slimhole drilling and testing in geothermal exploration. Sandia Report SAND99-1976, 1999.

Garg, S.K. and Combs, J. Use of slim holes for geothermal exploration and reservoir assessment: A preliminary report on Japanese experience. Sandia National Laboratories Technical Report SAND93-7029, 1993.

Garg, S.K. and Combs, J. Slim holes with liquid feed zones for geothermal reservoir assessment. Geothermics Vol. 26, No. 2, pp. 153-178, 1997.

Gehringer, M. and Loksha, V.C. - Geothermal Handbook: Planning and Financing Power Generation. Washington DC: World Bank Group, Energy Sector: 2012.

Goff, S.J., Duffield, W.A., Goff, F.E., Heiken, G.H., and Janik, C.J. Application of scientific core drilling to geothermal exploration: Platanares, Honduras and Tecumaburro volcano, Guatemala, Central America. Proc. 7th Int'l Symp./Observation of Continental Crust Thru Drilling, Santa Fe, NM, April 25-30, 1994.

Goff, S.J., Goff, F., and Janik, C.J. Tecuamburro volcano, Guatemala: Exploration gradient drilling and results. Geothermics, v. 21, no. 4, 1992.

Gunderson, R., Ganefianto, N., Riedel, K., Sirad-Azwar, L. and Suleiman, S. Exploration Results in the Sarulla Block, North Sumatra, Indonesia. Proceedings World Geothermal Congress, 2000.

Haraldsson, I.G. Geothermal activity in South America: Bolivia, Chile, Colombia, Ecuador, and Peru. UNU-GTP and LaGeo Short Course on Conceptual Modelling of Geothermal Systems, El Salvador, Feb 24-Mar 2, 2013.

Henkle, W.R. Phase 2 Reese River geothermal project – Slim well 56-4 drilling and testing. Western Geothermal Partners Technical Report, 2008.

Hickson, C., Rodriguez, C. Siefeld, G., Selters, J., Ferraris, F., and Henriquez. Mariposa geothermal system: A large geothermal resource in Central Chile (320 MWe inferred). Sernageomin Bulletin, 583-585, 2011(?).

Hochstein, M, Sudarman, S. History of geothermal exploration in Indonesia from 1970 to 2000. Geothermics 37, 2008.

Khubaeva, O. Geothermal mapping in the Krysuvik geothermal field. UNU-GTP Reports, no. 8, 2007.

LaFleur, J. and Hoag, R. Geothermal exploration on Nevis: A Caribbean success story. Proc. GRC Transactions, v. 34, 2010.

Lahsen, A., Sepulveda, F., Roja, J., and Palacios, C. Present status of geotermal exploration in Chile. Proc. World Geothermal Congress, 2005.

Lobato, M.L., Fujino, T., and Ayala, J.C.P. Amatitlan geothermal field exploration in Guatemala. GRC Bulletin, Nov/Dec, 2000.

Libbey, R., Bogie, I., Peng, W.F., Duasing, J., Payer, A., Zamhari, Z., Lojingau, D., Urzua, L., Ussher, G.N., and

Brotheridge, J. Insights into the Apas Kiri Geothermal System from AK-1D – Malaysia's first geothermal exploration well. GRC Transactions 41; 2017

Melosh, G., Fairbank, B., and Niggeman, K. Geothermal drilling success at Blue Mountain, Nevada. Proc. Stanford Geothermal Workshop, 2008.

Melosh, G., Moore, J., and Stacey, R. Natural reservoir evolution in the Tolhuaca geothermal field, Southern Chile. Proc. Stanford Geothermal Workshop, 2012.

Moore, J.N., Norman, D.I., Ellis, R. Geochemicalevolution Of The Vapor-Dominated Regime At Karaha-Telaga Bodas Indonesia: Insights From Fluid Inclusion Gas Compositions. Proceedings 24th NZ Geothermal Workshop, 2002.

Nakanishi, S., Abe, M., Todaka, N., Yamada, M., Sierra, J.L., Gingins, M.O., Mas, L.C., and Pedro, G.E. Copahue geothermal system, Argentina – Study of a vapor-dominated reservoir. Proc. World Geothermal Congress, 1995.

Nielson, D.L. and Garg, S.K. Slim Hole Drilling and Testing Strategies. Proceedings 6th ITB International Geothermal Workshop, Bandung, 2017.

Nielson, D.L. and Garg, S.K. Slim Hole Reservoir Characterization for Risk Reduction. Proceedings 41st Workshop on Geothermal Engineering, Stanford, 2016.

Nielson, D.L. and Shervais, J.W. 2014. Conceptual model for Snake River Plain geothermal systems. Proc. Stanford Geothermal Workshop, 2014.

Nordquist, J. and Delwiche, B. The McGinness Hills geothermal project. GRC Transactions, v. 37, 2013.

Osborn, W., Hernández, J., George, A. Successful Discovery Drilling in Roseau Valley, Commonwealth of Dominica. Proceedings, Thirty-Ninth Workshop on Geothermal Reservoir Engineering Stanford University, 2014.

Procesi, M. Geothermal Potential Evaluation for Northern Chile and Suggestions for New Energy Plans. Energies 2014, 7. ISSN 1996-1073, www.mdpi.com/journal/energies.

PT Madani Alam Lestari. Slimhole drilling. Brochure, July 2016.

Rejeki, S., Rohrs, D., Nordquist, G. and Fitriyanto, A. Geologic Conceptual Model Update of the Darajat Geothermal Field, Indonesia. Proceedings World Geothermal Congress, 2010.

Reyes, N., Vidal, A., Ramirez, E., Arnason, K., Richter, B., Steingrimsson, B., Acosta, O., Camacho. Geothermal exploration at Irruptuncu and Olca volcanoes: Pursuing a sustainable mining development in Chile. GRC Transactions, v. 35, 2011.

Riza, I. and Berry, B.R. Slimhole Drilling Experience at Darajat Geothermal Field, West Java, Indonesia. Proceedings 20th New Zealand Geothermal Workshop, 1998.

Siong, L.P., Intang, F., and On, C.F. Geothermal prospecting in the Semporna Peninsula with emphasis on the Tawau area. Geo. Soc. Malaysia, Bulletin, v. 29, pp. 135-155, 1991.

Sudarman, S., and Hochstein, M.P.. History Of Geothermal Exploration In Indonesia (1970-2010). Proceedings 36th New Zealand Geothermal Workshop 24 - 26 November 2014.

Thorhallsson, S. and Gunnsteinsson, S.S. Slim wells for geothermal exploration. Presented at "Short Course on Geothermal Development and Geothermal Wells", organized by UNU-GTP and LaGeo, in Santa Tecla, El Salvador, March 11-17, 2012.

Vázquez, M., Nieto, F., Morata, D., Droguett, Carrillo-Rosua, F.J., and Morales, S. Evolution of clay mineral assemblages in the Tinguiririca geothermal field, Andean Cordillera of central Chile: an XRD and HRTEM-AEM study. Journal of Volcanology and Geothermal Research, v. 282, 2014.

Vimmerstedt, V. Opportunities for Small Geothermal Projects: Rural Power for Latin America, the Caribbean, and the Philippines. NREL report : NREL/TP-210-25107, 1998.

White, P.J, MacKenzie, K.M., Brotheridge, J., Seastres, J., Lovelock, B.G. and Gomez, M. Drilling Confirmation of the Casita Indicated Geothermal Resource, Nicaragua. Proceedings 34th New Zealand Geothermal Workshop, 2012.

White, P.J., MacKenzie, K.M., Verghese, K. and Hickson, C. Deep Slimhole Drilling for Geothermal Exploration. GRC Transactions, Vol. 34, 2010.

Witter, J.B., Ronne, J.A., and Thompson, G.R. Exploration at the Reese River geothermal prospect in Nevada. GRC Transactions, v. 33, 2009.

Rosenberg, M., Wallin, E., Bannister, S., Bourguinon, S., Sherburn, S., Jolly, G., Mroczek, E., Milicich, S., Graham, D., Bromley, C., Reeves, R., Bixley, P., Clotworth, A., Carey, B., Climo, M., Links. GNS Science consultancy report, 2010/138.

Table A1. Examples of geothermal projects where slimholes have been utilised. Depth column colours indicate if the wells were drilled deep enough to assess the geothermal reservoir (green = yes, red = no). Outcomes column colours indicate if the well was successful in encountering a geothermal reservoir (green = yes, red=no, orange = possibly).

Project	Depth mMD	Outcomes	Flow	References
Argentina				
Copahue	1065-1414	Dry steam discharged from all 3 wells (max flow 2.5 kg/s). Max temps of ~230°C.	Yes	Nakanishi et al., 1995
Chile				
Apacheta	700	Found 210 °C. Not enough information to determine whether or not it intersected a reservoir.		Procesci 2014
Mariposa	659-900	Helicopter rig access for first well. Downhole temperatures of ~205°C measured delineate the top of the reservoir. Dominantly conductive gradients to the base of the wells.	Yes	Haraldsson, 2013; Hickson et al., 2011
El Tatio	571-735	6 slimholes Found the main outflow structure including temperatures over 250 °C	Yes	Cumming et al, 2002
Irruputuncu	800-1430	Downhole temperatures of 150 to 195°C. Well appears to be drilled to the west of a potential reservoir (as suggested by MT).	No	Reyes et al., 2011
Puchuldiza	428-1013	Max downhole temperatures of 175°C Not deep enough or on outflow	No	Lahsen et al., 2005
Tinguiririca	815	Max downhole temperatures of 230°C. Encountered a dry steam reservoir, thickness unknown	Yes	Aravena and Lahsen, 2013; Vázquez et al., 2014
Tolhuaca	1073-1274	Max downhole temperatures of 280-300°C. Wells flowed vigorously. Kicks experienced during drilling helped delineate steam zone.	Yes	Haraldsson, 2013; Melosh et al., 2013
Dominica				
Wotton Waven	1200 - 1613	Wells discovered productive reservoir and guided delineation 2 wells flowed (up to 29 kg/s). Max temp of 246°C.	Yes	
Guatemala				
Amatitlán	135	Intersected shallow 200°C aquifer. Helped refine conceptual model of system and locate upflow beneath higher elevation area.	?	Lobato et al., 2000
Mita	1200-1530	6 wells drilled. 4th well was discovery well. Max temps of 195-217°C. Resource was delineated at much lower cost than conventional wells. Flow tests provided information about the wider permeability characteristics of the reservoir.	Yes	McDowell and White, 2011
Tecuamburro	808	Max temps of 238°C measured. Well was temporarily flowed after swabbing, but stopped after drilling fluids were purged from the hole. Fish in the hole at 772 to TD.	Yes	Goff et al., 1992; Goff et al., 1994
Zunil	364-576	Step out exploration of existing field. Downhole temperatures of 235-247°C encountered. Help confirm the existence of steam zone above deeper liquid reservoir.	?	Asturias, 2003
Honduras				
Azacualpa	500-650	Downhole temperatures of 130-140°C Multiple shallow hot inflows encountered in AZ-1 (related to prominent fault target). AZ-1 was discharged Confirmation of low temperature resource.	Yes	Dal and Geotermica Italiana, 1988
Platanares	401-679	Many hot (160-165°C) water entries were encountered in the three wells. Flows obtained from 2 out of the 3 wells (PLTG-1 and -3); 5.5 to 8 L/s at WHP of 2 to 4 barg.	Yes	Goff et al., 1991; Goff et al., 1994; Finger et al., 1999
Iceland				
Krísuvik	800	Downhole measured temperatures of up to 262°C, but temperature reversals with depth.	?	Khubaeva, 2007
Indonesia				
Bedugal	685 – 1607	Found top of reservoir, but not permeability for production	No	
Darajat	1342-2310	Encountered reservoir in several wells. 2 had to be deepened to reach reservoir. Proved norther extent of the reservoir.	Yes	Riza and Berry, 1998
Karaha	1200 - >1500	Found > 250 °C and flowed in the southern Karaha area Flowed with acid fluids at Telaga Bodas.	Yes	Moore et al 2002
Blawan-Ijen	2000	High temperature (283°C) neutral pH fluid discovered. Temperature at the base of conductor in 3D MT data determined to be ~220°C (1400 mMD).	?	Daud et al., 2017; PT Madani Alam Lestari, 2016
Sarulla,	1709 – 2330	Used hybrid slimhole : rotary to deep levels, and cored bottom section. Successful discovery of two production areas. Max temps of 276-310°C measured.	Yes	Gunderson et al., 2000

Project	Depth mMD	Outcomes	Flow	References
Ulubelu	~1000 -1200	Wells helped delineate the reservoir that is an outflow system. ULB-2 had 224 °C and flowed.	Yes	Hochstein and Sudarman (2008)
Wayang Windu	~1500	Cost effective approach to delineating the margins of the productive resource. ~24 hr flow from one well	Yes	White et al., 2010
Japan				
Hohi	110-1800	About 15 slimholes drilled for deep exploration Penetrated the outflow which constituted the reservoir, but not deep enough to full demonstrate temperature inversion below 1600 m.	No	Garg and Combs, 1993
Oguni	500-700 1000-1950	15 slimholes drilled Achieved steam flowrates on 7 wells(3-8 tph steam)	Yes	Garg and Combs, 1993 Combs and Garg, 2000
Kirishima	500 -2000	23 slimholes drilled 10 wells flowed	Yes	Finger et al., 1999 Combs and Garg, 2000
Sumikawa	1600	15 slimholes drilled Penetrated reservoir and used for interference testing, 4 wells flowed	Yes	Garg and Combs, 1993 Finger et al., 1999
Takigami		11 slimholes drilled , 7 wells flowed	Yes	Finger et al., 1999 , Combs and Garg, 2000
Malaysia				
Apas Kiri	1449	Successful discovery well, with indications of permeability and high temperatures. Downhole temperatures of ~200°C measured. Unperforated NQ pipe from bottomhole to surface.	No	Libbey et al., 2017
Nevis				
Nevis	762-1127	Downhole temperatures of ~260°C measured in all 3 holes. N-3 flowed at 9.5 kg/s	Yes	LaFleur and Hoag, 2010
New Zealand				
Ngatamariki-Orakei Korako	1003 – 1570	Sentinel wells to test connection to adjacent protected system. Providing vital information for assessing the impact of the operation on the Orakei Korako thermal manifestations.	No	Boseley et al., 2012
Tauhara	880	Well encountered permeable horizons lateral equivalent to reservoir even if outside hot reservoir	No	Rosenberg et al, 2010
Nicaragua				
Casita	842	Despite wellbore restrictions (fish in hole), discharged dry steam for 10 days at ~4 tph (0.5 MW_e). Max temp of 232°C measured. Drilling difficulties highlighted need for on-site experience with geothermal conditions.	Yes	
Managua-Chiltepe	1000	Results suggested that the geothermal resource is sub-economic.	No	
PNG				
Lihir	1500	Proved significant temperatures(>220°C) 3 km beyond proven area.	Yes	
USA				
Blue Mountain, NV	645-1128	Would not sustain flow, but was air-lifted to collect chemical samples. Max temps of 148-163°C.	Yes	Melosh et al., 2008
Emigrant, NV	896		?	
Fort Bliss / McGregor Range, TX	615-1207	Max temps of 88°C reached.	No	Finger and Jacobson, 2000; Finger et al., 1999
McGinness Hills, NV	752	Max temps of 153°C reached. Flowed at 8.6 L/s. Success resulted in twinning of the well with a full-sized well (58B(P)-22).	Yes	Nordquist and Delwiche, 2013
Newberry Caldera, OR	1475-1634	High temperature (~200°C) but low permeability. Difficulties encountered during drilling (116 days to TD)	No	Finger and Jacobson, 2000; Finger et al., 1999
Pueblo Valley, OR	451	25 L/s artesian flow at wellhead P of ~5 barg (~150°C).	Yes	Finger et al., 1999
Reese River, NV	1198	Max temps of 124.5°C reached. Airlift flow test to collect chemical samples.	Yes	Henkle, 2008; Witter et al., 2009
Snake River Plains, ID	1821-1959	Max temps of ~150°C reached. Artesian flow from one well.	Yes	Delahunty et al., 2012; Nielson and Shervais, 2014
Salt Wells, NV	162	Successful discovery well for shallow low temperature resource. Stabilized flow of ~16 L/s. Max temperatures of 133°C	Yes	Finger et al., 1999
Steamboat Hills, NV	1220	Proven capability of extrapolating slimhole flow tests to larger diameter wells. Significant permeability encountered at deeper levels (possible 165°C resource or injection area)	Yes	Finger and Jacobson, 2000; Finger et al., 1999
Vale, OR	1775	Temp (max ~140°C) and permeability too low for commercial production.	No	Finger and Jacobson, 2000; Finger et al., 1999

ISBN 978-602-52132-0-5

HIGH NCG WELLS INTERFERENCE TEST FOR HIGH NCG WELLS OPTIMIZATION IN SALAK GEOTHERMAL FIELD

Doniberatus Imantoro, Abu Dawud Hidayaturrobi, Risa Prameswari Putri, Ayu Anandya Utami

Star Energy Geothermal Salak Ltd.

e-mail: dzih@starenergy.co.id; Abu.Dawud@starenergy.co.id;
risaprameswari@starenergy.co.id; ayu.utami@starenergy.co.id

ABSTRACT

The steam cap has significantly developed in East Salak resulting to dry steam production and higher Non-Condensable Gas (NCG) content in the most of East Salak wells, particularly Pad A and M- wells. Nowadays, Unit-4 experienced frequent curtailment (loss generation) due to high-NCG steam supplied by Pad A wells. Steam blending (among high- and low-NCG wells) was initiated by shutting-in or throttling high-NCG wells in order to maintain NCG content in Unit-4 below the maximum Gas Removal System (GRS) capacity (2.25wt.%). Unfortunately, this method did not give consistent results due to NCG interference among Pad A and Pad M wells.

NCG Interference was first evaluated in 2012 by observing changes in NCG concentration of certain wells after new make-up wells were POP'd or the existing wells were shutted-in. Another NCG interference evaluation was conducted on January 2014 – May 2015 to observed the optimum operation setting of high-NCG well in Pad A. However, several well still showing uncertain connectivity and camouflage by interference with other wells (Julinawati et al., 2017). Thus, an ideal interference test is needed to fully understand the NCG interference of high NCG wells. The ideal condition mentioned here is the condition where we only change 1 well per event and monitor the changes at surrounding wells. The NCG interference test was completed in 31 days operation and comprehensively shows clear NCG interference among Pad A and Pad M wells. This test result is used as reference to develop operational guideline of high NCG wells in Salak Geothermal field.

Keywords: Non Condensible Gas, Salak, High NCG, Wells Optimization, Interference

INTRODUCTION

Salak is the largest geothermal field in Indonesia and the sixth largest in the world with an installed capacity of 377 MWe. Commercial operations commenced in February 1994 with total production 59,514 GWhr (110.4 MMBOE) through the end of 2016.

Production levels have been maintained at or above the rated turbine capacity for 17 years through periodic infill drilling and injection system realignment. Currently, there are 76 production wells, 22 injection wells, four (4) monitoring wells and eight (8) abandoned wells in Salak. And more new make-up wells will be required to maintain full generation up to the end of the current Energy Sales Contract (ESC) in 2040.

BACKGROUND

Frequent curtailment experienced in Unit 4 due to high NCG steam from Pad A reaching the power plant. NCG itself could decreased the electricity power generation by reducing the vacuum level of condenser (a.k.a. back-pressure unit). If the steam entering turbine have NCG beyond handling capacity, it will significantly drop the power generation.

Thus, one of the most important issue at Salak is the NCG management. The NCG content in produced steam are expected to increase as the steam cap reservoir develops. Steam cap in eastern Salak was developed faster than in western Salak. At East Salak, Pad A has the highest NCG content with the highest NCG content from A-4, >11%. The high NCG in A-4 interference to almost all wells in Pad A if the A-4 shutted-in. Furthermore, the unsuccessful workover at A-4 (late 2015) caused the well to be shut-in and prevented the NCG from being vented. This impacted the NCG content in the steam supply by Pad A to Unit 4.

Non-Condensable Gas (NCG) is gas that is not able to condense to the liquid phase. NCG content is measured on-site using Wet-Test Meter. The NCG content (gas to steam ratio) of well can be calculated by measuring total volume of a dry gas and total volume (weight) of condensed steam collected over period of time. The dry gas volume is measured using a gas flow meter (Wet-Test Meter) and steam condensate is collected in a bottle trap and measure the volume or weighed. The NCG content (wt.%) is simply yielded by dividing the gas volume (weight) with the total weight (gas+condensate) (Wijaya et al., 2009).

As the solution, steam blending (among high and low NCG wells) was initiated by shutting-in or throttling high-NCG wells to maintain the NCG content in Unit-4 below the maximum GRS capacity. However, this method did not give consistent results due to NCG interference (or interconnectivitiy) among Pad A and Pad M wells.

NCG INTERFERENCE TEST DESIGN

NCG interference test was proposed to give better understanding of interference on NCG wells at current conditions. The idea of NCG interference test is to set ideal condition in observing NCG changes by controlling production setting. The NCG interference test program has followed this particular workflow (Figure 1).

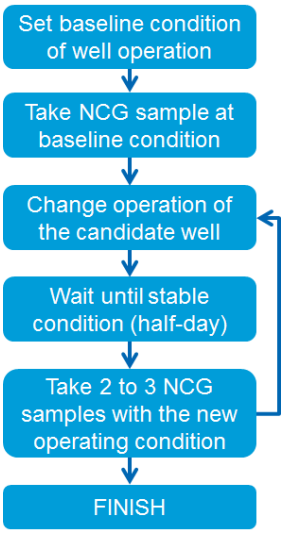

Figure 1. NCG Interference Test Workflow

First, set the baseline condition of wells. This step is very important to get the most reliable result. The NCG distribution on baseline condition will be used for analysis.

Second, change the operation condition of candidate well. The proposed conditions are venting through 10" SUV (commonly named production line), 3" (commonly named stimulation line), and 2" bypass SUV. Several things should be followed, such as:

1. Non-candidate wells should be strictly maintained at baseline condition.
2. There must be at least half-day retention time prior taking NCG samples in new operating condition.
3. Two (2) NCG samples is required to confirm the effect of operation disturbance

Repeat the workflow until all candidate wells have been tested.

There were 10 candidate wells chosen by the preliminary hypothesis regarding its relationship with A-4, which are: A-2, A-3, A-5, A-6, A-7, A-8, A-9, A-10, M-3, M-6. The sequence of the test considers well location on the field to minimize mobilization. Furthermore, in an attempt to minimize test duration, we also change 2 well condition within one day by turning the previous well candidate into baseline condition in the morning, then change the next well candidate into disturbance condition.

NCG INTERFERENCE EXECUTION AND RESULT

The first step is to set the baseline of operating well configuration and NCG of each well. The NCG content of all online wells at Pad A, M-3 and M-6 were sampled 1 day after the operation changes of the candidate wells. The NCG were measured for 2 to 3 days, before the well operation will changes again. Then, the NCG content was compared to the baseline condition. If there were increasing or decreasing trend after the candidate wells operation changes, then the online wells were concluded to have connection to the candidate well. Based on this NCG Interference Test, NCG of each well had respond specifically when the tested well put on shut-in or venting.

Table 1. Baseline Operating Well Condition, Test Well Condition & Initial NCG Content

Well	Baseline Well Condition	NCG content, wt.%	Test Well Condition
A-2	Fully open	2.2	Shut-in
A-3	Fully open	3.3	Shut-in
A-4	Shut-in	-	Shut-in
A-5	Venting through 3" to AFT	2.7	Venting through 10" SUV to AFT
A-6	Shut-in		Venting through 3" to AFT
A-7	Fully open	0.6	Fully Open
A-8	Shut-in		Venting through 3" to AFT
A-9	Throttled		Throttled
A-10	Shut-in		Venting through 2" bypass SUV to AFT
M-3	Throttled	3.9	Shut-in
M-6	Venting	5.9	Shut-in

Figure 2 shows that A-3 and A-5 respond directly to the change of operation in A-6. The green line is the event of A-6 changed operation condition from shut-in to venting through 3" to AFT. The NCG at A-3 and A-5 suddenly shows a drop.

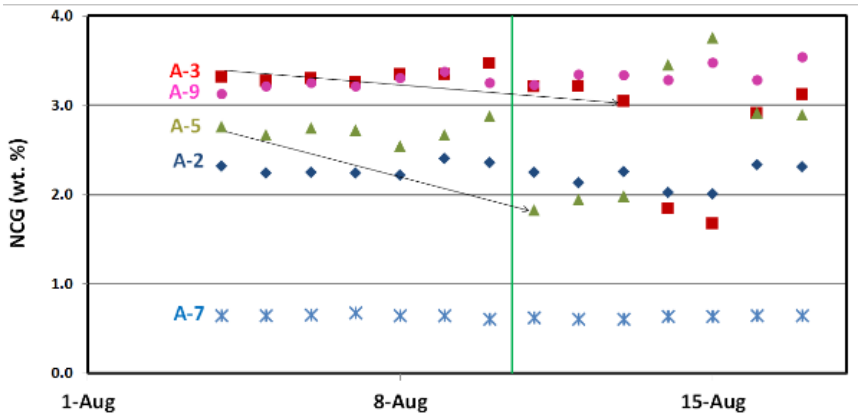

Figure 2. A-6 Interference Test Result

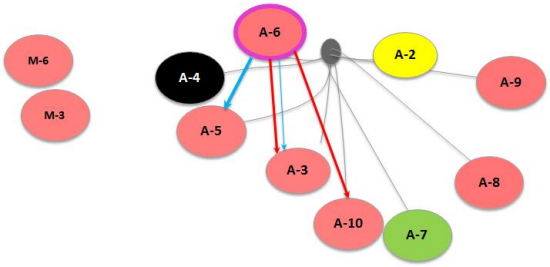

Figure 3. A-6 Interference Result Connection

This test concluded that A-6 interferred A-3 and A-5 (Figure 3). Further explanation of Figure 3,the blue line corresponds to result from 2016 NCG interference test and the red line corresponds to result from 2014 NCG interference evaluation. It means that for current condition, changing of operation in A-6 will impact on A-5 and A-3 NCG content. However, NCG interference between A-6 and A-10 that previously observed (from 2014 NCG Interference test) can not be analyzed due to those wells are currently in shut in condition.

In addition, the degree of connectivity can be classified into two types: strong and weak connection. After gathering all of the data trend, the simple statistical was used to make the classification. The assumption used is if the changes are more than Q2 of the population, then the connectivity is categorized as strong connection. Else, if it is less than Q2 of the population, then the connection is categorized as weak connection.

Table 2. NCG Interference Test Result

Source of Disturb-ance	Interfered wells	Baseline NCG (wt.%)	NCG after being interfered (wt.%)	% change
A-8	A-2	2.2	2.4	5
	A-3	3.3	3.5	6
	A-5	2.7	2.9	8
A-6	A-3	3.3	3	7
	A-5	2.7	2	26
A-5	A-2	2.2	2	10
	A-3	3.3	1.7	48
A-3	A-2	2.2	3	35
	A-5	2.7	2.9	9
	A-7	0.6	1	53
M-6	A-3	3.3	3.6	11
	A-5	2.7	3.8	41
	M-3	3.9	4.6	17
M-3	A-3	3.3	3.8	17
	A-5	2.7	3.6	34
	M-6	5.9	7.7	30
A-2	A-3	3.3	3.7	13
	A-7	0.6	0.8	25
Quartile 1				9
Quartile 2				17
Quartile 3				33
Quartile 4				53
Median				17

The full results of 2016 NCG Interference test shown in Figure 4.

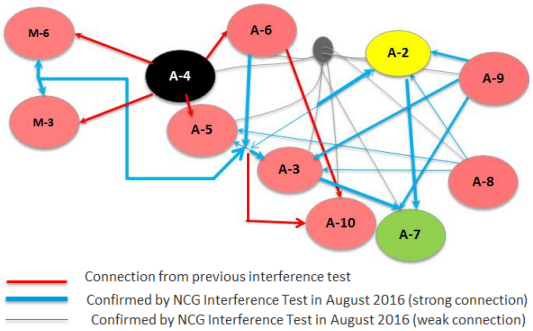

Figure 4 Salak NCG Interference Connectivity

The blue bold line represents the strong connection in NCG interference and the blue normal line represents the weak connection in NCG interference. For example, changing well condition of A-9 will significantly impact NCG content of A-2, A-3 and A-7. Figure 4 also explains that there is a change in source of interference. Previously, the source of interference is identified in A-4. A more complete account of A-4 interference can be found in Hidayatturobi et al., 2017 (this issue).

However, after A-4 shutted in, the source of interference change into A-5 and A-3. Both of them connected each other and will impact almost all of the surroundings if there is any changes in the operating condition.

NCG INTERFERENCE TEST ANALYSIS

Previously, some of the high-NCG wells were continuously put on venting to AFT and causing too many steam has been wasted. In addition, there is no any dedicated guideline on how to maneuver high-NCG well and what is the impact to surrounding producers when the well is maneuvered for logging or maintenance activities.

NCG Interference Test result shows the range of fluctuation in NCG content to other wells when specific well is maneuvered. This data then used to predict total NCG entering turbine by using simple chemical mixing concentration concept as follow:

$$\%\text{NCG to turbine} = \frac{\sum(m_i \times NCG_i)}{\sum m_i}$$

, with:

m_i : steam rate of well i that contributes to power plant, kph

NCG_i : wt%. NCG of well i

By combining the information of NCG interference and NCG blending calculation, a solution to improve current condition by manuevering some of well condition in Pad A can be gencrate.

Table 3. Initial Well Operating Condition & Initial NCG Content in Pad A

Well	Well Status	Steam Rate to Power Plant, kph	NCG content, wt.%	NCG rate, kph
A-2	Fully Open	110	2.45	2.70
A-3	Fully open	210	2.84	5.96
A-4	Shut-in	0	10.00	0.00
A-5	Venting	0	4.17	0.00
A-6	Shut-in	0	4.20	0.00

A-7	Fully open	140	0.64	0.90
A-8	Shut-in	0	2.82	0.00
A-9	Throttled	120	3.30	3.96
A-10	Shut-in	0	2.80	0.00
Total			580	13.52

Initial total steam contribution from Pad A was 580 kph. And by using NCG blending calculation, Pad A give NCG contribution to power plant at around 2.33 wt.%.

Table 4. Recommended Well Operation Setting & NCG Content in Pad A

Well	Well Status	Steam Rate to Power Plant, kph	NCG content, wt.%	NCG rate, kph
A-2	Fully open	110	2.38	2.62
A-3	Fully open	210	2.73	5.73
A-4	Shut-in	0	10.00	0.00
A-5	**Throttled**	**150**	**1.38**	**2.07**
A-6	Venting	0	4.20	0.00
A-7	Fully open	140	0.62	0.87
A-8	Bleed	0	2.82	0.00
A-9	Throttled	120	3.30	3.96
A-10	Bleed	0	2.80	0.00
Total			730	15.25

Table 4 shows a recommendation of well operation setting and NCG content in Pad A after applying the setting. After A-6 put on venting, A-10 put into bleed, and A-5 put online under throttled condition, total steam contributed to power plant is 730 kph. There is 150 kph additional steam from A-5. NCG blending from Pad A to power plant reduces to 2.09% with new operating condition.

CONCLUSION AND RECOMMENDATION

2016 NCG interference test came up with several conclusions, such as:

- Clear understanding on interference connection between Pad A and Pad M.
- Source of interference change from A-4 into A-3 and A-5.
- Steam supplied to the power plan had less NCG content that will lead to less curtailment.
- Wells that previously venting, could be produced based on his behavior of interfering surrounding wells. It means that additional steam can be obtained by applying the most efficient operating condition.

The NCG interference test result afterwards could be used to generate new operation protocol to optimize the steam production in high NCG wells. The operation protocol included fully open, throttling and venting some of wells. This recommendation resulted in full generation of 65.7 MW in Unit 4 even with 1 Cooling Tower Fan (CTF) stop operation.

ACKNOWLEDGEMENT

We would like to thank Star Energy Geothermal Salak (SEGS) and Pertamina Geothermal Energy (PGE) for granting permission to publish this work, especially to Star Energy Geothermal Salak Asset Development Department for supporting us in making this paper.

REFERENCES

Paramitasari, H., Putra, F.J., and Hidayaturrobi, A.D., *NCG Interference Evaluation*, CGS Internal Report, July 7, 2015.

Julinawati, T., Paramitasari, H., Putri, R.P., Hidayaturrobi, A.D.,*Salak NCG Interference Evaluation to Enhance Steam Production in High NCG Wells*, IIGCE 2017, August 2017.

Wijaya, B.A., Suminar, A. R., Ganefianto, N., *Resource Management Geosciences Well Sampling Two-Phase Flow Standard Operating Procedure*, CGS Internal SOP, May 2009.

Salak Asset Development Department, *2016 Salak Geothermal Field Asset Development Plan*, GPO Internal Report, October 2016.

HIdayatturobi, A.D., Simatupang, C.H., Permatasari, H.M., Putra, F.J.,*Successfull High NCG Wells Optimization in Salak Geothermal Field to Maintain Unit-4 Full Generation*, IIGCE 2017, August 2017.

EVALUATION OF THE DEEPEST PRODUCTION WELL IN SALAK GEOTHERMAL FIELD, INDONESIA

Frederick T. Libert

Star Energy Geothermal Salak

e-mail: flibert@starenergy.co.id

ABSTRACT

Well AWI 9-9 was recently drilled at the Salak (also known as Awibengkok) Geothermal Field, West Java, Indonesia, as a make-up steam supply well to support full load power generation at the 377 MWe power facilities. The well was also drilled to provide information on the temperatures in and the permeability of the undrilled portion of the southwest area of the Awibengkok field. AWI 9-9 was completed in 21 days to a total depth (TD) of 10,402 ft (3,170 m) making it the deepest production well drilled in the Awibengkok reservoir.

The well completion test indicated that AWI 9-9 has inter-zonal flow with the upflowing hot (610 °F or 321 °C) reservoir fluid from the bottom feed zone exiting the feed zone at ~6,532' (1,991 m) MD. The presence of an inter-zonal flow at AWI 9-9 creates difficulties in assessing the actual reservoir parameters encountered by the well. Adjustment of the conventional geothermal well characterization method thus needed to be made in order to fully characterize the well. The well's unique sub-surface condition also increased the risk of well control issues so these risks needed to be fully understand and mitigated.

The bottom entry in this well, the deepest permeable entry identified to date (10,032' or 3,058 m MD), confirms the interpretation of deep permeability at the Awibengkok reservoir. The presence of the deep feed zone in the MVS indicated that this formation is still permeable to sustain commercial production. The depth of recorded micro-seismicity events suggests that permeability could extend as deep as 13,000' (~4,000 m) BSL. At this depth, it is possible that supercritical fluid exists and that it can be harnessed to generate power outputs in order of magnitude greater than from conventional high-temperature fluid.

Keywords: Salak, completion test, deep well, supercritical fluid, interzonal flow, well control

INTRODUCTION

The Salak geothermal field is located about 60 kms southwest of Jakarta, West Java, Indonesia on the southwestern flank of the Gunung Salak volcano (2,211 m ASL). Commercial production started in 1994 with an initial 110 MW (Units 1 and 2) and was expanded to 330 MW by 1998 when Units 3, 4, 5 and 6 were installed. In 2002, following the Asian Economic Crisis of 1997-1998, turbine output was increased to 377 MWe (Ibrahim et al., 2005). Salak is presently the largest producer of geothermal power in Indonesia.

Salak is a fracture-controlled, liquid-dominated geothermal system with commercial reservoir temperatures ranging from 464 - 600 °F (240 – 316 °C), benign fluid chemistry and low to moderate non-condensable gas (NCG) content (~0.5-3%w/w) (Stimac et al., 2008). The reservoir is contained within a sequence of volcanic units of predominantly andesitic to rhyodacitic composition, with a basement of Miocene marine sedimentary rock cut by igneous intrusions. With a current installed capacity of 377 MWe and a proven reservoir area of about 18 km^2 (Figure 2), the field has a power density of about 20 MWe/km^2.

At the start of commercial operations in 1994, brine was injected infield in the hottest portion i.e the upflow zone of the reservoir at AWI 9 and in the southern edge of the field at AWI 10. The general belief then was that the "limited" brine produced from generating 110 MWe would not significantly harm the high-temperature reservoir. In 1998, the increase in generation capacity increased the produced brine to an average injection rate of 12,000 kilo-lb/hr (130,600 ton/day). Chemical breakthrough and thermal breakthrough were observed at the main production area and, as a result, infield injection has been minimized by transferring both condensate and brine injection to the edge and outside of the field's production area.

To maintain full generation of 377 MWe, the field has been developed through the periodic drilling of make-up wells. The most recent make-up well drilling campaign was in 2012-2013. During this period three new wells were drilled in the western-most production pad AWI 9, namely, AWI 9-7 in 2009, AWI 9-8 in 2012 and AWI 9-9 in 2013. These wells provide key reservoir information as they were drilled in a previously undrilled area at the southwestern edge of the field. At 620 °F (327 °C) AWI 9-7 has shown the highest temperature yet measured at Salak while AWI 9-8 confirms the lateral extension of the reservoir margin to the southwest.

The bottom of a geothermal reservoir is normally defined when the permeability of the rock is not sufficient to sustain commercial production. Data from the relatively deep make-up wells shows the potential for an extension of the depth of permeability. In addition, the depth of recorded micro-seismicity events suggests that permeability could extend as deep as 13,000 ft (~4,000 m) BSL especially in the southwestern part of the field (Libert et al, 2014). AWI 9-9 was designed to test temperature and permeability at depth in the area of the inferred upflow region of the Salak reservoir.

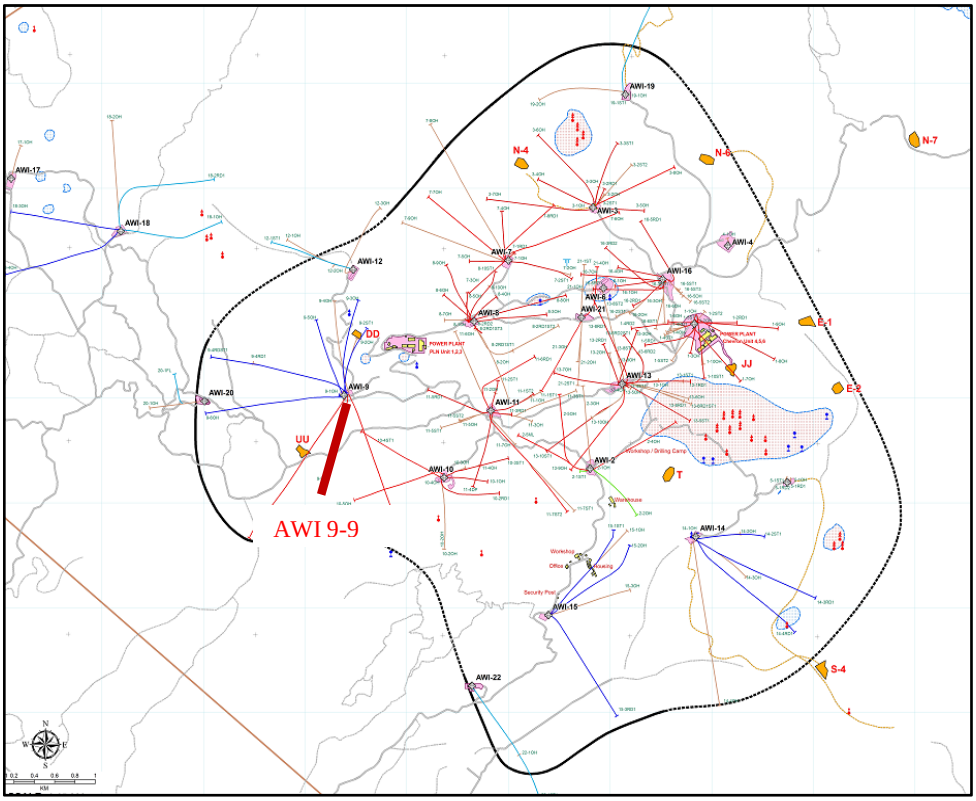

Figure 2: Map of the Salak geothermal field showing the commercial reservoir boundary (black solid/dashed line), production (red) and injection wells (blue). Also shown is AWI 9-9, the deepest production well drilled in Salak (bold red line).

DRILLING SUMMARY

AWI 9-9 was designed as a low inclination (17°) standard 2D directional well that targets production from the deep brine reservoir in the southwestern part of the field. Although relatively shallower than the original target, AWI 9-9 was drilled to 6,665 ft (2,032 m) BSL, still the deepest production well drilled in Awibengkok. Typical for a production well in the field, AWI 9-9 was completed as a big hole with a 13-⅜" production liner. The reservoir hole section was drilled in two hole sections, namely, 12-¼" and 9-⅞" diameter. Perforated 10-¾" production liner was installed in the 12-¼" hole section. (Figure 3).

SUBSURFACE GEOLOGY

AWI 9-9 penetrated a series of hydrothermally altered volcanic rocks to a depth of 6,504 ft (1,982 m) MD where mud circulation was lost. The rocks encountered by this well were similar to those of other wells drilled in the Field and can be divided into six formations (Table 1). The transition from argillic to propylitic alteration occurs in the Middle Andesite Formation and the Rhyodacite Marker (RDM). Phyllic alteration was also observed in the RDM at 3,660 - 3,920 ft (1,115 -1,195 m) MD and in the Lower Andesite Formation at 4,160 – 4,340 ft (1,268 -1,322 m) MD. RDM occurencess also supported by a significant spike ingamma ray value (Figure 4) suggests that the number of radioactive elements increase with increasing silica. Overall, the general lithology encountered at AWI 9-9 is similar to those encountered at AWI 9-7 and AWI 9-8.

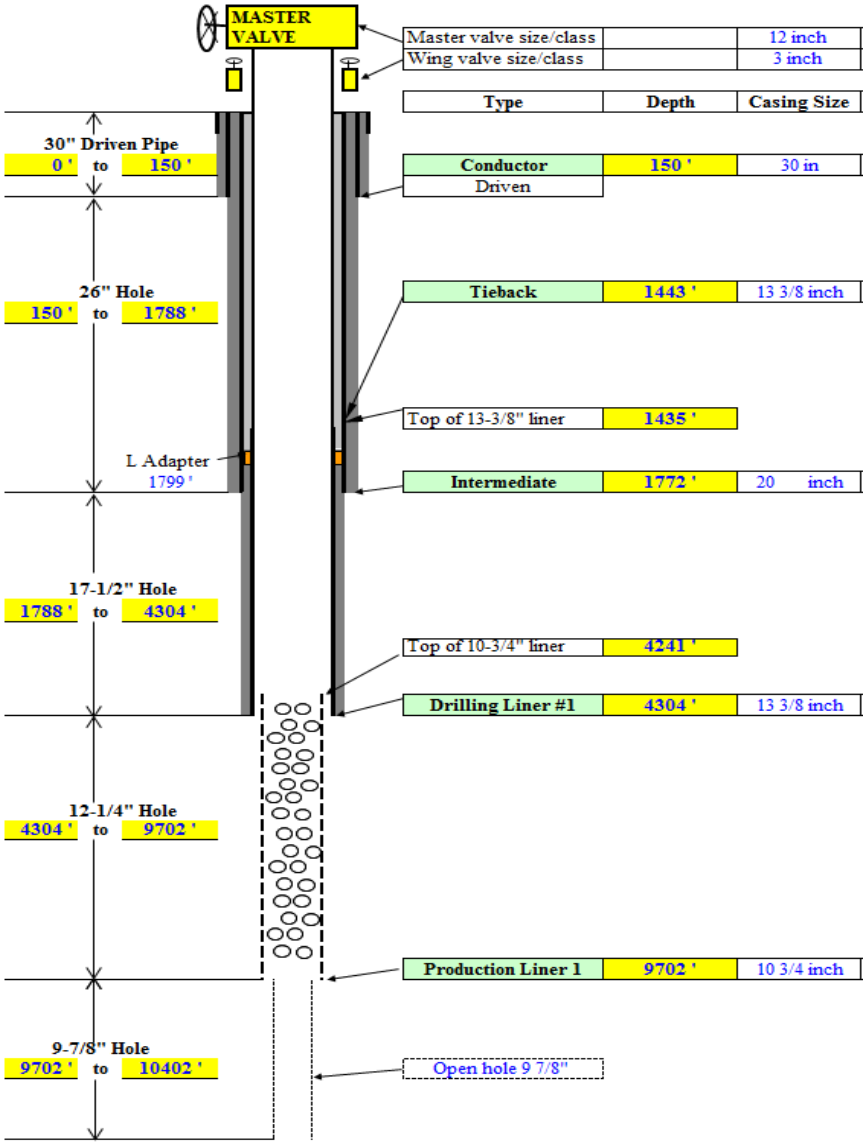

Figure 3: Well completion schematic of AWI 9-9

Table 1: Lithology and alteration of AWI 9-9 based on interpretation of rock cuttings

Depth	Lithology	Alteration
184 – 540 ft (56 – 165 m)	Upper Dacite	Unaltered to weakly argillic
540 – 840 ft (165 – 256 m)	Upper Andesite	Moderate to strongly argillic
840 – 1,280 ft (256 – 390 m)	Middle Dacite	Argillic
1,280 – 3,660 ft (390 – 1,115 m)	Middle Andesite	Weak to moderately argillic transitioning to propylitic
3,660 – 4,340 ft (1,115 – 1,322 m)	Rhyodacite Marker	Argillic; propylitic
4,340 – 6,504 ft (1,322 – 1,982 m)	Lower Andesite	Propylitic

WELL CHARACTERIZATION

Completion test

Upon completion of the drilling operations and the releasing of the rig, a completion test consisting of an injection Pressure-Temperature-Spinner (PTS) survey and a multi-rate injection test was performed. This was followed by heat up surveys or series of shut-in pressure and temperature (PT) surveys. The completion test and heat up survey analysis suggest that AWI 9-9 encountered three permeable entries. Analysis of the PTS data also revealed two directions of fluid movement during the injection test i.e. downflowing injected condensate and upflowing hot (610°F or 321°C) reservoir fluids from the bottom feed zone at ~10,032 ft (3,058 m) MD. Both fluid streams exit at the feed zone located at ~6,532' (1,991 m) MD (Figure 4).

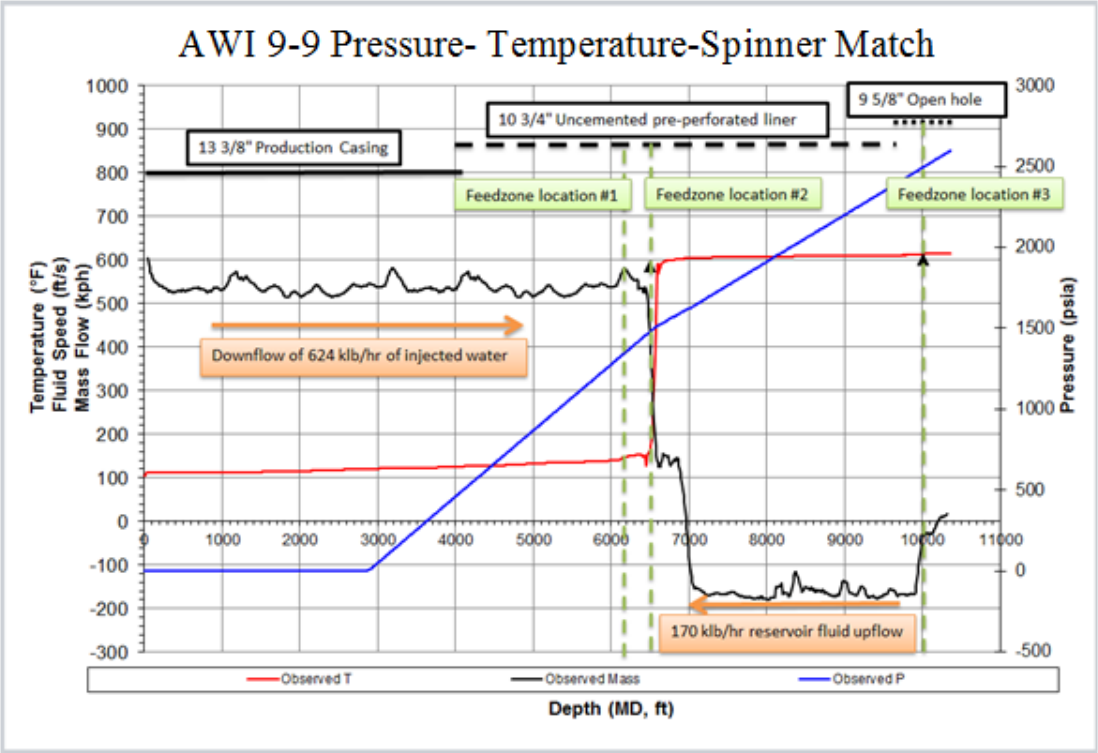

Figure 4: AWI 9-9 injection PTS analysis showing the three permeable zones encountered by the well. Black line is the mass flow calculated from spinner data, blue line and red line are measured injection pressure and temperature respectively.

Interpretation of the aforementioned phenomenon was based on at least three evidences observed in the PTS data. First is change in the direction of spinner rotation below ~6,532' MD. Second is temperature profile of the well above ~6,532' MD which is imprinting condensate temperature that is slightly heated up by the hot formation. Below ~6,532' MD the temperature jumps to 610°F (321°C) followed by isothermal profile down to the well TD. And lastly, injection pressure profile showed 2 different pressure gradient at above and below ~6,532' resulted from significant temperature differences and pressure drop from gravity and friction suffered by the upflowing zone.

The shallowest permeable entry is located at 6,182' (1,884 m) MD. Based on rock cuttings, the host rock is andesite lithic tuff of the Lower Andesite Formation. There was no indication of permeability at this depth during drilling, (e.g., no drilling breaks, fluid losses and drops in stand pipe pressure) and also this feedzone does not clearly appear during injection PTS survey. This uppermost feedzone was detected from the heat up survey data. The deep upflow creates a convective isothermal zone that was undisturbed during the completion test as seen in Figure 5. The upflow also provides convective heat transfer to the cold condensate column above the upflow exit point thus increasing the well heating up period (10 days to fully heat up). This dynamic condition triggers deep boiling in the wellbore where the steam-liquid interface (or top of the boiling zone) is controlled by AWI 9-9's shallowest feedzone. Without the existence of this uppermost feedzone at 6,182' the top of the boiling zone would be expected to be at a greater depth around the upflow exit point (~6,532' MD)

The second permeable entry is an extended interval of about 500 ft from 6,532 to 7032' MD (1991 to 2,143 m) MD. This feedzone is consistent with a drilling break at 6,499' (1,980 m) MD and Total Loss of Circulation (TLC) at 6,504' (1,982 m) MD.

The third feed zone is at 10,032' (3,058 m) MD, within the interval of blind drilling, Completion test data indicate that this entry is a high-temperature (610°F or 321°C) inflow which results in an interzonal flow that exits the well at 6,532' (1,991 m) MD. In addition, even though FMI analysis indicates no direct correlation between feed zone location and structure data, the interval range of the feed zone based on PTS to permeability indication (fracture/ fault cluster and significantly drop in pressure while drilling) is 67 feet (20 m), suggesting the range of feed zone with high-temperature feed zone near TD may still corresponds with a large fracture that identified at depth 9960 to 9965' (3,035-3037 m) MD (Figure 6).

The injectivity index (II) measured by an injectivity test was 20 kph/psi (or 36.5 kg/s/bar) (Figure 7). However, this measured value underestimates AWI 9-9's actual injectivity as it only calculates the change in downhole pressure as a function of changes in the condensate injection rate. The calculated II does not quantify the deepest feedzone permeability as it does not accept the injected fluid during the test (inflowing); moreover, the second feedzone at ~6,532' (1,991 m) MD has a higher injectivity to that calculated as this feedzone accepts both injected condensate and upflowing reservoir fluid from the deepest feedzone.

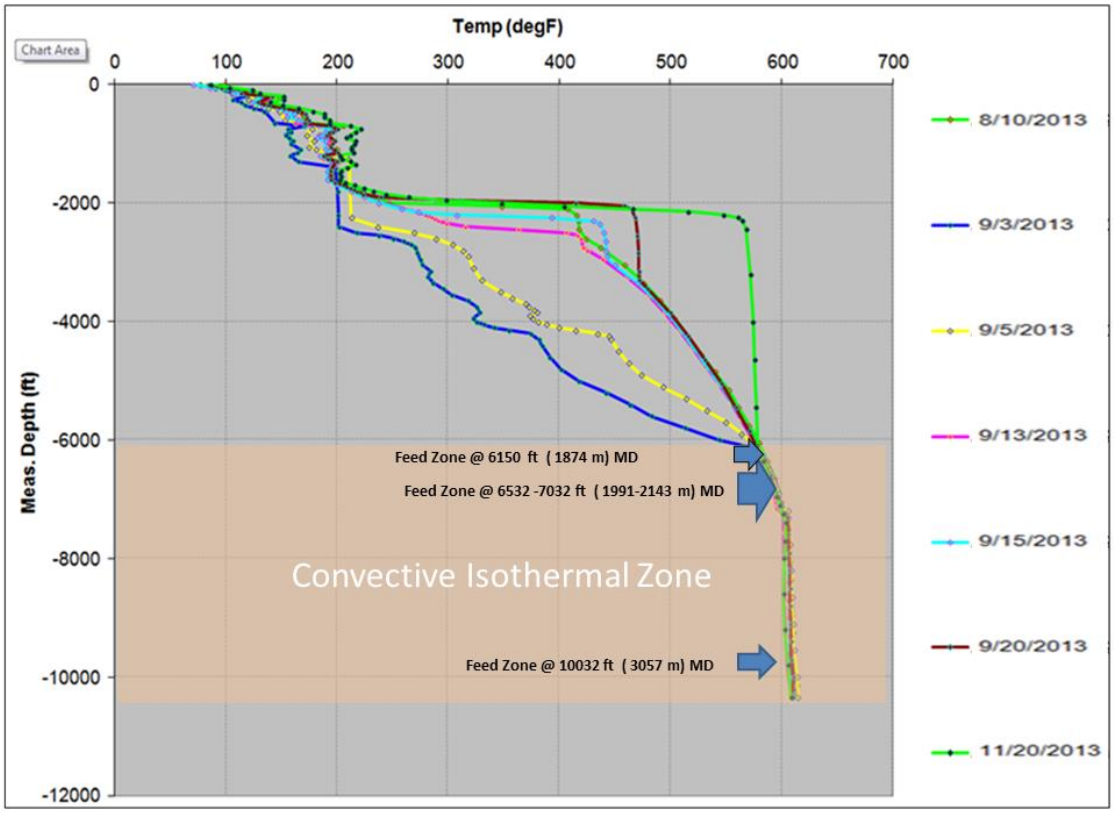

Figure 5: Chart showing the AWI 9-9 heat-up profile and the existence of a feed zone at ~6150' MD. This feedzone acts as a pressure reliever preventing the top of the boiling zone from going deeper. Also shown is a suggested presence of fluid movement from ~6500 ft-MD to the well TD as indicated by the isothermal temperature profile.

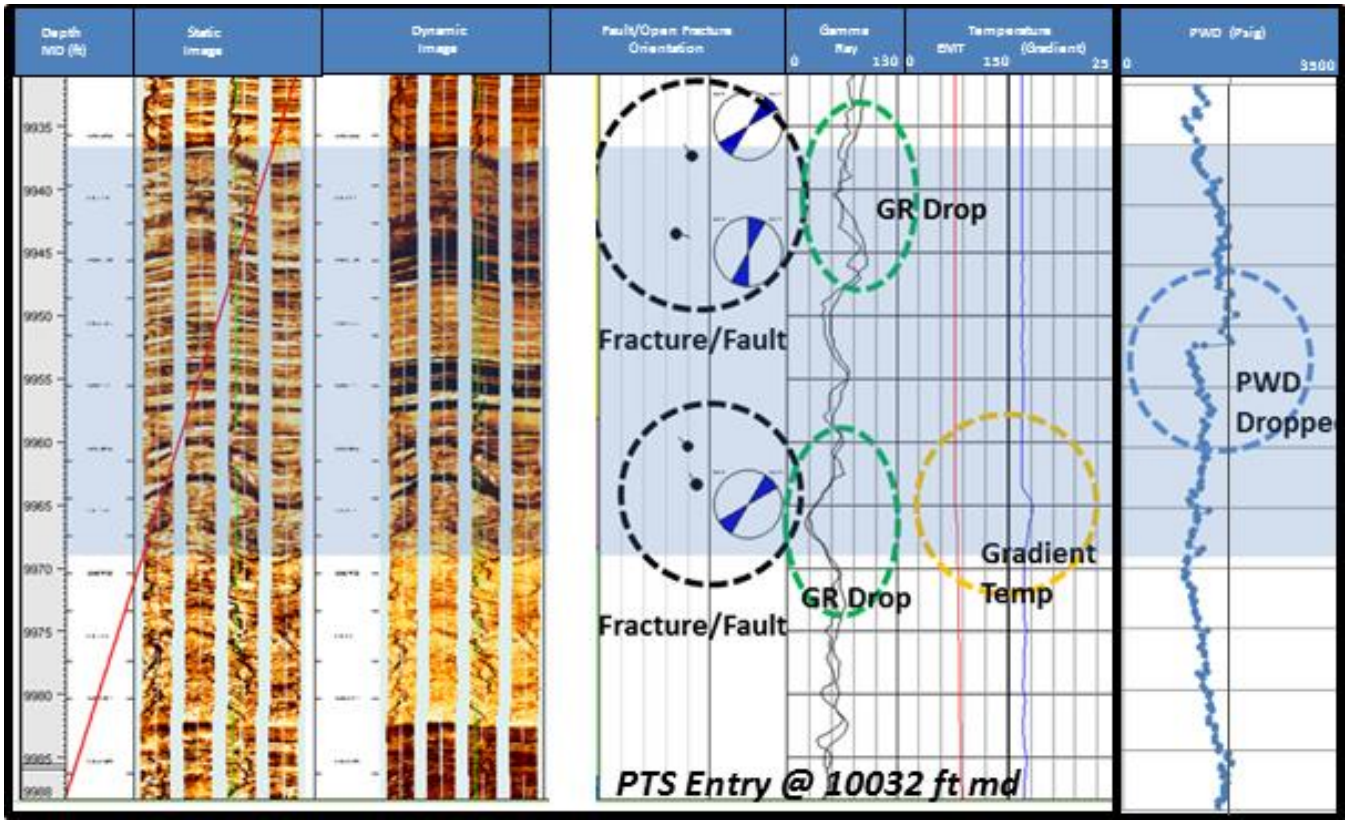

Figure 6: Screenshot showing FMI interpretation and GR, temperature gradient and PWD profiles of AWI 9-9. Although the injecting PTS data identified the bottom permeable entry at 10,032' (3,058 m) MD, it is believed that this feed zone is correlated with a NE-SW trending fracture/fault zone at 9,960'-9,965' (3,035-3037 m) MD.

The well injectivity was therefore estimated by calculating the injectivity of each feedzone based on injection PTS data (Table 3). Injection PTS analysis provides information of the mass flow rate of each feedzone, II is then calculated by dividing the mass flow rate with the differential pressure in the wellbore (from injection PTS data) and at the reservoir (from SI PT data). The total injectivity of AWI 9-9 is at minimum 27 kph/psi (or 50 kg/s/bar). The injectivity of the shallowest feedzone was neglected as it was hardly detected by the spinner. Due to the dynamic conditions in the wellbore, the reservoir pressure of the deepest feedzone was based on an estimated value that will be discussed in the next section (4.2). Despite all of the uncertainties and difficulties surrounding AWI 9-9 injectivity test interpretation, having II above 20 kph/psi (or 36.5 kg/s/bar) suggests that the permeability of the well is considerably high than that of other producers in the field.

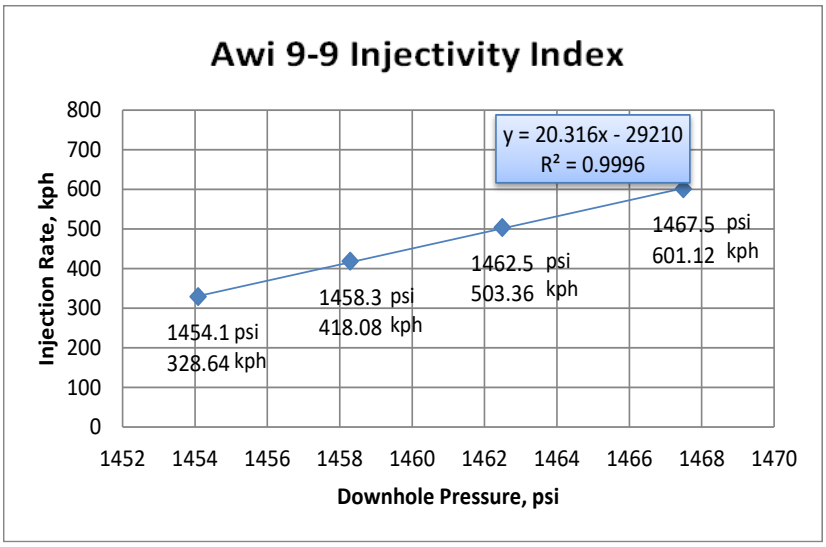

Figure 7: Injectivity index from a multi-rate injection test suggesting that AWI 9-9 has II of 20 kph/psi or 36.5 kg/s/bar which is an underestimation of the actual injectivity of the well

Table 3: Calculated Injectivity Index based on injection PTS data. AWI 9-9 has total II of 27.3 kph/psi or 50 kg/s/bar

Depth, ft-MD	6,532	10,032
Mass Flow, kph	748	170
Wellbore P, psia	1479	2494
Reservoir P, psia	1451	2682
II, kph/psi (kgs/bar)	26.2 (47.9)	1.1 (2)
Remarks	Mass flow rate is both injected condensate and upflowing reservoir fluid from the deepest feedzone	Reservoir pressure is estimated

Steam Deliverability Estimation

After the completion test, the well's deliverability was estimated using wellbore simulation with inputs from the completion test and heat up surveys. The required parameters to construct a Awi 9-9 wellbore model are feedzone' productivity index (PI), pressure, and enthalpy that can be computed from temperature. Feedzone PI can be obtained by converting the calculated II (APPENDIX A). However, the feedzone pressure and temperature cannot be obtained directly from SI PT data due to the presence of a hot upflow from the bottommost feedzone.

The interzonal flow in AWI 9-9 created difficulties in assessing the actual reservoir pressure and temperature encountered by the well. The upflow masks the actual formation temperature from 6,532' (1,991 m) MD to TD. The measured wellbore pressure also does not represent actual reservoir conditions. The measured pressure at the source of inter-zonal flow is lower than the actual reservoir pressure; consequently, the measured pressure at the exit point of the up-flow is higher than the actual reservoir pressure.

For this reason, the temperature and pressure of the feed zone at ~6,532' (1,991 m) MD were estimated based on offset wells data and analysis of the injectivity test respectively. During the injectivity test, the tool was hung at ~6,482' (1,976 m) MD, this meant the reservoir pressure at that depth could be estimated by calculating the intercept of the injectivity chart which is the bottomhole pressure at zero injection rate. The reservoir pressure of the feedzone at ~6,532' (1,991 m) MD could therefore be calculated by gravity correction of the reservoir pressure at ~6,482' (1,976 m) MD.

The temperature of the deepest feedzone is the upflowing fluid temperature. As for the reservoir pressure, it needed to be estimated by calculating the fluid mixture density from the measured pressure gradient (SI PT) and adjusting the measured reservoir pressure to get steam quality of zero, assuming that the fluid in the reservoir is in compressed liquid state. The steam quality can be computed with following formula :

$$Q = (Vmix - VL)/(VS-VL) \quad \ldots\ldots\ldots\ldots\ldots\ldots\ldots\ldots\ldots\ldots (1)$$

Where Q is the steam quality, and Vmix, VL, and VS are the specific volume of mixture, liquid, and steam in cu-ft/lb respectively.

Input data for the wellbore model is summarized in Table 4. The wellbore simulation results indicate that AWI 9-9 can produce about 650 kph (82 kg/s) of steam at system pressure (Figure 8). However, considering all of the uncertainties pertaining to the special conditions at AWI

9-9, this initial estimate of the well's deliverability may change pending conduct of a flow test to fully characterize the well and the reservoir in the southwestern part of the field.

Well Control

AWI 9-9 was completed with API-6D class 600 wellhead equipment. The maximum working pressure of the equipment is 1500 psig (103.4 barg) at temperatures below 200°F (93°C) and de-rated to 1210 psig (83.4 barg) at 600°F (316°C). The material selection was based on the maximum anticipated surface pressure of the well which was determined based on boiling zone at Awi 9 area which is around -1000 ft asl. At this depth, pressure and temperature at the boiling zone correspond to a shut-in wellhead pressure (SI WHP) of 940 psig (64.8 barg) at 530°F (277°C). The SI WHP could go as high as 1058 psig (72.9 barg) when NCG accumulation is present in the upper casing section. This value is an assumed worst case scenario where the accumulated NCG is 100 percent carbon dioxide (CO_2) that being heated up by underlying steam to reach critical condition. However, it is known that the accumulated NCG is a mixture of CO2 and other gases with lower partial pressure which will result in a lower SI WHP.

Approximately one week after the completion test, AWI 9-9 SI WHP started to build up and stabilized at ~1120 psig (Figure 9a), which was above the maximum anticipated SI WHP of the well. The casing head flange and the wellhead temperature record (Figure 9b) suggesting no casing growth was observed as the SI WHP building up. The low wellhead temperature (90°F or 32°C) indicating presence of NCG accumulation at shallow casing section which is contradictory to the fact that the critical pressure of the NCG is 1058 psig (72.9 barg).

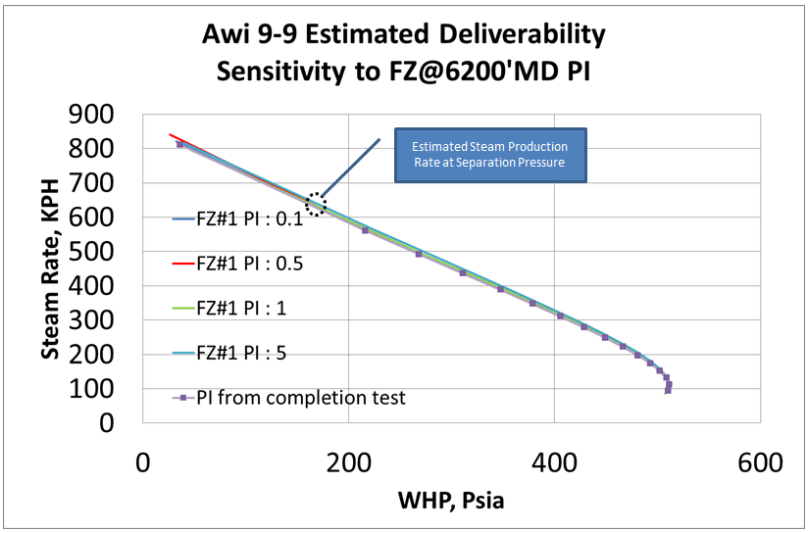

Figure 8: Chart showing synthetic deliverability curve of AWI 9-9; at current system pressure, the well can produce about 650 kph (82kg/s) of steam. The multiple curves represent sensitivity analysis of the shallow feed zone #1 which shows that it does not significantly affect well performance as the well's hydraulic condition is controlled by the 2nd and 3rd feedzone.

Table 4: Input data for wellbore simulation

Depth, ft-MD	II, kph/psi	PI, kph/psi	Reservoir Pressure, psia	Reservoir Temperature, °F	Enthalpy, btu/lb	Remarks
6,182	N/A	0.1 – 5	1328	550	550	Multiple runs of wellbore simulation with various PI since the feedzone is detected from the heat up survey
6,532	26.2	21	1451	570	575	Reservoir pressure estimated based on intercept of following equation from figure 11. Y = 20.316 X + 29210 Where X is bottomhole pressure at ~6,482' (1,976 m) MD
10,032	1.1	0.9	2682	610	630	Measured upflow temperature

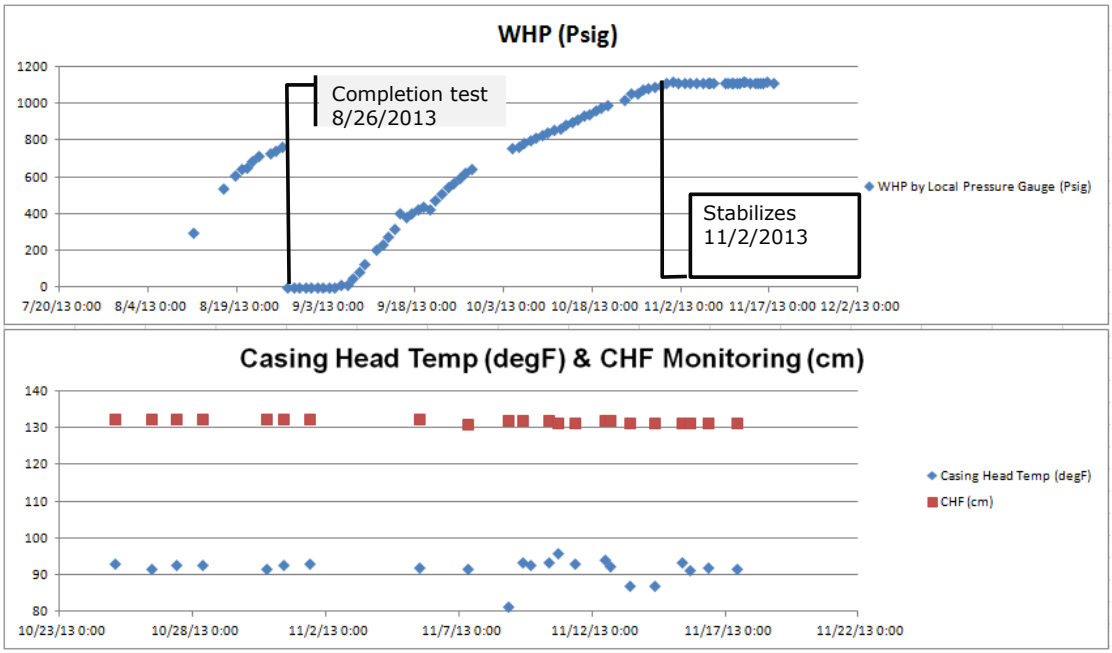

Figure 9: AWI 9-9 WHP monitoring (a) and record of casing head temperature and height (b)

Consequently, a shut-in PT survey was then performed to investigate the cause of the elevated SI WHP and to determine whether or not it was safe to vent/bleed the well to release the pressure. The survey revealed that the NCG (mainly CO_2) accumulated at the shallow part of the casing had reached supercritical condition as a result of pressurization of the steam from the boiling zone at 6182'.

CO_2 usually behaves as a gas in air at standard temperature and pressure (STP), or as a solid called dry ice when frozen. If the temperature and pressure are both increased from STP to be at or above the critical point for CO_2, it can adopt properties midway between a gas and a liquid. More specifically, expanding to fill its container like a gas but with a density like that of a liquid. This condition protects the wellhead from exposure to higher pressure and temperature. In the absence of NCG accumulation, Awi 9-9 SI WHP could be expected to reach 1205 psig (83 barg) at 569°F (298°C) (Figure 10).

Information from a static PT survey indicates that venting the well via a 3" bleed line would increase its WHP rather than reducing it. Under bleed conditions, the situation could be worse if dynamic conditions are created in the wellbore that allow higher pressures to be transmitted from the bottom of the well. This is a function of the temperature, pressure and the permeability of the zones.

For Awi 9-9, however, the sub-surface conditions are such that they should act to minimize the possibility of an increase in pressure; the deep temperature is "only" 610°F (321°C) and the pressure is over 2,500 psig (172 barg), which is well above the saturation pressure of 1,645 psig (113 barg). This means that under bleed conditions, flashing will occur higher up in the wellbore and the fluid will still have a relatively high density due to the relatively low enthalpy of 540 BTU/lb (1256 kj/kg), which will further decrease the pressure. The zone at 6,532' (1,991 m) MD also appears to have very high permeability. Thus it is expected that the wellhead pressure will still be controlled by the zone at 6,182' (1,884 m) MD even under bleed conditions. So the wellhead pressure may not change much from the shut-in condition as there is already an upflow occurring.

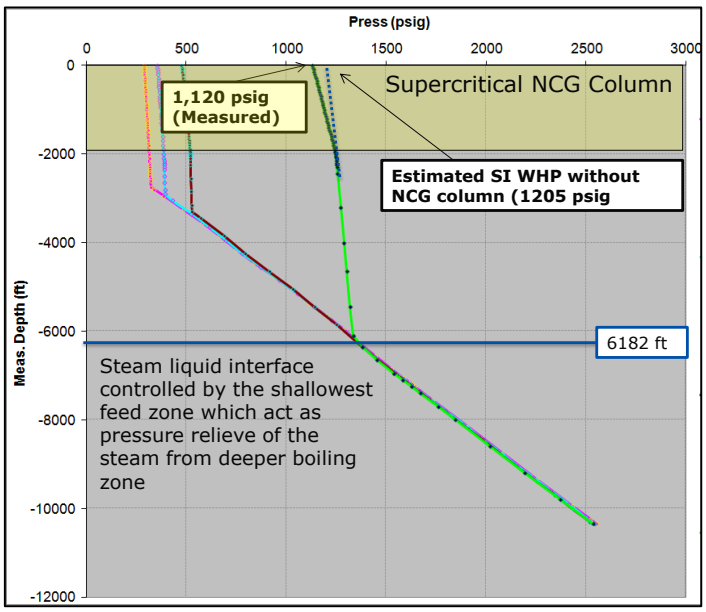

Figure 10: Shut-in PT survey of Awi 9-9. Presence of supercritical NCG column protecting the wellhead from exposure to higher pressure and temperature.

A different situation applied at Bul-108 (Mak-Ban geothermal field, Phillippines). The data from Bul-108 provides an example of what happens when conditions are more favorable for building up wellhead pressure. In this well, the bottomhole temperature was ~610°F (338°C), and a saturation pressure of 2,042 psig (140 barg). So flashing started much deeper in the wellbore. The well also has high permeability in the lower zone and low permeability in the shallow zone, which is also favorable for transmitting high pressures (Figure 11).

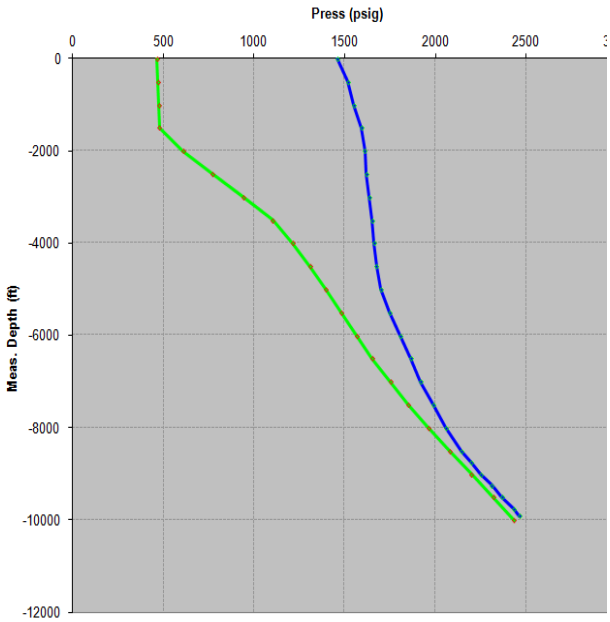

Figure 11 :The plots of shut-in and bleeding pressure of Bul-108. Green line shows the well's shut-in pressure profile, whereas the blue line shows that the dynamic condition in the wellbore (bleeding) causes the wellhead pressure to built up to near 1,460 psig (100 barg). Note that this well was completed with a ANSI900 series wellhead.

To mitigate potential exposure of the wellhead equipment to conditions above its design limit, the well was quenched and maintained under vacuum by 2 BPM (5 kg/s) of condensate injection. Continuous injection minimizes the thermal cycle and the injected condensate will mix with the hot upflow prior to entering the reservoir from feedzone at ~6,532' (1,991 m) MD. Based on simple heat and mass balance, the resulting mixture will have a temperature of ~500°F (260°C) which is considerably high and will not negatively impact the production area in the short run.

Well Operability, Monitoring, and Maintenance

There are several uncertainties that remain to be mitigated in order to safely operate AWI 9-9. The first is scaling potential. Under normal condition, the well's maximum expected surface pressure is 1205 psig (83 barg) at 569°F (298 °C) which is still lower (albeit by a thin margin) than the installed surface equipment maximum working pressure i.e. 1210 psig (83.4 barg) at 600°F (316°C). However, this condition is controlled by the uppermost feedzone at 6,182' (1,884 m) MD which may potentially be plugged if scaling occurred during the well's production life. Scaling could occur if the uppermost feedzone which is currently in a liquid state evolves into two-phase and/or dry steam which results ins a boiling and evaporation process that creates an ideal environment for scale precipitation. In addition, low enthalpy fluid (marginal recharge, brine injectate) inflow into the uppermost feedzone which induce cooling favorable for scale precipitation may occur in the future as the reservoir pressure declines.

Other uncertainties are related to the fluid characteristic and how the deep upflow will affect the wellbore hydraulic condition. These uncertainties apply because AWI 9-9 has not yet been flow tested. Several attempt to take liquid sample of the upflowing fluid have failed due to the high temperatures in the well. Recommendations for a specific well surveillance and monitoring program to address and mitigate these aforementioned uncertainties are shown in Table 5.

Table 5: Recommended surveillance and monitoring program for AWI 9-9

Type	Frequency	Remarks
Discharge test	1x prior to put online	Take discharged fluid sample, take down-hole fluid sample, run flowing PTS, and conduct flow performance test (FPT).
Downhole fluid sampling	Every 1-3 years	Obtain information on the deep upflow (pristine sample without mixing with shallower feedzone).
Surface gas and liquid sampling	Every 3-6 months	Monitor gas and liquid chemistry.
Casing condition monitoring (caliper, HTCC)	Every 1-5 years depends on fluid characteristic	Even though the Awibengkok reservoir fluid is known to be benign (Stimac et al., 2008), it is possible that the upflow from the bottommost feedzone has more magmatic influence which will increase the corrosion potential. Running caliper will enable to monitor corrosion, casing deformation, and scaling deposition.
Flowing PTS	At the beginning of production and when there is indication changes in well hydraulic condition	Understand well hydraulic condition under flowing condition with presence of the deep upflow.
Static PT	Annualy	Monitor reservoir pressure, temperature, and boiling zone evolution.
Maximum Clear Depth (MCD) Monitoring	In every downhole survey	Run dummy tool to tag MCD prior to any downhole surveys to evaluate wellbore clearance (fill from unconsolidated formation, corrosion product, scaling etc.)

Even though AWI 9-9 is the first well that intersected a high temperature upflow zone in the Awibengkok field and all other Chevron operated geothermal fields (i.e Darajat, Mak-Ban, and Tiwi) there are existing wells elsewhere with high SI WHP that intersect high pressure and a high temperature reservoir.

One example is Bul-108 (discussed above), the well had experienced surface pressure of 1,460 psig (100 barg) under bleeding condition, however, there was no well control issue as the well was completed with ANSI 900 series wellhead equipment. Up to the present there has been no wellhead or casing condition reliability issues (Libert, 2012) and the well behaves in a similar way to the

other two-phase producers in the Mak-Ban field (Menzies, *pers.comm*, 2014).

Another analog example are wells drilled in the Rotokawa geothermal field. The field is located in the Taupo Volcanic Zone (TVZ) of New Zealand. As in the case of Awibengkok, the Rotokawa reservoir has heterogeneous permeability with semi-sealing compartments with pressure differences ranging of 550 psi (38 bar) across the field. The wells drilled in Rotokawa encountered temperatures of 625°F (330°C) at 8,500' (2,500 m) depth (Hernandez et al., 2015). Corresponding to that reservoir condition, the wells in Rotokawa have very high SI WHP as well as flowing well head pressure (FWHP). These wells supply the Nga Awa Purua (NAP) power station which was commissioned in 2010. This power station operates the largest triple flash geothermal single unit in the world with a high pressure inlet of 340 psig (23.5 barg) (Horie, 2009). Consequently, the wells operate at high FWHP; some of them operate as high as ~580 psig (~40 barg) of FWHP (Libert, 2015). These wells as well as the entire surface facility were completed with class 900 series material (Zarrouk, *pers.comm*, 2015) to control the high pressure and high temperature system. After five years of operation, the NAP steam field has been safely and successfully operated with aforementioned design, in addition, the wells also behave in a similar fashion to common two-phase geothermal wells (Quinao, *pers.comm*, 2015)

Therefore, upgrading the existing wellhead equipment of AWI 9-9 from API 6D class 600 series to class 900 series is recommended. The class 900 series have higher maximum allowable working pressure (1815 psig (125 barg) at 600°F (316°C)) which will be sufficient to cope with the anticipated risk of higher pressure and temperature at the surface. In the worst case scenario where the uppermost feedzone at 6,182' (1,884 m) MD plugs up, the boiling zone in the wellbore will be controlled by the second feedzone at ~6,532' (1,991 m) MD where the subsurface condition at that depth will correspond to the surface condition of 1400 psig (97 barg) at 590°F (310°C). This worst case scenario is still below the class 900 maximum working pressure.

POTENTIAL UPSIDE

The AWI 9-9 well characterization reveals that deep permeability exists at the South-Western (SW) portion of Awibengkok reservoir. The well confirms the presence of permeable zone at 10,032' (3,058 m) MD which corresponds to a reservoir pressure and temperature of 2,682 psig (185 barg) and 610°F (321°C) respectively. This part of the reservoir has been identified as the upflow zone of the Awibengkok geothermal system (Acuna et al, 1997) and has been exploited mainly as an area for brine disposal since 1994. Approximately 4,000 kilo-lb/hr (43,500 ton/day) of brine has been injected in the AWI 9 area since 1994 and the number tripled in 1998 to 12,000 kilo-lb/hr (130,600 ton/day) when electricity generation expanded from 110 MW to 330 MW.

Despite the amount of brine injected, a high temperature zone still exists in the area. Moreover, AWI 9-7 which was drilled in 2012 found the highest temperature yet measured in the reservoir (620 °F or 327 °C). Data from recently drilled deep wells show the potential for an extension of permeability at depth. In addition, the depth of recorded micro-seismicity events suggests that permeability could extend to as deep as 13,000' (~4,000 m) BSL in this area (Figure 12)

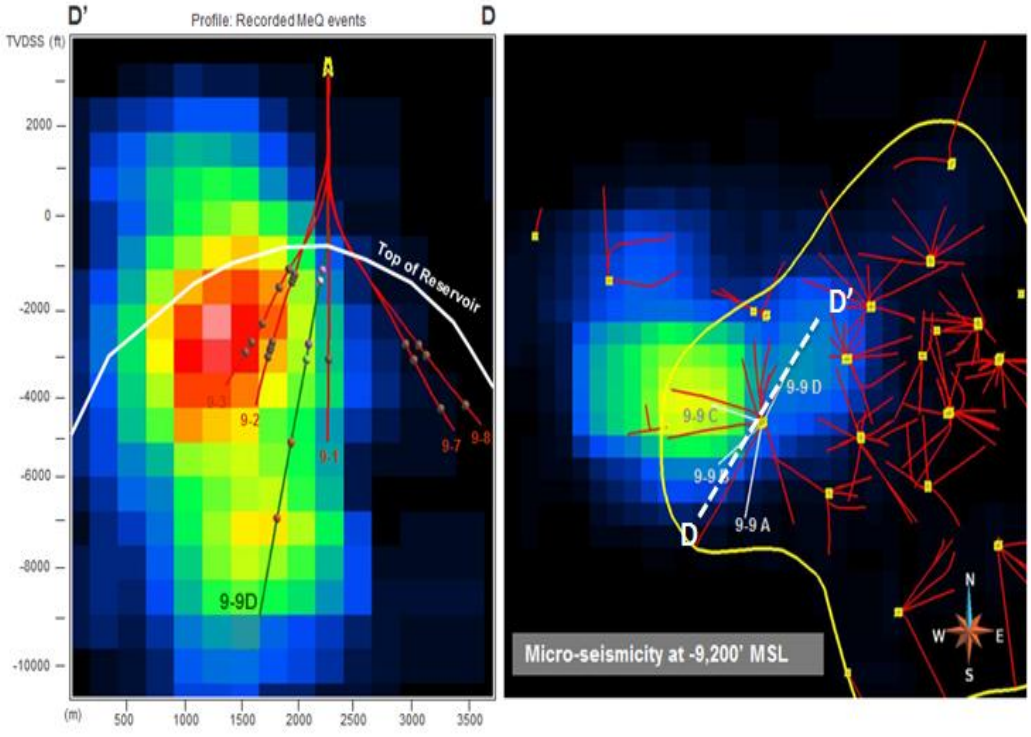

Figure 12 : Recorded MeQ event at pad AWI 9 due to injected fluid movement in the deep reservoir. The map shows cumulative MeQ events from 1998 until 2014.

At 13,000' (~4,000 m) the expected reservoir pressure is approximately 3,725 psig (257 barg) which is higher than the critical pressure of pure water. If the reservoir temperature at that depth is at or exceeds 705 °F (374 °C), supercritical fluid exists in the deep SW portion of the Awibengkok reservoir. Even though current highest maximum temperature recorded in this area is "only" 620 °F (327 °C), this peak does not means higher temperature do not exist at greater depth. This is especially the case because the area where the highest temperature was found has been affected by cooling from ~20 years of injection.

CONCLUSION AND RECOMMENDATION

The recently drilled AWI 9-9 in the southwestern portion of the Awibengkok field has revealed the presence of deep permeability below the current drilled depths of the reservoir. This deep permeability is located in Tertiary rocks in the Mixed Volcanics-Sediments (MVS) Formation which extends deeper than previously thought.

The well completion test indicated that AWI 9-9 has inter-zonal flow with the upflowing hot (610 °F or 321 °C) reservoir fluid from the bottom feed zone exiting the feed zone at ~6,532' (1,991 m) MD. This favorable result at AWI 9-9 confirms previous interpretations that the upflow of the geothermal system is beneath the Awi-9 pad. The bottom entry to this well, now the deepest permeable entry identified to date, confirms the interpretation of deep permeability in the Awibengkok reservoir. The presence of the deep feed zone in the MVS indicates that this formation is sufficiently permeable to sustain commercial production.

Upgrading the existing wellhead equipment from API 6D class 600 series to class 900 series is recommended in order to anticipate the risk of higher pressure and temperature at the surface due to scale deposition at the uppermost feedzone at 6,182' (1,884 m) MD and to also to anticipate potential anomalies in the well hydraulic condition because of the deep upflow.

Finally, supercritical fluid that has the potential to generate power outputs in order of magnitude greater than conventional high-temperature geothermal fluid may exist at greater depth in the SW portion of Awibengkok reservoir. Drilling an 'ultra' deep well or deepening existing deep wells to harness this source of energy may well be worth evaluating.

REFERENCES

Acuña, J., Astra, D., Molling, P., Prabowo, H., Stimac, J., and Sugiaman, F.: Awibengkok 1997 Conceptual Model Summary (edited by J. Stimac with contributions from W. Cumming, G. Nordquist, and J. Shemeta), *UGI In-house Report*, 1997

Ibrahim, R.F., Fauzi, A., Suryadarma: The Progress of Geothermal Energy Resources Activities in Indonesia. *Proceedings*, World Geothermal Congress 2005, Antalya, Turkey, Paper 0142, 7 pp.

Fournier, R.O., 1999 : Hydrothermal Processes Related to Moment of Fluid from Plastic into Brittle Rock in the Magmatic-epithermal Environment. *Economic Geology*, v.94, (8), pp1193-1211.

Friðleifsson, G. Ó., W.A. Elders, and A. Albertsson, 2014.: The Concept of the Iceland Deep Drilling Project. *Geothermics*, v.49, pp 2-8.

Hashida, T., G. Bignall, N. Tsuchiya, T. Takahashi, and K. Tanifuji, K., 2001.: Fracture Generation and Water Rock Interaction Processes in Supercritical Deep-seated Geothermal Reservoirs. *Geothermal Resources Council Transactions*, v. 25, pp 225-229.

Hernandez, D., Clearwater, J., Burnell, J., Franz, P., Azwar, L., and Marsh, A.,: Update on the Modeling of the Rotokawa Geothermal System: 2010 – 2014. *Proceedings*, World Geothermal Congress 2015, Melbourne, Australia.

Horie, T.: Kawerau and Nga Awa Purua Geothermal Power Station Projects in New Zealand, *Fuji Electr. Rev*., 55 (3), 2009.

Libert, F.: 620 Field Trip Report, *Internal report*, University of Auckland, 2015

Libert, F., Kusumah, Y., and Ryder, A.: Review and Evaluation of the the Initial Results of the 2012-2013 Salak Drilling Campaign: Production Make-Up Wells, *Internal report*, Chevron Geothermal Salak, May 2014.

Libert, F.: Well Reliability and Optimization Audit Result, *Internal report*, Chevron Geothermal Philippines, 2012

Muraoka, H., Uchida, T., Sasada, M., Mashiko, Y., Akaku, K., Sasaki, M., Yasukawa, K., Miyazaki, S., Doi, N., Saito, S., Sato, K., Tanaka, S., 1998 : Deep Geothermal Resources Survey Program: igneous, metamorphic and hydrothermal processes in a well encountering 500°C at 3729 m depth, Kakkonda, Japan. *Geothermics*, v. 27, (5/6), pp 507–534.

Rohrs, D., Gunderson, R., Melosh, G., Suminar, A., Nordquist, G., Molling, P. Sirad-Azwar, L., Acuña, J.: Awibengkok 2005 Conceptual Model Summary; *Internal report*, Unocal Geothermal Indonesia, 2005.

Stimac, J., Nordquist, G., Aquardi Suminar and Lutfhie, Sirad-Azwar.: An Overview of the Awibengkok Geothermal System, Indonesia, *Geothermics* 37 (2008) 300-331.

APPENDIX

RL is the part of the productivity index (PI) that does not depends on fluid properties. Injectivity index (II) obtained from a pressure-temperature-spinner survey can be corrected by mobility to obtain PI.

Constant PI (in kph/psi) can be defined as:

$$\frac{W}{PI} = (P^* - P_{wf}) \qquad \text{(A1)}$$

where W is mass flow rate in kph; P^* is the formation pressure in psi, and P_{wf} is wellbore pressure in psi.

In a steady-state radial flow **W/PI** can be expressed from Darcy's law (Paccaloni, 1979) as:

$$\frac{141.2WB\mu}{kh}\left(\ln\frac{r_e}{r_w}+s\right)=P^*-P_{wf} \quad \text{(A2)}$$

where r_e is the drainage radius in ft, r_w is the wellbore radius in ft, s is skin factor, B is the formation volume factor in bbl, kh is permeability thickness in md.ft, and μ is fluid viscosity in cP

Combining eq A1 and A2, RL can be defined as:

$$\frac{1}{RL}=\frac{141.2B\mu}{kh}\left(\ln\frac{r_e}{r_w}+s\right) \quad \text{(A3)}$$

Combining eq A1 and A3, RL (in (kph-cuft-cp)/(lb-psi)) is obtained by multiplying PI with VT (kinematic viscosity of mixture, in Cuft-cp/lb)

$$PI=RL\frac{1}{\nu_T} \quad \text{(A4)}$$

VT (kinematic viscosity of mixture, in Cuft-cp/lb) is calculated as:

Assuming $k_{rs} + k_{rw} = 1$

$$\frac{1}{\nu_T}=k_{rs}\frac{\rho_s}{\mu_s}+k_{rw}\frac{\rho_L}{\mu_L} \quad \text{(A5)}$$

In the wellbore simulator used for this project it is further assumed that k_{rw}~S_w to obtain:

$$\nu_T=X\frac{\mu_S}{\rho_S}+(1-X)\frac{\mu_L}{\rho_L} \quad \text{(A6)}$$

Where X is steam quality, k_{rs} is relative permeability of steam, k_{rw} is relative permeability of liquid, S_w is water saturation, ρ_s, ρ_L, μ_s, μ_L are steam density in lb/cuft, liquid density in lb/cuft, steam dynamic viscosity in cp, and liquid dynamic viscosity in cp respectively.

Therefore, PI can be calculated by first obtaining RL from II by multiplying it with kinematic viscosity of the injected fluid.

A LIFE CYCLE ASSESSMENT BASED COMPARISON OF A LARGE & A SMALL SCALE GEO-THERMAL ELECTRICITY PRODUCTION SYSTEM

Tianqi Yu[1], Joan Looijen[1], Freek van der Meer[1], Niek Willemsen[2]

[1]University of Twente, Faculty ITC, The Netherlands
[2]IF Technology, The Netherlands

e-mail: j.m.looijenl@utwente.nl; f. d.vandermeer@utwente.nl;
N.Willemsen@iftechnology.nl; tianqiyu0423@gmail.com

ABSTRACT

Greenhouse gas (GHG) emissions from fossil fuel electricity production cause a big problem on global warming. Using renewable energy, such as wind, solar and geothermal energy, is a more sustainable solution to produce electricity. During the operating phase of a geothermal energy power plant, there are much less GHG emissions compared to conventional power plants. But how sustainable are geothermal electricity production systems considering the whole life cycle, from construction, operation to closure of the power plant? Most research on the life cycle assessment (LCA) of geothermal energy (GTE) systems is conducted on large-scale geothermal power plants (installed capacity > 5MW) to assess their environmental performance. Little is known on the LCA of small-scale GTE systems.

In this study the environmental impacts of a large-scale GTE flash system (with an installed capacity of 110MW) is compared with a small-scale binary GTE system (the installed capacity is 500KW) using LCA, for the construction and operation stages.

The results showed that a small-scale binary system is more sustainable when considering the deep well drilling process and power plant building during the construction phase, while a large-scale flash system shows a better environmental performance when considering the process of power plant machinery production and pipeline construction. A small-scale binary system is more sustainable in the operation phase as there are no gas emissions.

Keywords: Geothermal energy systems, life cycle assessment (LCA), life cycle impact assessment (LCIA), sustainable energy systems

INTRODUCTION

Geothermal electricity production is considered to be more sustainable than the use of fossil fuels. But are they more sustainable if the whole life cycle, from construction, operation to the closure of the geothermal power plant is considered? And is there a difference between different geothermal energy systems: large and small scale systems? These are the questions addressed in this paper.

Burning fossil fuels to generate electricity produces carbon dioxide, one of most important greenhouse gases (GHGs) and therefore driver of climate change observed in the past few decades (Sullivan et al., 2010). Transition from fossil fuels to renewable energy sources is one of the biggest challenges for the coming decades if we wish to reach the agreements of COP21 (Paris Agreement) in view of combating climate change and global warming. Geothermal energy power is one of the sustainable solutions to generate electricity with minor greenhouse gas emissions.

Geothermal energy production does less damage to the environment than conventional fossil fuel electricity production systems (DiPippo, 2012). However, since geothermal steam and hot water contains hydrogen sulfide and other gases and chemicals that can be harmful in high concentrations, the environmental impacts of them cannot be ignored. Different geothermal energy systems deal with the harmful gases and chemicals differently. For example, in a flash system, the environment impacts of hydrogen sulfide and other gases need to be considered, while binary systems can inject these gases back into the geothermal well (DiPippo, 2012). Therefore, different geothermal energy conversion systems can have different environmental impacts. What's more, the gas emissions during the power generation phase do not completely cover all the environmental impacts of geothermal power plants. Large amount of energy and materials are utilized for the construction of the plant (Lacirignola & Blanc, 2013).This various for different geothermal systems and they in turn cause different environmental impacts. The inputs and outputs, as well as the environmental impacts of the different stages of a geothermal power plant can be assessed using a life cycle assessment (LCA) for different geothermal power production systems (Clark et al., 2012; Bayer et al., 2013; Pehnt, 2006).

LCA is a standard and normalized procedure (ISO 14040, 2006) to explore and assess environmental impacts during the different life cycle stages of a product (Hirschberg S.W. & Burgherr, P., 2015). Using LCA to calculate the total mass and energy consumption based on geothermal energy systems will help identify the environment impacts of the drilling, the construction of the power plant, the buildings and the operation of the power plant itself (Karlsdottir et al., 2010; Frick et al., 2010; Lacirignola & Blanc, 2013).

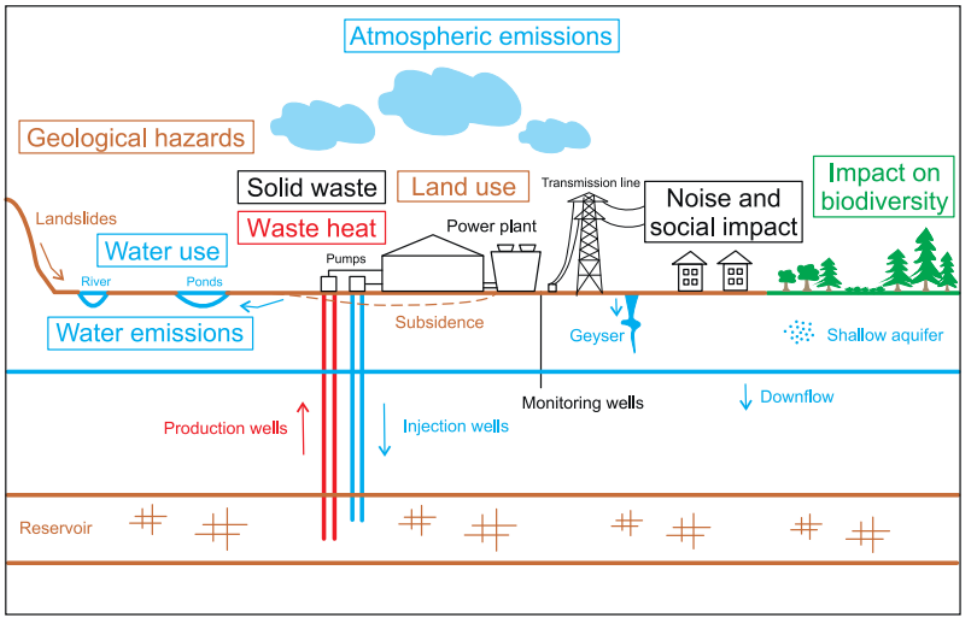

In this paper, the LCA of a large-scale flash system will be compared with a small-scale binary system, MiniGeo, for the construction and operation stages. The main reason to compare a large scale with a small scale geothermal plant is because little knowledge exists of the LCA of small scale geothermal plants. Wayang Windu is used as an example of a large-scale flash system. Wayang Windu Unit -1 was the first geothermal unit designed with a capacity of more than 100 MW (110 MW) and was therefore the first largest single flash geothermal power station in the world (Purnanto & Purwakusumah, 2015). MiniGeo is a project from IF technology (c http://www.iftechnology.nl/off-grid-electricity-production-with-minigeo). It is designed for the undeveloped (off-grid areas) areas, but can also be used in developed areas (with electricity grid). A small-scale system produces 0.5 MW. In this study, one large scale power plant (110MW) will be compared with 220 small scale geothermal power plants (0.5MW) to explore which GTE system performs better in terms of their environmental impacts, given the same electricity production.

Section 2 presents the LCA framework for geothermal energy systems. Section 3 explains the life cycle inventory (LCI) analysis for a large flash and a small scale binary geothermal plant. In Section 4 the environmental impacts of a large-scale flash system are presented for the construction, operation, and disposal phases. In Section 5 the environmental impacts of a large-scale flash system are compared with those of a small-scale binary system (MiniGeo), for the construction and operation phases. Section 6 includes the discussion, conclusions and recommendations.

LCA FRAMEWORK FOR GTE SYSTEMS

Figure 1 represents the goal definition and scope of a LCA of different GTE production system, life cycle inventory analysis and impact assessment.

GTE functional unit and system boundary

The GTE functional unit used in this paper is electricity production (kWh). LCA phases which are included within the system boundary of the considered system are as follow: 1) the production of raw materials and manufacturing of components 2) operational and maintenance phase and 3) end of life phase including the decommissioning and recycling or disposal of the components. The input materials for the GTE system are the materials and fuels used for the construction (such as deep well drilling, pipe construction etc.) and machinery. Maintenance and geothermal fluid are the two components considered for the operation phase. However, as there is hardly information available on maintenance, only geothermal fluid will be considered in this study. The output of the operation phase is electricity and hot water. The end of life stage of the GTE system usually involves the closure (filling up) of the wells and the power plant itself. On average a lifespan of thirty years is considered for a GTE power plant.

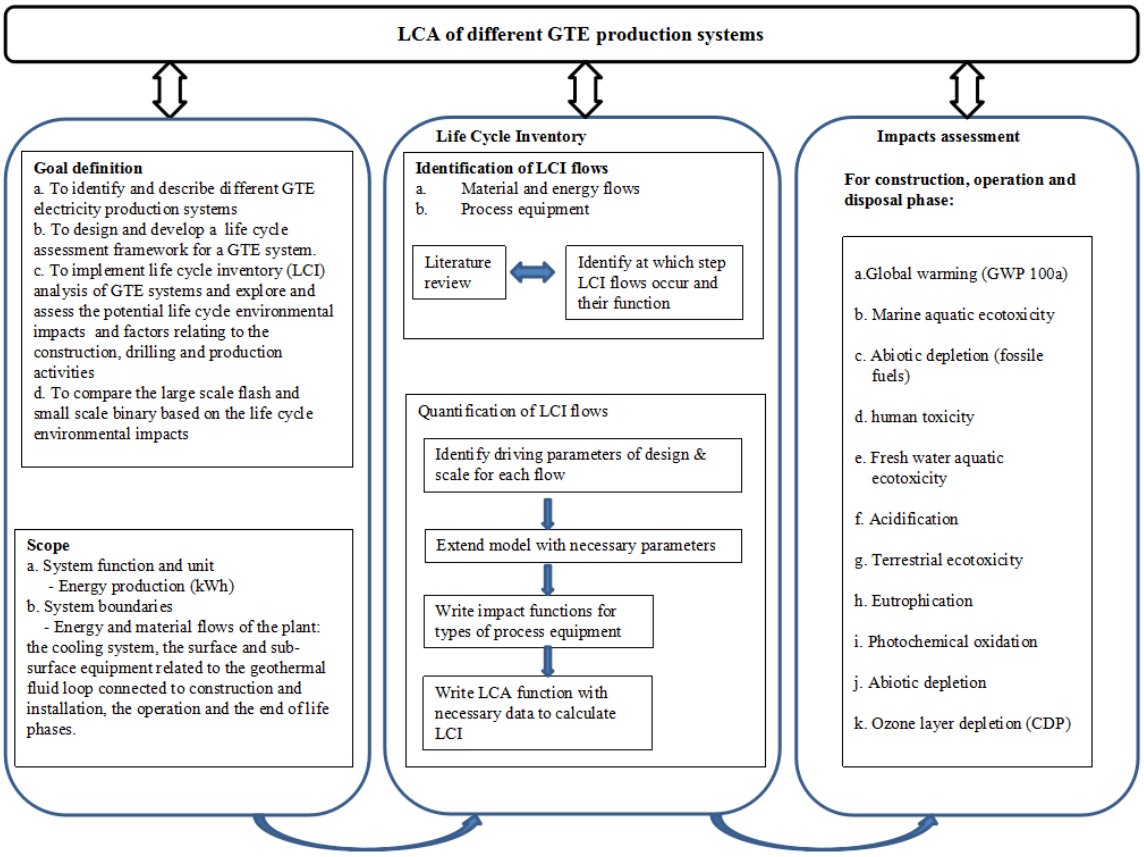

Figure 1 LCA framework for GTE electricity production systems

Life cycle inventory (LCI) analysis for GTE systems

The LCI involves the compilation and quantification of all the inputs and outputs for the construction, operation and disposal phases of the GTE system. The inputs/outputs for the geothermal energy production system includes raw material inputs, energy inputs and outputs, waste to be recycled and/or treated and emissions to the air. LCI is the most time consuming stage for conduction a LCA. The LCI data was obtained based on the literature reviews & expert knowledge. The construction phase includes all the materials (inputs and outputs) used for deep well drilling, pipeline construction, powerplant machinery and power plant buildings. For the operation phase CO_2, H_2S and CH_4, all outputs from geothermal fluid, were considered. Gravel and cement were the main components included in the LCI of the disposal phase. The LCI analysis can be conducted in LCA software, in this case SimaPro was used.

Life cycle impact assessment (LCIA) for GTE systems: impacts and indicators

An overview of possible environmental impact categories as well as specific impacts and emissions for a GTE system is given in Figure 2.

Figure 2 Direct life cycle environmental impacts of a GTE power plant (Source: Bayer et al., 2013)

When the LCIA is applied to geothermal energy systems, a number of impact metrics need to be identified. Table 3 - adapted from (European Commission - Joint Research Centre - Institute for Environment and Sustainability, 2010) shows the eleven impact categories considered in this study for the different LCA-stages.

LIFE CYCLE IMPACT ASSESSMENT OF A GTE LARGE-SCALE FLASH SYSTEM

In this section, the life cycle impact assessment (LCIA) of a large-scale flash system (Wayang Windu) is described. The impact assessment method and approaches are explained in section 3.1 and section 3.2 presents the life cycle impact assessment results for all GTE stages of a large-scale flash system.

Impact assessment methods

CML-IA (reference) is a LCA method developed by Leiden University. The method is a problem-oriented ('mid-point level') approach, in which eleven environmental impact categories are distinguished. The outcome of the LCIA in SimaPro includes a table showing the actual values for each of the eleven impact categories, for the different LCA processes. It is also possible in SimaPro to calculate the impact % each LCA process contributes to a particular impact, by dividing each impact value by the maximum value of that impact category. This is shown as a bar diagram, of which the first one will be illustrated in figure 3. Since the impact categories have different measurement units, ***normalization*** is used to make those categories more comparable. As there is no specific normalization method for Indonesia, the internationally accepted World 2000 normalization method was selected in SimaPro.

Life cycle impact assessment for all GTE stages

Table 3 shows the construction phase has the highest impact for all impact categories compared to the operation and disposal phases.

Table 3 The LCIA categories and values for the different stages of a large-scale flash system

Impact category	Unit	Total	Construction phase		Operation phase	Disposal phase
			values	%		
Marine aquatic eco-toxicity	kg 1,4-DB eq	1.97E11	1.97E11	99.9	-	8.95E6
Abiotic depletion (fossil fuels)	MJ	4.03E9	4.03E9	99.7	-	3.25E5
Human toxicity	kg 1,4-DB eq	5.2E8	5.18E8	99.6	2.16E6	7.3E3
Global warming (GWP 100a)	Kg CO2 eq	4.05E8	3.65E8	90.2	4.02E7	4.64E4
Fresh water aquatic eco-toxicity	kg 1,4-DB eq	1.27E7	1.27E7	Nearly 100		152
Terrestrial eco-toxicity	kg 1,4-DB eq	1.73E6	1.73E6	Nearly 100		56.8
Acidification	kg SO2 eq	1.62E6	1.61E6	Nearly 100		146
Eutrophication	kg $PO4^-$ eq	3.46E5	3.43E5	99.8		20.5
Photochemical oxidation	kg C2H4 eq	8.97E4	8.92E4	99.9	18.8	6.54
Abiotic depletion	kg Sb eq	1.49E3	1.23E3	99.7		0.0517
Ozone layer depletion (CDP)	kg CFC-11 eq	8.39	8.15	99.9		0.00266

The percentages per impact category for the four different construction processes and for the operation and disposal stages are shown in Figure 3. Deep well-drilling has overall the largest impact. Pipeline construction has a relatively larger impact on human toxicity and abiotic depletion. The impact of power plant buildings is mainly on abiotic depletion. The only significant environmental impact of the operation phase is global warming. Deep well closure (disposal phase) has an impact on marine aquatic eco-toxicity, abiotic depletion (fossil fuels), global warming and human toxicity.

Normalization

After normalization only the impact of deep well drilling on marine aquatic toxicity is prominent (see figure 4). Pipeline construction shows a relatively bigger impact on human toxicity than deep well drilling and has a minor impact on marine aquatic toxicity. The impact on the other environmental impact categories is very low.

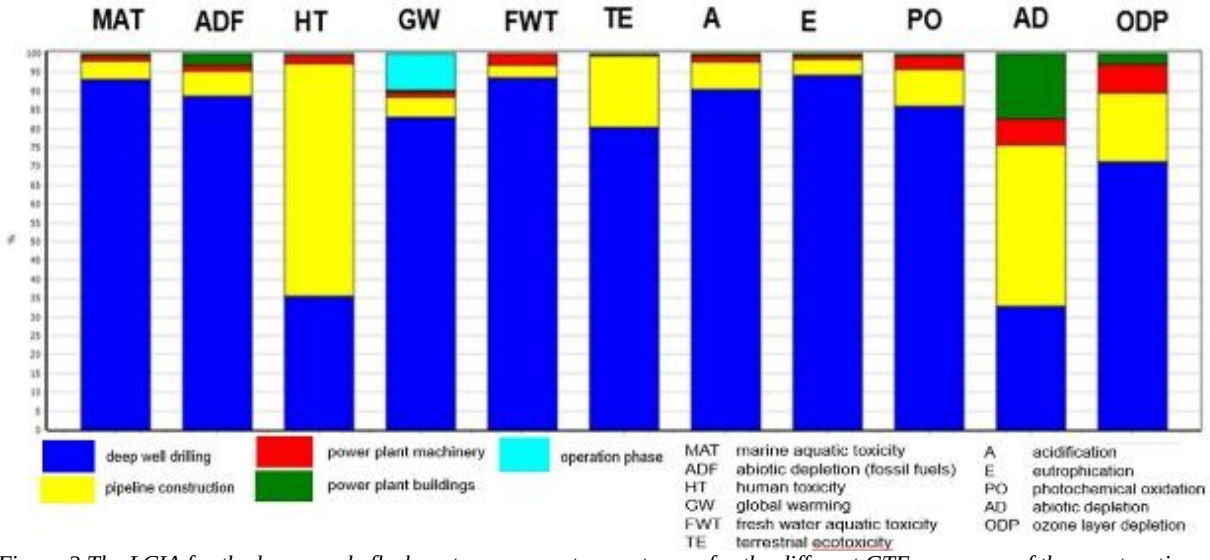

Figure 3 The LCIA for the large-scale flash system - percentage category for the different GTE processes of the construction, operation and disposal phases.

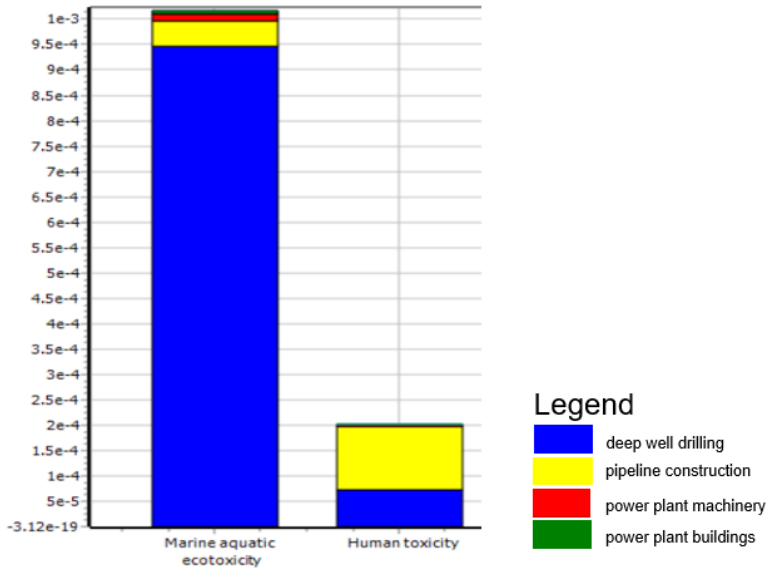

Figure 4 The normalized LCIA values of a large-scale flash system

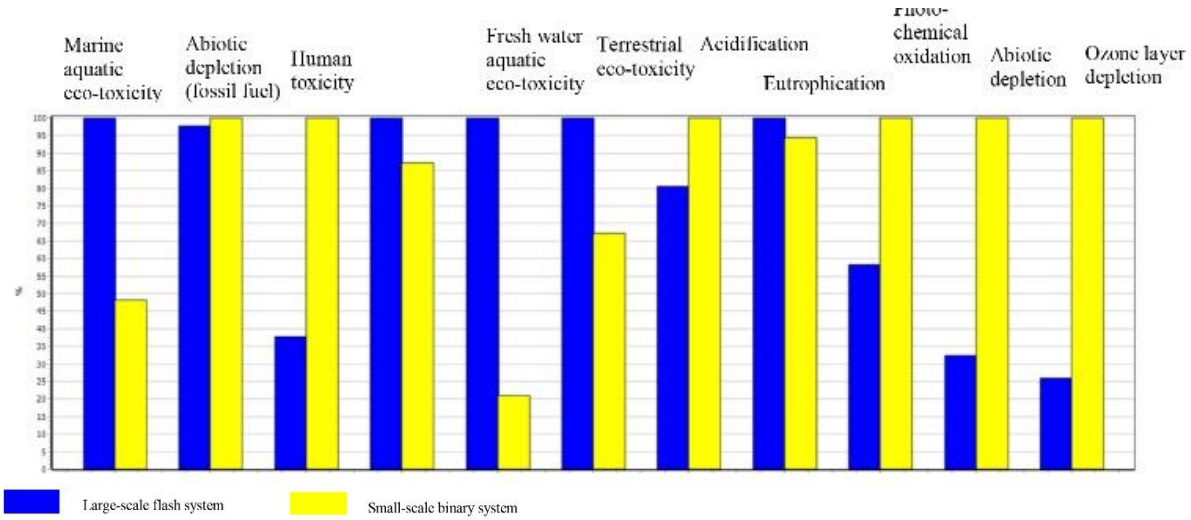

Figure 5 The LCIA of deep well drilling for the large-scale flash system and the small-scale binary system

COMPARISON OF A LARGE-SCALE FLASH WITH A SMALL-SCALE BINARY SYSTEM

For a binary system, there is no gas emitted from geothermal fluids, because a binary system has a closed loop. Therefore, there is no impact expected of the operation phase of a binary system. However, a large-scale flash system has the impacts mentioned in section 3.2. Also, the disposal phase was not considered as MiniGeo is not implemented yet and therefore no information is available on this stage for a binary small-scale system. As deep well-drilling showed overall the largest impact in the construction phase of a large-scale flash system, this phase will be given special attention first, followed by a comparison for all construction phases together.

Deep well drilling

In the process of deep well drilling**,** a large-scale flash system has relatively much more impact on fresh water & marine aquatic eco-toxicity and on terrestrial eco-toxicity and relatively more impact on global warming, abiotic depletion (fossil fuels) and eutrophication than a small-scale binary system. In contrast, the impact of a small-scale binary system is relatively much larger on ozone layer depletion, abiotic depletion and human toxicity, and relatively larger on photochemical oxidation. The impact on acidification is quite similar for both systems (see figure 5).

Comparison of GTE alternatives – all construction phases together

Figure 6 shows a large-scale flash system has more impact on marine aquatic toxicity, on fresh water aquatic eco-toxicity and terrestrial eco-toxicity than a small scale binary one. In contrast, a small-scale binary system has a bigger environmental impact on human toxicity, photochemical oxidation, abiotic depletion and ozone layer depletion than a large scale flash one.

Both systems indicate nearly the same impact on abiotic depletion, eutrophication and global warming.

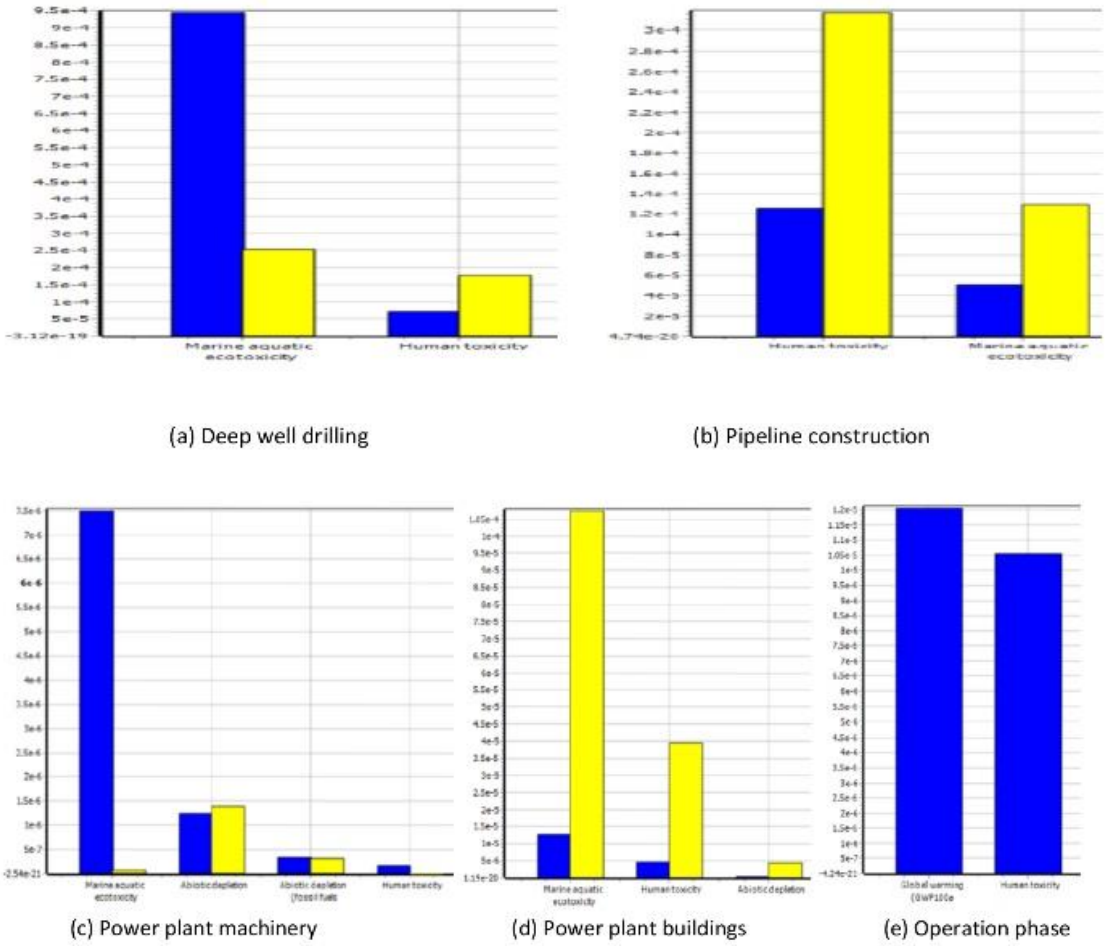

Figure 7 The normalized LCIA values of large-scale flash and small-scale binary system

Normalization

Figure 7 (a-e) shows the normalized LCIA values for the different construction phases (a-d) and the operation phase (7e) for a large-scale flash and small-scale binary system. The results are summarised in table 4.

Table 4 shows a small-scale binary system is overall more sustainable considering the construction and operation phases. Marine aquatic eco-toxicity and human toxicity are the main impacts. In the operation phase of a large-scale flash system global warming & human toxicity are prominent impacts.

DISCUSSION, CONCLUSIONS AND RECOMMENDATIONS

Accuracy assessment

An accuracy assessment was conducted using accuracy percentages between 10-30% for the different elements in the construction and operation phases. Only human toxicity, abiotic depletion and ozone layer depletion showed different impact results and those three impacts might therefore be either under estimated or over-estimated (Yu, 2017).

The LCIA method

Since there are different methods to perform a life cycle assessment, each having its own approach and normalization method, the LCA results can be affected by using a different method. The method chosen for this paper was the CML-IA baseline method. This method was compared with the ReCiPe method. As an example the LCA for deep well drilling in the construction phase of a large- scale flash system was discussed. When using the ReCiPe method, climate change appears to give the highest impact of deep well drilling, while this was marine aquatic eco-toxicity when using the CML-IA baseline method (Yu, 2017).

Comparison with results found in literature

Ketenagalistrikan et al., 2014, conducted LCIA for the process of deep well drilling specifically for the Wayang Windu GTE plant. Their findings showed a global warming potential ranging between 1.4 – 3.1 ton CO2 equivalent. In this research (Yu, 2017) a CO2 equivalent of 3 ton was calculated, which is within the range of the above mentioned research. In the operation phase, global warming potential (GWP) is a very important environmental impact in LCA (Marchand et al., 2015). The greenhouse values from the (Hondo, 2005), (Marchand et al., 2015) and (IPCC, 2011) are compared with the global warming potential results in this research. Their GWP values are between 38.5 and 47 g $CO_{2\ eq}$/kWh. The result in this research is 41.7 g $CO_{2\ eq}$/kWh. According to (IPCC, 2011), the medium value of global warming gas for other renewable energy electricity production systems are: 46 g $CO_{2\ eq}$/kWh (photovoltaic energy) and 12 g $CO_{2\ eq}$/kWh (wind energy). Meanwhile,

(IPCC, 2011) also reported the greenhouse gas emissions from non-renewable energy electricity production systems are: 840 g $CO_{2\ eq}$/kWh (fossil oil energy) and 1000g $CO_{2\ eq}$/kWh (coal). The production of geothermal energy seems to be comparable with the one of photovoltaic energy.

Site specific issues and parameters

The results of the LCA of GTE systems vary for different locations. For example, in Indonesia, materials used to drill wells are different from the materials used in Iceland. In addition, GTE power plants in developed countries, such as Switzerland and Germany, may use more sustainable materials than those in Indonesia. This may explain why e.g. carbon dioxide emissions are lower (Frick et al., 2010) than the ones presented for Indonesia. In some LCA studies, such as (Marchand et al., 2015), for GTE development, land use conversion (by the construction of wells, pipelines and power plant) as part of the construction phase, is included in the LCI.

The same is for the stimulation of wells to test the well performance. The stimulation process happens after the drilling of boreholes. As no information was available on those components, they could not be included in the LCA of this study.

In the operation stage, maintenance of the wells, machinery and the power station are important components in a LCA. Corrosion and geothermal scales are a problem, but could not be included in this study due to lack of data.Many LCA studies provide information on transport, which is an important component for all LCA stages. However, transport of materials to and from the site was not included in this research as no information was available on transport means, nor distances to transport materials and equipment. This, of course, will particularly increase the global warming values.

Table 4 Summarised comparison of a large-scale flash and small-scale binary system

	Large-scale Flash	Small-scale Binary
Construction phase		
Deep well drilling	**1**	2
Pipeline construction		1 & **2**
Power plant machinery		**1**, 2 & 3
Power plant buildings	**1** & 2	3
Operation phase	**4 & 2**	

1 = Marine aquatic eco-toxicity, 2 = Human toxicity, 3 = Abiotic depletion, 4 = Global warming potential

Conclusions

Geothermal deep well drilling is the most polluting phase during the whole life cycle of a large-scale flash GTE electricity production system, giving a high impact on marine aquatic eco-toxicity. Human toxicity is mainly caused by pipeline construction (also as part of the construction phase). The amount of abiotic depletion (fossil fuel) is large in absolute amount, but at a worldwide level, abiotic depletion is less of a concern.

Global warming is the only significant environmental impact in the operation phase, followed by human toxicity. This is mainly caused by gas emissions from geothermal fluid. The disposal phase shows very little environmental impacts in this research. The geothermal well drilling process in the construction phase of a large-scale flash system shows more environmental impact on marine aquatic eco-toxicity and fresh water aquatic eco-toxicity than a binary system.

A small-scale binary system can cause more acidification, photochemical oxidation, abiotic depletion and ozone layer depletion problems because more material are used while downscaling the power plant machineries of a small-scale binary system. Abiotic depletion and eutrophication impacts are nearly equivalent in both systems.

In the operation phase, this research assumed for a GTE system, the most environmental concern is from gas emitted from geothermal fluids. Since no gas will emit from a binary system in the operation phase, no impacts occur in this phase and therefore the operation phase of a small-scale binary system is considered more sustainable than of a large-scale flash system.

Summarized, a small-scale binary system is more sustainable when considering the deep well drilling process. In contrast, a large-scale flash system shows a better environmental performance when considering the process of power plant machinery production and pipeline construction. A small-scale binary system is more sustainable in the power plant building construction and operation phases.

Recommendations and suggestions for future research

Marchand et al., 2015 classified GTE systems into 3 categories: the type of energy produced (electricity or combined district heat and electricity), the type of reservoirs (conventional or unconventional) and the type of conversion technology. In future research, also a large-scale binary system and a small-scale flash system could be assessed. It would also be interesting to include different conversion technology scenarios. Also, different electricity production systems in Indonesia can be compared to figure out which is the most sustainable electricity production system.

Transportation should be included in all phases in a LCA research. The global warming potential values will be higher if also transportation is considered in a LCA study.

Finally, it would be nice to test how representative this research is when applied in another country or for other cases.

REFERENCE

Bayer, P., Rybach, L., Blum, P., & Brauchler, R. (2013). Review on life cycle environmental effects of geothermal power generation. *Renewable and Sustainable Energy Reviews*, *26*, 446–463. http://doi.org/10.1016/j.rser.2013.05.039

Clark, C., Sullivan, J., Harto, C., Han, J., & Wang, M. (2012). Life Cycle Environmental Impacts of Geothermal Systems. *Proceedings, Thirty-Seventh Workshop on Geothermal Reservoir Engineering*, (2010), 8.

DiPippo, R. (2012). *Geothermal Power Plants : Principles , Applications , Case Studies and Environmental Impact Third Edition*. http://doi.org/10.1016/B978-0-08-098206-9.00024-5

European Commission - Joint Research Centre - Institute for Environment and Sustainability. (2010). International Reference Life Cycle Data System (ILCD) Handbook : Analysing of existing Environmental Impact Assessment methodologies for use in Life Cycle Assessment. *European Commission*, 115. http://doi.org/10.2788/38479

Frick, S., Kaltschmitt, M., & Schr??der, G. (2010). Life cycle assessment of geothermal binary power plants using enhanced low-temperature reservoirs. *Energy*, *35*(5), 2281–2294. http://doi.org/10.1016/j.energy.2010.02.016

Hirschberg S. and Burgherr P. (2015). *Energy from the earth: deep geothermal energy as a resource for the future?* (2015 ed. S. Hirscheberg, s. wiemer and P. Burgherr, Center for Technology Assessment zurich, Switzerland, Ed.), *Energy from the earth: deep geothermal energy as a resource for the future?* http://doi.org/10.3929/ethz-a-010277690

Hondo, H. (2005). Life cycle GHG emission analysis of power generation systems: Japanese case. *Energy*, *30*(11–12 SPEC. ISS.), 2042–2056. http://doi.org/10.1016/j.energy.2004.07.020

IPCC. (2011). *IPCC, 2011: Summary for Policymakers. In: IPCC Special Report on Renewable Energy Sources and Climate Change Mitigation*. *Cambridge University Press*. http://doi.org/10.5860/CHOICE.49-6309

Karlsdottir, M. R., Palsson, O. P., Palsson, H., & Science, C. (2010). LCA of Combined Heat and Power Production At Hellishei Đi Geothermal Power Plant With Focus on Primary Energy Efficiency. *The 12th International Symposium on District Heating and Cooling*, (November 2015), 9. Retrieved from http://www.researchgate.net/profile/Halldor_Palsson/publication/256732536_LCA_of_combined_heat_and_power_production_at_Hellisheii_geothermal_power_plant_with_focus_on_primary_energy_efficiency/links/0046353563ef927b14000000.pdf

Ketenagalistrikan, P., Baru, E., Energi, K., Ciledug, J., Kav, R., Lama, K., & Selatan, J. (2014). Ketenagalistrikan dan Energi Terbarukan LAPANGAN PANAS BUMI WAYANG WINDU , JAWA BARAT LIFE CYCLE INVENTORY ANALYSIS OF GEOTHERMAL WELL DEVELOPMENT IN WAYANG WINDU FIELD , WEST JAVA I Made Agus Dharma Susila Ketenagalistrikan dan Energi Terbarukan dan Ener, *13*(2), 101–114.

Lacirignola, M., & Blanc, I. (2013). Environmental analysis of practical design options for enhanced geothermal systems (EGS) through life-cycle assessment. *Renewable Energy*, *50*, 901–914. http://doi.org/10.1016/j.renene.2012.08.005

Marchand, M., Blanc, I., Marquand, A., Beylot, A., Bezelgues-courtade, S., Guillemin, A. C., … Cedex, B. P. F.-O. (2015). Life Cycle Assessment of High Temperature Geothermal Energy Systems. *World Geothermal Congress 2015*, (April), 19–25.

Murakami, H., Kato, Y., & Akutsu, N. (2000). Construction of the Largest Geothermal Power Plant for Wayang Windu Project , Indonesia, 3239–3244.

Pehnt, M. (2006). Dynamic life cycle assessment (LCA) of renewable energy technologies. *Renewable Energy*, *31*(1), 55–71. http://doi.org/10.1016/j.renene.2005.03.002

Purnanto, M. H., & Purwakusumah, A. (2015). Fifteen Years (Mid-Life Time) of Wayang Windu Geothermal Power Station Unit-1: An Operational Review. *World Geothermal Congress 2015*, (April), 19–25.

Sullivan, J. L., Clark, C. E., Han, J., & Wang, M. Q. (2010). Life-cycle analysis results of geothermal systems in comparison to other power systems. *Energy Systems Division, Argonne National Laboratory*. http://doi.org/10.2172/993694

Yu, T. (2017). A life cycle assessment based comparison of large & small scale geo- thermal electricity production systems A life cycle assessment based comparison of large & small scale geo- thermal electricity production systems. MSC thesis, ITC, University of Twente. http://www.itc.nl/library/papers_2017/msc/nrm/tyu.pdf

IMPLEMENTATION OF RELIABILITY CENTER MAINTENANCE (RCM) PROGRAM USING FUZZY LOGIC ON THE STEAM TURBINE GENERATOR

Nasruddin[1], Nanang Kurniawan[2], Dimas Prasetyadi[3]

[1]Universitas Indonesia
[2]PT Pertamina Geothermal Energy
[3]PT Pertamina (Persero)

e-mail: nasruddin@eng.ui.ac.id; nanang.kurniawan@pertamina.com; prasetyadi.dimas@gmail.com

ABSTRACT

The Increasing complexity of Geothermal Power Plants (GPPs) installations and operations, along with growing public awareness to ensure higher levels of reliability, has put great pressure on the designers and operators to find innovative solutions to ensure reliability as well as economically viable operation. Reliability Centered Maintenance helps in finding such solutions and thus in gaining more importance in the industries, especially on Power Plants. A wide range of methodologies currently in use for RCM includes commercial and in-house software packages (specific to individual plants). The techniques with software produce very different results, raising serious concerns. Here, we present a simple and structured RCM methodology that can bridge this gap. The proposed methodology uses fuzzy logic to estimate risk by combining (fuzzy) likelihood of occurrence, (fuzzy) severity and its (fuzzy) detection.

Keywords: FMEA, fuzzy logic, RCM, steam turbine, geothermal power plants, RCM, strategies maintenance

INTRODUCTION

Renewable energy plays an important role in the provision of the secure supply of energy. Geothermal energy is one of the renewable energy forms that meet popular demand, especially in Indonesia. Geothermal becomes the important source for electricity needs in Indonesia. In order to generate stabile electricity, every equipment in the geothermal power plants must be maintained appropriately. Somehow, not every equipment needs excessive treatment, because it will need high cost and high amount of source. Some Critical Analysis Methods have been proposed to fix this problem. Failure Mode and Effect Analysis (FMEA) has been applied in some power plants to decrease potential failure modes in some power plants. The utilization of Failure Mode and Effect Analysis (FMEA) as a convenient technique for determining, classifying and analyzing common failures in typical GPPs in considered (Feili, 2013). As a result, an appropriate risk scoring of occurrence, detection and severity of failure modes and computing the Risk Priority Number (RPN) for detecting high potential failure is achieved. RPN (Risk Priority Number) is determined to rank the failure modes, however, the methods have been criticized for having some weakness (M Giardina, 2014). Fuzzy rule based assessment model has been applied to evaluate the RPN index to rank component failure (M Rafie F, 2015). The fuzzy assessment model is applied due to difficulty for the experts to give precise numerical inputs for the three risk factors and due to important factor for severity, occurrence, and detection, which never considered for rank the equipment criticality in geothermal power plants (M Giardina, 2014). The proposed methodology is applied to Geothermal Power Plants equipment) using MATLAB software, which never done before. Due to the complexity of geothermal power plants equipment, the proposed methodology can make the right decision to determine appropriate treatment for every equipment in geothermal power plants based on FMEA priority categorization. The obtained results allow the identification of the component faults that need to be known to achieve a better understanding. Those fuzzy logic approaches on FMEA application is applied on RCM (Reliability Centered Maintenance) program, In order to develop an appropriate maintenance task and build a living program.

FMEA

FMEA is a systematic method of identifying and preventing product or process problems before they occur (Mychael R. Beauregard, 1996).Thus, applying FMEA to Geothermal Power Plants to evaluate all the possible consequences of failure modes can be a useful technique to present a recommended action. Some of the experts give the score for every failure modes of each equipment. The risk ranking is based on the result of calculation among severity, occurrence, and detection.

$$RPN = S \times O \times D \quad (1)$$

The result of this calculation is RPN (Risk Priority Number). RPN is used to compare criticality of all equipment in the system. This method that the traditional FMEA employs to achieve a risk ranking is critically debated (M Rafie F, 2015). Various sets of O, S and D may produce an identical value of 3, 5, 2 and 2, 3, 5 for O, S, D respectively. For example, we consider two different events having values of 3, 5, 2 and 2, 3, 5 for O, S and D, respectively. Both this event will have 30 in RPN value, however, the risk implications of these two events may not necessarily be the same. In order to solute this problem, a fuzzy logic approach is used. Using expert knowledge and decision for input calculation in FMEA, a fuzzy logic approach could be used to improve the quality of the results and be applied especially in Geothermal Steam turbine system.

FUZZY LOGIC APPROACH

Generally the fuzzy logic approach proceed in the following steps (M Giardina, 2014):

- Fuzzification
- Fuzzy inference (apply implication method)
- Aggregation of all outputs.
- Defuzzification

The input parameter of the fuzzy logic approach is used gaussmf and gauss2mf membership function, such in

works (Tay KM, 2008) in order to gap between practical realities and mathematical modeling. While the output parameter is used trapezoidal and triangular membership function.

Gaussmf membership function

$$f\ (x;\sigma.c) = e^{\frac{-(x-c)^2}{2\sigma^2}} \quad (1)$$

The symmetric Gaussian function depends on two parameters σ and c factors.

Gauss2mf membership function

$$f\ (x;\sigma.c) = e^{\frac{-(x-c)^2}{2\sigma^2}} \quad (2)$$

The first part of the function of the *gauss2mf membership function* is specified by σ_1 and c_1, which determine the shape of the left-most curve. The second part of the *gauss2mf membership function*, specified by σ_2 and c_2, determines the shape of the right-most curve. Whenever $c_1 \leq c_2$, the gauss2mf function reaches a maximum value of 1. Otherwise, the maximum value is less than one. The order of the parameters follows: [σ_1 , c_1, σ_2 ,c_2] (Ratnayake, 2017).

Triangular membership function.

$$\mu_A(x) = \begin{cases} \frac{x-x_1}{x_2-x_1} & \text{for } x_1 \leq x \leq x_2 \\ \frac{x-x_1}{x_2-x_1} & \text{for } x_2 \leq x \leq x_3 \\ 0 & \text{For others} \end{cases} \quad (3)$$

Where $x_1 \leq x_2 \leq x_3$

Trapezodial membership function.

$$\mu_A(x) = \begin{cases} \frac{x-x_1}{x_2-x_1} & \text{for } x_1 \leq x \leq x_2 \\ 1 & \text{for } x_2 \leq x \leq x_3 \\ \frac{x-x_4}{x_3-x_4} & \text{for } x_3 \leq x \leq x_4 \\ 0 & \text{For others} \end{cases} \quad (4)$$

Where $x_1 \leq x_2 \leq x_3 \leq x_4$

Moreover, the other parameters of the fuzzy logic based expert system that has been selected for the current analysis are as follows: "AND" operator with "minimum", "OR", operator with "maximum", "Implication" with "minimum", "Aggregation" with "maximum" and "Defuzzification" with "centroid" algorithm. A fuzzy rule base has been developed using weighing factor as showm in Table 5 (Ratnayake, 2017). The toolbox simulator tool of MATLAB (R2015a) has been utilized to execute the suggested fuzzy inference process.

FMEA FUZZY LOGIC APPROACH

The input parameter are using gaussmf and gauss2mf membership functions, while The output risk is using triangular and trapezoidal membership functions. The input and output parameter have been decomposed into fuzzy sets as shown in figures 2-5. The values are based on ranking scales as shown in Tables 1-4, which describe some consequences explanation of each value (M Giardina, 2014).

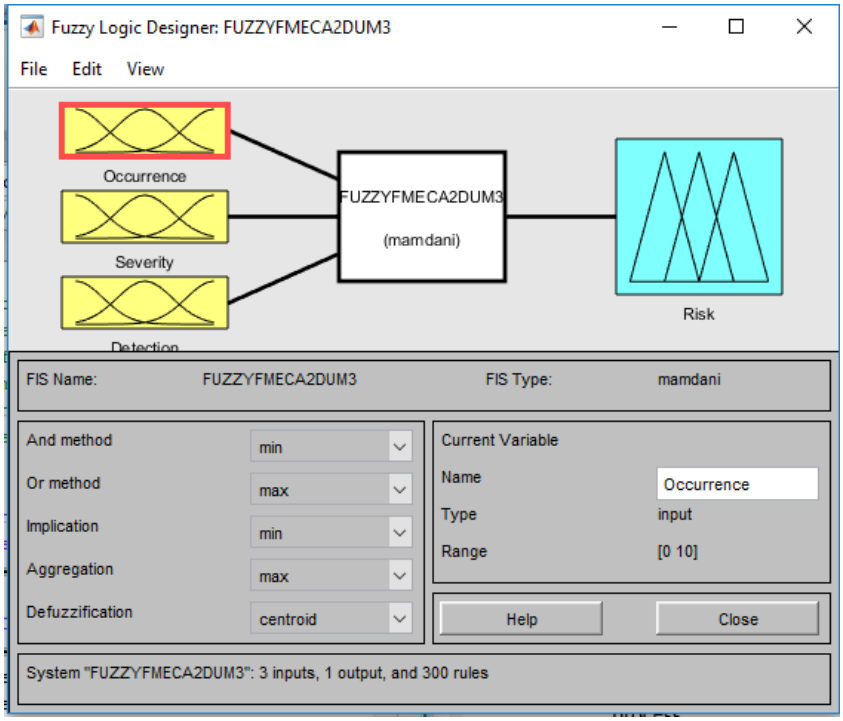

Figure 1 : Toolbox simulator tool of MATLAB (R2015B)

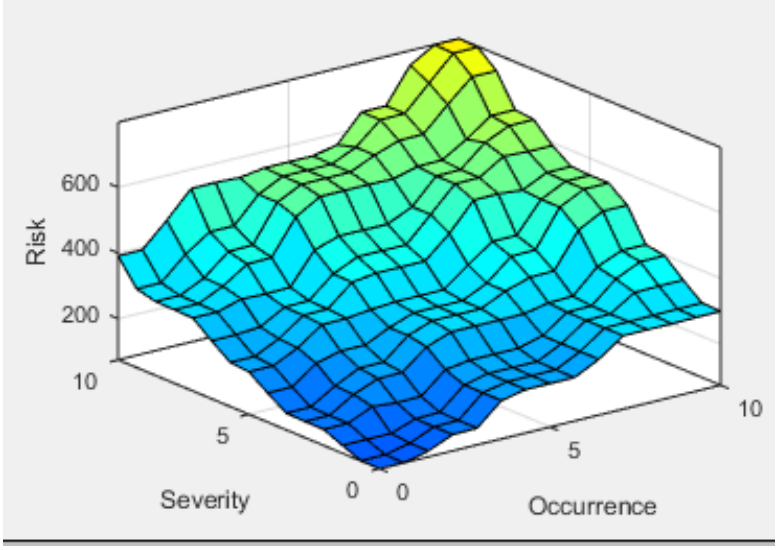

Figure 2 : Surface view of fuzzy logic

Table 1 : Occurrence ranking scale.

Rank of Occurence	Rating	Description	Linguistic Fuzzy	Weight (W)
1	Very Low (VL)	Failure unlikely,	[0.008493 0 0.3397 1]	0.2
2	Low (L)	Few Failures,	[0.34 2 0.34 3]	0.4
3,4,5	Moderate (M)	Occasional failures,	[0.3397 4 0.3397 6]	0.6
6,7,8	High (H)	Repeated failures,	[0.3397 4 0.3397 6]	0.8
9,10	Very High (VH)	Inevitable failure,	[0.3397 9 0.008493 10]	1

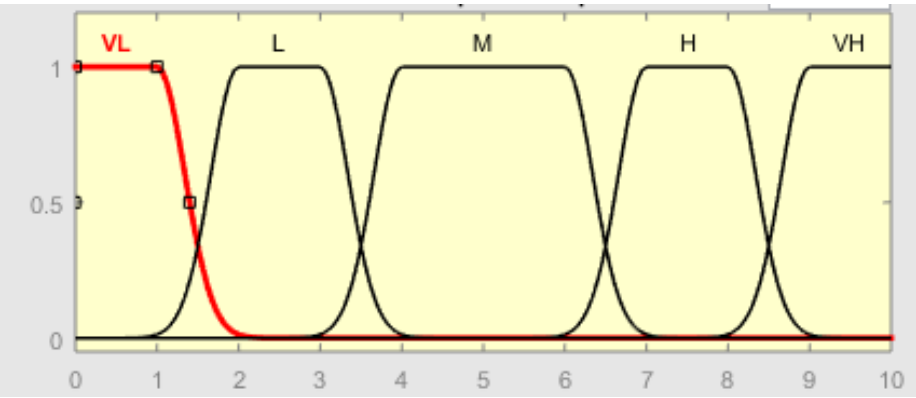

Figure 3 linguistic fuzzy value on Occurrence

Table 2 : Severity ranking scale.

Rank of Severity	Categorization	Description	W_S
1	No Effect (N)	No reason to expect failure. Slight annoyance-no injury to people.	0.1
2	Very Minor (VMR)	Very minor effect on product or system performance. The product does not require. Slight danger-no injury to people.	0.2
3	Minor (MR)	Minor effect on product or system performance. The product does not require repair. Very minor or no injury to people.	0.3
4	Very Low (VL)	Very low effect on system performance. The system does not require repair. Minor or no injury to people.	0.4
5	Low (L)	Moderate effect on system performance. The product requires repair. Very moderate danger-minor injury to people.	0.5
6	Moderate (M)	System performance is degraded. Some safety functions may not operate. The product requires repair. Moderate danger-minor to moderate injury to people.	0.6
7	High (H)	System performance is severely affected but functions (reduced level of performance). The system may not operate. The product requires repair. Very moderate danger-minor injury to people.	0.7
8	Very High (VH)	System is inoperable with loss of primary function. Failure can involve hazardous outcomes. Dangerous-may result in major injury to people.	0.8
9	Hazardous with Warning (HWW)	Failure involves hazardous outcomes. Very dangerous-may result in major injury or death of people.	0.9
10	Hazardous without Warning (HWOW)	Failure is hazardous and occurs without warning. It suspends operation of the system. Extremely dangerous-may cause death of people.	1

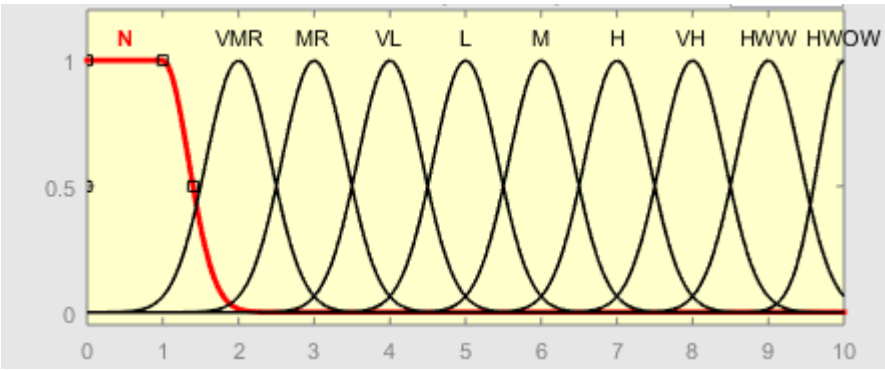

Figure 4 : llinguistic fuzzy value on Occurrence

Table 3 : Detection ranking scale.

Rank	Detection (%)	Description	Linguistic Fuzzy	W_D
1,2	0-15	Design control will almost certainly detect a potential failure mode/task error.	[0.008493 0 0.3397 2]	0.17
3,4	16-35	High chance that the design control will almost certainly detect a potential failure mode/ task error	[0.3397 3 0.3397 4]	0.33
5,6	36-65	Moderate chance that the design control will detect a potential failure mode/ task error (e.g. the defect will remain undetected until the system performance is affected).	[0.34 5 0.34 6]	0.5
7,8	66-85	Remote chance that the design control will detect a potential failure mode/task error (e.g. the defect will remain undetected until an inspection or test is carried out).	[0.3397 7 0.3397 8]	0.67

9	86-100	Defect most likely remains undetected (e.g. the design control cannot detect potential cause or the task will be performed in the presence of the defect).	[0.4247 9]	0.83
Rank	**Detection (%)**	**Description**	**Linguistik Fuzzy**	**WD**
10	90-100	System failures are not detect (e.g. there is no design verification or the task will certainly be performed in the presence of the defect). System failures are not detect (e.g. there is no design verification or the task will certainly be performed in the presence of the defect).	[0.3397 10 0.008493 10]	1

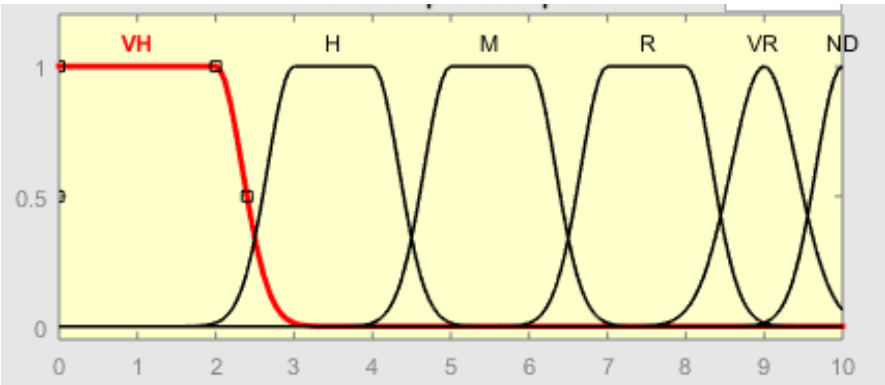

Figure 5 : linguistic fuzzy value on Detection

The linguistic term of the RPN fuzzy output and the pertinent weight W_{RPN} used within the proposed fuzzy if-then rules are identified using the value of the summation of the product of the relative importance factor and weight for each fuzzy input term (M Giardina, 2014):

$$W_{RPN} = R_O W_O + R_S W_S + R_D W_D \quad (5)$$

This W_{RPN} value allows for the identification of the output of the RPN linguistic terms as explained in the following examples (M Giardina, 2014):
Rule: If the occurrence is Moderate (with W_O=0.6) and the severity is No effect (with W_S = 0.1) and the detection is High (with W_D = 0.33), then the consequent part is obtained using equation (5), namely 0.4.0.6+0.4.0.1+0.2.0.33 = 0.346. This number is placed between W_{RPN} =0.3 of risk Very Low and W_{RPN} =0.4 of risk Low, but being closer to risk Very Low, therefore the result is Very Low with W_{RPN}=0.35
The rules have 300 combinations and Table 5 shows the fuzzy inference rules obtained by setting the linguistic terms of occurrence O as Moderate M and varying the linguistic terms of severity S and detection D. The W_{RPN} for each fuzzy rule are also reported.

Table 4 : Risk RPN ranking scale.

Linguistic value for RPN	**Rank**	**Linguistic**	**Fuzzy lingustik**	**W_{RPN}**
Almost unnecessary to take the follow-up actions	1-50	Unnecessary (U)	[0 0 25 75]	0.1
Minor priority to take the follow-up actions	50-100	Minor (MI)	[25 75 125]	0.2
Very Low priority to take the follow-up actions.	100-150	Very Low (VL)	[75 125 175]	0.3
Low priority to take the follow-up actions.	150-250	Low (L)	[125 200 300]	0.4
Moderate priority to take the follow-up actions.	250-350	Moderate (M)	[200 300 400]	0.5
High priority to take the follow-up actions.	350-450	High (H)	[300 400 500]	0.6
Very High priority to take the follow-up actions.	450-600	Very High (VH)	[400 550 700]	0.7
Extremely High priority to take the follow-up actions	600-800	Extremely High (EH)	[500 650 800]	0.8
Necessary to take the follow-up actions.	800-900	Necessary (N)	[700 800 900]	0.9
Absolutely Necessary to take the follow-up actions.	900-1000	Absolutely Necessary (AN)	[800 900 1000 1000]	1

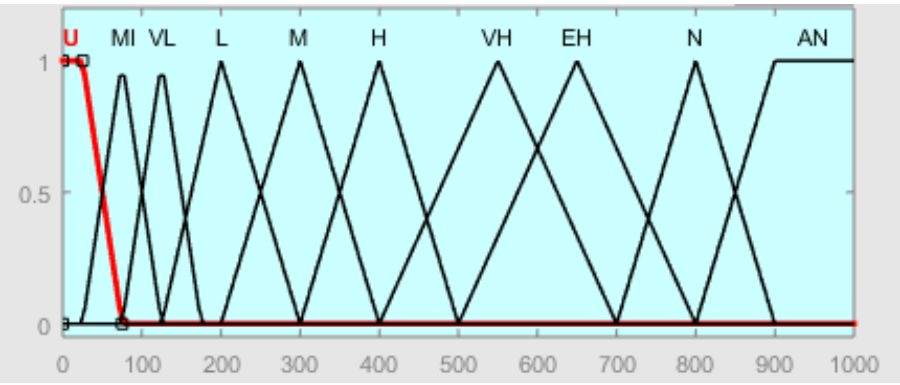

Figure 6 : linguistic fuzzy value on RPN (Risk Priority Number)

Table 5 RPN fuzzy inference rules.

				Occurrence (M)									
				R_o			0.4						
				W_O			0.4						
				Severity									
				R_D			0.4						
				N	VMR	MR	VL	L	M	H	VH	HWW	HWOW
				0.1	0.2	0.3	0.4	0.5	0.6	0.7	0.8	0.9	1
Detection	0.2	VH	0.17	0.23 MI	0.27 VL	0.31 VL	0.35 VL	0.39 L	0.43 L	0.47 M	0.51 M	0.55 M	0.59 H
		H	0.33	0.27 VL	0.31 VL	0.35 VL	0.39 L	0.43 L	0.47 M	0.51 M	0.55 M	0.59 H	0.63 H
		M	0.5	0.30 VL	0.34 VL	0.38 L	0.42 L	0.46 M	0.50 M	0.54 M	0.58 H	0.62 H	0.66 EH
		R	0.67	0.33 VL	0.37 L	0.41 L	0.45 L	0.49 M	0.53 M	0.57 M	0.61 H	0.65 H	0.69 EH
		VR	0.83	0.37 L	0.41 L	0.45 L	0.49 M	0.53 M	0.57 H	0.61 H	0.65 H	0.69 EH	0.73 EH
		ND	1	0.40 L	0.44 L	0.48 M	0.52 M	0.56 H	0.60 H	0.64 H	0.68 EH	0.72 EH	0.76 AN

RCM APPLICATION

Reliability Centered Maintenance is a process used to determine the maintenance requirements of any physical asset in its operating context (Moubrey, 1992). RCM application is used to determine the appropriate task and interval of maintenance scheduling.

RCM consists of 8 main process, which are listed below.

- **Prepare the Operating Context**
  Collect and identify all related data, in order to create an identification process comprehensive.

- ***Function***,
  Record what the asset does not what it is. Include desired standards of performance in its operating context.

- ***Functional Failure,***
  Document the ways in which the asset can fail to fulfill its function.
- ***Failure Modes,***
  Determine what causes each functional failure.

- ***Failure Effects***,
  Detail what happen if nothing were done to predict or prevent each failure mode.

- ***Failure Consequences***
  Determine how each failure mode matters.

Based on RCM book (Moubrey, 1992), there are several types of failure consequences.

1. Hidden failure consequences: Hidden failures have no impact, but they expose the organization to multiple failures with serious, often catastrophic, consequences.
2. Safety and environmental consequences: A failure has safety consequences if it could hurt or kill someone.
3. Operational consequences: A failure has operational consequences if it affects production (output, product quality, costumer service or operating cost in addition to the direct cost of repair).
4. Non-operational consequences: Evident failures which fall into this category affect neither safety nor production, so they involve only the direct cost of repair.

- ***Proactive Maintenance & Intervals***
  Determine if On-Condition or Preventive Maintenance is technically appropriate and worth doing. These are a task undertaken before a failure occurs, in order to prevent the item from getting a failed state. They embrace what is traditionally known as 'predictive' and 'preventive maintenance' although we will see later that RCM uses the terms *scheduled restoration, scheduled discard* and *on-condition maintenance* (Moubrey, 1992).

- ***Default Strategies***
  Determine if there are any other actions that are appropriate. RCM recognizes three major categories of default actions, as follows (Moubrey, 1992):
  1. Failure-finding: Failure-finding tasks entail checking hidden functions periodically to determine whether they have failed (whereas condition-based tasks entail checking if something is failing).
  2. Redesign: redesign entails making any one-off change to the built-in capability of a system.
  3. No scheduled maintenance: as the name implies, this default entails making no effort to anticipate or prevent failure modes to which it is applied, and so those failures are simply allowed to occur and then repaired.

The proposed methodology combines FMEA fuzzy logic and RCM, as shown in Figure 8.

RCM PROCESS

The process begins with identification system and related components. Critical Analysis is performed after identification has finished. Critical Analysis has used the application of fuzzy logic in order to prevent similarity of RPN value despite their differences implication risk input. The result of Critical Analysis would be the list of critical component and non-critical component based on their RPN value description. If the RPN value is low or below low, then the component would be registered as non-critical component and if the RPN value is moderate to very high then the component would be registered as critical equipment. After that maintenance tasks and intervals can be performed based on their characteristic. Those characteristics are achieved from the P-F interval (Potential to Failure Interval),showed in Figure 7.For non-critical equipment simple decision making is performed by experts, in order to get whether a simple task procedure or run to failure procedure. After that, all of the components will be reviewed by a team, in order to get an appropriate maintenance task. RCM would be developed and circulated, that we can conclude RCM is a living program.

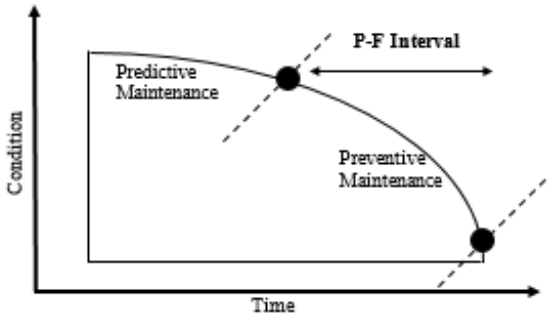

Figure 7 : P-F Interval

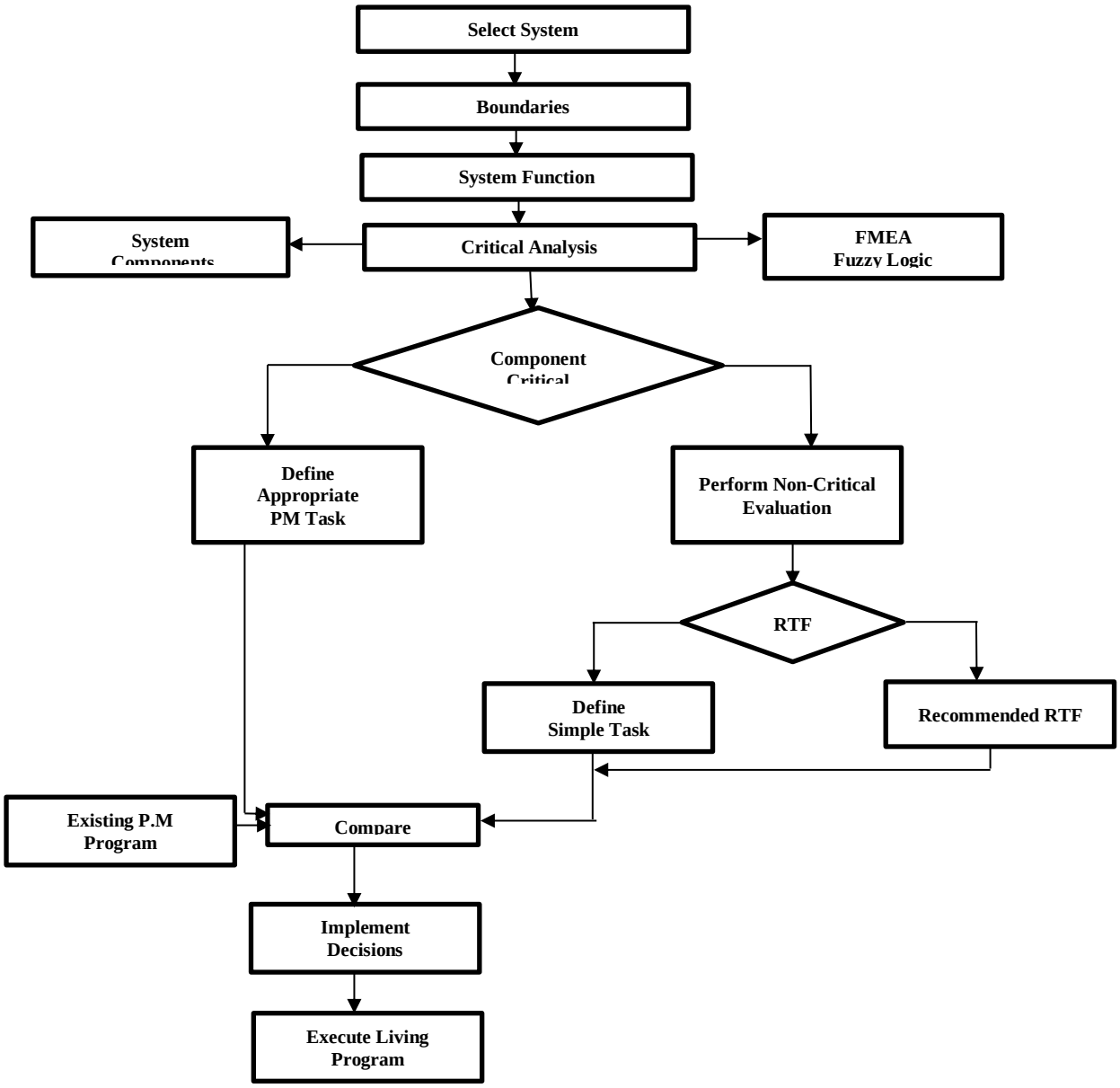

Figure 8 : RCM process diagram with fuzzy logic approach.

RCM IMPLEMENTATION USING FUZZY LOGIC

The proposed method is applied to geothermal steam turbine system. Geothermal steam turbine is an equipment to convert steam mechanical energy into power electricity. Geothermal steam turbine system composes of much complex equipment, therefore in this paper the boundary of discussion just talked about steam turbine and auxiliaries system, governing steam valve and lubrication oil system. After identifying each equipment root causes, FMEA fuzzy logic is applied due to determining equipment criticality as shown in Table 6.

Table 6 : FMEA fuzzy logic on geothermal steam turbine

No	Part	Failure Mode	S	O	D	RPN fuzzy	Indication
1	Moving blade	Blade erosion	6	4	6	391.4697	High (H)
2	Turning Gear	Gear can't latch with rotor	6	4	6	391.4697	High (H)
3	Rupture Disc	Relief diaphragm broken	6	4	6	391.4697	High (H)
4	Inner ring rotor	Material damage	6	4	5	389.3556	High (H)
5	Main Control Valve	Distortion	8	3	3	315.4406	Moderate (M)
6	Main Stop Valve	Distortion	8	2	3	307.1271	Moderate (M)
7	Turbine rotor	Mechanical damage to journal bearing and rotor	6	4	3	307.1271	Moderate (M)
8	Stationary Blade Ring	Crack on stationary blade ring	7	1	7	302.0877	Moderate (M)
9	Hold Stationary Blade	Crack at groove	7	1	7	302.0877	Moderate (M)
10	Coupling rotor	Misalignment	7	1	6	295.4384	Moderate (M)
11	Journal Bearing	Internal misalignment	5	3	6	295.4384	Moderate (M)
12	Thrust Bearing	Worn out	5	3	6	295.4384	Moderate (M)
13	Gland Steam	Control valve malfunction	5	3	4	220.4232	Low (L)
14	Pump (Main Oil Pump)	Leakage inside Main Oil Tank	5	3	4	220.4232	Low (L)
15	Gland Packing	Gland packing scratch	3	4	4	216.4706	Low (L)
16	Control Valve Gland Steam	Control valve malfunction	4	3	4	206.4572	Low (L)
17	Motor (Main Oil Pump)	Shaft misalignment	4	3	4	206.4572	Low (L)
18	Lube Oil Filter	Lube Oil Filter blocked	4	3	3	206.4532	Low (L)
19	Pump (Jacking Oil Pump)	Axial piston broken	4	3	3	206.4532	Low (L)
20	Lube Oil Cooler	Cooler tube leakage	4	3	3	206.4532	Low (L)
21	Steam Strainer	Strainer blocked by foreign object damage	4	3	3	206.4532	Low (L)
22	Pump (Auxiliary Oil Pump)	Shaft misalignment	4	2	4	206.4532	Low (L)
23	Casing	Seal package leakage	2	4	3	206.2122	Low (L)
24	Motor (Auxiliary Oil Pump)	Motor failure due to connection trouble	4	2	3	203.3434	Low (L)
25	Motor Jacking Oil Pump	Motor Malfunction	3	3	4	143.9447	Very Low (VL)
26	Pump on Emergency Oil Pump	Coupling misalignment	3	2	4	138.3511	Very Low (VL)
27	Motor Emergency Oil Pump	Bearing failure	2	3	4	133.7383	Very Low (VL)

The maintenance strategy is implemented after critical analysis is known. Task list of every equipment is based on the fuzzy RPN risk value indicator. If the RPN value is low or below low, then the component would be registered as non-critical component and if the RPN value is moderate to very high then the component would be registered as critical equipment. P-F interval is used to determine the exact time to do the preventive maintenance before failure occurring, known as Predictive Maintenance. Mean Time to Failure (MTTF) would be get by using predictive maintenance, otherwise they're using time based maintenance or preventive

maintenance. For non-critical equipment simple decision making is performed by experts, in order to get whether a simple task procedure or run to failure procedure. The maintenance strategy is shown in Table 7.

Table 7 : Maintenance strategy on geothermal steam turbine system based on FMEA fuzzy logic.

Rank	Part	Failure Mode	Indication	Maintenance Strategy	Task List	MTTF	Interval Task List (times/once)
1	Moving blade	Blade erosion	High (H)	Predictive Maintenance	Vibration trending	4 years	1 days
					Vibration monitoring		3 months
					Vibration Analysis		3 months
					Major Overhaul		4 years
					Precision Inspection		12 years
2	Turning Gear	Gear can't latch with rotor	High (H)	Preventive Maintenance	Inspection *turning gear*	-	2 years
					Function test turning gear		4 years
					Precision Inspection		12 years
3	Rupture Disc	Relief diaphragm broken	High (H)	Preventive Maintenance	Minor Overhaul and Replacement	4 years	4 years
					Major Overhaul		12 years
4	Inner ring rotor	Material damage	High (H)	Preventive Maintenance	Visual inspection for damage, deformation, looseness ,burrs	-	4 years
					Cleaning inner wall		4 years
5	Main Control Valve	Distortion	Moderate (M)	Preventive Maintenance	Visual Inspection	-	1 days
					Movement check stroke test		2 years
					Inspection and cleaning		1 weeks
6	Main Stop Valve	Distortion	Moderate (M)	Preventive Maintenance	Visual Inspection	-	1 days
					Movement check stroke test		2 years
					Inspection and cleaning		1 weeks

Rank	Part	Failure Mode	Indication	Maintenance Strategy	Task List	MTTF	Interval Task List (times/once)
7	Turbine rotor	Mechanical damage to journal bearing and rotor	Moderate (M)	Predictive Maintenance	Vibration trending	4 years	1 days
					Vibration Analysis		1 months
					Vibration Monitoring		1 weeks
					Lubrication Analysis		1 weeks
					Major overhaul, bearing inspection ,check bearing vibration, oil lubricating		4 years
					Inspection and cleaning		1 weeks
8	Stationery Blade Ring	Crack on stationery blade ring	Moderate (M)	Preventive Maintenance	Inspection and cleaning	-	1 weeks
9	Hold Stationary Blade	Crack at groove	Moderate (M)	Preventive Maintenance	NDT Test (Dye Penetrant) on the groove at stationary blade holder	-	4 years
					Visual Inspection		1 weeks
10	Coupling rotor	Misalignment	Moderate (M)	Preventive Maintenance	Check *alignment*	-	4 years
					Visual Inspection		1 weeks
11	Journal Bearing	Internal misalignment	Moderate (M)	Predictive Maintenance	Precision Inspection	4 years	12 years
					Oil Analysis		3 weeks
					Vibration trending		1 weeks
					Vibration Monitoring		3 months
					Vibration Analysis		3 months
12	Thrust Bearing	Worn out	Moderate (M)	Predictive Maintenance	Precision Inspection	4 years	12 years
					Oil Analysis		3 months
					Monitoring temperature thrust bearing and recorded data		1 weeks

Rank	Part	Failure Mode	Indication	Maintenance Strategy	Task List	MTTF	Interval Task List (times/once)
13	Gland Steam	Control valve malfunction	Low (L)	Simple Task	Check Vibration	-	1 weeks
					Visual Inspection		1 days
					Check shaft alignment		4 years
14	Pump Main Oil Pump	Leakage inside Main Oil Tank	Low (L)	Simple Task	Major Inspection	-	4 years
					Visual Inspection		1 weeks
15	Gland Packing	Gland packing scratch	Low (L)	Simple Task	Visual Inspection		1 days
					(major overhaul) Inspection gland & *labyrinth fin* packing	-	4 years
					Precision Inspection		12 years
16	Control Valve for Gland Steam	Control valve malfunction	Low (L)	Simple Task	Visual Inspection	-	1 days
					movement check stroke test		2 years
					Replace diaphragm		4 years
					Major Overhaul		4 years
17	Motor Main Oil Pump	Shaft misalignment	Low (L)	Simple Task	Replace bearing	-	4 years
					Check Vibration		1 months
18	Lube Oil Filter	Lube Oil Filter blocked	Low (L)	Simple Task	Visual Inspection	-	3 months
					Cleaning		4 years
					Major Overhaul		10 years
19	Pump Jacking Oil Pump	Axial piston broken	Low (L)	Simple Task	Monitoring discharge pressure	-	2 years
					Monitoring Oil Flow		2 years
					Inspection		4 years
					Precision Inspection		12 years
20	Lube Oil Cooler	Cooler tube leakage	Low (L)	Simple Task	Visual Inspection	-	1 weeks
					Cleaning		2 years
					Major Overhaul		4 years
21	Steam Strainer	Strainer blocked by foreign object damage	Low (L)	Simple Task	Visual inspection & Cleaning	-	1 weeks

Rank	Part	Failure Mode	Indication	Maintenance Strategy	Task List	MTTF	Interval Task List (times/once)
22	Pump Auxiliary Oil Pump	Shaft misalignment	Low (L)	Simple Task	Check Vibration	-	1 weeks
					Visual Inspection		1 days
					Check Shaft alignment		4 years
23	Casing	Seal package leakage	Low (L)	Simple Task	(Major Inspection) Inspection and cleaning casing split surface.	-	4 years
					Visual inspection		1 days
					Precision inspection		12 years
24	Motor Auxiliary Oil Pump	Motor failure due to connection trouble	Low (L)	Simple Task	Function test	-	3 months
					Inspection		2 years
25	Motor Jacking Oil Pump	Motor Malfunction	Very Low (VL)	Simple Task	Monitoring temperature winding	-	2 years
					Inspection		4 years
					Precision Inspection		10-12 years
26	Pump Emergency Oil Pump	Coupling misalignment	Very Low (VL)	Simple Task	Vibration analysis	-	3 months
					Visual Inspection		2 years
27	Motor Emergency Oil Pump	Bearing failure	Very Low (VL)	Simple Task	Function test		3 months
					Inspection		2 years

CONCLUSION

A fuzzy logic model has been applied to geothermal steam turbine system to determine the criticality of every component in steam turbine system. Based on the value RPN and RPN indication, it is easier to determine the appropriate task of the equipment. Furthermore, the application of fuzzy logic could be used to improve the quality of the results and be applied in the complex system, in order to reduce uncertainty.

REFERENCES

Zadeh. L. (1975). The concept of a linguistic variable and its application to approximate reasoning . Inform.Sci.

DiPippo, R. (2008). Geothermal Power Plants. ElSevier.

Feili, H. R. (2013). Risk analysis of geothermal power plants using Failure Modes and Effect Analysis (FMEA) technique. Energy Conversion and Management, 69-76.

H, M. E. (1974). Application of fuzzy logic algorithms for control of a symple dynamic plant. IEEE, 1585-88.

Zadeh A. L (1992). The calculus of fuzzy if/then rules. Al Expert.

M Giardina, F. C. (2014). Risk assessment of component failure modes and human errors using a new FMECA approach: application in the safety analysis of HRD brachytherapy. Journal of Radiological Protection (pp. 891-911). IOP Publishing.

M Rafie F, S. N. (2015). Uncertainty determination in rock mass classification when using FRMR Software. International Journal of Mining Science and Technology, 655-663.

Moubrey, J. (1992). Reliability Centered Maintenance. (New York:Industrial Press).

Mychael R. Beauregard, R. J. (1996). The Basics of FMEA,2nd Edition.

Pertamina. (2017). RCM Application on Lahendong Geothermal Power Plants. Pertamina.

Ratnayake, R. C. (2017). Development of Risk Matrix and Extending Risk-based Maintenance Analysis with Fuzzy Logic. 7th International Conference on Engineering,Project, and Production Management (pp. 602-610). ElSevier.

Sharma, R. K. (2005). Systematic failure mode effect analysis (FMEA) using fuzzy linguistic modelling.

International Journal of Quality & Reliability Management , 986-1004.

Tay KM, L. C. (2008). On the use of fuzzy inference techniques om assessment models: part II: industrial applications. Fuz Opti and Dec Mak, 283-302.

Yang Lifei, J. (2010). The Development of SRCM and The Applicatio at Home and Abroad. Proceedings of the 18th International Conference of Nuclear Engineering (pp. 1-6). ICONE18.

MATLAB R2015B

THE DEVELOPMENT OF DISABILITY EMPOWERMENT CAPACITIES IN GEOTHERMAL COMMUNITY THROUGH THE INTEGRATED COMMUNITY DEVELOPMENT (ICD) PATTERN: A PORTRAIT OF DESA CAANG PROGRAM IN DARAJAT, GARUT DISTRICT, WEST JAVA

Heri Mohamad Tohari and M. Panji Pranadikusumah

The Creative Institute and Star Energy Geothermal Darajat II, Ltd.

e-mail: herimohamadt@yahoo.co.id; panji@starenergy.co.id

ABSTRACT

Social investment is a valuable asset in supporting the growth and development of geothermal companies. One of investment that is sometimes forgotten is the empowerment of disability person. In accordance with Undang-Undang RI No. 8 in 2016 about persons with disabilities, the constitution requires any company to provide reasonable empowerment for individuals with disabilities. A reasonable empowerment is any change in the surrounding operation area that enables a person with a disability to enjoy equal opportunities within community.

Desa Caang Program attempts to address this issue by empowering disable person on the program. The program is to support the existence of Persons with Disabilities in the form of their potentials.

Object of analysis of this paper is at Nurul Falah Group, a small group of the community led by a female activist named Ottoh who have visual impairment, which specifically she bears blindness. As Desa Caang program is address her as a beneficiaries, it is also actively involving her on the community development program as well. A key goal of the program on this sector is to build inclusive communities, to ensure people with disability have the same opportunity to participate in all aspects of community life. The Program was developed to progress an approach within Disability Services where the community is the primary focus for change and development.

This paper contains of tribute, advancement, protection, and fulfillment of the rights of People with Disabilities to develop and empower all their abilities based on their interests and talents. Therefore, they can enjoy, participate and contribute optimally, securely, freely and in dignity in all life aspects around the area of geothermal mines in Darajat, Garut. This paper uses narrative-qualitative method.

Keywords: empowerment, Desa Caang, geothermal

INTRODUCTION

The discussion of Persons with Disabilities is interesting to be discussed. The existence of them must be reviewed in vision of humanity and Indonesian. In the context of humanity, everyone agrees that Persons with Disabilities are parts of mankind who have the right to live, to have education, to have religion, to be in culture and to be free from stigma. Almost in any religion and culture, there is always a calling to the concept of similarity for Persons with disabilities as an evidence of their vision of humanity.

Giving opportunities and providing accesses to Persons with Disabilities to express their potentials in all aspects of country and society implementation is a necessity. After all, Persons with Disabilities are citizens whose right and duties are recognized. The recognition of Persons with Disabilities is carefully guaranteed by the state. The state must exist to protect and recognize the existence of them.

Undang-undang number 8 in 2016 provides the limitations of meaning; Persons with Disabilities are those who have physical, intellectual, mental, and/or sensory limitation in a long time, which is, in interacting with their environment, they face some obstacles and they also experience the difficulty to fully and effectively participate with other citizens based on the similarity of right.

Referring to statistic data taken by WHO, it is obtained that 15% of people in earth have disabilities, and 80% from the amount are estimated to be in poor conditions. In the context of Indonesian, according to the data of Susenas in 2012, Persons with Disabilities are 2.45%.

West Java has the highest number of Persons with Disabilities in Indonesia, which is 152,294 persons with disabilities (Data Surveyor Indonesia, 2007). With the number, program of Persons with Disabilities empowerment must be the priority of the development of West Java. As so with Garut District, the number of Persons with Disabilities is very eye-popping. Considering the results of survey conducted in working area of geothermal production Darajat Garut, which consists of about 35 villages, at least there are 483 Persons with Disabilities around the operation area of Star Energy Darajat II.

The programs of social investment in the production working area are valuable assets to support the growth and development rate of the geothermal company. One of the programs, which are sometimes forgotten, is the empowerment of Persons with Disabilities around the company area. So, it is important to create an idea about the empowerment of Persons with Disabilities around the working area of geothermal production. One of them is the empowerment conducted in Darajat, Garut District West Java.

Desa Caang attempts to answer these issues through the vision of disability empowerment. The vision is to strengthen the presence of Person of Disabilities in form of climate growth and potential development so they could grow and develop as an individual or group of Persons

with Disabilities who are tough and independent in Darajat. The enhancement of the empowerment capacity of Persons with Disabilities uses Integrated Community Development (ICD) pattern.

This initiation of integrated pattern in ICD is very reasonable. Considering the issues of Persons with Disabilities in their environment are not merely issues about stigma and recognition of them, more than that, this program is designed to answer the whole root of the problems around the environment of Persons with Disabilities. It turned out to be true, UU no. 8 in 2016 states that the rights of Persons with Disabilities that must be fought for are not only the right to live and be free from negative stigma. Article 5 in *Undang-undang* mandates the necessity of the integration of the fulfillment of Persons with Disabilities in terms: privacy; equity and legal protection; education; occupation, entrepreneurship and cooperation; health; politics; religion; sport; culture and tourism; social welfare; accessibility; public services; protection from harms; habilitation and rehabilitation; concession; data collection; live independently and be involved in society; expressing; communicating and receiving information; move places and citizenship; and free from discrimination, neglect, torture and exploitation. The issues on Persons with Disabilities rights are so complex as mandated by *Undang-undang*, so the program of Persons with Disabilities empowerment through Integrated Community Development or ICD pattern is the right step.

Argumentations that support to take the pattern of empowerment ICD is also supported by field facts that the issues in Darajat society are so complex and not rely only on one sector. The result of research conducted by LPPM STAIPI and The Creative Institute in 2014 in Darajat, from the total 5,793 respondents, shows that 43.3% of the people are illiterate. The issue of poverty becomes an acute problem that ruins the dynamics of their life. A survey conducted by Chevron Geothermal Indonesia Ltd. Along with The Creative Institute describes how strong the poverty in that area. One of them is the number of electrification that is very low; there are 9,995 out of 41,239 families have not electrical facilities. This is so ironic; they have no electrical facilities within the area of power sources. As so with the issues of health, sanitation, low rate of school participation, malnutrition, disabilities, etc. become cycle chain that supports each other.

The object of the study of this paper is Nurul Falah Group that is led by women with disability named Ibu Totoh. She is a woman with disabilities who cannot see and live by herself in her house. This woman figure previously has no electricity in her house even though her students who come to her house need some lighting. Likewise, before the program of Desa Caang comes to her house, Ma Otoh does not have economic independence.

This figure is empowered by Desa Caang Program by giving free KWH for the people (Caang Listrikna/bright electricity), the involvement of this woman figure in economic empowerment (Caang Pesakna/ Bright Pocket), and education empowerment pattern by formulating the model of learning MASAGI or *Maca Sakali Ngarti* (understand by only reading once) (Caang Otakna/Bright Brain). The program of Desa Caang integrates the whole potential within the society by developing program in the field of disabilities, energy, economy, education, religiosity, health and environment empowerment.

WHY MUST DISABILITY EMPOWERMENT

Persons with Disabilities generally are in poor condition almost in every order of community life. They are not only poor economically, but also comparatively poor in many aspects such as access to health facilities, education, employment and community inclusivity. Moreover, Persons with Disabilities often time face stigma that restrict their voices to have decent and just life around the community or even in their own families.

For a long time, this condition is rarely reached by the sector of plan and development effort of community. This would be contributed to the increasing number of Persons with Disabilities who are in poverty line significantly. We would never be succeeding in decreasing injustice and creating inclusive community if we ignore Persons with Disabilities in the practice of community development. This is caused by there are so many practitioners of community development who see Persons with Disabilities only as objects of charity or philanthropy.

It is important to draw the issue of disability to the activities of community development as a part of social issues and global attention. Long before, Goldenson (1978) through his work entitled "*Dissability and Rehabilitation handbook*" explains the issues that are often time faced by people with disabilities especially those with blindness; inferiority and live in poverty or prone to social-economic conditions. The failure to involve people with disabilities in community development sector, can only cause people with disabilities to continue their life in poverty line.

We pay attention to the issues of people of disabilities who are generally marginalized and receive discrimination acts. In the operation area of Star Energy Geothermal Darajat II at leats there are 483 persons with disabilities who have not become a common concern. Company realizes that the involvement of persons with disabilities in the activities of community development needs to be implemented carefully. Referring to a statement of Goldenson about general issues that are faced by persons with disabilities that are feeling of inferiority and economic downturn, it can be defined that persons with disabilities tend to be more sensitive in social interaction. Based on those, the method to be chosen must be conducted in a manner that would not give negative impact emotionally and can be accepted by persons with disabilities.

MEANING AND PHILOSOPHY OF DESA CAANG

"Caang" is Sundanese language. It means "bright". Bright means clear or shining. The antonym of bright is dark. Dark means no light, dim, not bright. Through the program of Desa Caang, it is expected to be a speck of enlightenment in building community that is bright in all its dimensions of life.

Desa Caang was officially planned in 2015 through the synergy of Chevron Geothermal Indonesia Ltd., Pertamina Geothermal Energy, PLN, ESDM, Local Government, Central Government and The Creative Institute. As the company acquired, which is previously

by Chevron, now the program is under the control of Star Energy Geothermal Darajat II.

In its first year, the program of Desa Caang was driven to build an integrated system to be an independent village. Through the effort to increase the ratio of electrification an also by considering integrated pattern and to enlarge multiplier effect on other development such as in the field of economic an education, the jargon of Desa Caang Philosophy in the first year at least is described in its three fields of concern (Figure 1), that are:

1. Caang Listrikna (Bright Electricity), means bright lamp or light. The target community is expected to achieve "cerah energi" or independence towards energy.
2. *Caang Pesakna* (Bright Pocket), means bright financially. The target community is expected to be "economically bright" or have qualified economic independence.
3. *Caang Otakna* (Bright Brain), means smart thinking. The target community is expected to have "bright education" or educational independence.

Afterwards, in the second year there was an expansion of community development in the sector of health and environment. Thus, Caang Warugana program that means bright body and Caang Alamna or bright nature were created.

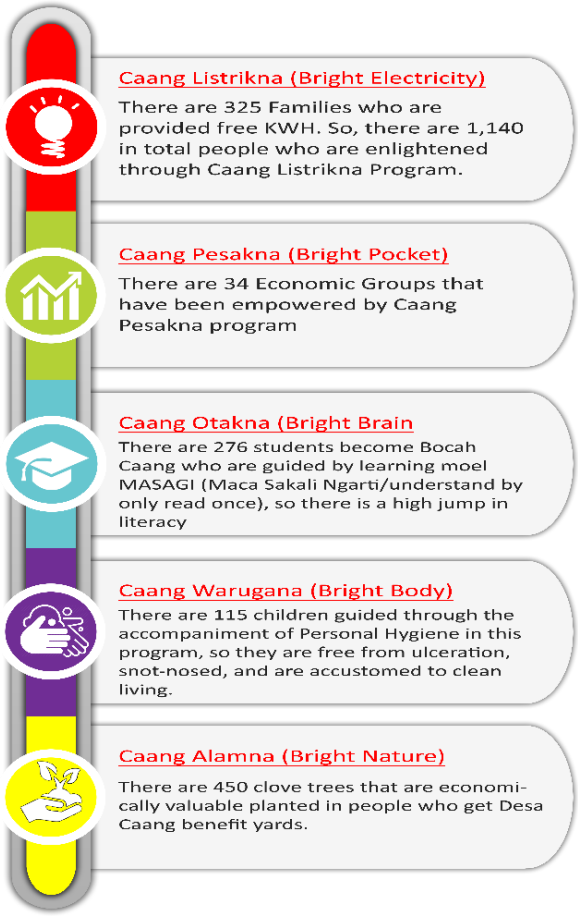

Figure 1: The achievements of Desa Caang program until 2017

Besides, Desa Caang as an integrated community development program, attempts to do a focused approach to involve people with disabilities in community development program. Since some of beneficiaries are having disabilities, they are given knowledge and life skills to be independent in all fields.

EMPOWERMENT OF PERSONS WITH DISABILITIES SKETCH IN DESA CAANG

Mekarjaya village sub-district of Sukaresmi Garut West Java has aportrait of persons with disabilities. One of the beneficiaries of Desa Caang program in the village is Mak Otoh, a woman with blindness, caused by error handling in medical action when she was 3 years old. Until now, he has been actively teaching Al-Quran to at least 70 students in Panagan village RT 04 RW 03.

Through the program of Desa Caang, Mak Otoh is encouraged to be a figure of change for people. Program interventions that have been performed are as follows:

1. Electrical installation. This is meant to help the process of teaching performed by Mak Otoh towards her students goes effectively. Mak Otoh actually does not need electrical enlightenment because of her disability, but her students need that. Before the existence of this program, they learn religious things using *dammar* (light produced by kerosene).
2. The support of economic empowerment program. Before the existence of this program, Mak Otoh has no economic independence. She lives from the mercy of her students who always bring their crops. Now, after the program exists, Mak Otoh has economic independence; she has a small stall that consists of typical child snacks. It is because the segmentation of the buyer is children who are her students.
3. The arrangement of stall managerial scheme and Mak Otoh life. Santri or students that are considered to be mature take turns shops the needs for stall periodically. As for who attend the stall is Mak Otoh every night, because she lives by herself. Some of them help to keep he stall and help her daily life. All schedules ensure that Mak Otoh has the access to social facilities. The effort also includes ensuring Mak Otoh economic empowerment program can continue.
4. Creating integrated education curriculum. Most of Mak Otoh Students live in the illiteracy environment. There are many students there who do not have good reading abilities compared to students in their ages in other places. With this condition, there comes up learning model MASAGI or the abbreviation of "*Maca sakali ngarti*" or understand by only read once. This model of learning has succeeded to make a leap of ability in literacy of Latin script. MASAGI is initiated by young lecturers from several colleges in Garut District. MASAGI curriculum is delivered in 12 stages of program: Gymnastic Literacy, Snake-ladder Literacy, Puppets Literacy, Singing Literacy, etc. the success story of this learning model MASAGI has been several times aired on national private television in Indonesia.

Other educational curriculum is integrating education with children health. Education through the figure of Mak Otoh has succeeded to do health accompaniment to children. So, children are free from diseases like: ulceration, runny-nose, and are accustomed to healthy living. All of these

educational programs are delivered with a relaxed and measurable approach. The children are trusted to cultivate their characters according to their interests, talents and abilities. In the end, as time goes by, children will grow and develop and directed to be the subject of community changes. The portrait of the activity is shown in Figure 2.

Figure 2: The portrait of the activity

At a glance, this empowerment seems to be usual. However, it needs to be analyzed that this empowerment views a Person with Disability as a subject of change. As for other empowerments views a Person with Disability as an object of empowerment. Treatment of this empowerment is done by encouraging Persons with Disabilities to play a maximum role beyond all of their physical limitedness. This is what occurs in Mak Otoh figure.

Mak Otoh is an inspirational woman figure. The figure of Mak Otoh has exceeded everything and covered all of her weaknesses. She even becomes inspiration to other Persons with Disabilities who are empowered by this program. For instance, she becomes inspiration for Mak Enit who has child with disability. Then, Mak Enit's child is directed to have future goals to be someone like Mak Otoh. Mak Enit and Mak Otoh are beneficiaries of Desa Caang.

People after-empowerment view Mak Otoh as a public figure. So that it is easy for her to inspire people and people with disabilities. This is done through the involvement of Mak Otoh in public events. The examples of the events are event of Bocah Caang, praying in community official event, *syukuran*, etc. This disability empowerment has brought Mak Otoh to be new public figure in the community. Mak Otoh is so confident in living her daily life. This program of empowerment has succeeded in arranging Mak Otoh's daily agenda, assistances from her students to accompany her when she is on trip, and has also brought her to have economic independence.

In this case, Desa Caang does not position Mak Otoh as an object of the program, but as a part of the program. This is done by positioning Mak Otoh as an agent of change in people paradigm toward people with disabilities. So, Mak Otoh is expected to inspire people with disabilities around to be actively involved in community's life.

CONCLUSION AND PROGRESS

This paper seems to be important to understand social limits and life experience faced by people with disabilities. This is meant for us to manifest inclusive community for all without exception. The role of Mak Otoh as a main pillar of the quality improvement of education for the community plays an important role in Mekar Jaya village. In the context, Mak Otoh can be said as an agent of change manifestation who becomes a model for general society and especially for people with disabilities.

Plan of further Desa Caang program mapping would start to involve people with disabilities as objects or parts of community development program drives. Thus, with similar pattern done to Mak Otoh, the persons with disabilities who become the objects of empowerment are directed to find their potentials, so later they would be encouraged to be the subjects of change. This is the significance of the program that has directed the persons with disabilities from objects to be subjects. Gradually, they would be involved in community empowerment program. The points of main goals of the involvement of people with disabilities in Desa Caang program are as follows:

1. Promoting equity and fundamental freedom for people with disabilities to be positioned equally in community's life.
2. Changing community's view towards the presence of people with disabilities. This covers discriminative treatments towards people with disabilities around the community.
3. Ensuring people with disabilities to have access to social facilities and services.
4. Creating open and inclusive community with the figure of Person with Disability who act as a subject of change in the community.

REFERENCES

Data Surveyor Indonesia. 2007. *Disabilities in Indonesia.* Jakarta: Surveyor Indonesia.

Goldenson. 1978. *Dissability and Rehabilitation Handbook*.

Heri Mohamad T. 2014. *Potret Tematik Literasi di Kecamatan Sukaresmi*. Kerjasama: LPPM STAI Persatuan Islam Garut, The Creative Institute, dan Pemprov Jawa Barat.

_____. 2015. *Electricity Study*. Chevron Geothermal Indonesia Ltd. dan The Creative Institute.

Kementerian Kesehatan. 2014. *Situasi Penyandang Disabilitas: Refleksi Data Susenas 2012*. Jakarta: Pusdatin.

Tim Penyusun BPS. 2016. *Garut dala Angka tahun 2016*. Garut: BPS Garut.

Undang-Undang No. 8 tahun 2016.

EXPERIMENTAL STUDY OF FIBRE OPTIC PHOTON COUNTING APPLICATION: REAL TIME-FREE CALIBRATION DISTRIBUTED TEMPERATURE MEASUREMENT AND ENTHALPY ESTIMATION FOR GEOTHERMAL WELL

Anggoro Wisaksono

School of Engineering, University of Glasgow

e-mail: a.wisaksono.1@research.gla.ac.uk

ABSTRACT

Temperature, pressure and enthalpy data is very important and valuable, both during geothermal drilling and in well operation. The study will research the possibility of direct downhole measurement of temperature and free calibration, which will result in a real time pressure and enthalpy reporting model. The research will report on the development of a downhole geothermal brine pressure and enthalpy model, applied to the state-space T-p-X delineations and density (ρ) correlations in flowing gas, liquid and two-phase systems, using the H2O–NaCl geothermal brine thermodynamic formulation. The model was implemented in C programming, running in the NI Lab Windows/CVI user interface. The model is highly dependent on the fibre optic temperature sensor system for a direct temperature measurement. The experiment works to extend the range of an existing calibration-free fibre optic temperature sensing technique based on photon counting measurements by Raman backscatter (previously developed in collaboration with the US National Institute of Standards and Technology). The research aim is to extend the range of the system to a kilometre length, by increasing the optical power per pulse and reducing the repetition rate of the excitation laser. For this experiment, the test will employ superconducting single photon detectors with improved efficiency (5%) housed in a practical, closed-cycle cooling system. The experiment managed to demonstrate the temperature measurement and estimate the enthalpy using 2 meter of fibre under test, which represent 2 meter of depth. Meanwhile, the experiment of 100 meter of fibre under test are still under investigation after successfully measured low temperature.

Keywords: geothermal, brine, H2O-NaCl, two-phase, fibre optics sensor, temperature sensing, enthalpy

INTRODUCTION

Temperature data plays an important role in many geothermal downhole procedures, including depth temperature profiles in well logging processes (PT and PTS logging) and real time thermal measurements to monitor the performance of producing wells (Brown, 2009; Blankenship and Finger, 2010). Recent numerous studies have presented analyses of temperature measurement using fibre optics in monitoring temperatures in application to hydrogeology, oil and gas surveys and geothermal energy (Bolognin and Hartog, 2013). Temperature measurement using high-resolution, single-mode fibre optic distributed Raman sensors has been developed in previous research using meter-scales of fibre optic cables. The research intends to extend the range of a calibration-free fibre optic temperature sensing technique based on photon counting measurements of Raman backscatter, developed in collaboration with the US National Institute of Standards and Technology by Tanner et al. (2011) for geothermal applications in downhole temperature measurement. In addition to temperature measurement, this study will also model the real-time known temperature pressure-enthalpy relationship based on directly measured temperature. The potential users typically need confidence that a certain geothermal field is capable to produce sufficient energy at affordable cost. Information on enthalpy conditions within wells and reservoir, equip engineers with better insight into reservoir and well performance.

The ultimate research goal is to obtain temperature data continuously along 1 km fibre optic cable with the obtained temperature readings input to the enthalpy measurement model application. Calibration-free fibre optic temperature sensing techniques based on photon counting measurements of Raman backscatter have been investigated recently (Dyer et al., 2012). Most of the system was constructed from cheap fibre-optic components from the telecommunication industry, with a few less common components including filters and amplifiers. The outputs of the model comprise graphs of depth-temperature, depth-enthalpy and pressure-enthalpy.

Section 2 will explain the theoretical context of the target geothermal fluids. Section 3 will explain the fibre optic distributed Raman temperature sensor and Section 4 will describe the prototype system. The experimental results and discussion are presented in section 5, followed by the conclusions in section 6.

HYDROTHERMAL FLUIDS

The hydrothermal reservoir is assumed to contain H_2O, CO_2, H_2S and NaCl. The flow in the reservoir is assumed to be a one or two phase flow, with fluid mixtures of brines, which might be H_2O with NaCl, KCl or $CaCl_2$ or sulphate waters (H_2O - SO_4) or bicarbonate waters (H_2O – HCO_3). The present phase of the research focusses on H_2O-NaCl geothermal brine, typical of most hydrothermal brines. In the first phase of the experiment, the research will measure single-phase saturated water (H_2O) followed by H_2O-NaCl liquids.

Saturated water (H_2O)

Programming assumes saturated water and vapour according to measurements for known temperatures for the first phase of the experiment. The temperature accords with equation (19) (see section 3).

The basis of the enthalpy measurement programming is the formula standard of The International Association for the Properties of Water and Steam (IAPWS). The programming is valid for properties of saturated water and steam. The study use the following constants; T_{crit}=

647.096 K, p_{crit}= 22064000 Pa, ρ_{crit}= 322 kg/m^3, α_0= 1000 J/kg, ϕ_0= α_0/T_{crit}, θ= T/T_{crit} and τ= 1-θ. The study use linear interpolation of the steam thermodynamic table for model validation.

At given temperature, pressure of saturated liquid (p_w) can be approximated using coefficient values through the following formulae:

$$p_w = p_{crit} e^{\frac{T_{crit}}{T}[a_1\tau + a_2\tau^{1.5} + a_3\tau^3 + a_4\tau^{3.5} + a_5\tau^4 + a_6\tau^{7.5}]} \quad (1)$$

$$\frac{dp_w}{dT} = \left(\frac{-p_w}{T}\right)\left[ln\left(\frac{p_w}{p_{crit}}\right) + b_1 + 1.5b_2\tau^{0.5} + 3b_3\tau^2 + 3.5b_4\tau^{2.5} + 4b_5\tau^3 + 7.5b_6\tau^{6.5}\right] \quad (2)$$

At any given temperature, the specific enthalpy of saturated liquid can be approximated through the following:

$$h_{wliquid} = \alpha + \frac{T}{\rho_{liquid}}\frac{dp}{dT} \quad (3)$$

The specific enthalpy of saturated gas can be solved using the following:

$$h_{wgas} = \alpha + \frac{T}{\rho_{gas}}\frac{dp}{dT} \quad (4)$$

Where α and the density (ρ) using the following:

$$\alpha = \alpha_0[b_0 + b_1\theta^{-19} + b_2\theta + b_3\theta^{4.5} + b_4\theta^5 + b_5\theta^{54.5}] \quad (5)$$

$$\rho_{wliquid} = \rho_{crit}\left[1 + c_1\tau^{\frac{1}{3}} + c_2\tau^{\frac{2}{3}} + c_3\tau^{\frac{5}{3}} + c_4\tau^{\frac{16}{3}} + c_5\tau^{\frac{43}{3}} + c_6\tau^{\frac{110}{3}}\right] \quad (6)$$

$$\rho_{wgas} = \rho_{crit} e^{\left[d_1\tau^{\frac{1}{3}} + d_2\tau^{\frac{2}{3}} + d_3\tau^{\frac{4}{3}} + d_4\tau^3 + d_5\tau^{\frac{37}{6}} + d_6\tau^{\frac{71}{6}}\right]} \quad (7)$$

	0	1	2	3	4	5	6
a		-7.8595178	1.8440826	-11.7866497	22.6807411	-15.9618719	1.80122502
b	-1135.9056277	-0.0000000565134998	2690.66631	127.287297	-135.003439	0.981825814	
c		1.99274064	1.09965342	-0.510839303	-1.75493479	-45.5170352	-674694.45
d		-2.03150240	-2.68302940	-5.38626492	-17.2991605	-44.7586581	-63.9201063

Table 1: Coefficient values for saturated water pressure and enthalpy

	0	1	2	3
m	0	3.57384	-0.00379475	0.00159816
n	2500	2.85416	-0.00799981	0.00000889497

Table 2: Coefficient values for saturated geothermal brine pressure and enthalpy.

The study developed a computer program based on the above formulae in C language. The LabWindows/CVI user interface is used to run the program. The user interface then produced temperature-depth and enthalpy-depth graph, based on the Raman temperature sensor readings.

H20-NaCl brine

After the preceding development for saturated water, the study then proceeded to further develop the model for H20-NaCl brine by extending the saturated model by adding formulations for state-space T-p-X delineations and density (ρ) correlations for flowing gas, liquid and

two-phase systems for geothermal brine, following Palliser and McKibbin (1998). The programming formula are limited to geothermal brine in T ≤ 647.096 K.

The saturated brine pressure (p_{brine}) formula is as follow, where t = (T/374)^2:

$$p_{brine} = e_1 t + e_2 t^2 + e_3 t^3 + e_4 t^4 + e_5 t^5 \quad (8)$$

The saturated static enthalpies for saturated liquid ($h_{liquidSAT}$) and gas (h_{gasSAT}) geothermal brine are:

$$h_{liquidSAT}(T) = f_0 + f_1 T + f_2 T^2 + f_3 T^3 \quad (9)$$
$$h_{gasSAT}(T) = g_0 + g_1 T + g_2 T^2 + g_3 T^3 \quad (10)$$

Meanwhile for two phase flow brine liquid enthalpy (h_{l2p}), for T ≤ 647.096 K

$$h_{l2p} = h_{wliquid} + \left[h_{liquid} - h_{wliquid}\right]\left[\frac{p_w - p_{2p}}{p_w - p_{brine}}\right]^{\frac{1}{1.4}} \quad (11)$$

Two phase flow brine vapour enthalpy (h_{gs}), for T ≤ 647.096 K

$$h_{g2p} = h_{wgas} + \left[h_{gas} - h_{wgas}\right]\left[\frac{p_w - p_{2p}}{p_w - p_{brine}}\right]^{\frac{1}{1.7}} \quad (12)$$

However, the determination of the downhole two-phase pressure (p_{2p}) is needed in two phase systems in order to get the value of enthalpy. Therefore this model took the pressure value samples from the existing two phase systems.

FIBER OPTIC RAMAN DISTRIBUTED SENSOR

The sensors make use of optical time-domain reflectometry, in which measurements typically employ a pulsed source and determine position information from backscattered photons from the tested fibre. The experiment is well justified by the link between Raman backscattering and temperature that has been already demonstrated. The Stokes and anti-Stokes contribution to the total backscattering can be approximated as follows (Dyer et al., 2012).

$$I_u = \eta_u \Delta v_u P_0 L |g_R| N(\Omega_{up}) D_c \quad (13)$$

where I_u is the backscattered photons per second, the subscript u is either S or a for Stokes or anti-Stokes, η_u is the detection efficiency (DE) of the sensors, Δv_u is the bandwidth of the Stokes or anti-Stokes filters, P_0 is the peak pump power [4, 5], L is fibre length, g_R is the Raman gain factor, D_c is the duty cycle of the pump signal, Ω_{up} is the radial frequency detuning between the pump and the mean Stokes or anti-Stokes wavelengths, and N is the phonon population as follows:

$$N = \begin{cases} \frac{1}{exp\left(\frac{\hbar|\Omega_{up}|}{k_B T}\right)-1}, \Omega_{up} < 0 \\ \frac{1}{exp\left(\frac{\hbar|\Omega_{up}|}{k_B T}\right)-1} + 1, \wedge\, \Omega_{up} \geq 0 \end{cases} \quad (14)$$

Detuning Ω_{up} as constant over the filter bandwidths and assuming an equal value in the Stoke and anti-Stokes case, the ratio of Stokes to anti-Stokes is given by:

$$\frac{I_s(x) - B_s}{I_{as}(x) - B_{as}} = \frac{\eta_s \Delta v_s |g_R|}{\eta_{as} \Delta v_{as} |g_R|} e^{\frac{\hbar|\Omega_{sp}|}{k_B T(x)}} \quad (15)$$

Based on equation no. 17, the temperature model developed in this technique is:

$$k_B T(x) = \frac{\hbar|\Omega_{sp}|}{ln\left(\frac{I_s(x)}{C[I_{as}(x)]}\right)} \quad (16)$$

Where $[m]$ is the measured temperature, $\hbar$ is the reduced Planck constant, Ω_{sp} is the radial frequency, is the Boltzmann constant. C is the reference temperature. Should the fibre optic temperature sensor is the initial measurement, then C will be neglected.

SYSTEM DESCRIPTION

The experiment will demonstrate a high resolution single mode fibre optic distributed Raman sensor that was originally developed in 2011 (Tanner et al., 2011; Dyer et al., 2012). The distributed sensor for temperature, followed by geothermal brine T-p-x model used for the experiment is OTDR. According to Tanner, et al. (2011), Raman-based OTDR sensors are already sufficient for some commercial applications, such as monitoring of oil and gas wells, and also the detection of hot spots along the steam pipes of power plants, where a spatial resolution much better than 1m is required. The diagram of the assembled detectors are shown in Figure 1.

Femtosecond fibre laser with a spectrum near 1560 nm is used as source of light. The fibre under test (FUT) is standard low-loss single-mode commercial telecommunications fibre SMF28 by Corning (η = 1.452) with a mode field diameter of 10.4μm and attenuation less than 0.2 dB/km at a wavelength of 1550 nm.

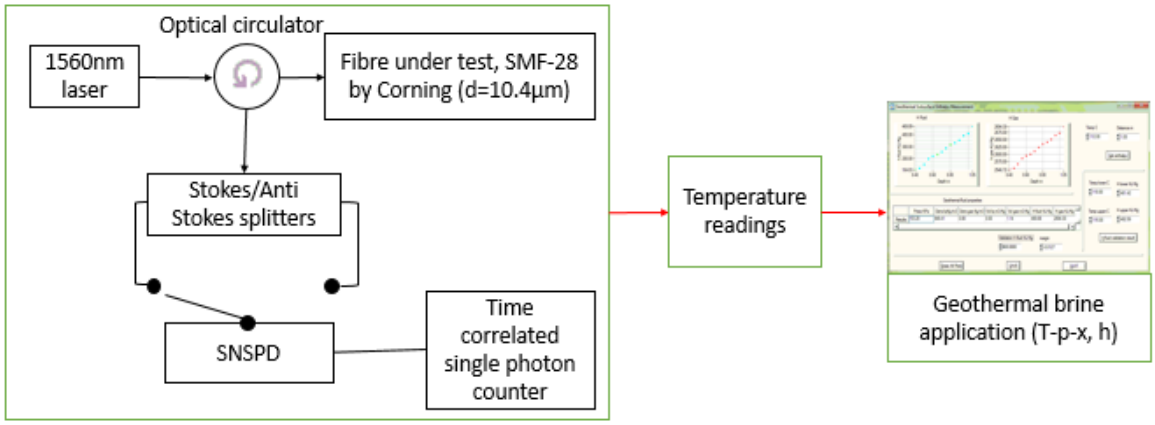

Figure 1: Simplified diagram of free calibration temperature measurement and real time pressure-enthalpy estimation.

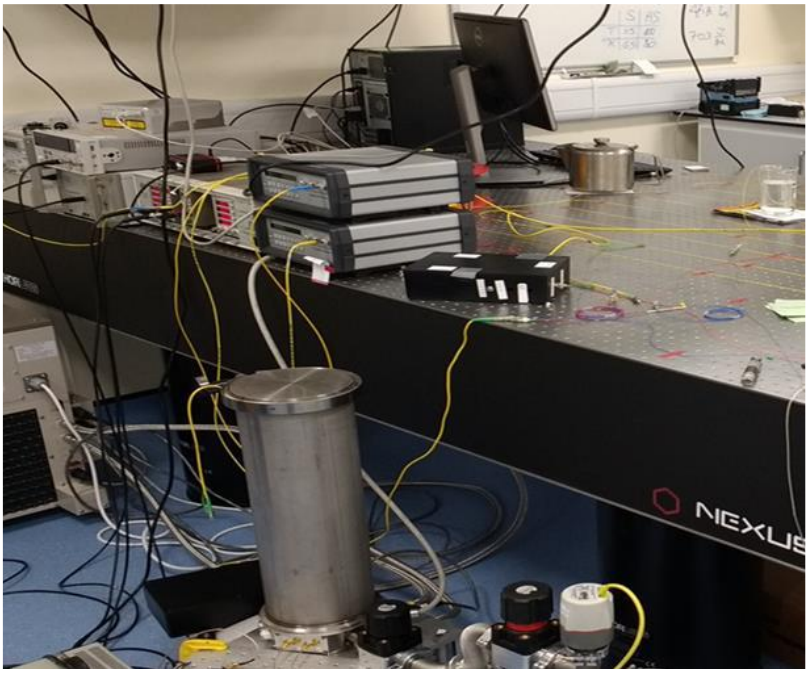

Figure 2: Experiment set up. (1) Laser, (2a) 2m red fibre under test cable, (2b) 100m yellow fibre under test fibre, (3) circulator, (4) Series of splitters, (5) cryogenic refrigerator, with SNSPD temperature sensor inside, (5) Hydraharp, (6) Measured liquid.

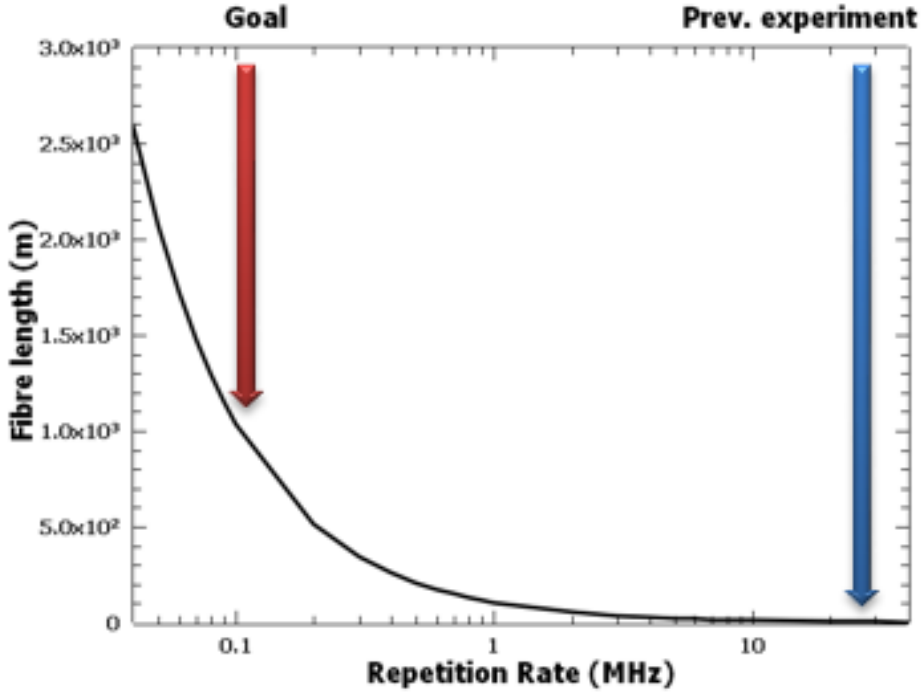

Figure 3: Extension of the fibre as a function of the RR of the pulsed laser source.

The length of the fibre is affected by the repetition rate (RR) of the pump laser that determines the period of time between each pulse. A single laser pulse. is required in order to get position information on the photon detected The time measured between a pulse sent into the fibre, and the scattered photon returning back down the fibre and being detected, gives the position in the fibre that the scattering happened. The greater the time interval between pulses, the more time the pulse can stay in the fibre and the longer the fibre can be. Basically, the repetition rate shall be less than 1 MHz to achieve results yet not seen in literature (Figure 2). Be l the length of the FUT and η its refractive index of the core, be c the speed of the light, the relationship is thus the following (Gold, 1985):

$$l = \frac{c}{RR*2\eta} \tag{20}$$

Pump filters were installed before and after the fibre amplifier and attenuator. Each filter provides 25 dBm rejection of unexpected wavelengths and remove the broadband amplified spontaneous emission from the pump. The light that is backscattered from the FUT is directed by the circulator to a series of filters that have been chosen to reject the pump wavelength. Then S-band and L-band splitters are used, which are 1470 nm and 1666 nm at peak and the maximum shift is at 440 cm^{-1}. Band splitters are to separate and filter the Raman backscattered photons. The pump wavelength reject filters chosen to be approximately equally spaced between the S- and L-bands. Unwanted photons at the pump wavelength would reach the detector without these filters. Superconducting nanowire single-photon detectors (SNSPDs) is the photon detector. They are single-pixel meander with an active area of 15x15 μm^2. SNSPDs work properly below at extra low temperature, therefore the first operation is the installation of the mounted chip inside a cryostat refrigerator. The one used for the following measurements is a Gifford-McMahon cryostat, assembled by the photonic research group at the University of Glasgow, on a Sumitomo SRDK-101D-A11C helium cryogenic cooler. The lowest temperature the cryostat can reach is ~2.4 K. Then, time-interval analyser used to create histograms of the time delays between a laser clock electrical pulse and the electrical pulses created by the detection of photons at the SNSPDs. The temperature readings were then inputted to the geothermal brine model application to get the thermodynamic data for the water and then for the range of geothermal brine mixtures. The initial experiment used only water to check the reliability of the measurement and the model program.

EXPERIMENTAL RESULT

Demonstration for 2 m fibre under test

The study's initial goal is to have the same test profile with the previous research using 1m fibre under test. In this experiment, the study also tried 2 m long fibre. The experiment managed to capture the peak temperature when the fibre under test was put inside a hot water kettle. Figure 7 represents the measured saturated water temperature along 2 m fibre under test. It measured approximately 318 K. The spatial resolution of 1.35 cm

has been recorded. The speed of the measurement in this test was recorded at 3 to 4 minutes.

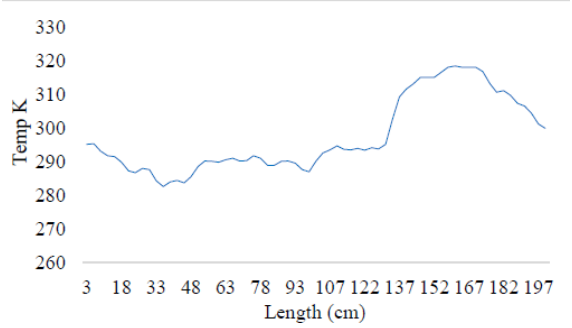

Figure 7: Temperature measurement test using 2 m fibre optic cable.

The process then inputed the data into the geothermal brine model application software, which has been developed using LabWindows/CVI. The results are shown in figure 8 and 9. The model's results have been validated using linear interpolation from value taken from widely used IAPWS thermodynamic table.

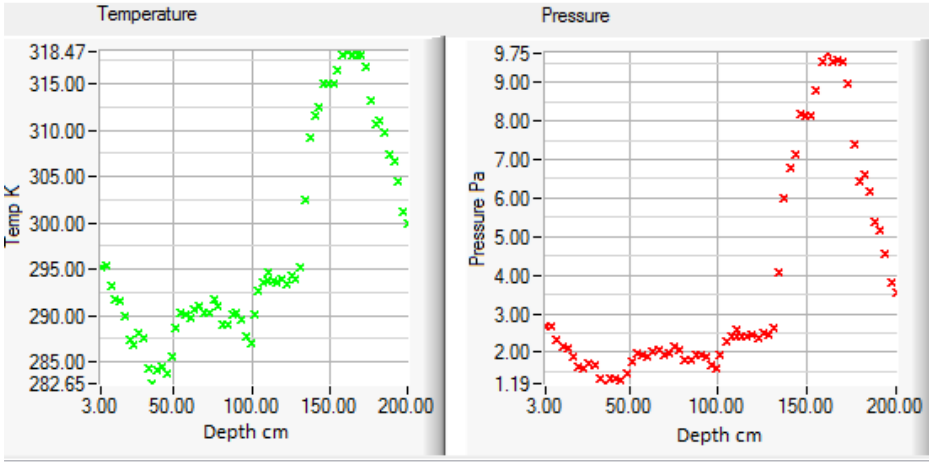

Figure 8: LabWindows/CVI Temperature and pressure data output of measured saturated water temperature along 2m fibre under test.

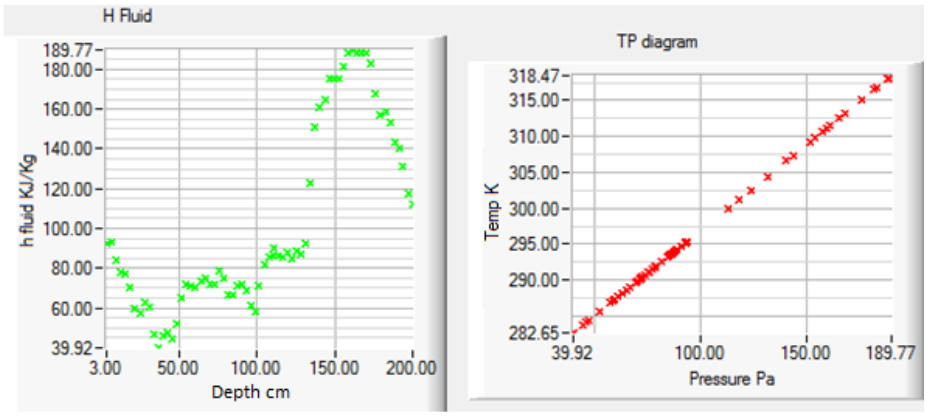

Figure 9: LabWindows/CVI fluid enthalpy data and TP graph output of measured saturated water temperature along 2m fibre under test.

Demonstration for 100 m fibre under test

The second phase of the project is to extend the fibre under test into hundreds of meters. The latest experimental outcomes are shown in figure 10. This time, the 100 m cable reels have been placed inside a freezer. The objective of this test is to check the time resolution of Raman backscattered photon counts when travelling in a longer cable and how the sensor reacts to cold temperature. The outcome is shown in figure 10.

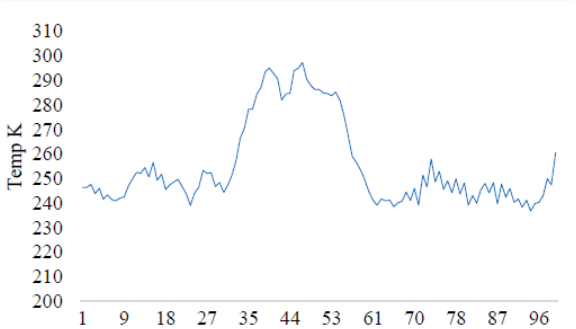

Figure 10: Measured freeze temperature along 100m fibre under test.

The experiment is still ongoing when this report was written, hence no enthalpy and pressure estimation were demonstrated.

CONCLUSION

The initial temperature measurement and enthalpy-pressure estimation of 2 m and 100 m length of fibre optic under test, leading up to use in conjunction with a fibre temperature set up utilising superconductor nanowire single-photon temperature sensor currently under construction at the University of Glasgow. This will allow temperature to be measured over a hundreds of meters and kilometre of fibre, using the Raman backscattered photons.

Although laboratory experiments are still ongoing at the time of writing, initial findings vindicate the hypothesis of the real time pressure and enthalpy reporting model, from direct and free calibration downhole measurement of temperature.

Following laboratory tests using water in saturated conditions and real geothermal brine, the study's future aim is to test the tool in one of the geothermal boreholes in the UK, to test the efficacy of the real-time pressure and enthalpy model, based on temperature sensing results, up to 1 km depth and initially over the temperature interval 270 – 647K.

ACKNOWLEDGEMENT

I would like to express gratitude to fellow researchers in this project Andrea Pizzone, Nathan R. Gemmell, Robert H. Hadfield, Paul L. Younger and James H. Sharp. Financial support by Indonesia Endowment Fund for Education (LPDP) of Ministry of Finance Republic of Indonesia, is highly appreciated and gratefully acknowledged.

REFERENCES

Brown G 2009 *Oil. Rev.* **4** 34

Blankenship D and Finger J 2010 *Handbook of Best Practices for Geothermal Drilling* (Albuquerque: Sandia National Laboratories)

Bolognin G and Hartog A 2013 *Opt. Fib. Tech.* **19** 678

Tanner MG et al. 2011 *App.Phy. Let.* **99** 1

Dyer SD et al.2012 *Opt Exp* **20** 4 3456

Gold MP 1985 *Lig. Tech* **3.1** 39

Palliser C and McKibbin R 1998 *Tran. in Por. Med*. **33** 65

Palliser C and McKibbin R 1998 *Tran. in Por. Med*. **33** 155

Pitzer KS et al 1984 *Phy. and Chem*. **1**

Palliser C and McKibbin R 1998 *Tran. in Por. Med*. **33** 129

SOIL STABILIZATION USING HORIZONTAL DEEP DRAINAGE AT AWI-14 BRINE LINE PIPE AND WELL PAD, STAR ENERGY GEOTHERMAL SALAK FIELD, WEST JAVA, INDONESIA

Adi Gunawan TP[1], Satrio Wicaksono[2]

[1] Star Energy Geothermal Salak, Sukabumi, Indonesia
[2] Star Energy, Sentral Senayan II, 26th Fl, Jakarta, Indonesia

e-mail: adipandiangan@starenergy.com, satriowicaksono@starenergy.com

ABSTRACT

Salak geothermal field has several locally steep slopes that could yield the possibility for large-scale landslides. During heavy rains on 2003, Salak recorded significant landslides that caused major damage and shut down a part of Salak operations for 3 months. Over the period 2010-2012 several new landslides have been identified around the Awi-14 injection location. The landslides have significantly impacted surface facilities including pipeline, road, and well pad, and will have a potential to impact injection strategy within Salak field.

Steep slopes, high rainfall, high porosity, and loosely consolidated near-surface rocks were the main contributing factors to the landslides in the area that will threatening the Awi-14 brine line pipe. During heavy rain, the soil has the tendency to become over-saturated, triggering slope failure that can lead to landslide depending on the nature of the underlying soil.

On 2011, several geotechnical analyses have been applied including shallow drilling for soil investigations, geo-electrical, geological engineering mapping, and geophysics survey. Those applications have helped to identified landslide mechanisms around the pad, quantify the risks at identified critical areas, and provided recommendations for cost effective mitigation measures. High groundwater level at Awi-14 brine line pipe has identified as the main problem, it has decreased the soil strength so one of the solution is to lowering the groundwater level. Design and installation of Horizontal Deep Drainage (HDD) systems were done for lowering the ground water level. This method would prevent occurrence of further landslides and restore the stability and viability of Awi-14 as an injection well in the Salak field.

Keywords: Salak, Awi-14, geothermal, geohazard, landslide 2010, geotechnical analysis, geological engineering, construction

INTRODUCTION

Salak field is located 60 km south of Jakarta in the West Java province, at an elevation between 1,100 - 1,500 meters above sea level (Figure 1). It is one of the world's largest liquid-dominated geothermal fields with a current total capacity of 377 MW. Based on morphology this field located in a high terrain or mountainous area. The highest peaks are inactive andesitic volcanoes of Gunung Salak, Gagak, Perbakti and Endut that lie along the main trend of Sunda Volcanic Arc. Several fault also identified all over Salak area with dominant N-NE and subsidiary NW and E-W trending (James Stimac, et.al, 2007). This geologic circumstance leads the possibility of the area to have several kind of geohazard; one of the examples is landslide which have affected to Salak field assets.

Figure 1. Location map showing Salak and Darajat geothermal field operated by Star Energy

Back to 2003 Salak field experienced series of landslides and debris flows that disrupted the production facilities capability to provide and control resource supply steam to PLN Power Plants Units 1, 2, & 3. The landslide created releases of brine, condensate and steam from pipelines, blocked access roads to well sites and created hazardous conditions to numerous operational locations, causing stopped operation activities for about 3 months (URS Indonesia, 2004). Specific to Awi-14 area, still in the same year 2003, landslides also occurred on the northern area of Awi-14, at that time Salak operation have immediately commenced implementing a remedial works program for the repair of damaged facilities and civil engineering infrastructure to improve pad stability (Sagala,Birean, et.al, 2003).

During period of prolonged intense rainfall in the year of 2010 and 2015, landslide and soil subsidence reoccurred in well pad area Awi-14, this time landslide appeared in the cross country zone between this well pad and Awi-14 and at northern site of well pad, precisely behind sheet pile area. Preliminary observation from resulted that most of landslides in this area considered to be due to a combination of concentrated run off related to erosion effects, together with a partial loss of soil strength (suction) caused by saturation of the soils. Hence detail geological engineering studies and slope stability analysis were needed to assess the most safety, most effective and effective programs to stabilize the area and mitigate further geohazard.

METHODOLOGY

On November 2010, landslide was identified at between brine lines Awi-2 to Awi-14 (Figure 2). There are some cases to geotechnical issue found from preliminary observation such as identified landslide near pipe support where three trees fell down and shifted brine pipe line, other landslide observed along pipeline 40 m, width 24 m and subsidence 3 m depth, other landslide indication also discovered i.e. brine line pipe hanging, pipe support moved and tilted (Gunawan, Adi, et.al, April 2011). The brief recommendation at that time was covered landslide area with tarpaulin/ terram to stop water infiltration on unconsolidated soil surface, protected soil dirt spill to the Cibeureum River and avoided further slope erosion (Salak Operation, 2010 – 2011).

As a long term mitigation program, several geotechnical works were conducted in early 2011 (Figure 3) prior the permanent engineering construction, the geotechnical works focus on the landslide area, in order to collate both surface and subsurface data (shallow), understand the soil characterization analyze rock strength and slope stability to develop representative geotechnical models for typical and critical sections of the slopes (Safety Factor). These models were then used as a basis for construction design.

The geotechnical investigations consist of:

- Fieldwork detail surface geological mapping to map out lithology, structure and landslide risk location (data combined from 2003 and 2011)
- Shallow borehole for soil investigation including, mechanical Cone Penetrometer Tests (CPT), Standard Penetration Tests (SPT)
- Laboratory testing. Soil properties analysis, also includes index properties, shear strength consolidation, and permeability tests.
- Shallow geophysical survey using 2D electrical resistivity and SP survey (Self Potential)

Hereafter on December 2015, subsidence case also happened at northern of Awi-14 well pad behind of sheet pile (Figure 4). Soil subsided 1 to 2 m depth and shifted the sheet pile 2 to 3 m away from well pad.

Figure 2. Fallen tree and pipe movement on Awi-14 brine line pipe

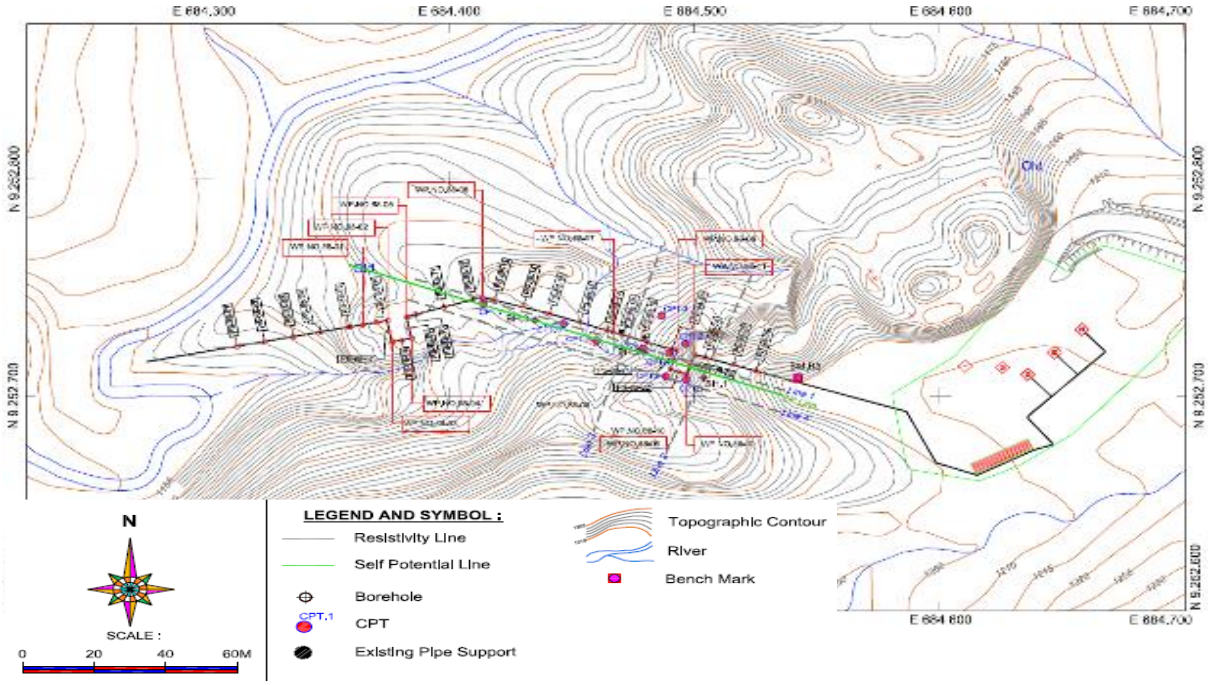

Figure 3. Layout location for CPT point, Borehole SPT,2D Resistivity and SP geophysical survey

Figure 4. Soil subsidence and sheet pile shifting at Awi-14 well pad

Rain gauge monitoring added information about high intensity (52 mm/hour) of rain was observed in Salak field prior the landslide happened (Salak Operation, December 2010). It was strengthen the preliminary interpretation during field study that mechanisms of landslide in Awi-14 were most likely triggered by the significant rise of the groundwater level and therefore by the dramatic changes in the subsurface stream of the groundwaterr (Figure 5 & Figure 6). High groundwater level will have the tendency of over-saturating the soil in the vicinity, triggering a chain of events that could lead to a bigger washout or worse a massive landslide depending on the nature of the underlying soil. Several soil movement indicators were also indicated at landslide area such as minor tension crack, heave, and water springs occurrence.

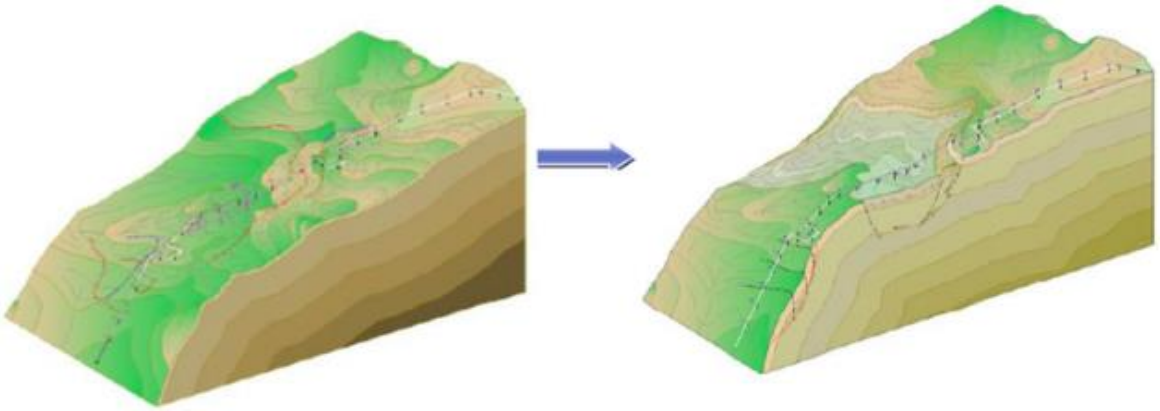

Figure 5. Left picture is original topography and right picture is a translational landslide that occurred acrosss Awi-14 brine line pipe route, wtih slip failure at 10m below ground level (measure from BH-3)

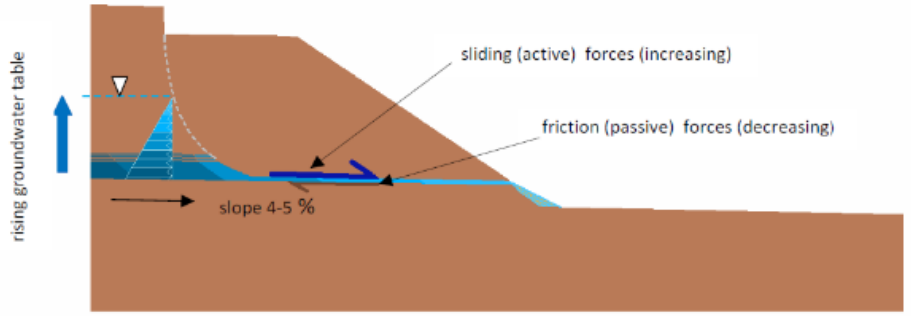

Figure 6. Cross section showing the increasing of active sliding forces, decreasing of passive friction forces, and rising of hydrostatic pressure

INTERPRETATION

Detail Geological Mapping

From several observation spots during the mapping, landslide areas mostly consist of debris (colluviums), Orange Tuff, reworked Tuff and Lahar (Figure 7). These deposits mostly comprise weathered, with very low – low strength rock materials, and the Tuffaceous deposits are more typically fine-medium grained soils in accordance with standard engineering classifications.

Top soil has characteristics as soft, blackish brown, and root fragment. While the light brown, Orangeish to grayish brown Lahar, is the oldest geological unit encountered at the site, consists of Andesite, Dacitic and Tuff sub-angular to sub-rounded fragments up to cobbles to boulder size. The unit is commonly poorly consolidated, and occurs as silty gravel and boulder soil. Lahar layer is overlain by light brown, cream, brown and Orangeish reworked Tuff or transported Tuff characterized by firm to stiff or medium dense soil. This unit shows laminated and graded bedding structure.

Special explanation for Orange Tuff (Figure 8) unit, which blanketed most of the site area (generally less than 3m in thickness), occurs as medium plasticity clay soil. Some thin intercalations of Silty Tuff frequently also occur within this unit. Hydrothermal processes have altered the Tuffaceous soils into light grey to blue grey, high plasticity, soft to firm clay which is an expansive or reactive soil due to the presence of montmorillonite (smectite) minerals, in other words Orange Tuff material usually stables in undisturbed condition but it becomes very sensitive to the water in disturbed condition. It also found that the landslide failure plane often coincides with the hydrothermally altered clay layer which occurs at the base of the Tuffaceous soil deposits.

As additional information to this study regarding alteration zone, there are most active thermal complex in Salak (Kawah Cibeureum) located on the north area of Awi-14 pad with distance of about 500m – 700m; and based on Salak geological map 2007, Cibeureum fault was confirmed existed at the side of Awi-14, with N-S fault trend, and passing Cibeureum mud pool area (Stimac, et.al, 2007).

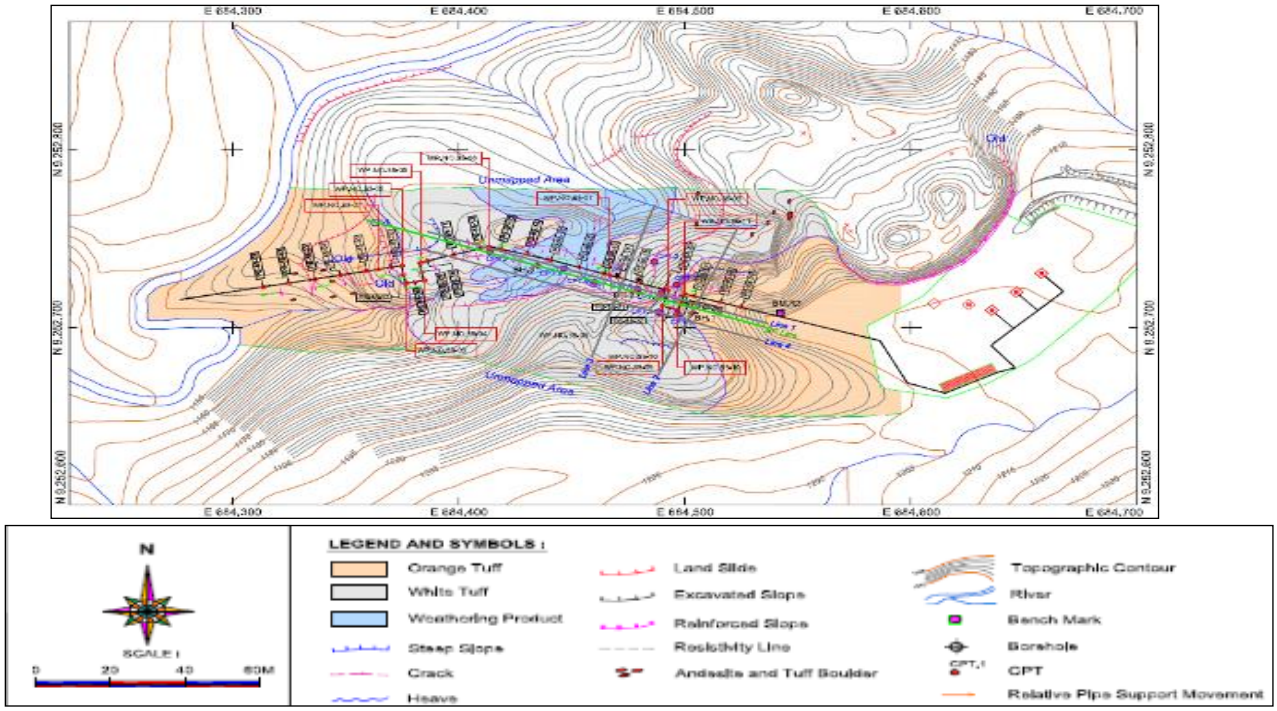

Figure 7. Geological Engineering Map at Landslide Area showing dominantly Orange Tuff at Awi-14

The typical of Tuff stratification in Salak area is following the original topography with various thickness, color and grain size. While some thin paleosoil is usually found between Tuff layers with various thicknesses.

Figure 8. Orange tuff in core box

Soil Investigation

In order to gain direct information about the soil character beneath surface, then geotechnical soil investigation should be conducted (LAPI ITB, 2011). The works consisted of CPT and shallow drilling with SPT (Figure 9).

The CPT cone test has been carried out at 9 points, utilizing DCPT device of 2.5 tons capacity in accordance with ASTM D3441-75T. The cone resistance value and local friction or friction sleeve value has been observed at every 20 cm depth interval. The penetration speed is maintained at approximately 2 cm/sec. Those tests have been performed to reach cone resistances value >160 Kg/cm2

.

Figure 9. Soil investigation activity Awi-14 pipeline

CPT work resulted a graph that shown the correlation of ground layer depth and the value of :

- Cone penetration (kg/cm2)
- Local friction (kg/cm2)
- Total friction (kg/cm1)

Shallow drilling & SPT works also conducted for total depth 25 meter that is performed at 3 point of boreholes. SPT has been performed at 2 meter interval. Number of blows for sample penetration of 1 foot was recorded for each test. The weight of hammer is 63.5 kg. The hammer

used in this test shall be free from friction using effective device according to ASTM D 1586-58T. The sampler used in SPT has an outside diameter of 51 mm & an inside diameter of 35 mm and length of 810 mm. The CPT, borehole & SPT result shown below (Figure 10)

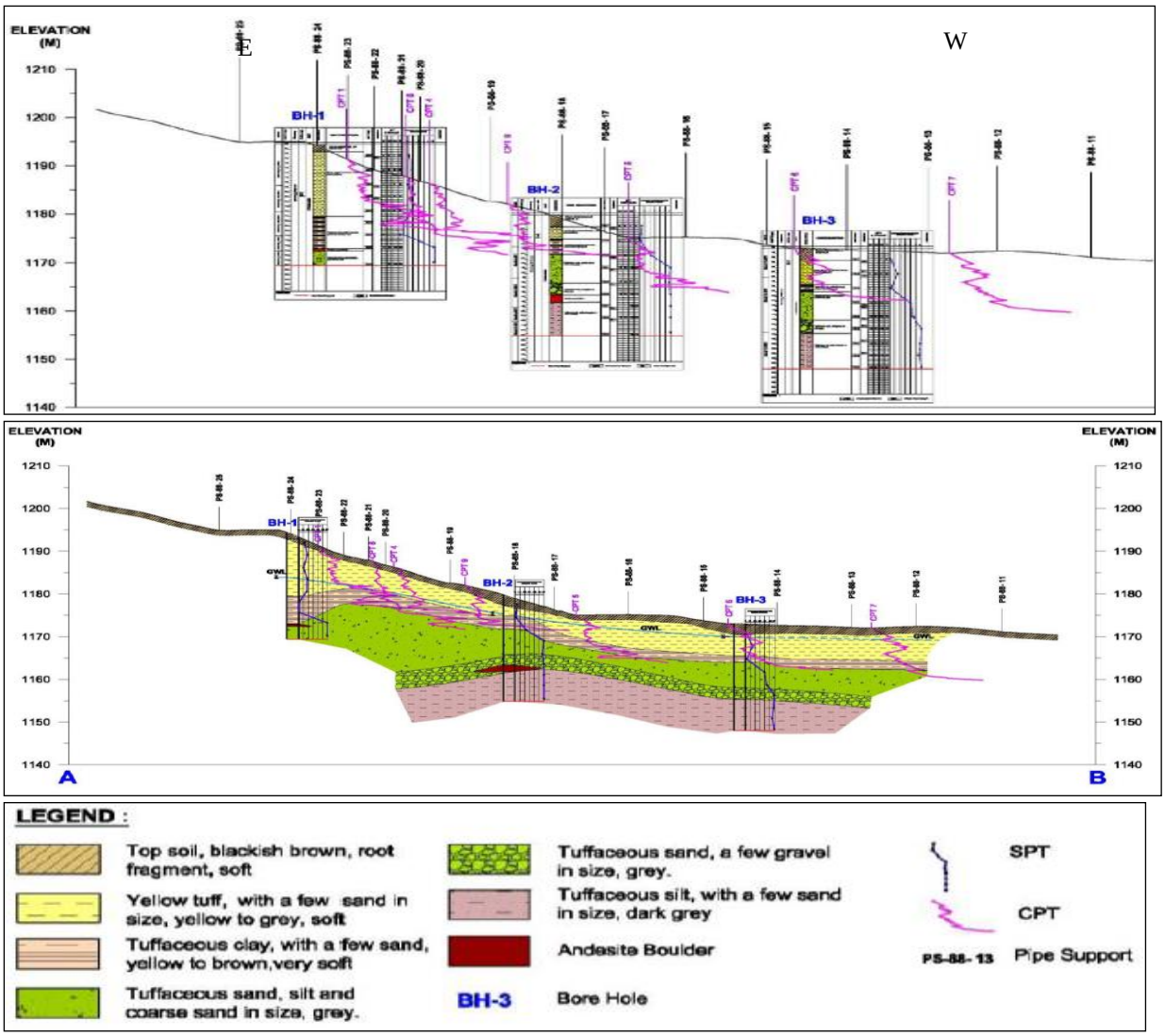

Figure 10. Data & interpretation CPT & Shallow Drilling Log BH-01, BH-02, & BH-03 in cross section along the slope & Awi-14 pipeline (E to W)

The drilling locations has been chosen as representative as possible. Using Toho D2G single core rotary machine, a shallow drilling activities has been carried out to soil investigation. The machine could drill up to 150 m depth. The outer diameter of the core barrel is 89 mm. This is entirely performed to obtain a reliable and efficient recovery sample.

Soil investigation results from BH-01, BH-02, &BH-03 samples, showed that there are six layers of soil:

a. At the top layer of soil formation consisted mainly of soil blackish brown with root fragment with SPT or N-value of this layer varied from 2 to 6 blows/ft
b. Second layer is Orange to brown Tuff in sand size SPT or N-value varied from 3 to 26 blows/ft
c. Third layer is Orange to brown Tuffaceous clay with minor sand, very soft SPT or N 1 blow/ft
d. Fourth layer is Tuffaceous sand, silt & coarse sand in size, grey with SPT or N-value varied from 13 to > 60 blows/ft
e. Fifth layer is grey Tuffaceous with sand & gravel, SPT or N-value varied from 25 to 60 blows/ft
f. Sixth layer is dark grey Tuffaceous silt with sand, SPT or N-value varied from 17 to > 60 blows/ft.

2D Resisitivity, SP SURVEY, & Sr (%)

The electrical resistivity is one of geophysical techniques that use variations of electrical resistivity value to determine subsurface material. This method is carried out by injecting current into the ground through the steel current electrodes and measuring potential difference using steel potential electrodes. The aim of injecting current and measuring potential difference is to determine the resistivity value distribution beneath the electrical resistivity line. The electrical resistivity survey is conducted in four lines

Data result has been converted from apparent resistivity to inverted resistivity using numerical inversion program.

The inverted resistivity data has been conducted to construct subsurface profile based on electrical properties of material. The vertical axis indicated the elevation and the horizontal axis indicated the horizontal distance along the line. The color in the cross section showed the distribution of electrical resistivity value.

The model inversion result at line 1 showed that a high resistivity value is detected from 70 meter to 105 meter, which is indicated intensive fracturing area. A low resistivity value is indicated massive clay / very fine tuff. The model inversion result at line 2 showed that there is no structure features in this line. A high resistivity value is indicated Tuffaceous sand. Orange tuff layer is distributed at top layer (Figure 11).

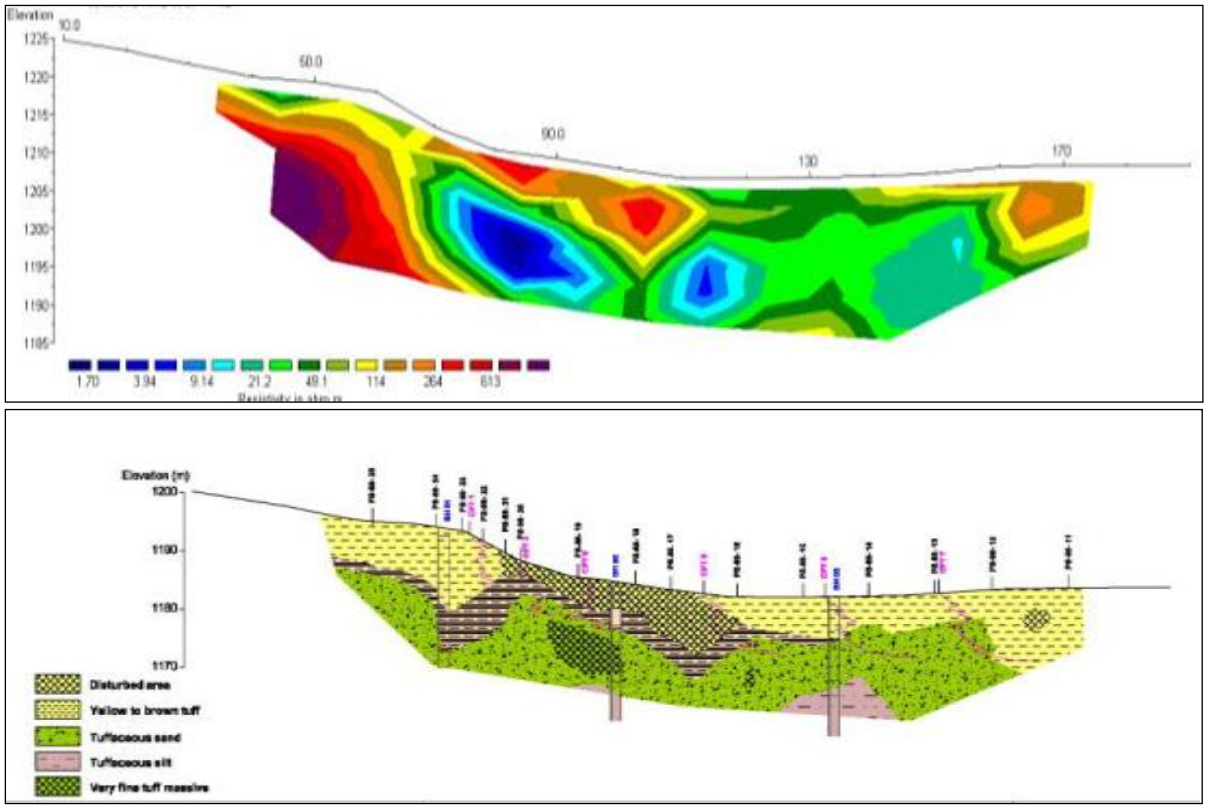

Figure 11. 2D resistivity Inversion model and Soil profile interpretation from Line-1of Awi-14 pipeline

The model inversion result at line 2 showed that there is no structure features in this line. A high resistivity value is indicated tuffaceous sand. Orange tuff layer is distributed at top layer. From the line 3 showed that there is clearly indicated of landslide movement. A high resistivity value is indicated tuffaceous silt. A low resistivity value indicated tufaceous clay with highly fracturing area is occupied at top layer, which is indicated by high value resistivity at top layer. Line 4 showed that there is clearly indicated of landslide movement, a high resistivity value indicated an intensive fracturing area and low resistivity value indicated very fine tuff / massive clay in this location.

As addition from geophysics survey, a single line of self-potential survey performed along pipeline route at Awi-14. The SP line has been conducted through length 225 meter parallel to pipeline route.

The SP survey resulted anomaly profile and the fluctuating potential differences occurred from beginning measurement to last failure pipe support. Indicate that there was intensive fracturing filled with water. The constant potential difference is occurred from several spot, which indicated dry area. At the end of line, there is a high anomaly that possibly spring water (Figure 12). High ground water table potentially exist at soil under Awi-14 pipeline

High saturated degree or Sr (%) was got from laboratory test that taken from soil data at Awi-14 well pad (Figure 13)

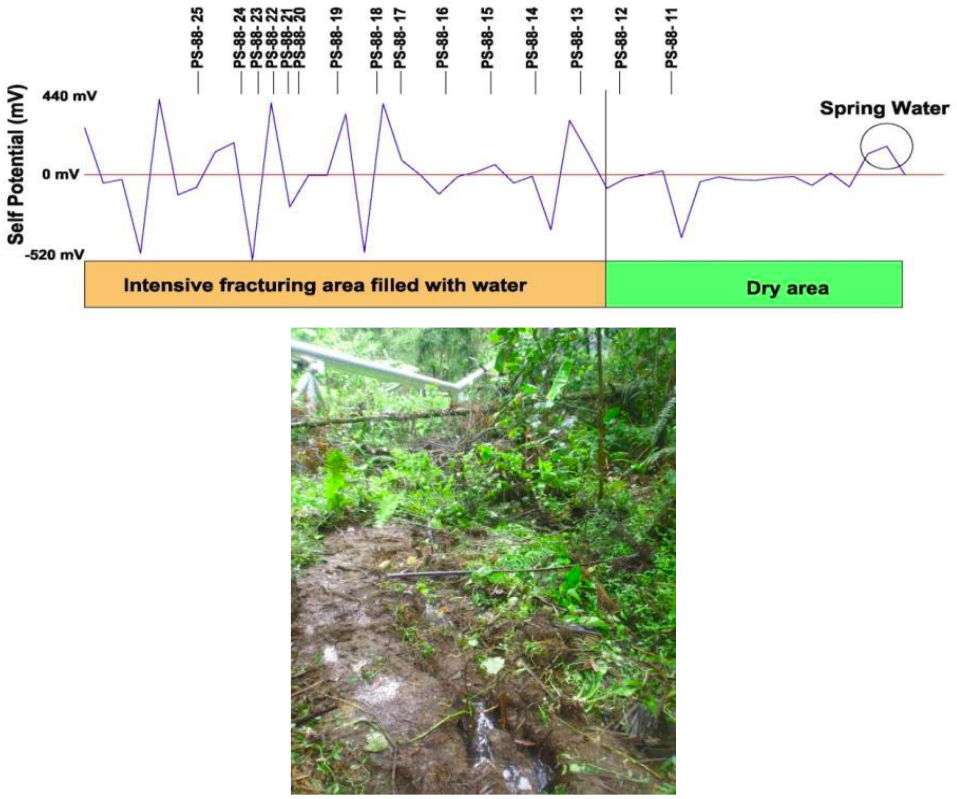

Figure 12. Self-Potential profile at crack area along Awi-14 brine line pipe, crack filled with water

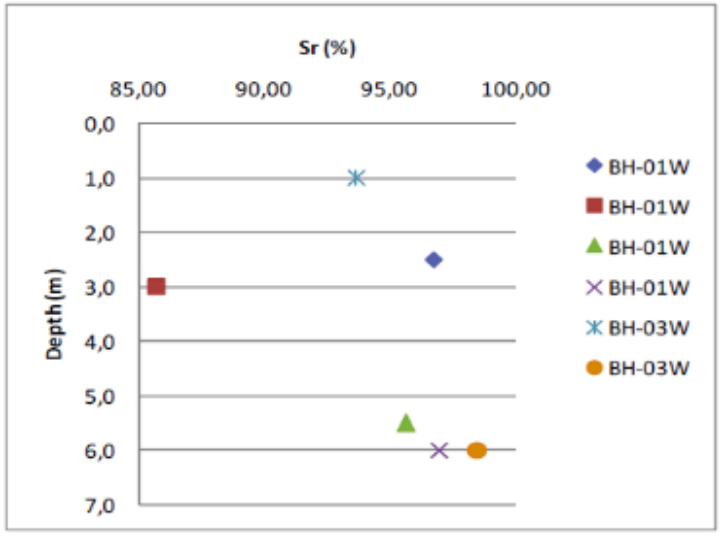

Figure 13. Sr (%) for various depth at Awi-14 well pad taken from BH-14-01-W & BH-14-03-W

Laboratory Test

Laboratory test on recovery samples (undisturbed soil). The following tests have been carried out:

- Index properties
- Grain size analysis
- Atterberg limit
- Tri-axial UU
- Tri-axial CU
- Direct shear

All the laboratory test was utilize as input data for geotechnical and slope stability analysis as conclusion for this study.

CONCLUSION

From all geotechnical analysis it was confirmed that main cause of geohazard or landslide within Awi-14 area was due to steep slope relief, high ground water table, and genuine soil condition surrounding location which dominated by orange tuff with soil characteristic silt and coarse sand so dewatering is the appropriate solution to increase the slope stability safety factor (JACOBS, 2014). The orange tuff usually stable in undisturbed condition but it becomes very sensittive to the water in disturbed condition. During mapping was found that these deposits (orange tuff) mostly weathered and having very low to low strength rock materials, coupled with poor drainage uncontrolled water run-off from heavy rainfall, then

overflowing water will have the tendency of over-saturating the soil in the vicinity, triggering a chain of events that could lead to a slope failure, bigger washout or worse a massive landslide.

These types of landslides had been triggered by the significant rise of the groundwater level, and therefore by the dramatic changes in the subsurface stream of the groundwater, several cases the sliding soil volume is so enormous (sometimes several hundred-thousands m³) that is it nearly impossible to stop it with engineering structures (or if is it possible, the costs are extremely high). The efective systems to stabilize and prevent this type of landslide is the Horizontal Deep Drainage (HDD) as a perfect tool to minimize the water table level (Istvan Szemesy, 2011). Technical reason of using this method can explain as below formula interpretation:

$$\tau = \sigma' \tan(\varphi') + c'$$

where,

τ = soil shear strength
φ' = soil friction angle
c' = soil cohesion

σ' = $(\sigma - u)$
= effective soil stress
σ = total soil stress
u = pore water pressure that correlated with ground water level (h_w)

Soil shear strength (τ) will be increase if effective soil stress (σ') increase so in condition of landslide triggered by high ground water level or high pore water pressure (u), the best solution is to decrease pore water pressure (u) and this condition will only been achieved by lowering ground water level (h_w).

Awi-14 brine line pipe landslide restoration project was executed on November 2014 with scope of work: installation of five (5) line of HDD that consist of horizontal drilling and installation of perforated HDPE pipe 6", while Awi-14 well pad restoration project was executed on May 2016 with only two (2) line of HDPE perforated pipe 6" installed (Figure 14). Horizontal drill machine type DDW-500C with pull back capacity 50 ton was used to execute this project, the work sequence as following flow chart (Figure 15).

Prior horizontal drilling, pilot bore plan must be provided. This bore plan will ease the operator to track the drilling distance, elevation, and angle of drilling in accordance with HDD design layout plan and elevation (Figure 16 and Figure 17). Completed installation of HDD has shown the result of water release from landslide area (Figure 18). This condition will improve the slope safety factor.

Figure 14. Horizontal drilling activity and HDPE perforated pipe 6" preparation before pulling back

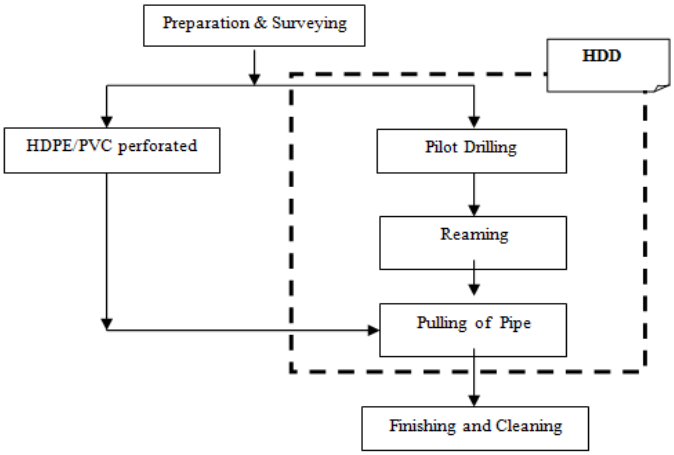

Figure 15. Horizontal drilling activity and HDPE perforated pipe 6" installation flow chart

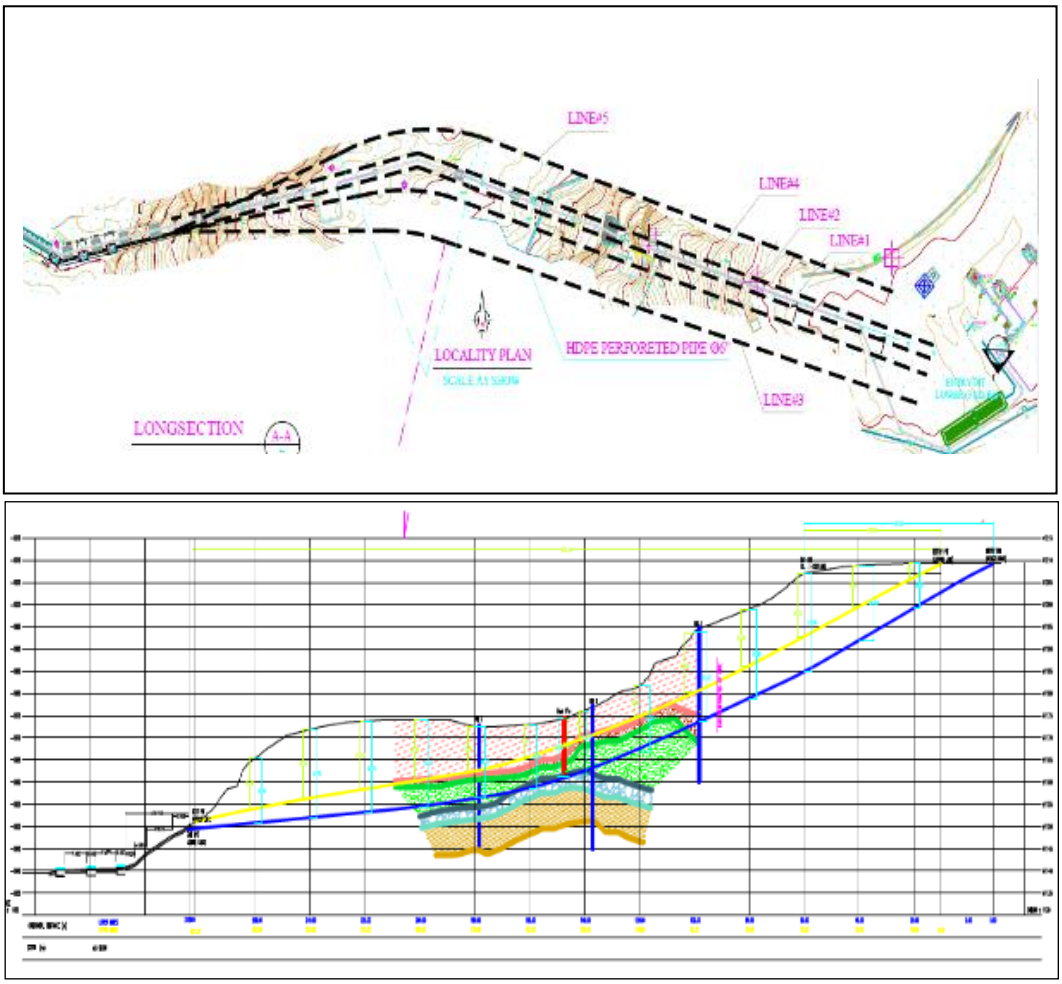

Figure 16. Five (5) line of Awi-14 brine line pipe horizontal deep drain layout and cross section

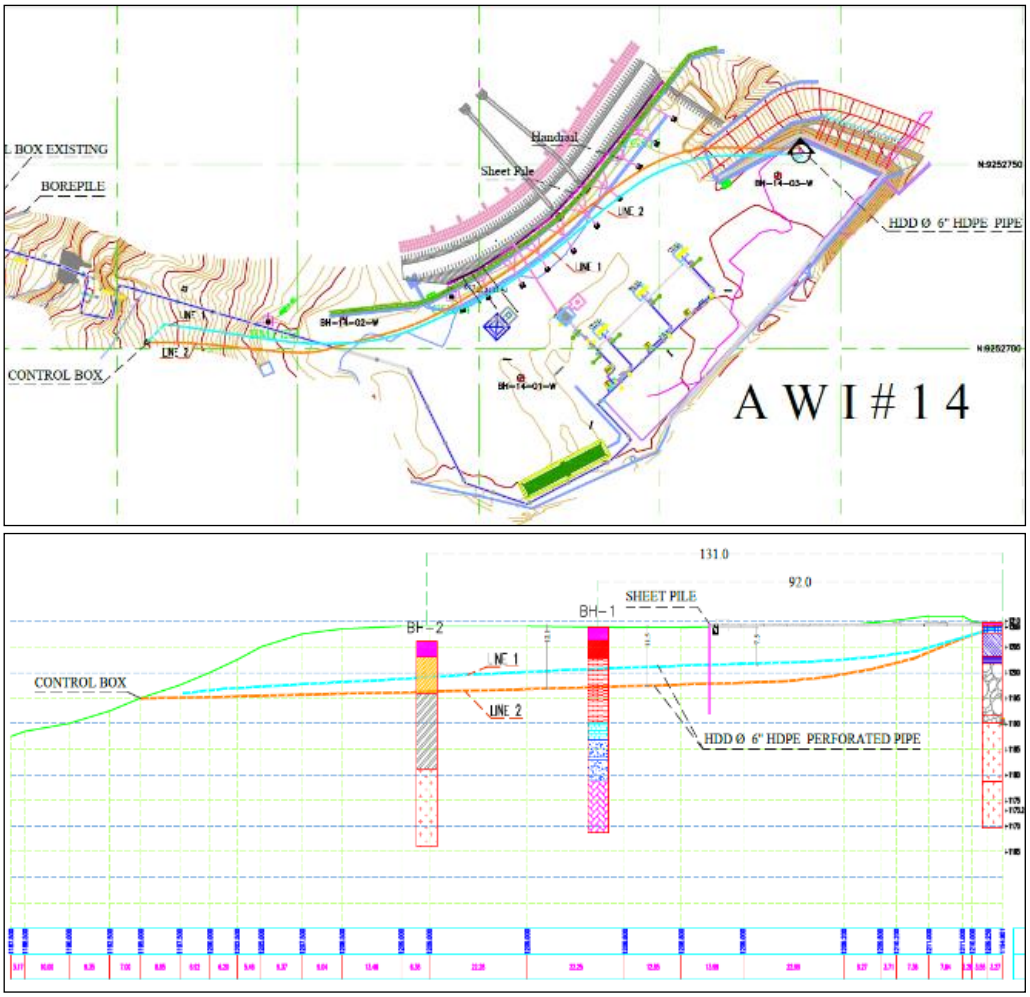

Figure 17. Two (2) line of Awi-14 Well pad horizontal deep drain layout and cross section

Figure 18. Completed installation of five (5) line of HDD at Awi-14 brine line pipe (left photo) and two (2) line of HDD at Awi-14 Well pad (right photo). Those HDD has successfully dropped ground water level

Prior the installation of HDD, measurement ground water level has conducted (Figure 19) in order to have a baseline data. To measure the ground water level, project team has installed one (1) unit vibrating wire piezometer and one (1) unit stand pipe piezometer. Those two (2) piezometer installed near bore hole 3 (BH-3) as the highest ground water level that measure during soil investigation. After HDD installed, ground water level dropped drastically to the level that expected -13 to -15 m. It could be read from piezometer that installed (Figure 20)

Water Level Monitoring BH1,2,&3 at Brine Line AWI 14

Date		2011	2012													
		Maret	November		Desember											
		16	28	29	4	5	6	7	8	9	10	11	13	15	17	18
Brine Line																
Water level Monitoring from surface (m)	BH-1	10,8	7,1	7,7	7,65	7,7	7,9	7,87	7,9	7,8	7,7	7,7	7,8	8	8	8
	BH-2	3,6	2,3	1,58	1,62	1,69	1,68	1,67	1,65	1,45	1,6	1,45	1,48	1,63	1,6	1,62
	BH-3	3,55	0,27	0,17	0,46	0,5	0,65	0,49	0,46	0,46	0,45	0,44	0,44	0,42	0,4	0,4

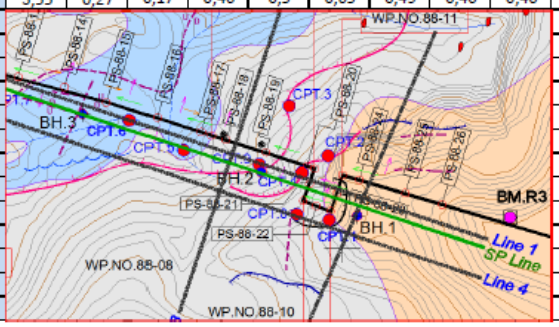

Figure 19. Table of GWT level measurement at AWI brine line prior HDD installation

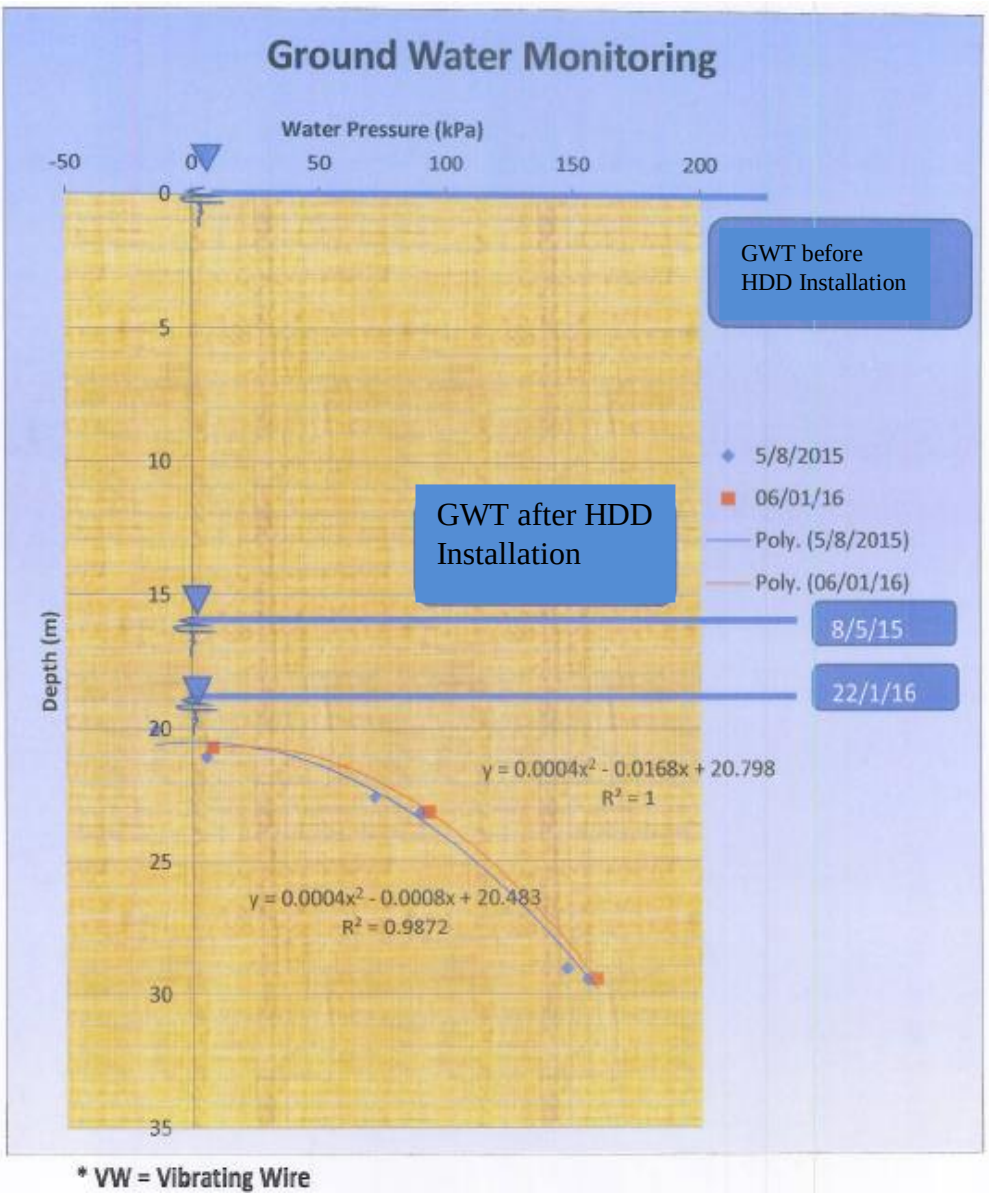

No	Month	Date	Weekly	Water Level below ground surface (m)			Water Pressure (Ton/m²)		
				SP (25m)	SP (15m)	SP (5m)	SP (25m)	SP (15m)	SP (5m)
1	July	7/10/2015	1	13.4	12.5	NA	11.6	2.5	NA
		7/15/2015	2	13.2	12.6	NA	11.8	2.4	NA
		7/20/2015	3	13.2	12.6	NA	11.8	2.4	NA
		7/30/2015	4	13.2	12.9	NA	11.8	2.1	NA
2	August	8/10/2015	1	13	12.9	NA	12	2.1	NA
		8/15/2015	2	13	13.3	NA	12	1.7	NA
		8/20/2015	3	13.1	13.3	NA	11.9	1.7	NA
		8/30/2015	4						

* SP = Stand Pipe

Figure 20. Data of GWT level and hydrostatic pressure taken from vibrating wire piezometer and stand pipe shown the decreasing of GWT after HDD installed

ACKNOWLEDGEMENT

The authors wish to thank to the management of Star Energy Geothermal Salak for supporting this project and granting permission to publish this paper. This project also could not have been undertaken without the support of co-author Satrio Wicaksono the ES-Geologist.

REFERENCES

James Stimac, et.al, 2007. "An Overview of the Awibengkok Geothermal System, Indonesia", Geothermics.

Gunawan, Adi, et.al, April 2011, "Report of Landslide Mitigation on Awi-2 and Awi-14 Brineline Area", Internal Presentation Report for Chevron Geothermal Salak

LAPI ITB, 2011, "Report of Soil Investigation at Landslide Area – Awi-14", Prepared for Chevron Geothermal Salak

Salak Operation, 2010 - 2011 "Routine Geohazard and Subsidence Monitoring", Internal Report for Chevron Geothermal Salak

Salak Operation, December 2010 "Salak Weather Monitoring", Internal Report for Chevron Geothermal Salak

Sagala, Birean, et.al, 2003, "Report on Soil Structure Investigation Awi-14 Pad Location", Internal Report for Chevron Geothermal Salak

URS Indonesia, 2004, "Salak Recovery Project Landslides Assessment", Prepared for Unocal Geothermal of Indonesia, Ltd.

Istvan Szemesy, 2011, "Stabilization and prevention of water triggered landslides", 10-th Slovak Geotechnical Conference

JACOBS, 2014, "Awi 14 Existing Brine Line Restoration", Design Review Report (ZP01581-RPT-GE-100 | A) prepared for Chevron Geothermal Salak, Ltd.

ISBN 978-602-52132-0-5

THE ROLE OF INFORMATION TECHNOLOGY PROCESS CONTROL NETWORK IN SUPPORTING THE SURVEILLANCE SYSTEM ON GEOTHERMAL SALAK AND DARAJAT OPERATION

Budi Darmawan

Star Energy Geothermal Salak and Darajat, Planning and Information Technology
Sentral Senayan II Office Tower, 25th Floor, Asia Afrika No. 8, Jakarta 10270, Indonesia

e-mail: budid@starenergy.co.id

ABSTRACT

Star Energy Geothermal Salak and Darajat asset have been operated for many years of operation. To ensure reliability and availability of the steam field and power plant, the company had been implementing surveillance system technology. The benefits achieved by implementing the surveillance system have been numerous. This surveillance system enables all stakeholders to monitor, collect and analyze historical data of steam field and power plant critical parameters also established information sharing at the highest level as well as enhanced company productivity, secure collaboration, operational transparency and reliability, and create image of integrity and safety to the stakeholders. This paper will discuss in brief the role of Information Technology Process Control Network in supporting the implementation of surveillance system in Star Energy Geothermal Salak and Darajat operation.

Keywords: Geothermal Operation, Information Technology, Process Control Network, Surveillance System

INTRODUCTION

Geothermal energy is another alternative solution to solve the power shortage in Indonesia, which is a fast growing economy and its energy demands are growing rapidly. Geothermal is a clean and renewable energy that could help Indonesia to reduce greenhouse gases emissions. Indonesia is a country that has a lot of geothermal resources and enormous geothermal energy potential with approximately 40% of the world geothermal energy resources (Munandar and Widodo, 2013).

Geothermal resources potential spreads along the entire trajectory of volcanoes in Indonesia which is usually found only in remote locations, therefore requires adequate facilities as well as infrastructure development. Steam field and power plant performance monitoring for all production areas and company-wide daily information and reporting systems in geothermal industry is one of the critical aspects to supporting company's vision, mission and performance measures (Rozaq *et al.*, 2015).

Salak geothermal field is located about 70 KM south of Jakarta (Nordquist *et al.*, 2010) and Darajat geothermal field is located about 150 KM southeast of Bandung in West Java, Indonesia (Intani *et al.*, 2015). Both of the geothermal field is located along the Sunda Volcanic Arc in West Java Province (Stimac *et al.*, 2010). Currently, Star Energy Geothermal Salak and Darajat are the largest geothermal field in Indonesia and the sixth largest in the world (Pasikki *et al.*, 2011). The location map Star Energy Geothermal Salak and Darajat fields in West Java Province, Indonesia as shown in Figure 1.

Figure 1. Location map Star Energy Geothermal Salak and Darajat fields in the West Java Province, Indonesia

As one of the biggest steam field and power generation geothermal company in Indonesia, thus the stakeholders need easy tools to monitor or visualize the real-time or historical operations data of the facilities, especially during critical operation periods. With the tools, the critical to the success of the geothermal operation is the ability to collect and analyze real-time information throughout the entire process, from steam field to power plant. As part of the power generation, company also require to provide ongoing reports on steam field and power plant operations to several stakeholders, to ensure that comply with all compliance and regulation. Use of collaboration tools has also provided an improvement in ensuring data quality and the ability to spot discrepancies for troubleshooting purposes and optimizations process.

Previously, the surveillance activity has been relying on operator report and operator routine duty check list. The monitoring activity was facing many obstacles such as administrative task, weather condition, road condition or interruption by other more important job. There is also gap in quality of facilities performance data in term of its accuracy, interval time, availability and accessibility which lead to inability to detect the declining of plant performance as well as to perform accurate and timely evaluation of any facility problem or discrepancy. The benefit includes early warning system for facility down or any discrepancy which enables operator to recognize the critical parameters problem and take appropriate action in timely manner so that the loss production opportunity impact will potentially be reduced, and the, objective to operate wells safer more efficient, and more reliable will potentially be achieved.

Gunnarsdóttir (2013 and 2015) said that in many cases geothermal data are not yet stored in computerized file form and may only be preserved in word or text processed reports in computers. Geothermal data that has been computerized may then not be stored in central computers as yet, but different parts of the information only kept in computers of individual employees. It can be said that proper data storage is lacking far and wide, which puts it at great risk of time consuming data recovery and even permanent data loss. The benefits of implementing relational database management system is to make the most use of the data, to get benefits as to maximize data security, ensure data consistency, avoid duplication of data, minimize human error, and to increase the accessibility of the data.

INFORMATION TECHNOLOGY

Definition, Role, and Function

Nowadays, Information Technology (IT) touches nearly every aspect of modern life. IT enables seamless integration and communication between businesses anywhere in the world. To keep IT systems running, a large workforce is needed to maintain networks, create new software, and ensure information security (Matthews, 2012). Information Technology is considered a subset of information and communications technology (ICT). ICT hierarchy level contains some degree of commonality in that they are related to technologies that facilitate the transfer of information and various types of electronically mediated communications (Zuppo, 2012).

IT is helping companies simply to survive and support their operations. IT has become the major facilitator of business activities in the world today (Tapscott *et al.*, 2000, Dickson and DeSancis, 2001; and Huber, 2004). IT is also a catalyst of fundamental changes in the strategic structure, operations, and management of organizations (Carr, 2001). According to Wreden (1997), IT capabilities may support the five business objectives, such as improving productivity, reducing costs, improving decision making, enhancing customer relationship, and developing new strategic application. Indeed, IT is creating a transformation in the way business is conducted, facilitating a transition to a digital economy. Brynolfsson *et al.*, (2003) and Liebowitz (2002) said, the digital economy refers to economy that is based on digital technologies, including digital communication networks, computers, software, and other related information technologies.

The business model in the digital economy, companies need to react frequently and quickly resolve the problem and opportunities resulting to new business environment (Arens and Rosenbloom, 2003 and Drucker, 2001). Because the pace of change and the degree of uncertainty in tomorrow's competitive environment are expected to accelerate, organizations are going to operate under increasing pressure to produce more, using fewer resources. Boyett and Boyett (1995) emphasize this dramatic change and describe it with a set of what they call business pressure or drivers.

These business pressures are forces in the organization's environment that create pressures on the organization's operations. In order to succeed in this dynamic world, companies must not only take traditional actions such a lowering costs, but also undertaken innovative activities or devise a competitive strategy. According to Simpson (2003) and Aren and Rosenbloom (2003), IT is the only solution to face these business pressure.

The world is moving faster and faster. Decisions need to be made very quickly, and speed is needed to remain competitive. To mitigate, the business pressure so that company need to leverage real-time operations (Gates, 1999; Davis, 2001; and Huber, 2004). According to Huber (2004), the schematic view or relationships among business pressures, organization responses, and activities supported by IT are shown in Figure 2.

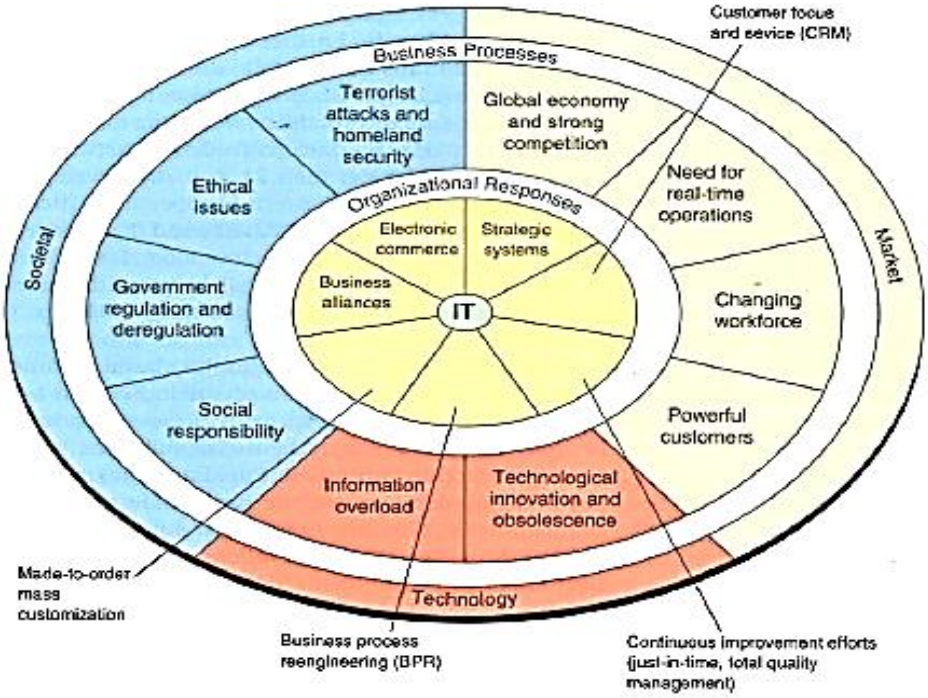

Figure 2. Business pressure, organizational responses and IT support

Process Control Network

Process Control Network (PCN) is a communications network that is used to transmit instructions and data between control and measurement units and Supervisory Control and Data Acquisition (SCADA) equipment (Byres *et al.,* 2005). According to terminology definition where PCNs are networks that mostly consist of real-time industrial process control systems used to centrally monitor and (over the local network) control remote or local industrial equipment such as motors, valves, pumps, relays, etc.

Process Control Systems are also referred to as Supervisory Control and Data Acquisition (SCADA) systems or Distributed Control Systems (DCS) (Peerlkamp and Nieuwenhuis, 2010). SCADA systems have been common used in the geothermal industry. These systems are used to monitor critical infrastructure systems and provide early warning of potential disaster situations. One of the most important aspects of SCADA has been its ability to evolve with the ever-changing face of technology that is now referred to as Information Technology systems. SCADA has evolved from a monolithic architecture to a networked architecture (Stouffer *et al.,* 2006).

In recent years, SCADA, PCN systems have increasingly relied on commercial information technologies such as Ethernet, TCP/IP and Windows for both critical and non-critical communications. The use of these common protocols and operating systems has made the interfacing of industrial control equipment much easier, but there is now significantly less isolation from the outside world. Network security problems from the enterprise network and the world at large can be passed onto the SCADA and process control network, putting industrial production and human safety at risk (Antal and Maghiar, 2008).

THE SURVEILLANCE SYSTEM

System Requirement

The geothermal stakeholders are requiring a high level confident of surveillance integrated in steam field and power plant systems to measure and understand the critical parameters and its characteristic. The surface facility monitoring, data collection and surveillance system is designed to ensure a successful of geothermal operation by collecting key important surface facility and turbine performance data. Achieving this objective is also the main goal of having surveillance system. Another key objective of the surveillance system is having a reliable data for both subsurface and surface production aspects to obtain a reasonable power generation baseline.

The surveillance systems installed on Star Energy Salak and Darajat operation must have at least two functionalities, such as operational and managerial functionalities. Users working in the operation section have capability to use the data for analysis by generating graphical user interface and trending as well. Users in managerial section use real time web-based application as the main application. Managerial section is using a thin client technology that works within a web-based environment to provide access to real-time and historical data via company intranet. Additionally, with the use of add-in functions to the spreadsheet menu bar and dialog boxes, users can quickly populate the spreadsheet with both real-time and historical data without need to use complex import functions.

The surveillance system must formed by a three-tier Information Technology architecture that is based on the server/client networking and information management concept dominating most business applications today. This combined with the use of web-based technology, Industrial Ethernet communications, and a component-based software structure. The ultimate goal of surveillance system is to develop supervisory and data acquisition monitoring system with the following purposes i.e. collecting the real-time and historical data from steam field and power plant parameters, saving the data in the application server that can be withdrawn anytime for the performance review and further evaluation, and monitoring/viewing the data from the control room and remote offices.

Together with all stakeholders involve, the functional team was carefully reviewed the products selection that were available on the market using following criteria, i.e. ability to sustain 24/7 operation, robust data processing capable of producing around 20K data items per second, easy to install and maintain, a reliable system from a well-established company. The steam field and power plant facilities better decision-making and reporting for operator, engineers and supervisors, while optimizing the costs for operation and maintenance. It can integrate all of the available data for the steam field and power plant operations group into a user friendly, consistent interface to better predict future events, and adapt to all systems in order to make them as efficient as possible.

Design Architecture

Surveillance system and data flow diagram on Star Energy Geothermal Salak and Darajat operation as shown in Figure 3. The architecture design has been followed company policy and procedure by doing risk assessment and getting IT concurrence process from IT management level. In Operating System side, implementation of all PCN-IP technical controls is mandatory and will be part of requirement to be fulfilled by vendors when they install the application. Data historian collectors will be installed in each asset connected to DCS and others SCADA system network to collect data sources and feed to historian server.

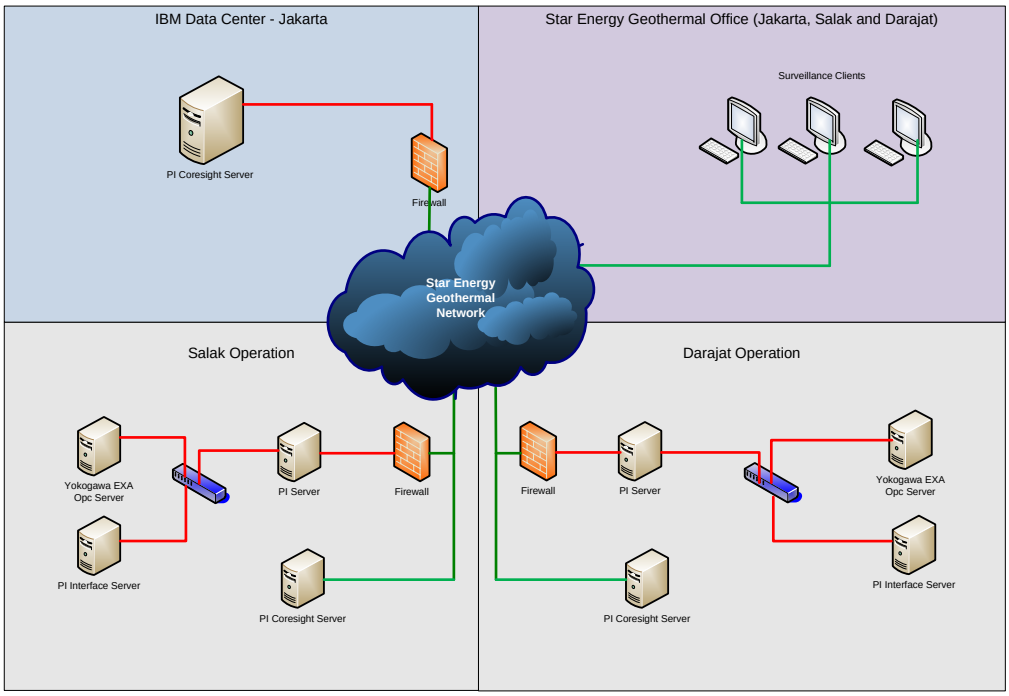

Figure 3. Surveillance system and data architecture flow diagram

The surveillance data architecture adopted the ISA S99 standard provides the SCADA and control systems industry with a model for segmenting networks at levels 2 and above to ensure that SCADA and control systems are isolated from the Enterprise IT networks through a DMZ (demilitarized zone). As the lower levels 0 and 1 typically contain instrumentation, meters, PLCs, RTUs and other field embedded devices move to IP communications, additional considerations for security must be taken into consideration (Djiev, 2002). One commonly suggested security solution is to isolate the SCADA and PCN system from the corporate and Internet systems through the use of firewalls (Byres and Hoffman, 2002).

A firewall is a mechanism used to control and monitor traffic to and from a network for the purpose of protecting devices on the network. It compares the traffic passing through it to a predefined security criteria or policy, discarding messages that do not meet the policy requirements. In effect, it is a filter blocking unwanted network traffic and placing limitations on the amount and type of communication that occurs between a protected network and other networks, or another portion of a site's network) (Mahan *et al.*, 2011).

Technology Solution

Client and Server technology is the next information technology for enabling the implementation. This technology enables for empowering users to access the information directly and timely. In Star Energy Geothermal Salak and Darajat operation, since 2007s we have been leveraging the OSIsoft's PI Systems® as data historian and surveillance system tools to collect real-time data on steam field and power plant operations and integrate with a variety of information sources throughout the steam field and power plant, along with DCS, other supervisory control and data acquisition system.

The PI data engine is used to collect and store all the raw data from the DCS, PLC's, manual logger and the field including pressure, temperature, flow rate, frequency, voltage, wattage, level, and others online analysis, which implement the actual monitoring of the process performance. The PI System provides real-time event management, retrieval, and deep archiving of volumes of data for scalable management of relevant variables and events enterprise wide.

PI System brings all operational data into a single system than can deliver it to users at all levels of the company from the plant floor to enterprise level. The PI System keeps all critical operation data online and available in a specialized time-series database so it is always available. With the help of the PI System's reporting and analytical tools, the wealth of data in our operation can drive meaningful, empowered and informed action.

The OSIsoft's product such as PI DataLink® by Microsoft Excel add-in, PI ProcessBook® and PI Coresight® by monitoring graphs and trends, created by the plant engineers. Statistical Quality Control is applied in order to monitor the process variables efficiently, and maintain operational quality through control charts that have upper and lower control limits. The operators and engineers are able determine the cause-effect relationships between steam field and power plant parameters and determine key process variables. Knowing the cause and effect enables the staff to maintain better (OSIsoft, 2016).

The sample displays PI DataLink real-time surveillance system for Salak and Darajat operations may show in Figure 4.

The PI DataLink established a direct connection the OSIsoft PI System and Microsoft Excel. Users can display real-time as well as historical data in Microsoft Excel so they can create and publish reports and perform complex data analysis. By providing direct access to PI System data, PI DataLink makes the performance of such tasks as data gathering, reporting, modeling, analysis, forecasting, and process planning fast and dependable.

The PI ProcessBook as easy-to use graphical interface makes it possible to efficiently display real-time and historical data reading in the PI System and other sources. User can use PI ProcessBook to create interactive graphical displays that can be saved and shared with others. Users can quickly switch between view and build modes to create dynamic, interactive displays and populate them with live data. They also can write scripts that automate displays and trends by using Microsoft Visual Basic for Applications, which is seamlessly integrated into PI ProcessBook. The sample displays PI ProcessBook real-time surveillance system for Salak and Darajat operations may show in Figure 5.

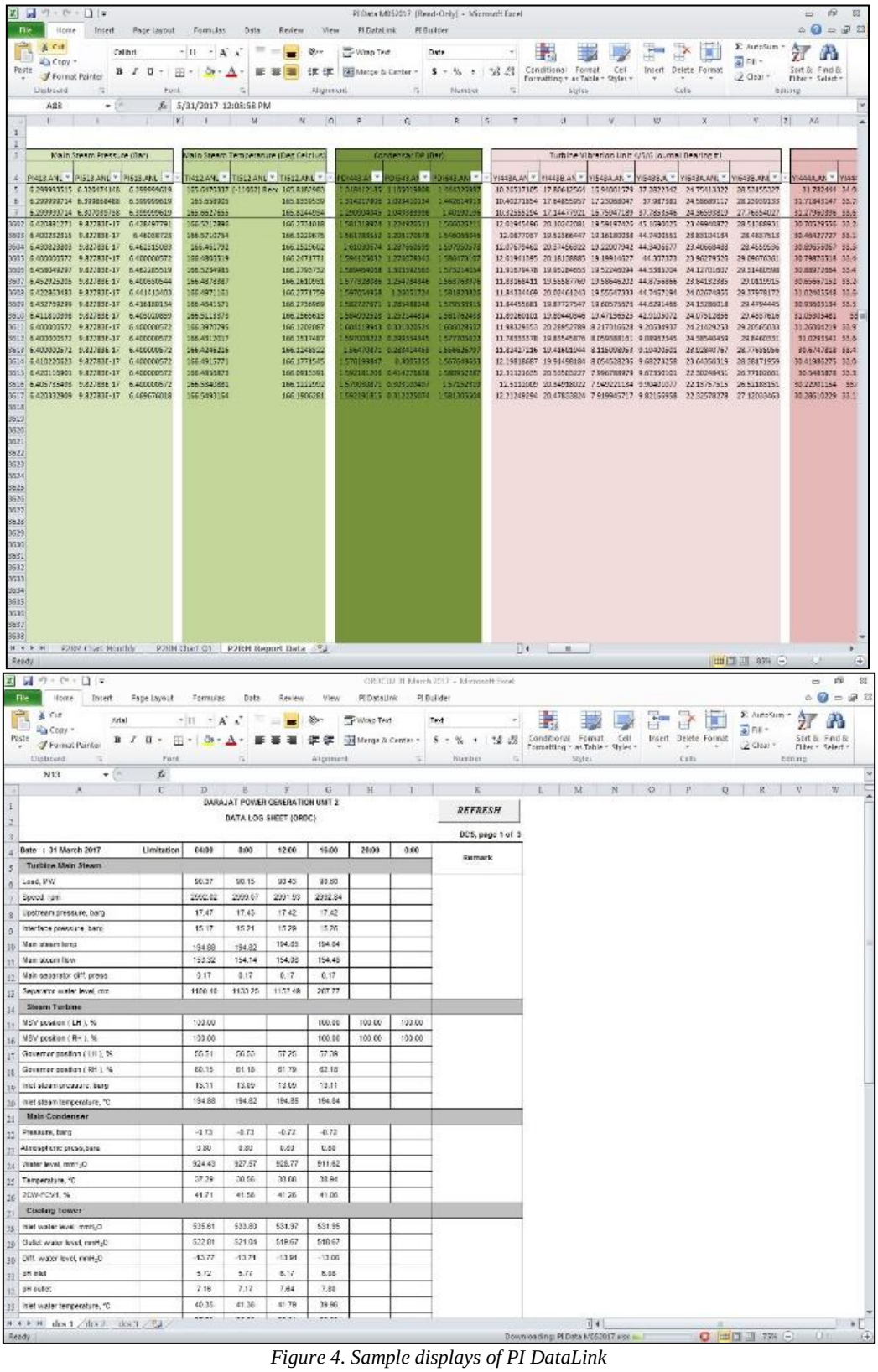

Figure 4. Sample displays of PI DataLink

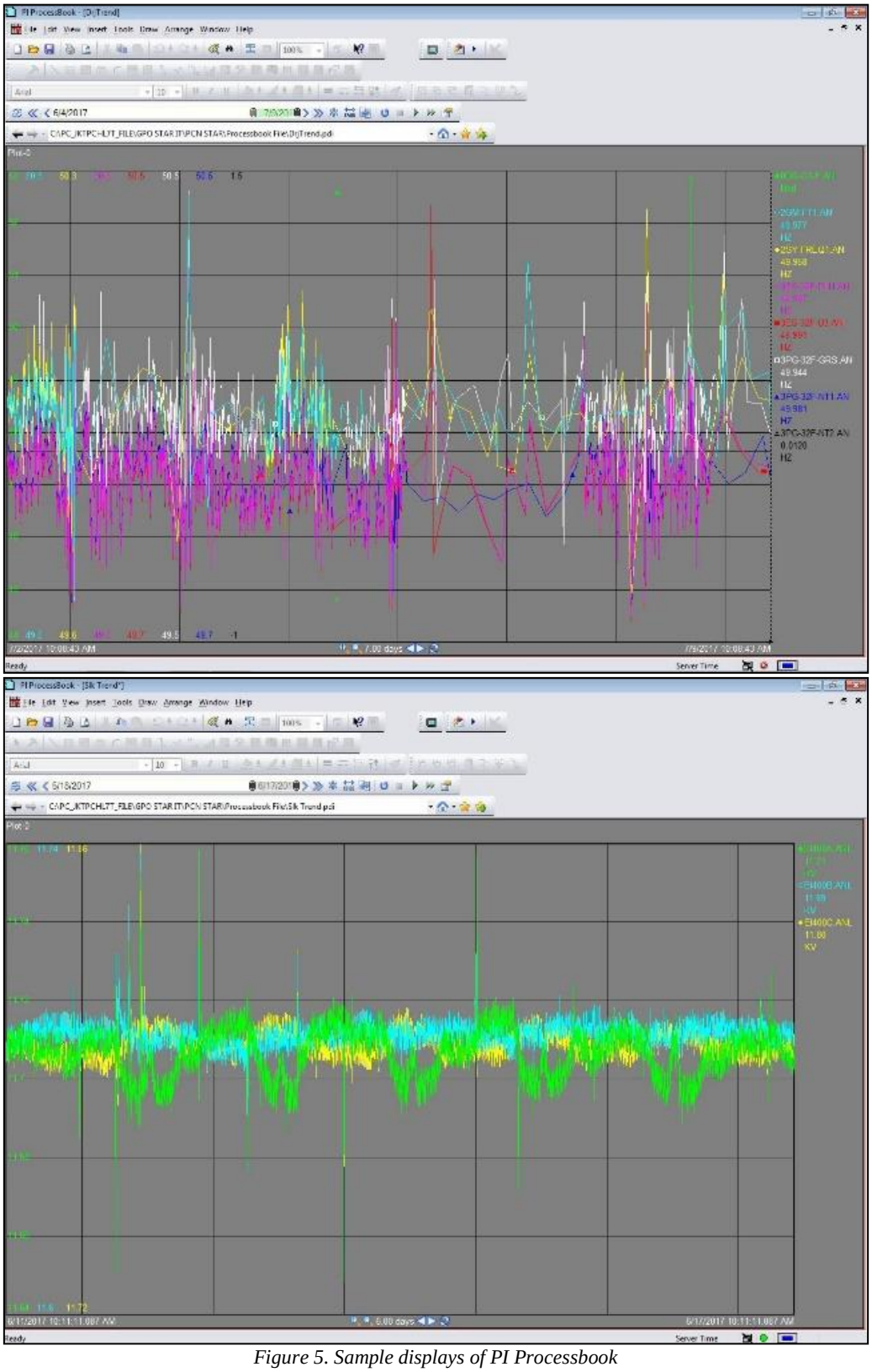

Figure 5. Sample displays of PI Processbook

The web-based real-time surveillance system portal site was developed using OSIsoft's PI Coresight®. While the core portal pages were developed by IT team, users have the ability to create their own customized graphic screens of the field that are incorporated in the portal site to display specific information based on their need. Custom and legacy data was consolidated along with PI System data. The site is also dynamic, allowing users to customize the layout and work with trends. The PI Coresight is thin clients that are integral components to the PI System products suite. The web-based applications allow users to investigate real-time information including time series, relational, and web services information, all within a familiar with internet browser-based environment. The sample displays web-based real-time surveillance system for Salak and Darajat operations may show in Figure 6.

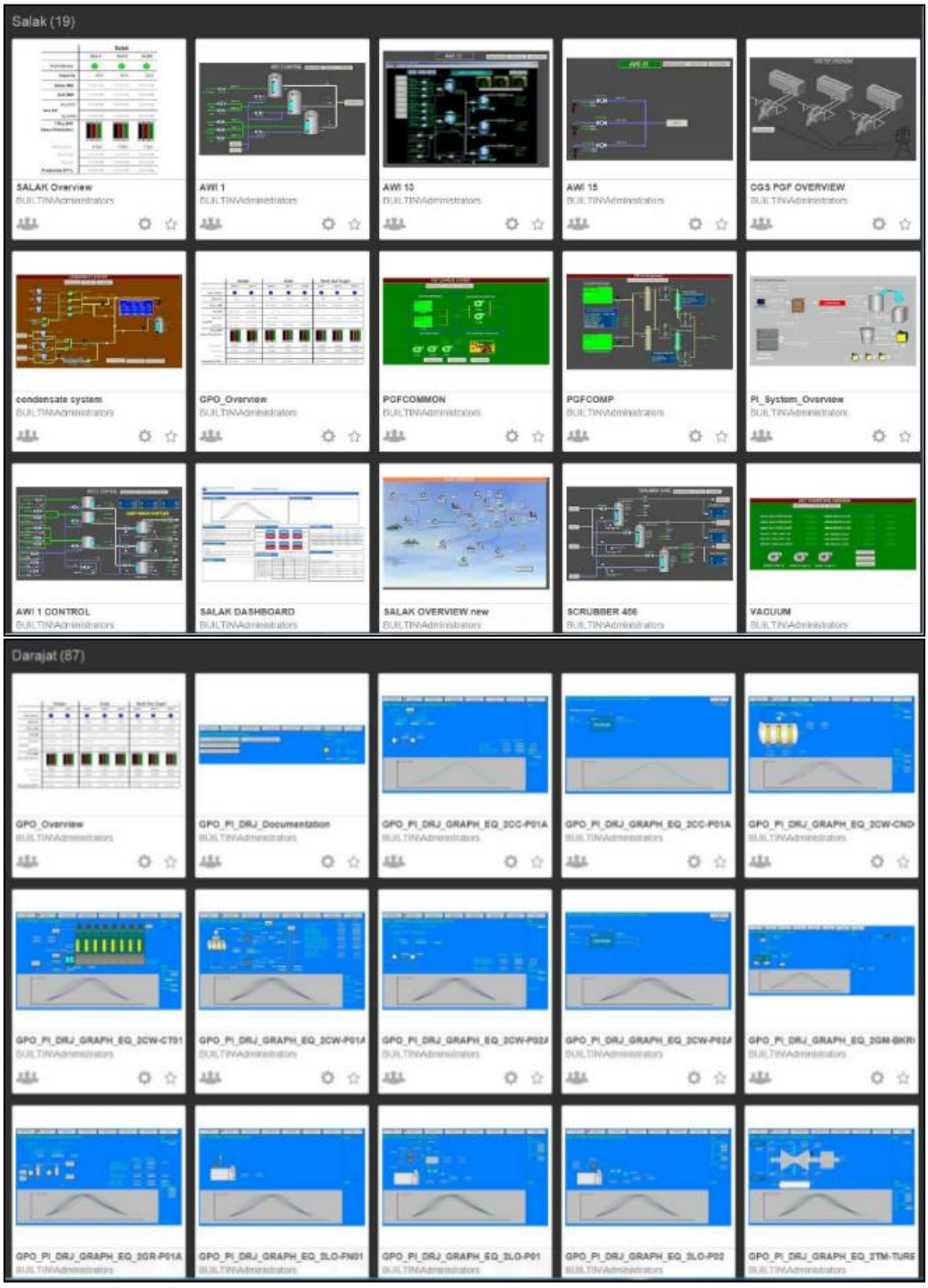

Figure 6. Sample displays of PI Coresight

Enhancing the Portal capability then engineers can drill down to view how the individual systems or equipment are working, to help operators and engineers focus on problem areas, color coded tabs have been incorporated to immediately identify areas of concern. A navigation bar, populated by the module database, is include on all pages to help choose with systems or equipment parameters data that they want to see or investigate. The portal site is Internet Explorer-based so it is very intuitive and easy for end user to use and understand.

CONCLUSIONS

The implementing surveillance system on Star Energy Geothermal Salak and Darajat operation have been numerous such aim of providing a tool for users to assess, improve and optimize the plant operations, allow more than one user to access data from historian database system simultaneously, faster data retrieval into spreadsheet for reporting purpose, provide real time plant performance monitoring tool, a centralized information or database available, extendable archive data files, a better system performance that existing historian system, integrates with existing DCS and other supervisory

control and data acquisition, improved accessibility and user friendly (thin client, web server and etc.), on-line notification based on process discrepancy to maintenance personnel to perform necessary repair on certain instrument/equipment, and minimize or eliminate common mistakes in gathering manual operating data.

The surveillance system has been providing economically viable energy generating, establishing information sharing at the lowest and highest level as well as enhanced the productivity tools, secure collaboration, operational data transparency, improve reliability, availability and created an image of integrity and safety to stakeholders. Integration and interconnectivity are creating a new world of opportunities for process control network to support the success of geothermal industry expected gain will be obtained if surveillance system is implemented such as reduction loss production opportunity as result of faster operator response time, and gain production optimization by improved steam field and power plant surveillance system.

The surveillance also can provide information for support decisions and thereby helps to offset negative effects of operational issue and reduce the decision uncertainty by transforming data into information to further manage costs and improve value, significantly reduce clerical function and change into analytical function, and highly secure environment with no interference in regular control room work.

ACKNOWLEDGMENTS

We thank Star Energy Geothermal Salak and Darajat operation for supporting and granting permission to publish this paper. Also, this paper could not have been undertaken without the support and encouragement of Mr. Wowok Meirianto, Mr. Bambang Santoso and Mr. Darel Nasri.

REFERENCE

Antal, C. and T. Maghiar. (2008), Automatic Control and Data Acquisition (SCADA) for Geothermal Systems. University of Oradea, Romania. UNU G.T.P., Iceland, report 1, 30 pp.

Aren, Y., and P.S. Rosenbloom. (2003), Responding to Unexpected. Association for Computing Machinery: Communication of the ACM.

Boyett, J.H., and J.T. Boyett. (1995), Beyond Workplace 2000: Essential Strategies for the New American Corporation. New York: Duntton.

Brynolfsson, E., *et al*. (2003), Consumer Surplus in the Digital Economy: Estimating the Value of Increased Product Variety at Online Book sellers. Management Science, 49(11).

Byres, E.J. and D. Hoffman. (2002), IT Security and the Plant Floor", InTech Magazine, Instrumentation Systems and Automation Society, Research Triangle Park, NC, p. 76.

Byres, E., J. Carter, A. Elramly and D. Hoffman. (2005), Worlds in Collision: Ethernet on the Plant Floor, ISA Emerging Technologies Conference, Instrumentation Systems and Automation Society, Chicago.

Davis, B. (2001), Speed Is Life. New York: Doubleday.

Dickson, G.W., and G. DeSantis. (2001), Information Technology and the Future Enterprise: New Models for Managers. Upper Saddle River. NJ:Prentice-Hall.

Djiev, S. (2002), Industial Networks for Communication and Control.

Drucker, P. F. (2001), The Next Society. The Economist.

Gates, H.B. (1999), Business at the Speed of Thought. New York. Penguin Books.

Gunnarsdóttir, S. (2013), Basics of Modern Databases – Mainly the Relational One. Iceland GeoSurvey. 15 p.

Gunnarsdóttir, S. (2015), Design and Use of Relational Databases in the Geothermal Sector. Iceland GeoSurvey. Proceedings World Geothermal Congress 2015 Melbourne, Australia, 19-25 April 2015.

Huber, G. (2004), The Necessary of Future Firms: Attributes of Survivors in a Changing World. San Francisco: Sage Publication.

Intani, R.G, C. Simatupang, A. Sihombing, R. Irfan, G. Golla and F. Pasaribu. (2015), West Edgefield Evaluation of the Darajat Geothermal Field, Indonesia. Proceedings World Geothermal Congress 2015. Melbourne, Australia, 19-25 April 2015.

Liebowitz, S. (2002), Rethinking the Network Economy: The True Forces that Drive the Digital Marketplace. New York. AMACOM.

Mahan, R.E., J.R. Burnette, J.D. Fluckiger, C.A. Goranson, S.L. Clements, H. Kirkham, C. Tews. (2011), Secure Data Transfer Guidance for Industrial Control and SCADA Systems. Pacific Northwest.

Matthews, C. 2012. The App Economy Estimated to Contribute Nearly Half a Million Jobs in U.S. http://business.time.com/2012/02/08/the-app-economy-estimated-to-contribute-nearly-half-a-million-jobs-to-the-u-s/.

Munandar, A. and S. Widodo. (2013), Geothermal Resources Development in Indonesia. Proceedings of the 10th Asian Geothermal Symposium, 22-24 September 2013.

Nordquist, G. A., J. Acuña and J. Stimac.(2010), Precision Gravity Modeling and Interpretation at the Salak Geothermal Field, Indonesia. Proceedings World Geothermal Congress 2010. Bali, Indonesia, 25-29 April 2010

OSIsoft. (2016), Operational Intelligence and Data Infrastructure | PI System OSIsof. https://techsupport.osisoft.com/

Pasikki, R.G., J. Maarif, A. Joeristanto, F. Libert, N. Kay. (2011), Studies and Implementation of Injector Well Conversion During Salak Field Operation. PROCEEDINGS, Thirty-Sixth Workshop on Geothermal Reservoir Engineering Stanford University, Stanford, California, January 31 - February 2, 2011.

Peerlkamp, S.F. and M.B. Nieuwenhuis. (2010), Process Control Network Security: Comparing frameworks to mitigate the specific threats to Process Control

Networks. Postgraduate Study Programme on EDP Auditing Vrije Universiteit Amsterdam.

Rozaq, K., D. Rahayu, and B. Bramantio. (2015), Development of Geothermal in Indonesia – PGE. Proceedings World Geothermal Congress 2015. Melbourne, Australia, 19-25 April 2015.

Simpson, R. L. (2003), Today's Challenges Shape Tommorow's Technology, Part 2. Nursing Management.

Stimac, J., M. Baroek, A. Suminar, and B. Sagala. (2010), Integration of Surface and Well Data to Determine Structural Controls on Permeability at Salak (Awibengkok), Indonesia. Proceedings World Geothermal Congress 2010. Bali, Indonesia, 25-29 April 2010.

Stouffer, K., J. Falco, K. Kent. (2006), Guide to Supervisory Control and Data Acquisition (SCADA) and Industrial Control Systems Security. Computer Security Division Information Technology Laboratory National Institute of Standards and Technology Gaithersburg, MD 20899-8930.

Tapscott, D. (2000), Digital Capital. Boston: Harvard Business School Press.

Wreden, N. (1997), Business-Boosting Technologies. Beyond Computing.

Zuppo, C. M. (2012), Defining ICT in A Boundaryless World: The Development of A Working Hierarchy. International Journal of Managing Information Technology (IJMIT) Vol.4, No.3, August 2012.

PRELIMINARY STUDY OF GEOTOURISM PLANS IN GEOTHERMAL AREA: A CASE STUDY IN BUKIT DAUN GEOTHERMAL PROJECT

Ilham Dharmawan Putra, Fathidliyaul Haq, Hendra Maulana Irvan, Agus Hendratno

Universitas Gadjah Mada
Grafika Street, No. 2, Engineering Faculty of Universitas Gadjah Mada

e-mail: Ilham.dharmawan.p@mail.ugm.ac.id; Fathidliyaul.haq@mail.ugm.ac.id;
hendra.maulana.i@mail.ugm.ac.id; gushendratno@yahoo.com

ABSTRACT

Bukit Daun is an area located in Bermani Ulu subdistrict, approximately 20 km from Curup City, Bengkulu Province and located about 700 – 1000 masl. This area now is one of the geothermal exploration sites in Indonesia to be developed for electricity purpose. In general, Observations in some geothermal fields show that social supports are one of the most important factors that determine the success rate of development activities in the geothermal area. In the other hand, the Geothermal area provides geotourism potentials and shows promising benefits to educate people because geotourism has been widely accepted by all kinds of society as their welfare. Departing from this point of views, we want to construct a plan that linked geothermal potentials in Bukit Daun area to geotourism in order to serve a good way in educating the people in Bukit Daun area. The method that we conducted to builds a construction plan is literature study, field, and social observations, as well as comparing it to other geothermal fields as case studies and interpretations to choose the most suitable ways of constructing it. The field observation shows that this area has some prospectus places to be developed as geotourism sites, they're Bukit Daun itself that offers beautiful landscapes, geothermal manifestations, Lakes, and Waterfalls. Also, certain places in this area act as recharge area and contain fertile soil to grow any plants including Rafflesia and Amorphophallus as national rare flowers. The main concept that we propose to the plan is "Geodiversity in Geothermal Geotourism", that based on following main values, 1) Rewarding, 2) Enriching, 3) Adventuring, and 4) Learning. From this values, the concept will be brought to education and conservation purpose by providing scientific information about the natural phenomena especially in a geothermal area that based on the appreciation of those phenomena, enrich the people's knowledge and abilities, and initiate participation of people in geotourism activity. Also, in this study we consider other values such as cultural

value to find the most suitable ways to deliver the information to society, economic value to give the benefits to the economic side of local people that lived in the geothermal area, and aesthetic value of the geotourism sites to attract and encourage people's curiosity. From this plans, we believed that geotourism could become good way to educate people in a geothermal area especially in exploration area like Bukit Daun.

Keywords: Bukit Daun, geothermal, geotourism, educations, society

INTRODUCTION

Bukit Daun is an area located in Bermani Ulu Raya subdistrict, Rejang Lebong, Bengkulu Province. This area located about 90 km from Bengkulu's Capital City, and in elevation about 700 – 1000 masl. Bukit Daun is found within the geological – geomorphological setting of Bukit Barisan Mountains. This area is well known as an area that has several potentials, one of it is geothermal potential. The geothermal potential in the area is shown by the presence of manifestations, such as hot pools, hot springs, Mud pools, and altered rocks. These conditions draw some of the national geothermal company to explore and exploit the potential of the area.

Learning from the past events, some of the geothermal development found to be very complicated, especially in social side, where oppositions from society rise up in the early or middle phase of geothermal development, especially when drilling process is about to begin.

Geotourism is a concept of tourism activities that visiting interesting geological spots (Sampurno, 1995 in Hendratno, 2002). Two important elements in geoturism concept are conservations and educations through appreciations a learning (Newsome & Dowling, 2010 in Kubalíková and Kirchner, 2016). Geotourism potential is presented in geodiversity but through exploration and exploitation, only those potential can be used for geotourism purposes (Pralong & Reynard, 2005 in Kubalíková and Kirchner, 2016).

Geodiversity is a concept of diversity of earth features and its systems. Human activities and environments are linked through geodiversity because geodiversity contains geological, natural processes, landforms, landscapes, soils, climates, and others as fundamental elements in affecting human activities (Kubalíková and Kirchner, 2016). Cultural and economics sides of society also the affected by geodiversity because of elements in geodiversity is found to support each other to form conditions for human life, i.e groundwater will be fundamental for residential places, or mountainous landscapes found to be suitable places to grow agriculture's. One of the products formed by geodiversity is geoturism potentials, which its parameter is: 1) geological, 2) geomorphological, 3) soil features (Gray, 2004).

When discussed geotorism, important terms used are geomorphsite and geosite based on Kubalíková and Kirchner (2016). Geosite means some sites on earth/ geosphere that represents geological history based on its prevailing feature, i.e. volcanic, or geothermal (Reynard, 2004, in Kubalíková and Kirchner, 2016). Geomorphsite means geosites that had been defined as landforms comes along with several values thanks to human perceptions. Geomorphsites values can be divided into two main values, there are scientific and added values, where scientific values contains information about genesis, process, evolutions, and dynamics of geomorphsites, while added values contains socials, cultural, aesthetics, ecological, economical, and others (Panizza, 2001 in Kubalíková and Kirchner, 2016).

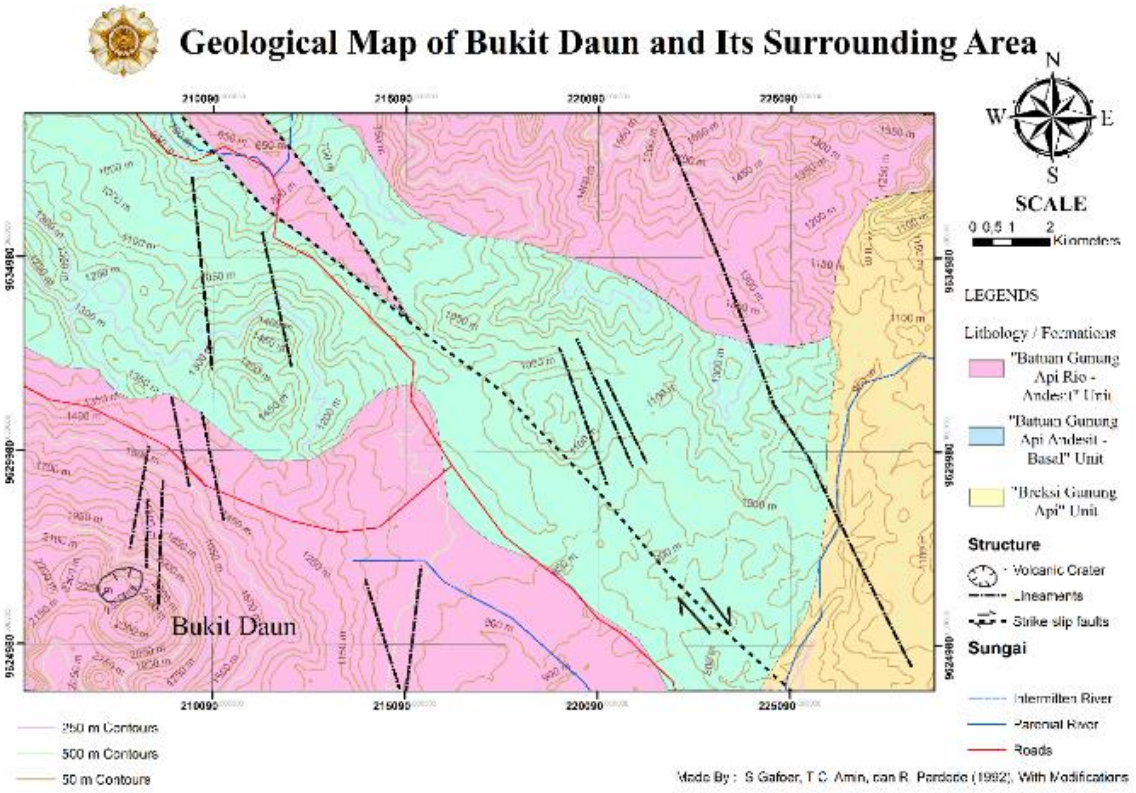

Figure 1:. Geological map of Bukit Daun and its surrounding area (Gafoer et al, 1992)

The concept of geodiversity, geosites, geomorphsites, and geoturisms are very important, also could be applied on some of geothermal area where geodiversity is rich that appear as geosite and geomorphsites that have potentials to be developed as geotourism. In this case, preliminary studies are needed to explore and exploit the geotourism potentials. In this study, we proposed a concept that will be used as a "tool" in educating the people that live within or around the geothermal area.

GEOLOGICAL AND GEOMORPHOLOGICAL CONDITIONS

Regional Geomorphology

Bukit Daun Area is located at Bukit Barisan mountains region geomorphologically. The study area is volcanic landform and surrounded by some hills/ mountains, such as Mt. Kaba, Mt. Condong, Mt. Kalang, Mt. Lalang, Mt. Naning, Mt. Hulupalik, Mt. Sanggul, Mt. Hulupalak, Mt Engas, Mt. Basa and others. Some Lineaments are found in study area showing N – S orientations (Gafoer et al, 1992).

Regional Geology

The study area is consists of some geological formations and rocks units, according to Gafoer et al (1992), the formation/ rock units are:

"Breksi Gunung api" Unit

This unit is composed of Volcanic breccia, Lava, Andesitic – Basaltic Tuff. Mt Kaba, Mt. Dempo, Mt. Lumut, Mt. Hulusulup, Mt. Balai, and Mt. Besar is expected to be the main source of this rocks unit.

"Batuan Gunung Api Andesit – Basal" Unit

This unit is composed by Lavas with the main composition are Andesite to Basalt, Tuff, and Laharic Breccia. Mt. Lumut, Mt. Hulusulup, Mt. Daun, and Mt. Dingin are expected to be the main source of this unit. The thickness of this unit is about 300 meters.

"Batuan Gunung Api Rio – Andesit" Unit

This unit is composed by Rhyolitic Lavas, Dacites, and Andesites, Hybrid Tuff, and Volcanic and or Pumice Breccia. The thickness of this unit is about 350 meters.

METHOD

To complete this paper, the method we use is literature studies, social observation, as well as performing interpretation to build a preliminary geotourism plan in Bukit Daun area. The early stage of method is done by collecting the related publications and literature to the study area. Then, the analysis is done by comparing and also analyzing the other geothermal fields to look for the parameters that made a geothermal field accepted or denied by society. Also, qualitative and quantitative analysis of some geomorphsites are done in order to found out the gaotourism activity can be done in each geomorphsites, also the further development can or must be done in each geomorphsites. Through that analysis, the parameter produced appear as the point of questions will be used in constructing geotourism plan and considering the challenge that needs to overcome.

GEOTOURISM EDUCATION IN GEOTHERMAL AREA

The main goal of this geotourism's preliminary study is to looking for some ways where geotourism activity could enriched the local people's and visitor's knowledge about geothermal and the fitures in it as well as to be linked on

indirect use electricity development of Bukit Daun Geothermal area. By looking from some events in the past, lack of knowledge of the geothermal system and how geothermal indirect use development are done have created some obstacles, that conduct local people resistence in the reasons of social, culture, and nature. By Serving geothermal education thorough geotourisms activity, educations and conservation of the geotourism sites could be reached through appreciations and learning (Newsome & Dowling, 2010 in Kubalíková, 2013).

In a geothermal area, education of geothermal are needed in order to create the well-understood society of geothermal, as they will be the organizer of the geotourism activity. Thorugh field observation in one of the well-developed geotourism sites in Lahendong Geothermal Area, the educative geotourism activity are done by could be held by serving: 1) Educative infrastructures, such as information signs, 2) provides the once-in-a-year geothermal celebrations that invite all group society, Childrens, Teenagers, and adults to participates in it, 3) Created the geothermal lover community or geothermal geoturism community as pioneers in passing the latest information and issue in geothermal utilization developments, 4) Creates a collaboration of Stakeholders, people, and CSR Progam fro company developer im developing to build a Geothermal Education Center that contains all kinds of informations for local people and tourists, 5) Inviting the social activity from all of the nations that have interests in Geothermal society character buildings, like Kuliah Kerja Nyata (KKN), 6) others.

In order to create the educative geothermal geoturism activity, 1, 2, 5, 10, or even 15 years are needed as the process of development, so that the indirect use development have to be developed together with the geothermal geotourism so that the the people not only act as the eye-witness but also have roles, one of it in geothermal society-based geotourism activity. As the organizer, knowing about geothermal and how to conserve it are basic capability for local people. In the end, all of the process will created the atmosphere of geothermal in harmony of geothermal development. In order to educate the society, the simplest way are needed in the first, and growing as the knowledge of the society are increased.

Figure 2: Information signs that contains geothermal informations are one of the ways to educate the local people and tourists to learn about geothermal, in order to create the society that approve the geothermal indirect use electricity development (Photo credit to Halim dkk, 2015)

Figure 3. Geothermal Education Center (GEC) of Lahendong Geothermal Field as the center of informations of basic scientific of geothermal science, geothermal development, and many kinds of geothermal utilization for society. GEC are formed by the collaborations of Pertamina Geothermal Energy, Tomohon City's Staholder, and BPPT, with the initiation from KKN PPM UGM 2017

GEOTOURISM COMPARISON WITH OTHER GEOTHERMAL FIELDS

Comparison are done to look for the parameters that can be considered in developing the geotourisms plan in Bukit Daun Geothermal Area. The geothermal fields that'll be compared are chosen by these parameters that have the same conditions in Bukit Daun Geothermal Area, those are: 1) Area must be a located at residences area 2) Area are in contact with protected rainforest, 3) society of the geothermal area development isn't well understood about geothermal activity and development

Lahendong Geothermal Field

Lahendong Geothermal Field is located in North Sulawesi Province. Geologically, the area is located at arc-arc collision zone from the collision of Sangihe arc and Halmahera Arc (Utami et al, 2015). Field and literature studies show that several parts of society accept the geothermal development and the other parts denied it. It is considered, the education and cultural conditions of the society are the main reasons why the conflict happens between Geothermal development company and society, because of the villager's area lived there before the geothermal development. Until now, educations steps are done by stakeholder and its partners to serve an information to geothermal and its dynamics through geoturisms development and direct uses plan of geothermal potentials, even actually the society is lived for a long time with geothermal phenomena, but the information doesn't reach the society, so that the resistance happened.

Kamojang Geothermal Field

Kamojang Geothermal Field is at West Java Province. Geologically, the area is located at island arc subduction zone from subduction of Indo-Australia and Eurasia tectonic plates. The Kamojang geothermal area estimated area is about 21 km2, which its electric potential are estimated 300 MWe (Sudarman, 1995, in Utami, 2000). Literature studies show that geothermal development and society are live in harmony with each other. In Kamojang, direct use utilization is present in order to give

opportunities to society who comes and stay after Kamojang WKP (*Wilayah Kerja Panas Bumi*) area are developed. Direct use utilization can be found in Kamojang are educative geo tourism, such as a beautiful landscape enriched with agricultural activity i.e. Tea garden and hot water bathing activity has given a good potential of geotourism for visitor, and also direct use utilization in agricultural activity, i.e. Oyster Mushroom cultivated (Suyanto et al, 2010 ; Fadli et al. 2015).

Dieng Geothermal Field

Dieng Geothermal Field is located in Central Java Province. Geologically, the area is located at island arc subduction zone from subduction of Indo-Australia and Eurasia tectonic plates (Harijoko et al, 2010). Field and literature studies show that Dieng is an area where society and geothermal development company are lived in harmony, even if sometimes there are conflicts between them. Educative geotourism and direct uses of geothermal are the ways of society to take parts in geothermal activities in Dieng Geothermal Area, where society developed a special interest in tourists activity, also by geothermal exploitation of the company, some of the unexploited fluids are used by people as direct uses utilization, i.e. Bathing, also in Dieng visitor could find many kinds of local products. Some of the geotourism activity can be seen in Kawah Sikidang Dieng, where local people build a semipermanent house to sold sulphuric mud in bottles or handicrafts as local products of Kawah Sikidang, also by built photobooth like-infrastrucutres, the visitors can take photos. The geotourism activity of Kawah Sikidang is also enriched with the knowledge of local people who know about the history of natural geothermal activity and its development. (Geomagz, 2015; Diengnesia, 2016).

Lawu Geothermal Field

Lawu Geothermal Field is located at two Province, Central and East Java Province. In 2016, the project of Lawu geothermal field geothermal development was suspended in order to mass protest of some communities. The reasons of the protest are based on the WKP area are located at Lawu conservational forest where many people depend on it as life resources, i.e. water, food, and also the Lawu area act as the center of spiritual activity in Java (Konsorsium Pembaruan Agraria et al, 2017). Some steps are done in order to negotiate the people that lived in Lawu Geothermal Field, such as held socializations, but until now the status of geothermal development in Lawu geothermal Field is still unclear.

Bedugul Geothermal Field

Bedugul Geothermal Field is located in Bali Province. The project of geothermal development is suspended in 2005, where some oppositions come from public communities in Bali, also with the support from Bali House of Representatives. The reasons of the oppositions are because of the WKP area of Bedugul Geothermal forest are located in the sacred forest of Bali, also because of the forest act as water recharge area, so it must remain undisturbed. In society's opinion, geothermal development activity in the Bedugul Geothermal Field could disturbed the nature balance of the forest and also disturbed the cultural activity (Richter, 2015).

STUDY AREA CONDITIONS

Social Condition of the Study Area

The study area is consists of several conditions in social sides. The people lived in the study area mainly is original people who've lived for a long period in Bukit Daun area, they are Rejang ethnics, with a little number of other ethnics. Social observation shows that the people that lived in Bukit Daun area reach the number of 10.294 persons, with the growth rate is 6 – 24% (*Badan Pusat Statisik (BPS), 2016)*. Social observation based on several parameter like: 1) Education, 2) Heatlh, 3) Labor force. Observation shows that the education activity in Bukit Daun area are in good conditions which mean the each stage Preliminary school, Junior, and senior high school are presents, even if there are some problems where after graduate from senior high school, the people prefer to choose continuing their agricultural activity, or even there are some groups that didn't attend the school. The health condition of society is in good conditions where health faccility such as Clinic, *Puskesmas*, and *Posyandu* are present, but, not in very good conditions like the ones that present in the Rejang Lebong capital's. The latest data shows that labor force number in Bukit Daun geothermal field area, especially in Bermani Ulu Raya district is diversed in some of economical activity, but the largest number shown the agricultural activity as the most (BPS, 2016).

Figure 4: Lahendong Geothermal Field now was using Geotourism and direct use geothermal utilization as the ways to educate society, one of it is Linow Lake. (Photo Credit to Muhammad Sidqi)

Economic Conditions of the Study Area

The study area consist of several conditions in economical sides. The Society that lived in Bukit Daun area is mainly lived in need to agricultural activity, where about 62% of the society of Rejang Lebong lived in Agriculture by, especially in the study area, where the percentage is higher (BPS, 2015). Agricultural activity are done by planting vegetables, coffees, fruits, woods, and even teas.

Figure 5: Geotourism activities in Dieng Geothermal Field, the beautiful and unusual views of Geothermal field, enhanced with infrastructure development has made this is very attractive for tourism, one of it is in Kawah sikidang (Photo credit to the author)

Culture Conditions of the Study Area

Bukit Daun area is a place that still holding tight their cultural activities. In the study area, special culture day is celebrated, i.e. youngs marriage by showing traditional dance "Kejei". Some history, legends, and myths are also present like Pat Petulai or presence of Spirits that stayed in Bukit Daun forest, and the others.

INVENTARIZATION AND ANALYSIS OF BUKIT DAUN GEOTHERMAL GEOTOURISM POTENTIALS

Qualitative Analysis

Qualitative analysis is done through describing the conditions of geomorphsites in the study area that producing geotourism potentials, geological, geomorphological, and soil features, as well as describing the activity can be done in each of geomorphsites (Gray, 2004). Activity in the geotorism spots is analyzed based on REAL TRAVEL from Hendratno (2002), that which the parameters are rewarding, enriching, adventuring, and learning in order to build a concept of the geoturism plan in Bukit Daun area.

Seven colors Hot pools

Seven Colours hot pools are geothermal manifestations. Those spots are located at coordinates ranges from 212800.8 - 214688.6 Easting and 9631379.1 - 9629148.4 Northing. These spots are located in Rimbo Pengadang, Bermani Ulu Raya administratively. The elevation of those spots is about 1097 masl. This place located in Bukit Daun national park, and to reach it, the visitor has to do it by walking pass the Bukit Daun Forest National Park. Some of geotourism potential are present thanks to the geological conditions of the area. Geotourism potential appears as the product of geothermal activity from Bukit Daun Tertiary-Quaternary-aged volcano.

Geotourism potential can be found in this area are:

a. Attractive adventuring geotourism
b. A good place to photo shooting especially when it comes to nature
c. Beautiful view of seven pools that have different colors
d. Good place in learning about geothermal activity and its dynamics that showed by its manifestations
e. Others

Through further developments, the geotourism potential can be created are: (further development, see in quantitative analysis)

a. By the presence of information signs, this spot could be an educative and adventuring geotourism b. An enjoyable and safe place for learning about geothermal activity
c. With some photobooth-like infrastructure, A good photo shootings place when it comes to nature and scientific knowledge
d. A place to find local products of Geotourisms, like sulfur powder, or sulfuric mud for healty skin
e. Others

Figure 6: One of the hot pools foundin Bukit Daun area Where through this spots could be a good way to deliver the information to the society of tourism visitor (Photo credit to Redi Harisusanto)

Bukit Daun "Garden of Tea"

Bukit Daun "Garden of Tea" is located at coordinates 213269.8 Easting and 9623960.2 northing, 1259 masl. Administratively, this spot is located in Air Dingin Villages, Bermani Ulu Raya Subdistrict, Rejang Lebong. To reach this spot, the visitor can do it by using motor vehicles. Geotourism potentials in this spots appear thanks to its geomorphological and soil features, where geomorphology has gave the beautiful views and conditions, i.e. temperature, and rate of rainfall that support the grow of vegetations, as well as the fertile soil feature that gace the nutritions to the vegetations.
Geotourism Potential can be found in this place are:

a. A Good place for family recreation
b. Some good views of Bukit Daun volcanic landform are presented
c. Volcanic deposits that covered all of this area from Bukit Daun eruption has enriched the floras and faunas, on of them is Tea
d. There are some beautiful spots for photo shooting
e. Others

Through further developments, the geotourism potential can be created are: (further development, see in quantitative analysis)

a. By a little direct-use improvement from the tea company developer, The Tea as local products can be sold right on the spot
b. By infrastructure additions, Presence of fun attractive games, like outbound, or paragliding.
c. By the presence of cottage or rest house, this spot could be nice resort to spend the holidays with family or colleagues
d. Others

Figure 7: Bukit Daun Garden of Tea is serving nice geomorphological views of Bukit Daun volcanic landform (Photo credit to Kurniawan Oka)

Telapak Lake

Telapak Lake is located in the proximal zone of Bukit Daun Volcanic Landform. Located in Rimbo Pengadang Village, Bermani Ulu Raya, Rejang Lebong District. Geographically, this spots located in 208013.6 Easting and 9625667.9 Northing, 2371 masl. Telapak lake is believed to be the leftover of past volcanic processes that forming a depression where surface water and shallow groundwater accumulated. To reach it, visitor need to walking pass the Bukit Daun forest to the one of the peaks in Mt. Bukit Daun, where Telapak Lake lies and expected as the edifices product of past volcanic activity.

Geotourism potentials can be found in this place are:

a. Good place for nature-based adventuring
b. A good place for enjoying the beautiful view of volcanic lake
c. A place to saw and learn some of the endemic flora and fauna
d. Good destination for nature lover students/ community
e. Others

Through further developments, the geotourism potential can be created are: (further development, see in quantitative analysis)

a. By the presence of tracks/ trails, safer adventuring activity through tracks/trails while enjoying the view of Bukit Daun National Park
b. By the presence of information signs, information of the Telapak lake characteristics will reach the visitors
c. By its unique shape, Telapak lake's shape could be the icon of the geotourism activity in Bukit Daun
d. Others

Figure 8: A bird view of Telapak Lake of Bukit Daun, where past volcanic activity produced this lake (Photo credit to Dio Gala Putra)

Bukit Daun National Park

Bukit Daun National Park located in the proximal zone of Bukit Daun Volcanic Landform. This area is located 200330.3 – 210675.8 Easting and 9621176.9 – 9626293.2 Northing, 926 – 2449 masl. Administratively, this area located in Bermani Ulu Raya area subdistrict, and continued to exceed the administrative border of Rejang Lebong, Lebong, and North Bengkulu district. In 2014, Bukit Daun exceeds 176.290 ha. Geotourism potentials present as the product of geological, soil feature and geomorphological of the area as the main factor, where volcanic deposits that cover all of the areas have enriched the variety of vegetations in the study area. High rainfall rate also accelerates the weathering process that produces fertile soil as the medium of the vegetations to grow.

Geotourism potentials can be found in this place are:

a. Nature-based adventuring geotourism
b. A good place to study about the heterogenization of vegetations in rain forest
c. One of the best places for Rafflesia flower to grow, especially Rafflesia arnoldi and Rafflesia bengkuluensis that only can be found in Bengkulu.
d. Good views for Flora and Fauna photoshoot in its natural habitat
e. A place to feel the cleanest air in the rain forest
f. Others

Through further developments, the geotourism potential can be created are: (further development, see in quantitative analysis)

a. By additions of guard station or safety infrastructures, enjoyable and safer sites for geotourisms could be created
b. By Presence of tracks/ trails, good views of Bukit Daun forest can be seen more
c. By the presence of information signs, the visitor could learn much about the Bukit Daun Forest
d. By presence of local tour guide, visitor will get more information
e. Others

Figure 9: Geotourism activity in Bukit Daun National Park. A tourist that took photo with Refflesia arnoldi as one of rarest flower in the world, that naturally only can be found in Bengkulu Province (Photo credit to Danang Prasetya)

Quantitative Analysis

Quantitative analysis is done by giving some scores to several parameter and subparameter from 0 – 1. By giving some scores, can be seen that in each of geomorphsites have different scores in subparameters that showing the sides that need to be improved in order to serve a good geotourisms activity. The quantitative analysis used in this study will be based on several parameters that proposed by Kubalíková (2013), that based on five main parameters, such as Scientific and intrinsic value, educational, economical, conservational, and added value.

Table 1: Assessment of Geotourism potentials (Kubalíková, 2013)

Parameters	
Scientific and Intrinsic Values	
Integrity	0 – Totally destroyed site 0,5 – Disturbed site, but with visible abiotic features 1 – site without any destructions
Rarity (number of similar sites)	0 – more than 5 sites 0,5 – 2-5 similar sites 1 - the only site within the area of interest
Diversity	0 – only one visible feature/ processes 0,5 – 2-4 visible feature/ processes 1 – the only sites within the area of interest
Scientific Knowledge	0 – unknown site 0,5 – scientific paper on national level 1 – high knowledge of the site, monographic studies of the sites
Educational Values	
Representativeness and Visibility/ Clarity of the Features / Processes	0 – low representativeness/ clarity of the form and the processes 0,5 – medium representativeness, especially for scientists 1 – high representativeness of the form or processes, also for public
Exemplarity, Pedagogical use	0 - very low exemplarity and pedagogical use of the form and process 0,5 - existing exemplarity, but with limited pedagogical use, 1 - high exemplarity and high potential for pedagogical use, goedidactics and geotourism
Existing Educational Products	0 - no products 0,5 - leaflets, maps, web pages 1 - info panel, information at the site
Actual Use of a Site for Educational Purpose	0 - no educative use of the site 0,5 - site as a part of specialized excursions (students), 1 - guided tours for public
Economic Values	
Accessibility	0 - more than 1000 m from the parking place, 0,5 - less than 1000 m from the parking place 1 - more than 1000 m from the stop of public transport
Presence of Tourist Infrastructure	0 - more than 10 km from the site existing tourist facilities, 0.5 - 5 – 10 km tourist facilities 1 - less than 5 km tourist facilities

Local Products	0 - no local products related to a site, 0,5 - some products, 1 - emblematic site for some local products.
Conservational Values	
Actual Threat and Risk	0 - high both natural and atrophic risks, 0,5 - existing risks that can disturb the site, 1 - low risks and almost no threats
Potential Threat and Risks	0 - high both natural and athrophic risks, 0,5 - existing risks that can disturb the site, 1 - low risks and almost no threats
Current Status of a Site	0 - continuing destruction of the site, 0,5 - the site destroyed, but now with management measures for avoid the destruction, 1 - no destruction
Legislative Protection	0 - no legislative protection, 0,5 - existing proposal for legislative protection, 1 - existing legislative protection (Natural monument, Natural reservation…)
Added Values	
Presence of Cultural Value	0 - no cultural features, 0,5 - existing cultural features but without strong relation to abiotic features, 1 - existing cultural features with the strong relations to abiotic features
Ecological Value	0 - not important, 0,5 - existing influence but not so important, 1 - important influence of the geomorphologic feature on the ecologic feature
Aesthetical Value: number of colors; structure of the space, viewpoints	0 - one color, 0,25 - 2-3 colors, 0,5 - more than 3 colors; 0 - only one pattern, 0.25 - two or three patterns clearly distinguishable, 0.5 - more than 3 patterns; 0 - none, 0.25 - 1-2, 0.5 - 3 and more

From the quantitative analysis, can be seen that there are some of the parameters needed to be improved in order to construct a geotourism plans in Bukit Daun area.

From the scientific and intrinsic values, can be seen that the range of the values is 62,5 – 100%. The lowest value is lies at Bukit Daun Garden of Tea, and the highest value lies on Seven Colors Hot Pools "*Putri 7 Warna*". it happened because in some spots can be found some destruction processes that can threaten the sites, i.e. the human activity who throw garbage in the sites. The acts that need is to raise the integrity and scientific values of the sites

From the educational values, the values are ranged from 25% to 50%. Low values are present in order to the lack of the educational products of the sites, and also the places are still highly nature status where people are seldom using the sites for geotourism activity and only small number of people who already know about the sites. The acts need to do in order to increase the values are to serving more information to the visitor about the sites, the information may come from the information boards, flyers, brochures, websites, or even by serving a guide in geotourism sites.

From the economical values, the values are ranged from 0 – 66,7 %. Low values are present because mainly in accessibility and local products. Low accessibility happened because of the area are located in national parks of Bukit Daun forest, so that only small number of accessibility could be accessed. Low values of local product are also present because of the society in this area gave less-aware of their area's geotourism potentials. The acts need to do are by increasing the accessibility and presence of local products value. Accessibility as parts of infrastructures is needed by building a safe trail/ tracks to reach the geotourism sites, as well as to serving local product of each sites, in order to serving visitors something to bought to their relations as gifts.

From the conservational values, the values are ranged from 75 – 100%. Such a high values are present because of the area are a conservation area of Bukit Daun national park. The acts need to be done is just to determine the regulations how to keep the area keep conserved when the geotourism activity is about to begin, to keep the area from any threats of destructions that could lower the values of geotourisms itself.

Added values are presents because of the difference in cultural, aesthetical, and ecological in each site. The presence of added values are believed could relate the abiotic features and processes to cultural issues as biotic features (Kubalíková, 2013). The acts that need to be done are to promote more of these added values in order to create a more interactive geotourism activity.

Table 2: Assesments of Potential Geotourism Spots in Bukit Daun Geothermal Area

Parameter		Bukit Daun Garden of Tea	Seven Colors Hot Pools "*Putri 7 Warna*"	Telapak Lake	Bukit Daun National Park
Scientific And Intrisic Values	*Integrity*	0.5	1	1	1
	Rarity (number of similar sites)	1	1	1	1
	Diversity	0.5	1	0.5	0.5
	Scientific Knowledge	0.5	1	0.5	0.5
%		62.5%	100%	75%	75%
Educational Values	*Representativeness and Visibility/ Clarity of the Features / Processes*	1	1	1	1
	Exemplarity, Pedagogical use	1	0	0	0.5
	Existing Educational Products	0	0.5	0	0
	Actual Use of a Site for Educational Purpose	0.5	0.5	0	0.5
%		50%	50%	25%	50%
Economical Values	*Accessibility*	1	0	0	0
	Presence of Tourist infrastructure	0.5	0,5	0.5	0.5
	Local Products	0.5	0	0	0
%		66.7%	16,7%	16.7%	16.7%
Conservational Values	*Actual threat and Risk*	1	0.5	1	1
	Potential Threat and Risks	0.5	1	1	1
	Current Status of a Site	0.5	1	1	1
	Legislative Protection	1	1	1	1
%		75%	86,6%	100%	100%
Added Values	*Presence of Cultural Value*	0	1	0,5	0,5
	Ecological Value	1	1	1	1
	Aesthetical Value	0.5	0,5	0,25	0,25
	%	60%	100%	70%	70%
Mean		**62,84 %**	**70,66%**	**57,34%**	**62,34%**

GEOTHERMAL GEOTOURISM EDUCATION PLAN

Based on social condition and other analysis results, and linked to comparison to other geothermal fields, the the parameters need to be considered to construct an educative geothermal geotourism plans are summarized below:

The geotourism concept must answer the curiosity of the society and visitor about the nature of geothermal activity in Bukit Daun Geothermal field

1) The geotourism concept must serve an amusing activity of geotourism to the society and the visitors
2) How to involve the Society as the organizer of the geotourism activities?
3) How long will it be needed to build the infrastructures for those geotourism plans?

The geotourism concept must answer how to rises up the conservational value as reward for natureThe concept we proposed of geothermal education based on values proposed by Hendratno (2002), those values are REAL Travel, means 1) Rewarding, 2) Enriching, 3) Adventuring, and 4) Learning. Rewarding means reward for geological and environmental phenomenon objects, enriching means enrichment of knowledge for geological and environmental phenomenon objects, adventuring means doing an active trip to observe geological objects, and also learning means that trip there are learning aspects for geological and environmental phenomenon objects. In order to connect the abiotic features (Geological uniqueness) to biotic features, added values are something important that needs to be analyzed (Kubalíková, 2013). Several added values are present in the study area are cultural values, aesthetic values, ecological, and economical.

Cultural Values

One of the most interesting values that can supports this geotourism plan is cultural values in Rejang Lebong called *Pat Petulai*. *Pat* means four, and *Petulai* means *mergo* or groups of member of Rejang Ethnic. Those member of Rejang Ethnic are Mergo Bermani, Mergo Bejinggo, Mergo Sepanjang Jiwo, dan Mergo Bimbo, which are spreaded in North Bengkulu, Kepahiang, Rejang Lebong, and Central Bengkulu districs.This cultural values can be linked with four geotourism spots as four main geotourism spots with its own uniqueness.

The other values can be seen is the presence of myth that in the Seven Colors Hot Pools "*Putri 7 Warna*", there are tutelary spirits with with the appearance of princess, that lives in white hot pool, for the other six hot pools, it's believed to be the place where the guardians of the princes-like spirit lies.

Ecological and Aesthetical Values

As a district that located within and around of Bukit Daun National Park, and also from activity of people who dominantly do agricultural activity, ecological conditions of Bukit Daun Geothermal field could supports the geotourism activity. Agricultural activity could serving beautiful view of vegetables or fruits that has been planted, or by creative thoughts, the farm/ field owner could let the visitor pick the vegetables or fruits itself, this also could increase the economical values of the geotourism activities.

Figure 8: An example of Curup's Strawberry farm (20 Km to the East of Study Area) where the visitor could picks the farm's product by themselves (Photo credit to Yurike Anggraini).

RESULTS

From the Concept of Real TRAVEL (Hendratno, 2002), we proposed a concept of geotourism in Bukit Daun Geothermal Area. The concept of geotourism we brought is *Geodiversity in Geothermal Geotourism*. It Means that geodiversity in geothermal could become powerful tools to educate the society. The geotourism concept plan are brought because of it contains the values summarized in Table 1. besides of educational purposes, thanks to it, geotourism spots has to be conserved thorugh geoconservation as the basis of geotourism activity (Kubalíková, 2013).

Geodiversity in geothermal geotourism also a concept we proposed by linked geological, cultural, economical, and social sides of society lived within and around the Bukit Daun geothermal area in order to construct a geothermal geourism plan, so that the society will be ready to act as the organizer of those geotourisms sites, but that does not mean their old social-economical activity is gone after geotourism activitites are present. The cultural value of the Rejang Lebong such as Pat Petulai also could enrich the value of geotourism. Those are what it means what we proposed about geodiversity in geothermal geotourism, so that the visitors could found an exciting area with all of the uniqueness in Bukit Daun geothermal area, and to fill the visitor expectations; 1) sightseeing as a part of trip agenda, 2) Uniqueness photo opportunities, 3) scientific or educational study interest, and 4) curiosity and ambitions to see something unusual (Erfurt-Cooper, 2010)

Four main spots of Geotourism, Bukit Daun Garden of Tea, Seven Colors Hot Pools "*Putri 7 Warna*", Telapak Lake, and Bukit Daun Protected Rain Forest could act as the main "actors" to educate the society and visitor that lived within the Bukit Daun geothermal area differently based on their geological, Geomorphological, and soil features uniqueness , such as :

a. Bukit Daun Garden of tea, could give the information about the relation between biotic especially many varieties of vegetations with geological conditions and geomorphological conditions, that geological conditions supports the biotic features to be present, and also the economic activities in Bukit Daun. Bukit

Daun Garden of the also gives the informations about the geomorphological phenomena of Mt. Bukit Daun.

b. Seven Colors Hot Pools "Putri 7 Warna, could give the informations about how the geothermal system works as a cycle where its elements support each other to transport the heats below to the surface, and appear as manifestations, as well as the other processes appear within and around the manifestation area, i.e. hydrothermal alterations.
c. Telapak Lake could give the information about how past volcanic activity of Mt. Bukit Daun could created something amazing, in this issue is Telapak Lake. Telapak Lake also gives the information about how are the processes happened between the surface water, Lake, and the forest that support each other in their existences.
d. Bukit Daun National Park, could give the information how the volcanic activity of Bukit Daun produce volcanic deposits, and by its geomorphological conditions has made special soil features, and serving a very good place for vegetations to grow, the Bukit Daun forest itself. One of the most spectacular products of this area is Rafflesia arnoldi and Rafflesia bengkuluensis flower as provinces and national icon that only can be found in Bengkulu with Bukit Daun as the place where most of the Rafflesia flower lives.

CHALLENGES

Developing a geotourism plans is a long ways and steps, there're no guaranteed that developer does will be the success. Based on analysis before, there is five main question that needs to fulfill by developers in developing geoturism in Bukit Daun Sector, for educational purposes about geothermal phenomena and potentials, they are:

1) How are preparations we need to do in developing geothermal geotourism especially in a populated area and rain forests? The presence of rainforest is also the main factor need to be considered, because large scale of geoturism activity can be held in protected areas. The background of this question is because usually a conflict will happen between the society and the developers in the populated area where the local people are afraid if their area are exploited for some self-importance.
2) What Infrastructures are needed to build a geotourismactivity? Infrastructures are the important sides need to be improved through geotourism spots, because it will attract visitors to come to the place, besides it will serve a better and safer tourism activity, both for society and the visitor.
3) How to create the conditions where the roles of society in geotourism activity will be the organizer of it? To create the geotourism that based on education, the society have to be the organizer of the tourism activity, so they'll have to know the conditions of the area
4) Who and how the management and further development activity will be done? The further development is needed in order to create a geotourism based educations, to create it, stakeholder and the company are the responsible parties who has a better power and sometimes better knowledge about the geological and other conditions of the area.
5) How to perform geoconservation of the Bukit Daun Geothermal Area? Conservation of the sites is the final relationship and responsibility between Stakeholder, Developer company, society, and visitors to keep the nature in its good state. The acts need to do is to serve a sanitation facilities, as well as to serve the functionary staffs. is to serve a sanitation facilities, as well as to serve the functionary staffs.

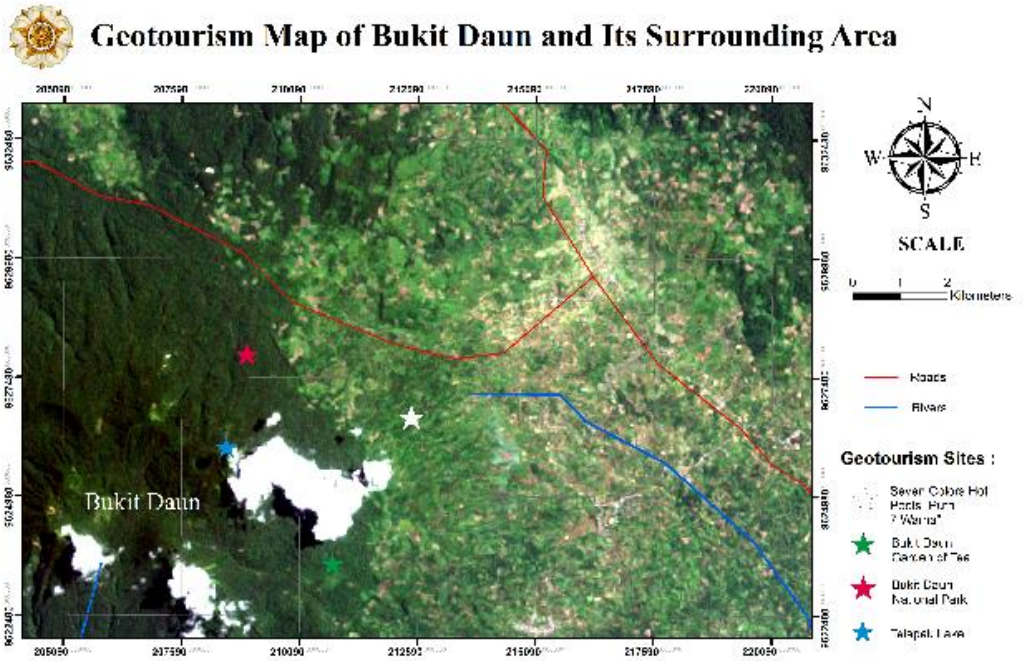

Figure 9: Geotourism maps of Bukit Daun Geothermal Area (Landsat 8 OLI/ TIRS)

CONCLUSIONS

The conclusions from this publications are Bukit Daun Geothermal Fields contains some sites/ places that have high potentials to be developed in geotourism, they are Bukit Daun Garden of tea, Seven Colors Hot Pools " Putri 7 Warna, Telapak Lake, and Bukit Daun National Park, but now the utilizations is only in its simplest ways. The collaboration of Stakeholder, company developer, and society are needed to construct a geotourism activity that based on rewarding, enriching, adventuring, and learning.

ACKNOWLEDGEMENT

In completing this paper, the authors want to say thanks to Danang Prasetya, Tri Intan Putri Kinanti, Kurniawan Oka, and the others as the informans for geotourism sites in Bukit Daun Geothermal Fields.

REFERENCES

Badan Pusat Statistik Kabupaten Rejang Lebong, 2015, Kabupaten Rejang Lebong dalam Angka, Percetakan Merdeka Curup, 464 h.

Badan Pusat Statistik Kabupaten Rejang Lebong, 2016, Kabupaten Rejang Lebong dalam Angka, Percetakan Merdeka Curup, 370 h.

Diengnesia, 2016, Sejarah Panas Bumi Dieng, [Online] http://www.diengnesia.com/index.php/2016/03/10/sejarah-panas-bumi-dieng/ (Accessed 7th July, 2017)

Erfurt-Cooper, P., 2010, 'The Importance of Natural Geothermal Resources in Tourism', *Proceedings World Geothermal Congress 2010, Bali, Indonesia*, hh. 1-10.

Gafoer, S, Amin, T. C., & Pardede, ., 1992, *Geological Map of The Bengkulu Quadrangle, Sumatra*, Geological Research and Development Centre.

Gray, M., 2004, 'Geodiversity: Valuing and Conserving Abiotic Nature'. Chichester: John Wiley, 450 h.

Hendratno, A., 2002, 'Perjalanan Wisata Minat Khusus Geowisata Gunung Merapi (Studi di Lereng Merapi Bagian Selatan, Yogyakarta)', *Jurnal Nasional Pariwisata*, vol. 2, no. 2, hh7-23.

Kubalikova, L., 2013, 'Geomorphosite Assessment for Geotourism Puposes', *Czech Journal of Tourism*, vol. 2, no. 2, hh80-104.

Kubalikova, L., Kirchner, K., 2016, 'Geosite and Geomorphosite Assessment as a Tool for Geoconservation and Geotourism Purposes: a Case Study from Vizovicka vrchovina Highland (Eastern Part of Czech Republic)', *Geoheritage*, hh5-14.

Konsorsium Pembaruan Agraria (KPA), 2017, Siaran Pers: Tolak Eksploitasi Panas Bumi di Gunung Lawu, [Online]. http://www.kpa.or.id/news/blog/siaran-pers-tolak-eksploitasi-panas-bumi-di-gunung-lawu/ (Accesed 7th July, 2017)

Kurnia, A., 2014, *Riwayat Panas Bumi di Kamojang*, MAGZ-Majalah Geologi Populer, Badan Geologi, dilihat pada 10 Juli 2017, <http://geomagz.geologi.esdm.go.id/riwayat-panas-bumi-di-kamojang/>.

Listrik.org., 2016, Pertamina Menang Lelang Wilayah Kerja Panas Bumi Gunung Lawu [Online], available from: http://listrik.org/news/pertamina-menang-lelang-wilayah-kerja-panas-bumi-gunung-lawu/ (Accessed 5th July, 2017)

Martin-Duque, J. F., Garcia, J. S. & Urqui, L. C., 2012, 'Geoheritage Information for Geoconservation and Geotourism Through the Categorization of Landforms in a Karstic Landscape. A Case Study from Covalagua and Las Tuerces (Pelencia, Spain)', *Geoheritage*, hh93-108.

Priatna, 2015, *Panas Bumi Dieng*, GEOMAGZ-Majalah Geologi Populer, Badan Geologi, dilihat pada 10 Juli 2017, <http://geomagz.geologi.esdm.go.id/panas-bumi-dieng/>.

Putra, G. Z. M., Sutrisno, Fandi, P. M. I. & Hendratno, A., 2016, 'Analisis Geosite dan Geomorphosite Pantai Menganti sebagai Potensi Geowisata Indonesia', *Proceeding Seminar Nasional Kebumian Ke-9*, hh. 951-969.

Richter, A., 2015, Continued opposition to Bedugul project in Bali, Indonesia. [Online] available from: http://www.thinkgeoenergy.com/continued-opposition-to-bedugul-project-in-bali-indonesia/ (Accessed 4th July, 2017)

Suyanto, Surana, T., Agustina, L. & Subandriya, A., 2010, 'Development of Direct Use Application by BPPT', *Proceedings World Geothermal Congress 2010, Bali, Indonesia*, hh. 1-5.

Utami, P, 2000, 'Characteristics of the Kamojang Geothermal Reservoir (West Java) as Revealed by Its Hydrothermal Alteration Mineralogy', *Proceedings World Geothermal Congress*, hh1921-1926.

Utami, P., Widarto, D. S., Atmojo, J. P., Kamah, Y., Browne, P. R L., Warmada, I. W., Bignall, G., Chambefort, I. 2015, 'Hydrothermal Alteration and Evolution of the Lahendong Geothermal System, North Sulawesi', *Proceedings World Geothermal Congress*, hh1-10.

ISBN 978-602-52132-0-5

Asosiasi Panasbumi Indonesia (API)
Apartemen Menteng Square, BR-9 Tower B
Jl. Matraman No 30 E, Jakarta Pusat - 10320 Indonesia
Email: api.inaga@yahoo.co.id